

Pilkington Library

Author/Filing Title ZARIFI, A

Accession/Copy No. 040129658

Vol. No. Class Mark

	LOAN COPY	date due :-
06 MAY 1997		
- 9 NOV 1997	22 NOV 1998	24 DEC 1999
30 NOV 1997	11 DEC 1998	LOAN 3 WKS. + 3
11 MAR 1998		UNLESS RECALLED
	26 MAR 1999	KP95791
21 MAY 1998	FOR REFERENCE ONLY	
		19 FEB 2001

040129658X



**Integrated inspection of sculptured surface
products using machine vision and a
coordinate measuring machine**

by


AssadAllah Zarifi

A Doctoral Thesis
Submitted in partial fulfilment of the requirements
for the award of

Doctor of Philosophy of Loughborough University

1996

© by AssadAllah Zarifi 1996

 Loughborough University Library
Date: Jun 97
Class:
Acc No. 640129658

9/6446837

**To my wife who gave me full support, love, appreciation and without her help this work
could not be completed,**

and

To my parents who taught me the merits of discipline and the rewards of education,

and

To my brothers and sisters who always supported and encouraged me in my way.

Acknowledgements

I would like to express my sincere gratitude to my academic adviser, Dr. Roy Jones, for his guidance and encouragement during my years at the Loughborough University of Technology. His extensive knowledge, professional guidance, support and constructive criticism have greatly influenced my life and work.

I would like also to thank Professor Keith Case my director of research for his excellent support and help during the course of this research.

I further extend my appreciation to Dr Ali Mamma and Mrs. M. Green of the department of Mathematics for their expert help and discussions on developing optimisation method and correcting the mathematical equations for this project. I thank the following individuals for their precious roles during the course of this study:–

Mr. JagPal Singh for his endless practical help and useful discussion on the measurement,

Mr. Terry Smith for his professional work in taking photographs included in this project,

Mr. Robert Doyle for his help and ideas for the CAD section of this project, and Mr. David Walters for his help and support on computing matters,

Mr. Trevor Downham and Mr. Derrick Hurrell of the machine tools laboratory for their invaluable help and support during the project,

Mr. Richard Price for his help and especially the work on the plastic modelling of the ball,

Mr. Robert Temple, John Jones and David Hardwick for their generous support and help for this project.

Mr. Nicholas Ball for his kind support during my study at Loughborough University,

Miss Tess Clark for her assistance help during my time at Loughborough University,

I further extend my appreciation to all of the colleagues and department staffs for their endless help and efforts which made the job possible.

Synopsis

In modern manufacturing technology with increasing automation of manufacturing processes and operations, the need for automated measurement has become much more apparent.

Computer measuring machines are one of the essential instruments for quality control and measurement of complex products, performing measurements that were previously laborious and time consuming. Inspection of sculptured surfaces can be time consuming since, for exact specification, an almost infinite number of points would be required. Automated measurement with a significant reduction of inspected points can be attempted if prior knowledge of the part shape is available. The use of a vision system can help to identify product shape and features but, unfortunately, the accuracy required is often insufficient. In this work a vision system used with a Coordinate Measuring Machine (CMM), incorporating probing, has enabled fast and accurate measurements to be obtained. The part features have been enhanced by surface marking and a simple 2-D vision system has been utilised to identify part features. In order to accurately identify all parts of the product using the 2-D vision system, a multiple image superposition method has been developed which enables 100 per cent identification of surface features. A method has been developed to generate approximate 3-D surface position from prior knowledge of the product shape.

A probing strategy has been developed which selects correct probe angle for optimum accuracy and access, together with methods and software for automated CMM code generation. This has enabled accurate measurement of product features with considerable reductions in inspection time.

Several strategies for the determination and assessment of feature position errors have been investigated and a method using a 3-D least squares assessment has been found to be satisfactory. A graphical representation of the product model and errors has been developed using a 3-D solid modelling CAD system. The work has used golf balls and tooling as the product example.

Acronyms

A/DC	Analog/Digital Converter
AERS	Automatic Error Representation Scheme
AGV	Automated Guided Vehicle
AI	Artificial Intelligence
AIPS	Active Illumination Projection System
ANSI/ASME	The American National Standard Institute/American Society of Mechanical Engineers
ASP	Active Stereo Probe
CAI	Computer Aided Inspection
CAPP	Computer Aided Process Planning
CCD	Charged Couple Device
CIM	Computer Integrated Manufacture
CMM	Coordinate Measuring Machine
CNC	Computer Numerical Control
CRS	Controlled Random Search
CSG	Construction Solid Geometry
DCC	Direct Computer Control
DCP	Dimple Clearance Position
DME	Dimensional Measuring Equipment
DMIS	Dimensional Measuring Interchange Specification
DF	Discrepancy Factor
DR	Discrepancy Radial
DS	Dimple Sphere
DSS	Dimensional Sculpture Surfaces
DTI	Department of Trade and Industry
DZP	Dead-Zone Percentage
EDA's	Edge Detection Algorithms
EDM	Electro Discharge Machining
EDS	Electronic Data Systems
FMS	Flexible Manufacturing System
GKS	Graphical Kernel System
IGES	Initial Graphics Exchange Specification
LSBFM	Least Squares Best Fit Optimisation Method
LVDT	Linear Voltage Differential Transformer (linear displacement transducer)

MIST	Multi-Image Superimposed Technique
MCG	Machine Checking Gauge
MM4	Micro-Measure-4
NBS	National Bureau of Standards
NC	Numerical Control
PDES	Product Data Exchange Standard
RMS	Root Mean Square
RSM	Random Search Method
SSC	Stereo Scene Coding
STEP	STandard for data Exchange Product
SVP	Surface Virtual Point
TTP	Touch Trigger Probe
TACP	Tip Angle Changing Position
UG	Unigraphics
3-DSS	Three Dimensional Sculptured Surfaces

Integrated inspection of sculptured surface products using machine vision and a coordinate measuring machine

CONTENTS	Page
Chapter 1	Introduction..... 1
1.0	Introduction..... 1
1.1	Automated inspection 1
1.2	CNC code generation 2
1.3	Geometric and feature measurements..... 3
1.4	Automated measurement of sculptured surfaces..... 4
1.5	Vision directed inspection and recognition..... 7
1.6	Integration of vision and CMM..... 12
1.7	CMM and CAD integration..... 13
1.8	Research objectives and proposed approach..... 14
Chapter 2	Digital image processing system..... 17
2.0	Introduction 17
2.1	Digital image representation..... 17
2.2	Fundamental steps in image processing..... 18
2.3	Vision system and its elements..... 19
2.4	Machine vision fundamentals..... 20
2.5	Review on vision system for measurements of objects..... 22
2.6	The vision system used for this work..... 24
2.6.1	The Matrox vision system..... 24
2.6.2	Illumination and filtering system 26
Chapter 3	Coordinate Measuring Machine (CMM)..... 28
3.0	Introduction 28
3.1	CMM and it's elements..... 29
3.2	Types of probes and sensors used by CMMs..... 30
3.2.1	Contact probes 31
3.2.2	Non contact probes 34
3.3	CMM measurement techniques..... 36
3.3.1	Digitising, scanning and types of measurements by CMMs.. 37
3.4	Review on CMM applications, integration and related matters..... 39
3.5	Factors affecting CMM performance..... 42

3.5.1	Geometric and kinematic errors on CMMs.....	43
3.5.2	Probe error sources within a kinematic/resistive probe....	43
3.5.3	Errors due to environmental effects.....	45
3.5.4	Volumetric accuracy.....	46
3.6	The CMM systems used for this work.....	46
3.7	Future developments of CMMs.....	47
Chapter 4	Feature detection using machine vision and a CMM..	50
4.0	Introduction	50
4.1	Golf balls	50
4.2	Review of vision system application methods for feature identification.....	53
4.2.1	Automated inspection by CMM.....	55
4.2.2	Review of previous work at Loughborough University...	57
4.3	Proposed integration method in this work.....	58
4.3.1	Method of feature detection.....	59
4.3.2	Identification of dimples.....	59
4.3.3	Dimple centre detection from 2-D images.....	61
4.4	2-D lens correction factor for spherical products.....	63
4.5	Calculation of feature height.....	67
4.5.1	Z-layer approach	67
4.5.2	Segmentation approach.....	68
4.5.3	3-D calculation of dimple locations	69
4.6	System of part and the ball holder.....	74
4.7	Probing strategy.....	75
4.7.1	Restrictions on different CMMs.....	75
4.7.2	Dimple probing techniques.....	76
4.8	Discussion.....	79
Chapter 5	Multi-Image Superimposing Technique (MIST) for pattern features on spherical surfaces.....	81
5.0	Introduction	81
5.1	Feature identification by multi-images.....	82
5.2	Proposed one camera multi-image superimposed method.....	83
5.2.1	System configuration.....	84
5.2.2	Filter arrangement.....	86
5.2.3	View arrangement and axes transformation.....	86

5.3	Overlapped areas.....	87
5.3.1	Data-set sorting.....	90
5.4	Mathematical evaluation of the overlapped areas.....	92
5.4.1	Calculation of the detectable ring diameter for optimum overlap.....	92
5.4.2	The approximate overlapped evaluation method.....	96
5.4.3	The surface integration method.....	98
5.4.4	Calculation of Dead Zone Percentage (DZP).....	100
5.5	Experiments and results.....	102
5.6	Reduced MIST.....	110
5.7	Discussion.....	111
Chapter 6	The system error model.....	112
6.0	Introduction.....	112
6.1	Review on error evaluation methods.....	112
6.2	Dimple pattern problems.....	114
6.3	Possible solutions to dimple problems.....	115
6.3.1	Introduction to optimisation.....	116
6.3.2	Definition of optimisation problems.....	117
6.3.3	Classification of optimisation problems.....	117
6.3.4	Unconstrained optimisation.....	118
6.3.5	Constraints optimisation.....	120
6.3.6	Least squares best fit.....	121
6.4	Possible solutions worthy of evaluation.....	122
6.5	Proposed random search method for optimisation.....	123
6.5.1	RMS experiments on the golf ball patterns.....	123
6.6	Proposed Least Squares Best Fit Optimisation Method (LSBFM)	129
6.6.1	Cartesian approach.....	130
6.6.2	Calculation of the domains.....	133
6.6.3	Polar approach.....	136
6.7	Discussion and Results.....	138
Chapter 7	Interfacing CAD and CMM.....	141
7.0	Introduction.....	141
7.1	Review of CAD/CMM integration.....	142
7.2	Generation of CAD data/Reverse engineering of parts.....	143
7.3	CAD generated models.....	145

7.4	Interfacing and 3–D graphical presentation of results.....	146
7.5	Machine code generation for an optimised measurement.....	152
7.6	Discussion.....	153
Chapter 8	Discussion.....	155
Chapter 9	Conclusions.....	163
Chapter 10	Recommendations for future work.....	165
References.....		167
Appendix A. LSBFM Results for cubic and icosdhh(432) patterns..		176
Appendix B. Polar approach.....		184

CHAPTER 1

INTRODUCTION

1.0 Introduction

Free form or sculptured surfaces are of great importance in engineering and are particularly related to aerodynamic shapes in today's industries. Inspection and measurement of these surfaces to high orders of accuracy can be time consuming since the new designs tend to have more complex forms and for exact specification, an almost infinite number of points would be required. Generally the most effective way of measuring these surfaces is by the use of a three dimensional Computer Numerical Control (CNC) Computer Measuring Machine (CMM).

In recent years, CMM's have become one of the most essential instruments for quality control and measurement used in manufacturing processes, performing measurements that were previously very laborious and time consuming to make. Generally, the state of the art in the operation of the CMM requires on line teaching methods before performing inspection. However, if prior knowledge of the part shape is available automated measurement with a significant reduction of inspected points can be attempted. One successful way of identifying these objects is by employing a perception system which means that the objects to be measured need to be identified. This provides the possibility for considerable time reduction when the inspection process is dealing with complex and accurate shapes. Vision systems are being used increasingly to automate the measuring process. Their use can help to identify product shape and features but unfortunately for high accuracy their cost is prohibitive.

Therefore, if an integrated inspection system could be developed which could identify the surface features in minimum time, measure them to high accuracy with speed and suitable analysis then the above mentioned problems could be avoided.

Thus, an essential step in obtaining a flexible inspection system is to integrate a machine vision system with a CNC CMM incorporating probing. Further enhancement and data transfer could also be achieved with the integration of a CAD system.

1.1 Automated inspection

Inspection is an essential part of the manufacturing process to ensure a constant output quality, and automated inspection in industry, is sufficiently new and the technology is still emerging. For manufacturing companies to be competitive it is crucial to automate this process. The automating

of the inspection process is not merely determined by technical feasibility or finance alone but by the interaction of all relevant economic factors [1].

Elshennawy [2] categorised inspection in automated manufacturing into four groups; (1) deterministic metrology, (2) in-process inspection, (3) post-process inspection, and (4) inspection performed in a separate inspection laboratory where automated equipment is located for that purpose. However, he describes how it is important to integrate computer controlled measuring machines like a CMM into an automated manufacturing environment where a constant demand for increased productivity is coupled with a growing demand for higher quality.

For dimensional measurement there are devices and procedures to follow in order to obtain the best possible results. These devices can be grouped into CMM's, vision systems, optical comparators, robotic measuring devices, photogrammetry and laser based measuring devices/3D scanners. The functionality, duty and the environment in which each device can operate is particular to that device. Apart from their physical restrictions other important factors such as flexibility or the economic viability will have an impact on the feasibility of the system.

The issue of automated inspection has been considered by some researchers using CAD systems, vision system or a feature based database system [3,4,5,6,7,8,9,10,11]. In all of these inspection systems, one common characteristic is that they employ computer technology to integrate different computer numerical control devices together. A typical integrated system can consist of a CAD/CAM system and a CMM as the main elements and with auxiliary elements which depends on the application, for example for a system to be used for an automated inspection in a machining cell extra elements could be a robot, a cell control computer, a machining centre and storage/retrieval facilities for parts and tools.

The advantages of automated inspection can be listed as temporal, locational and operational. Information on the product being inspected is acquired and will be processed at electronic speeds. The speed of inspection usually matches production speeds which will save time in material handling. Furthermore those products which were only inspected on a sample basis because time was not available may now be 100 per cent inspected if so desired.

1.2 CNC code generation

For CNC machines the CNC code generation is the process that determines exactly how a particular machine will position or operate on the part. The majority of CNC applications have been directed towards machining. However, in contrast to the machining process, relatively little research effort has been directed towards inspection CNC code generation. In this study the

automated generation of CNC code for inspection machines will be considered.

Due to the development of CNC machines and software packages, measurement of free form sculptured surfaces can now be done with a three axis measuring machine. Many software modules are now available to aid measurement an example is the direction vector of the measuring probe. The direction vector consists of a tilting and rotation angle [12] of the probe and with graphical capability the inspection or machining path can be animated which allows the operator to visually check the inspection path for inefficient moves and collisions. As will be mentioned later (section 1.7) Dimensional Measuring Interchange Specification (DMIS) is one standard CNC code generation language for CMM's in a neutral programming languages. In general the output of a typical CNC code generator software for a CMM is the machine code for the CMM with codes for probing path, probe change orientation station and direction and clearance positions for the probe.

1.3 Geometric and feature measurements

Generally, in manufacturing industries components often consist of geometric primitive elements, for example, lines, circles, and so on. In machining industries workpieces not only consist of the above mentioned elements but also of form features such as holes, slots, steps and pockets. To measure a geometric element a set of three dimensional measurement points is required from the elements surface. The values of these 3-D points will be fed into mathematical equations which develops them into an element or a feature. Conceptually features represent a higher level description of the part than primitive volumes that are traditionally used in CAD systems.

Each type of geometric element requires a specific minimum number of measurement points. Generally, the more complex the element, the higher is the minimum number of points, for example, the minimum number of points required for a line is 2 and 3 points for a circle. To increase the precision of a measurement it is suggested to take more than the minimum required number of points [13,14].

There exists a large number of industrial parts whose shapes do not have any primitive geometric form. They form compound surfaces which can be defined by the number of segments (patches) which are joined together with some specified continuity conditions. Many researchers have worked to identify and localise these surfaces with the use of CMM. They either developed object scanning methods [15,16,17] or developed CAD driven inspection systems [3] which rely on the existence of a CAD data base.

Corrigal and Bell [11] worked on inspection planning process in which they introduced probe approach directions for the probe to have maximum access to each surfaces. Their methods required a Construction Solid Geometry (CSG) model of the object which is typically built from geometric primitive shapes, this method also requires a list of surfaces that need to be inspected.

Merat et al. [7] followed a feature based procedure. Their approach was to develop an intelligent inspection planning subsystem for a computer integrated manufacturing environment for mechanical part where the specific problem was to use form feature information to guide the inspection planning process. In their work an inspection planner takes the part model consisting of a specification of the part geometry as well as dimensioning and tolerancing information and produce an inspection plan, which gives detailed instructions on how to inspect a manufactured part to determine whether it is within tolerance.

Generally the most difficult operation in measuring a sculptured part is to identify the feature boundaries which can be caused by not knowing the location and the shape of the feature. If a fundamental and easier method can be developed to locate or to recognise the shape of a feature detailed boundary information of the feature is less crucial and tedious evaluation of the feature can be done easily by the measuring equipment. If prior knowledge of the feature shape exists then the evaluation of the extent of the boundary is not essential. With prismatic parts this is an easy operation, since if the feature is a plane, then so long as the points taken are within the plane the extended form of the plane can easily be developed. With sculptured parts this is not so easy, however, if the general part shape is known and the approximate feature centre can be identified a measurement search process can be constructed to determine the feature shape.

1.4 Automated measurement of sculptured surfaces

The development of automatic measurement of sculptured surfaces has generated a need for new flexible systems to deal with its problems and peculiarities. A number of attempts have already been made in the last decade to automate the inspection of parts and surfaces by many researchers, some of whom have used CAD systems while others exercised a combination of a CAD and a vision system.

Duffie et al. [18,19] presented a CAD directed inspection method to automatically inspect sculptured surfaces. Their defined method uses bicubic parametric surface patches. The bicubic parametric surface patch is the lowest order of parametric surface representation that can conveniently be used to describe nonplanar shapes. With patches of higher order than three a smaller number of patches may be needed to represent a whole shape. Not only the manipulation of these parameters becomes more difficult but also unwanted oscillations in surface shape can occur

more easily for composite surfaces when higher order polynomials are used.

The inspection process is initiated by the user selecting the patch or group of patches that require measurement so that the inspection planner can automatically determine the coordinates of the points to be measured. The points are spread uniformly over each patch in a grid-like formation dependent on the size and proportions of the patch. For each surface point specified by the system another two points (guidance points) are determined which lie equidistant and normal to the surface. The pairs of guidance points are used such that one point is outside the surface and the second point is inside the surface on the same normal vector to the surface patch. The probe tip of the CMM is moved in and out of the part by the use of guidance points on either side of a surface patch. Fig. 1.1 depicts this arrangement.

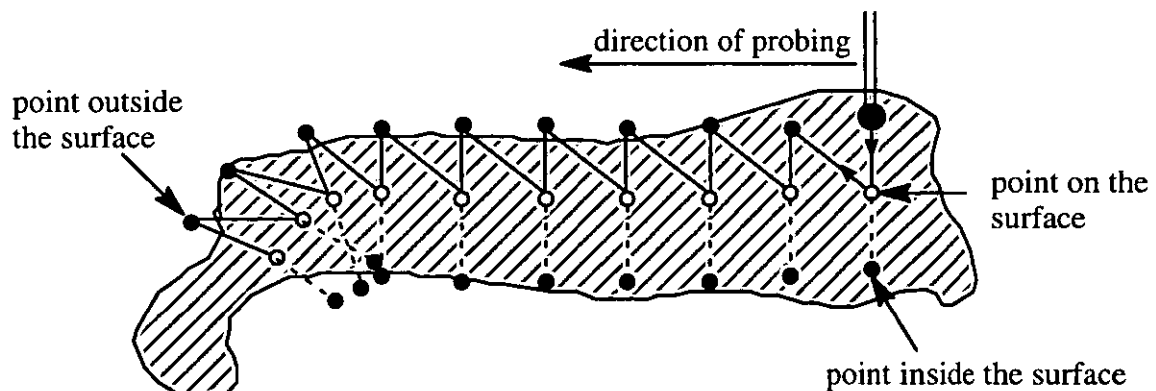


Fig. 1.1. Motion path for CMM probe.

During the measurement phase the probe traverses fast to the point in front of the surface and then slowly to the point behind so that it touches the surface somewhere between the two guidance points. The coordinates of the measured point will be fed into the inspection planner in order to determine the actual surface point. There is no argument that the coordinates could be corrected along the normal direction since the stylus ball radius is constant, this was based on the assumption that the calculated surface normal was correct which may not always be the case. The authors discussed the effects of surface normal errors on the measurement and conclude that they could be reduced in magnitude by using the smallest possible stylus ball and in addition more than one measurement might give a better estimation of the actual surface.

The CMM records the centre point of the undeflected stylus ball which in this case the inspection planner must be able to interpret and correct the uncompensated points in order to determine surface points. The approach proposed a simple but effective method for compensating the measured values and acknowledges the problems of surface normal errors. The implied use of a constant

value for probe deflection may not be valid as the magnitude of deflection varies according to the attack angle [20,21]. However, the inspection planner does not determine probe set-up, component set-up or collision-free safe rapid paths.

Van Den Berg [3] described the development of an automated machining cell to make small batches of precision turbine parts. The automated machining cell was integrated with a CMM to produce a flexible manufacturing system. To maximize productivity of the cell the time to measure and analyse a manufactured part needed to be less than the time required to manufacture the next part. In order to achieve such an automated cell further areas such as automatic material transfer, automatic inspection and automatic error analysis (this may include estimation of the cause of error and determination of a correction strategy) needed to be considered.

Inspection of the part was carried out using both the machining centre's touch trigger probe and the CMM to capture measurement data. A menu driven system allowed the user to interactively develop inspection programs, however as with the previous system of Duffie et al. only points could be measured. It is not clear whether there was any intelligent assistance in the determination of probing points, but the machining centre used a drilling cycle to measure, so each inspection point needed to be formulated as part of a drill cycle. The measured points are sent to the cell controller for interpretation by a user written programme which accesses the machine library of analysis functions. Measurement data from both the machining centre and CMM are analysed for error analysis.

The manufacturing analysis is a two step process. Firstly the observed errors should be matched against the possible sources of error in the manufacturing process model, which creates a model of how the errors observed in the measurements were caused. The second set-up involves the application of corrective strategies to the manufacturing process.

Two methods of error analysis are employed within the system; the first is tolerance analysis, which determines whether the measured point is out of tolerance and the second is manufacturing analysis, which determines the cause of the error and a correction strategy. The tolerance analysis facility is capable of checking for position, orientation and form errors by calculating the error vector of each point with respect to the surface and then by determining the transformation matrix necessary to fit the measured points to the defined surface. The position and orientation errors could be extracted from the net rigid body fitting transformation, from which the form errors could be extracted from the error vectors.

1.5 Vision directed inspection and recognition

In order to achieve a highly effective inspection system, the inspection process should be interfaced to a machine vision. Machine vision endows an inspection system with a sophisticated sensing mechanism to respond to its environment in an intelligent and flexible manner. Vision inspection can be defined as the process of extracting, characterizing, and interpreting information from images of a 3-D world.

The application of computer-based image analysis is an emerging technology. Many useful applications are possible with existing technology which include finding flaws, identifying parts, detecting surfaces, gauging, determining X, Y, and Z coordinates to locate parts in three dimensional space for robot guidance and many other application [22]. Use of machine vision in a manufacturing process not only can avoid the production of scrap but also improve quality of production, reduce set-up time, increase equipment utilization and bring many other benefits.

The vision directed inspection has been studied by a number of researchers [6,8,23,24,25,26,27, 28,29]. Generally the major issue in this research area is the development of representation or feature extraction of 3-D objects by fusing multi images of an object which are taken from different view points or from the same view point with different illumination.

The technique described by McMichael [23] represents an image intensity gradient in two derived maps of gradient magnitude and orientation. The initial research objective was to consider techniques that are insensitive to poor lighting since the lighting is a neglected area in industrial image processing and poor lighting is often taken to imply specular reflection, shadow, and low image contrast. In the proposed method several images of the object to be inspected taken from the same view point, but illuminated differently, are fused together to attenuate the effects of shadow and image contrast variation. The method appears to be faster and uses more of the information available from the gradient orientation map. The technique thresholds on gradient magnitude and deletes regions of high variation of gradient orientation, which allows the edge segments to be detected and can be shown graphically.

There is also too much information regarding edge regions (i.e., pixel locations). A method of information compression is required to identify parametric edge segments by their orientation, length and centre. The method of edge segment extraction using gradient magnitude and orientation mapping can be achieved by either finding the segment orientation directly from the orientation map or by determining the edge from the distribution of pixel locations. The former is perceived by the author to be useful for short edge regions and diffuse edges, while the latter gives highly accurate results with long straight edge regions. However, fusing the results of both

methods improves reliability. Extracting an accurate gradient field from an image is not easy. Such issues as orientation accuracy and bandwidth, aliasing, edge intensity bandwidth, signal to noise ratio and localisation need to be taken into account. The weaknesses of the system are a reliance on global thresholds, computation time, and, lack of the powerful software to detect complex edges. However, the system appears to be good at finding the edge structure of scenes with straight edges and sharp corners, furthermore it seeks to extract information about objects rather than images.

McDonald et al. [28] and Urquhart et al. [26] researched on methods concerned with stereo scene coding or active animated stereo vision. In their work a set of hardware and software tools are developed around the Active Stereo Probe (ASP) which uses structured pattern projection. Scene objects are illuminated by patterns projected by the ASP Active Illumination Projection System (AIPS). Images of patterns, disrupted by the scene, are then captured using the ASP stereo camera head and analysed using a technique called Stereo Scene Coding (SSC) to recover 3-D information.

The ASP head consists of two cameras independently actuated. The AIPS which allows projection of patterns onto the viewed scene, is positioned below the sensor head such that it projects onto an inclined mirror situated between the cameras. The mirror is also actuated in elevation and azimuth allowing the reflected structured illumination pattern to be steered so that it is maintained within the camera's fields of view. The performance of the combined AIPS/ASP system is critically dependent on the system's ability to project and image patterns. The overall model can predict captured image characteristics relative to the projected pattern, given object reflection characteristics and details of ambient light conditions.

In SSC images the scene to be analysed is captured by the left and right cameras during the projection of each pattern. Analysis of the distortions of each pattern are used to make 3-D measurements about scene points.

The complexity grade of the system is high and is believed to work once the system is set-up and the cameras are calibrated. The quality of measurements made using stereo scene coding is directly dependent on the quality of the input pattern images. The field of the camera's view is a controlling factor, however, the given accuracy of the order of ± 0.5 mm RMS in height for 3 m range is good. Although, the camera's focal lengths are 500 mm or more, it is not stated what would be the top limit of the object size before the accuracy will deteriorate. The quality of measurements using SSC and performance of algorithm utilising the combined AISP/ASP system is directly dependent on the quality of image patterns, for example high quality input images (full

frequency content, high contrast ratio and high signal to noise ratios) result in high measurement accuracy. Both the projection and imaging process are subject to corruption by noise and degradation through loss contrast ratios and optical blurring.

Clarke et al. [25] discussed another 3–D measurement system using multiple camera views that are obtained from different viewpoints. The work describes the basic method of photogrammetry [30,31,32] and discusses the potential for automated high accuracy measurement in an industrial context. The method involves identifying homologous targets or patterns (i.e., reflective marks) on images of an object which have been obtained from different viewpoints. These image measurements are then used to capture, the 3–D coordinates of the locations of the targets or patterns on the object being measured. Each point on the object is related to a set of measurements made in the image space by a set of colinear equations through the theory of a central perspective projection. Each colinearity equation contains unknowns such as: the location and orientation of the camera at exposure time; the X,Y,Z coordinates of the object point; and its corresponding image coordinates in 2–D X,Y image space.

Since real imaging systems only approximate to the central perspective projection, equations must also be included to model departures such as those caused by the real lens system, and any geometric distortion of the image due to the camera sensor characteristics.

There are a number of steps before measurement can take place such as; placement of target points, setting cameras and lighting, collection of images from each view–point and estimation of camera locations and orientations (position of the camera relative to the object). Further steps are identification and labelling of the targets, calculation of correspondences between targets from all viewpoints, initialisation of focal length, principal point position, lens distortion parameters, least squares adjustment with initial estimated parameters to check that the program converges and that the change in the coordinates is within some pre–determined limits. If this occurs then the programme is terminated otherwise it is required to check for errors (i.e., incorrectly located targets or matched targets) and repeat the adjustment process with new adjusted values. The resulting 3–D coordinates of the target points after determination are transferred into a CAD system and used to derive a 3–D B–spline surface.

The accuracy of the method is dependent on several factors including; the number of observations, the type of target or surface feature, camera stability, the strength of the measurement network and operator experience. The system appears to be flexible, there is no limit to the size of the measured object, and the measuring system is portable. The system has some disadvantages such as the high level of computation involved, the significant setting up procedure required for

each measurement case, a high degree of expert knowledge, and the lack of techniques for fast or dynamic automated measurement.

The 3-D object recognition from multiple views can be employed to build structured models of bodies in a scene by identifying classes of simple objects (e.g., wedges, bricks, etc.) and their interrelationships (e.g., in front of, next to, supported by, etc.) in each view to build a prototype model. Martin and Aggarwal [33] used multiple views to build a volumetric model of 3-D objects, although their algorithm allowed learning and refinement it required explicit knowledge about each viewpoint during learning and recognition.

Seibert and Waxman [27] worked on the automated recognition and representation of 3-D objects from exploratory view sequences of unoccluded or nonpolyhedral objects. The work concentrated on 3-D appearance modeling and succeeded under favourable viewing conditions by using simplified processes (edge detection algorithms and view transition matrices) to segment objects from the scene and drive the spatial arrangement of the object features. The test objects were model aircraft in flight. In building the models, processed frames, of a video sequence are clustered into view categories called aspects which represent characteristic views of an object invariant to its apparent position, size, 2-D orientation, and limited foreshortening deformation. The cameras were repositioned coarsely during intervals of the transitions between the aspects which were used to build a representation of the 3-D object in the aspect network representation of the object. At each camera repositioning the object recognition hypotheses were reset to allow unbiased competition among the objects during the new view sequence. The subsequent view sequence is compared with the previously built object representations. If a sufficiently close match is found, then the representation of that object is refined; otherwise, a representation for new object is constructed.

Liu and Tsai [34] proposed a recognition system for 3-D curved objects using multiple 2-D camera views. They used two cameras, one placed at the top of the object with the other placed at a lateral position. The object was placed on a rotating table for translation and rotation in the recognition process. The recognition process used a top view of the object, and then normalized the top view shape by translating the shape centroid beneath the top camera and rotating the principal axis of the shape to align with the X-axis of the image plane. Another 2-D object image was taken again and matched against the object models/reference models (organised in the form of a decision tree). If the top view shape was comparable with any object models the recognition was completed, otherwise the lateral camera would take a side view image of the object from a fixed direction with respect to the centroid and the principal axis of the top view shape. The side view object

shape was then matched against side view shape of the object models for further discriminations. This method uses features extracted from 2-D object shapes directly as the object model, this accomplishes 3-D object recognition by matching sequentially input 2-D silhouette shape features against those of model shapes which have been taken from the set of fixed camera views.

The reason for this recognition of 3-D objects by 2-D silhouette shape is based on simple shape features, but the learning process for the decision tree set up is not yet automated and needs to be specifically arranged. However, the computation is not seen to be complicated and a high recognition rate for most industrial parts is envisaged. Difficulties in recognizing a part could occur due to an improper threshold selection for feature comparison, resulting in the assignment of input objects to incorrect tree nodes. Another source of error was the camera sensitivity to light changes in the environment, resulting in undesirable changes of shape boundaries and object features. It was suggested that the above problems could be improved by the use of autoregressive models to represent object boundaries, making features less sensitive to boundary distortions and the adoption of sophisticated pattern classification algorithms to discriminate the object shapes more radically. The proposed method may be employed for sculptured surface recognition, however, it is not easy to install a rotary table on the CMM and measurement errors can occur because of the rotary table. Also, if the object has a rotationally symmetric base, it is not easy to recognize the object.

Al-Kindi et al. [6] have worked on automatic 2-D component inspection with assistance of machine vision for engineering components. Their extensive work is based on the use of edge detection with new developed algorithms for application when contour tracing methods fail to detect localized edges in a complex scene. They restated that the use of 2-D object inspection using computer vision can be approached in 3 ways: (1) an interactive approach where the user selects and shows the required feature to be examined, (2) a teaching approach which assumes that the system has previous knowledge of features to be inspected, (3) a full automated approach where the system has no prior information about the object or its position.

In edge detection operations there are three types of error which sometimes cause the operation to fail. These are: (1) missing valid edge points, (2) failure to detect localized edge points and (3) failure to separate noise. The Edge Detection Algorithms (EDA's) are classified in two groups, namely, differential type operators and model fitting methods. A new algorithm for edge finding was proposed by the authors which they believed to be beneficial for most applications where contour tracing fails to detect localized edges in a complex scene. It is not always obvious which of the EDA's will be the most effective in a particular application unless tests for suitability

are made for use in component inspection. 2-D inspection could be divided into inspection of the features of component silhouette and inspection of the internal features, typically the boundary of a hole. The algorithm designed by the authors traces and identifies the silhouette of a component which is created by the boundary pixels. The algorithm uses two substituted arrays for the 2-D binary image matrix. One of the arrays contains the row boundary data while the other has the column numbers of the boundary pixels stored in the image matrix. A further algorithm has been designed to distinguish between an internal and external boundary contour. The resolution of the identified silhouette by recognition of the edge is directly affected by the image processing hardware configuration.

1.6 Integration of vision and CMM

Integration between machine vision and automated systems such as a CMM often relies on intelligence provided by designers. Integration of such did not gain that much attention from researchers in the past, however recently with needs of flexible manufacturing and automation systems there has been an increase in vision and CMM integration [35].

Cho et al. [36] researched on CMM and vision and CAD database integration. The research objective of their work was the development of a flexible 3-D inspection system for sculpture surfaces. They used a 2-D machine vision with a CNC CMM. The machine vision was mounted on the column of the CMM. Two images, which were needed for the 3-D shape construction, were taken at two positions along the X-direction of the CMM while the Y and Z-coordinates of the camera remain unchanged. The method of finding the Z coordinate of a point was explained through the use of a stereo method [30,31]. It is necessary to calculate the pixel coordinate representation into CMM coordinates which is made by calibrating the vision system to determine the camera mounting error, and a transformation matrix used to convert the pixel representation to CMM coordinates. This method could generate 3-D coordinates of a required point on the surface without prior knowledge about it. For an accurate measurement or surface determination the CMM will use these approximations to assess and evaluate the surface. The system appeared to have some difficulties to detect features and surfaces at the side of the object or on the planes which are not directly under the cameras.

As mentioned previously Liu and Tsai [34] used a similar integration by placing the two cameras, one above the CMM table and one at a lateral position to the table. However, their work on surface and shape recognition is different to that of Cho et al. since the method uses multiple 2-D views and in a systematic way they compared and recognised the object by finding 2-D shapes when matched within the set of the reference models. Less computational work is involved by this

method, however more errors could be introduced since a rotary table is used.

1.7 CMM and CAD integration

CMM's are widely used tools for performing fast accurate measurements of industrial components. In order to achieve a high degree of flexibility and higher productivity in an automated inspection environment an integration of a CNC CMM with a CAD system has a major role. The primary objectives of such integration will be the development of techniques for automatically generating inspection procedures from CAD data (off-line programming) and access to part design (CAD) databases for quality assurance.

The concept of CMM and CAD integration has been around for less than a decade, its major advantage is the reduction in inspection planning. Harris et al. [37] explained a type of integration which allowed nominal and measured data to be exchanged between CAD and CMM systems for graphical interactive programming of the CMM. The data exchange between these two systems needed to be of a bidirectional data exchange standard such as DMIS [38].

Cowling and Mullineux [39] explained the type of information required for such integration. They pointed out that the ability to transfer data between CAD and CMM systems requires intelligence of the human user by specifying the critical features and the inspection strategy for measuring them. In their study the CMM was simulated in software and the model of the component to be inspected existed within the CAD system called "origin CAD model". The CMM held a second model, the "physical component". Differences between these models represent errors in manufacture.

By returning coordinates of the points between the physical model on the CMM and the probe inspection path, a second model can be created within the CAD model. By interrogating the CAD data from the third model geometric entities or features could be passed to the CAD system to decide where faults were.

Their suggested solution strategies for CAD and CMM integration are concentrated on areas such as data fitting, since the component may not comprise exact lines and arcs. Further work was concerned with determination of the end points of entities since they are in different positions to the corresponding end points in the original CAD model and finally a recursive subdivision scheme for inferring good representation of the entities of the physical component. Often the required degree of accuracy could not be achieved if a small number of data points was used.

The issue of CAD and CMM interfacing was further investigated by Schwartz and Karadayi [40]. They designed and developed an intermediate system in the form of a translator buffer named

Expert DIMS Graphical Editor Simulator (EDGES). They focused on problems that would be expected once this integration took place, such as reduction in speed of inspection, robustness of DMIS, and lack of operator knowledge. They considered operator difficulties in this area to be considerable. The need for extensive system training of CMM personnel is significant since the machine and system integration are complex.

1.8 Research objectives and proposed approach

There are many problems that must be addressed in the 3-D automated measurement of high technology sculptured surfaces products such as, the type of sensing system to be used, the cost effectiveness of the system, the degree of accuracy and the speed of measurement. If using a non-contact sensing method such as a vision system problems such as arranging a suitable lighting system and developing image analysis methods for different applications have to be resolved. It has been mentioned previously that vision systems are not flexible enough to be integrated cheaply and easily into an automated inspection environment for sculptured surfaces, because they do not have the required capabilities for high accuracy. Therefore high accuracy applications are limited to the use of a touch probing approach. The automatic generation of NC code for this inspection approach for the sculptured products presents an additional problem since it is a time consuming business. One approach to overcome this problem is to use a cheap or inexpensive 2-D vision system which would give a first approximation to the location of the object features and then use this information as an input to generate the NC drive code for a touch probe CMM. The objective of this research is to develop an automated inspection system for the measurement of sculptured surfaces using this approach. A number of secondary objectives were identified which are;

1. Integration of the various elements.
2. A method for recognition and identification of the product features.
3. A method for NC drive code generation with a measurement optimisation procedure to achieve accuracy and speed.
4. A suitable method of displaying the information graphically.

In order to develop the system a golf ball has been selected as the sample product since it contains 3 dimensional curved surfaces and features together with repeated surface patterns. The schematic diagram of the proposed inspection system is shown in fig. 1.2.

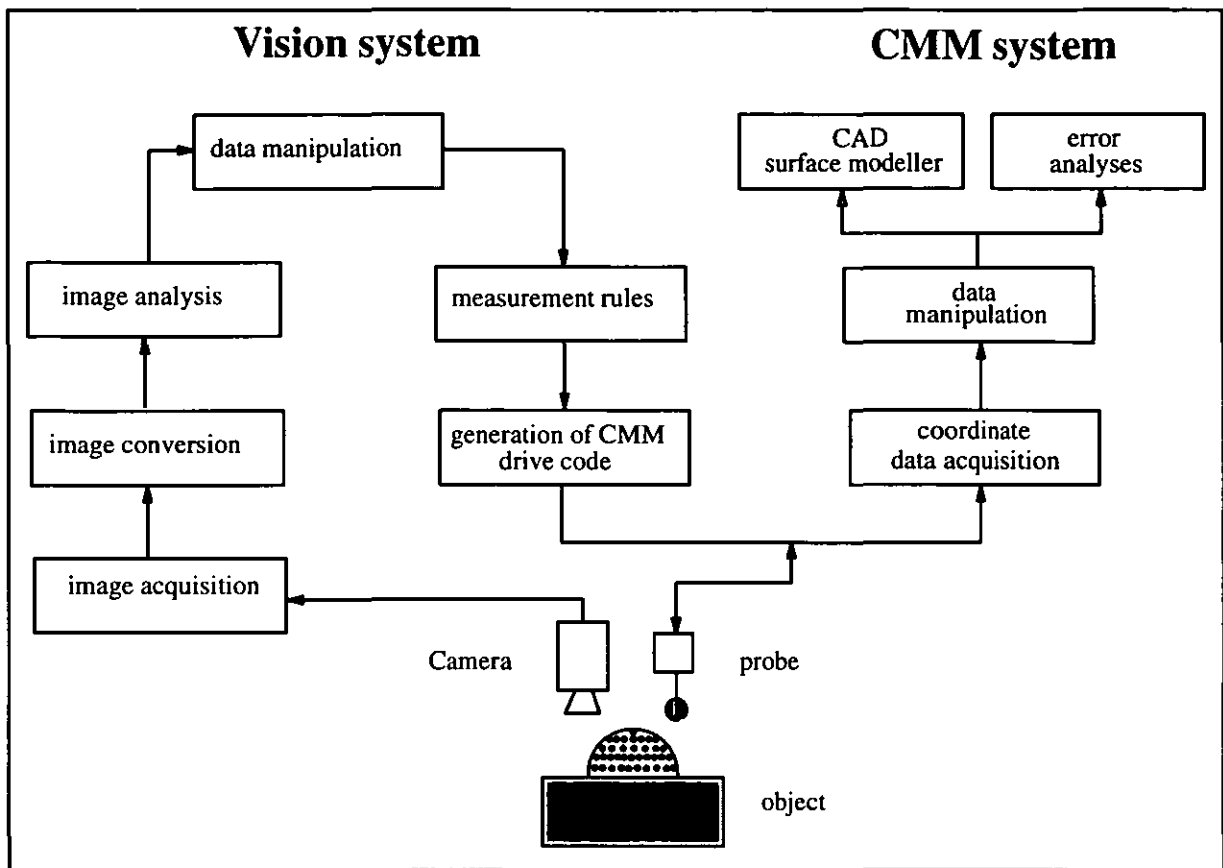


Fig. 1.2. An Automated Measurement of Golf Balls.

To achieve the above mentioned objectives the following work has been carried out in this research:

1. Development of feature enhancement: Several feature enhancement methods have been generated by using vision system facilities and use of manual marking. The simplest method used was by placing a mark or dot onto centre of each feature.
2. Development of a new feature identification procedure: The feature identification procedure is developed by employing the vision system, which is arranged to capture five images of the object for superimposition. The system is named Multi-Image Superimposed Technique (MIST) and a binary image processing technique is used to determine the 3-D location of the features.
3. Development of a CNC code generation method with auto-probe selection strategy: A 3-D CNC code generation method for the CMM is proposed to automatically measure the identified features. The method uses vision system data to automatically select a suitable tip orientation for optimal evaluation of the relevant feature.
4. Graphical CAD model representation: The inspected features are represented on a CAD system

to visualise the results and for CAD and CMM data comparison.

5. Error model generation: Two applications of optimisation methods are proposed to model pattern errors. The model handles errors existing between the nominal and actual data. The first method uses a random search method technique to propose an optimum position for features patterns, the second method uses a least square best fit strategy.

6. Experiments and results analysis: Several different types of golf balls and hobs were used and their features identified and inspected automatically based on the proposed method of the vision integrated CMM. Finally, the measured model is graphically represented and its error model generated and analysed.

CHAPTER 2

DIGITAL IMAGE PROCESSING SYSTEM

2.0 Introduction

Digital image processing is a term given to the process of analysing electronic images which are taken by Charged Couple Device (CCD) sensors. The procedure is similar to normal photography but instead of using a negative, the image is converted from an optical picture by use of a electronic photo sensitive elements to a digital image. A digital image consists of a matrix of pixels (a pixel is the smallest picture element i.e., photosite) which can be represented by 8 bits (a byte) or higher order of gray level. The 8 bit gray level generates 256 shades of intensity which gives an image of various shades, unlike people, who can interpret and characterise as many as 4000 colours/shades. Machine vision systems available today generally only interpret colours into the shades of gray defined by the specific system [22]. They generally cannot distinguish between object colours and can become confused if two colours have the same gray value.

The term computer vision (or machine vision) is a general name given to a system which includes a digital image processing unit. The applications of computer vision are increasing at a fast rate, and the use of these machines can be seen in industrial inspection, surface measurement, manipulator guidance, vehicle guidance, medical applications, civilian applications and the food industry. One of the most difficult tasks facing image processing and computer vision is the development of systems that emulate the visual cognitive ability of high level biological visual systems.

2.1 Digital image representation

Conceptually, a digital image is an image $f(x,y)$ that has been discretized in both spatial coordinates and brightness. The use of monochrome images [31] refers to a 2-D light intensity function of $f(x,y)$ s, where x and y denote spatial coordinates and the value of f (function) at any point (x,y) is proportional to the brightness (intensity or gray level) of the image at that point. Fig. 2.1 illustrates the common axis convention used for image representation.

A digital image representation can be considered as a matrix where row and column indices identify a point in the image and the corresponding matrix element value identifies the gray level at that point. A typical size 512×512 array with 256 gray levels is a common vision element which

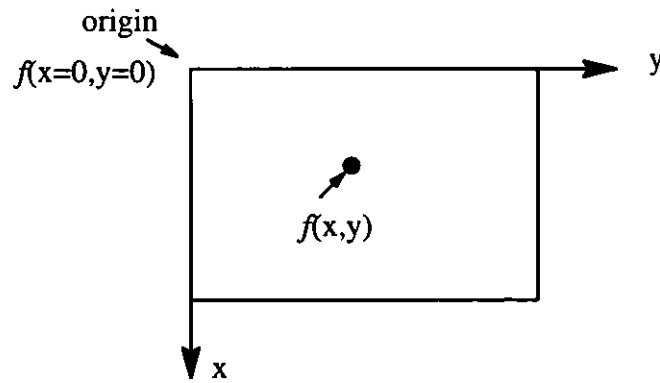


Fig. 2.1. Axis and coordinate convention for digital image representation.

can be seen in the majority of current machine vision applications.

2.2 Fundamental steps in image processing

The fundamental steps which are required to perform an image processing assignment are shown in fig. 2.2. From the figure it can be seen that there are six principal areas in image processing: sensing, pre-processing, segmentation, description, recognition, and interpretation [41].

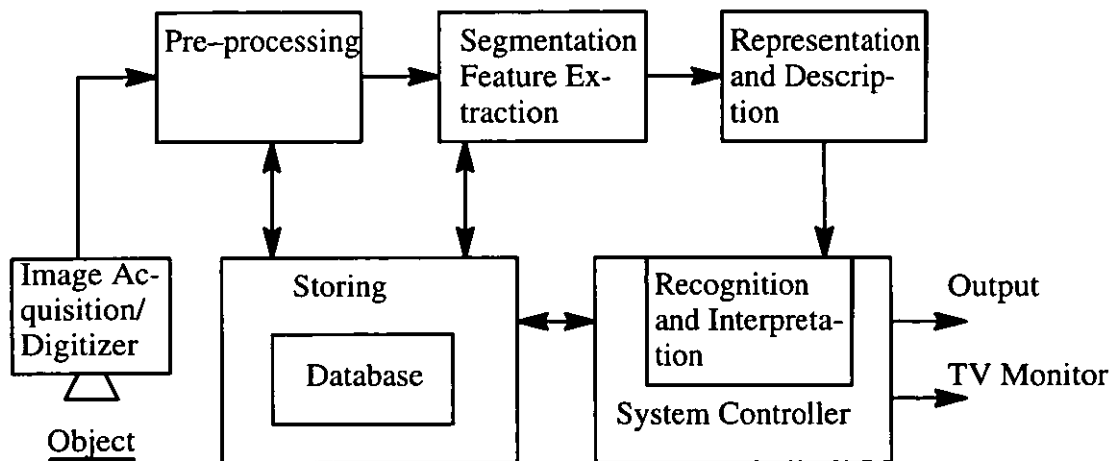


Fig. 2.2. Block diagram of fundamental steps in digital image processing.

Apart from the computer hardware and software requirements necessary to operate the image processing unit, the first step in image processing is image acquisition. This requires an imaging sensor and the capability to digitize the signal produced by the sensor such as a CCD camera. The next step is pre-processing the image which deals with techniques for enhancing contrast, removing noise, and isolating regions. Segmentation then takes place which is the process that partitions an image into objects of interest. This is an important role in image processing, since erratic or

weak segmentation algorithms almost always result in eventual failure. A robust or rugged segmentation procedure is an important factor in the successful solution of imaging problems. The output of the segmentation stage is usually raw pixel data which needs converting into a suitable form for computer processing. However, the image segmentation either comprises all the points in the region or constitutes the boundary of a region.

After segmentation, representation and feature extraction takes place. This section deals with the computation of features (e.g. size and shape) suitable for differentiating one type of object from another. The data can represent a boundary when the focus is on external shape characteristics, such as corners, straight edges, or concave to convex curvatures. It can also represent a complex region which is more appropriate for representing internal properties, such as texture and structure or skeletal shape.

The main task of representation is to transform the raw data into a suitable form for subsequent processing. In order to achieve this a complementary method should also be specified for describing the data so that the features of interest can be selected. Extracting features from a class of objects in an image needs descriptors which are called feature selectors. These feature selectors can also help to differentiate one part of the feature from another. The final processing stage involves recognition and interpretation, the former is the process that identifies and assigns a label to an object based on the information provided by its descriptors while the latter assigns meaning to a collection of recognized objects.

The knowledge is stored in a database which may interact with processing modules individually. The system can operate with simple or complex knowledge which would be fed back to the relevant module in order to enable the module to process the task better. For example if the process is in the segmentation or representation module the problem can be resolved for a better bounding representation or a region representation. The feature knowledge can refer to regions of an image where the interested information is known to be located, therefore the search can be easily conducted in seeking information, whereas in images with unknown and interrelated regions information is not so easily detectable.

It is important to note that not all image processing applications require the complexity of interactions shown in fig. 2.2.

2.3 Vision system and its elements

In image sensing a sensor converts visual information into electrical signals (voltage signals). A CCD sensor is composed of discrete silicon imaging elements, called photosites, that have a volt-

age output proportional to the intensity of the incident light. The output voltages are amplified and input to an Analog/Digital Converter (A/DC) in which the system characterizes the scene into a grid of digital numbers. This process is called digitizing, or sometimes image sampling/quantizing. The amplitude digitization is called intensity or gray level quantization. This is applicable to monochrome images and reflects the fact that these images vary from black to white in shades of gray. For a more detailed description of these processes references [22,31,41] provide adequate explanations.

The sections of a simple vision system can be listed as; acquisition, storage, processing, communication, and display. The image acquisition section is usually a CCD sensor coupled with A/DC as mentioned earlier. The digital storage for image processing can be divided into three sections; temporary (short term storage for use during processing), on-line storage (for relatively fast recall), and archival storage for any time access. Storage is measured in bytes (8 bit), for an eight bit image of size 512×512 pixels about $1/4$ of a million bytes of storage are required. In processing generally the image will go through various operations including, image enhancement, coding, and analysis. These processes can be handled in hardware or in software and the processes are usually expressed in algorithmic form, the hardware implementation is often faster than software execution but with less flexibility.

Communication in digital image processing performs local or network communication between image processing systems and remote communication from one point to another. To be able to implement such a connection hardware and software requirements of the standard communication protocol needed to be considered. Finally, the display section shows the digital images, common examples are monochrome and colour television monitors which are used in modern image processing systems. The display unit is fed by the output from the image display module hardware which is situated in the host computer of the image system. However, there are other sorts of display such as slides, photographs, and transparencies.

2.4 Machine vision fundamentals

There are a number of aspects to be considered prior to processing of digital images, examples of these are illumination, reflection effects, uniform image sampling, gray level quantization, relationships between pixels (i.e., connectivity or distance measurement) and imaging geometry.

Illumination has a direct effect on the image processing and suitable images for processing are those with a high contrast images, low specular reflections, low or no shadows and no extraneous details. This could be a reason why arbitrary lighting of the environment is often not acceptable. A good lighting system illuminates a scene so that the complexity of the resulting image is mini-

mised, while the information required for object detection and extraction is enhanced. The lighting system is usually dictated by the application, specifically, the properties of the object itself and the task, such as inspection, flaw checking, counting objects, character recognition or robot control.

As mentioned earlier image sampling or digitization and quantization are required for computer image processing. The most important point is that for consistent and uniform output sampling and quantization of an image. A suitable mathematical form should be used since a digital image is a 2-D function whose spatial coordinates of the pixels and amplitude value of each pair is now in the form of integers rather than analog. Apart from the above mentioned functions it is also required to specify the number of discrete gray levels to display the image. This point is worth considering before purchasing image processing software since the degree of discernible detail (resolution) of an image depends on above mentioned parameters. This is one reason for the number of image processing softwares which work on 256 gray levels and a resolution of 512×512 (square type).

There are some basic rules which need to be considered about pixels in a digital image such as neighbours, and connectivity which can be used for detailed image processing. Specific arrangements can be made to use these pixel relationships to detect edges, feature measurements, and labelling of connected components which would establish boundaries of objects and components of regions in an image. Further processes are used for extra pixel manipulation such as arithmetic and logic operations, the former works on multi-valued pixels (i.e., grey level) and the latter applies only to binary images. These operations are used in most branches of image processing in order to analyse shape, feature detection, filtering, and for masking purposes. Arithmetic operations can be grouped as addition, subtraction, multiplication, and division of pixels and the principal logic operations are AND, OR, and COMPLEMENT which are functionally complete and they can be combined to form any other logic operation.

Another set of operations belong to image geometry which mainly involves transformations used in imaging. These operations can be used to deal with problems involving image rotation, scaling, translation, perspective transformations, camera position (which deals with two coordinate systems, the camera and the world coordinate systems) and camera calibration [31].

2.5 Review on vision systems for measurements of objects

Machine vision has developed extensively since its uncertain beginnings in the 1980s. At that time systems were costly and early machine vision systems worked well in the laboratory but were unable to cope with the vibration and dust of the production environment. After overcoming the difficulties in transferring benchtop technologies to real world working environments machine vision systems are now being applied increasingly to applications in the following industries: automation, inspection, measurements, defence, electronic, food, health care, medical (pathology and life sciences), pharmaceutical, security and, to many other fields of technology.

The biggest end users of industrial vision systems are the electronics sectors, with the automotive industry in the second place. In electronics, production values are high and the implications of product failure can be severe, thus a need for 100 per cent quality inspection is essential. A vision system will not only identify faulty components but the system can also produce immediate statistical information on the type of rejects (e.g., measured dimensions). The investment in machine vision can generally only be cost effective for high volume production. One main location when using machine vision systems in the production lines is at the exit, where products can be checked for inadequate marking or wrong packing [42].

Currently the implementation of neural networks in vision system applications for developing expert systems is taking place. They are predicted to be common in system controllers and processors by the year 2000. This is why the Department of Trade and Industry (DTI) is investing 3.75 million pounds over the next 3 years to promote industrial awareness in the use of neural network [43]. Examples of these implementations are in signature verification, identification, food processing, and vision inspection where grading of fruit using a vision system and neural network uses surface defect classification techniques.

In measurement applications machine visions are applied at various degrees in detailed and complex measurement applications [44,45] where relatively high orders of accuracy are not required (of the order of one millimetre). Typical application areas are measurement of chocolate bars; grading of vegetables for size and even in automated butchery [46] where the locations and size of each beef forequarter is determined prior to cutting. The inspection industry is focusing [47] on how the vision information can be modelled and used in other industries. This arguably would imply the use of a computer network based on an emerging communication standards. This will resolve problems such as how the data can be transferred between vision machines and other computer systems.

Svetkoff et al. [48] and Mahon [8] employed vision system in the electronics industry to inspect

component boards and solder pastes on surface mount printed circuit boards, where 100 per cent inspection is required. Svetkoff et al. utilised a combination of gray scales and a 3-D sensing system to check minimum solder paste content and alignment of the paste to nominal pad locations. The examples given indicate that when the contrast is low, inspection will generally require to implement high speed 3-D information which could be based on a triangulation method. Mahon considered the volume of paste, mean paste height, and individual pad measurement vectors. The printed circuit boards were viewed under the camera and the board alignment was done by placement of the fiducial marks on the board at different locations. The detection of these marks was made by the vision system and the recognition procedure took place by comparing the component marks in a CAD database system. From the results the type of board and the locations for the inspection of the pastes could be determined. 2-D and 3-D algorithms were used to calculate the locations of pads in X and Y directions, the area and centroids of each pad were individually measured. From knowing the location of each pad a grey level threshold for the area could be set using the grey scale histograms of the paste and background images which could lead to an area measurement. To calculate the height of the blob a structured light technique similar to Svetkoff et al. was used. The inspection system seems fast and effective although the averaging method which was designed to give a higher degree of accuracy was questionable since blobs are not square in practice and they might not be spread consistently in their positions as assumed in the article. The system also experienced some difficulties to process light colour boards.

Blake [49] used a vision system in conjunction with two separate intersecting arrays of light from different projectors. This arrangement was used to digitise awkward 3-D shapes. Each of the projectors transmits a set of fringes at right angles to each other. The camera picks up the images of the two projections separately, and the grid intersection points are then determined by the use of projective geometry.

At Georgia Institute of Technology various researchers have employed machine vision to do intelligent tasks. Brown [50] used a vision system to help mobile robots home in on targets without following predetermined guide paths, by using prior knowledge of the environment. This robot guidance system used a video camera with a series of algorithms for image processing. The overall process followed a sequence which would find a potential workstation location, compare its image with a stored model, guide the robot to approach the target, and then slow it down for docking.

Pastorius [51] used a machine vision for surface quality inspection of objects up to 8 (feet) in length. The system could analyse magnified surface waves of the order of magnitude of 50 mi-

crons. The computer system provided a number of analysis algorithms for quantifying the gray scale waviness seen in the images. Two panel masters were selected for calibration and assigned values of "0" and "100", then test plaques (i.e., plastic, metal, or composite materials) were tested and rated in relation to these masters.

As the use of machine vision in industries is increasing improvement of these non-contact systems have been faster than the demand. Work has been done on making a smart vision camera [52] which consists of a computer that does some image analysis before the data leaves the camera. However, what the manufactures have been really waiting for, is higher resolution solid-state CCD cameras with resolution above 1000×1000 and their price is currently too high for many users.

2.6 The vision system used for this work

A measuring system has been developed which is primarily based on a CMM, a touch trigger probe, and a vision system. The vision system used for this work consists of a 2-D CCD sensor Matrox MVP-AT, and an illumination system equipped with a filtering system.

2.6.1 The Matrox vision system

The Matrox vision system includes a vision board, a CCD camera with a 25 mm lens and a Hitachi mono visual display unit. The vision system board operates in an IBM-PC environment run by the Matrox software. The board requires two adjacent 16 bit AT slots for installation and occupies 64 Kbytes of memory location and thirty two 8 bits I/O locations in the host computer address space. The system software consists of:

1. Control packages to control the CMM (will be discussed in Chapter 3).
2. Imager-AT vision system.
3. PC-IMAGE vision software for vision analysis.
4. A developed programme named MARZ for vision analysis.
5. A developed programme named BALLINSP for golf ball inspection.

The software Imager-AT [53] is a software library which contains a set of primitive imaging buffer arrangement, graphics and I/O commands for image processing. The software has libraries of routines which can be used off line together with any other necessary programmes written in the "C" language.

The original image buffer provided by the software consists of a 1024×1024 image frame buffer with each pixel being 8 bits to represent intensity levels. The system program divides this frame

buffer into four 512×512 image frame buffers as shown in fig. 2.4.

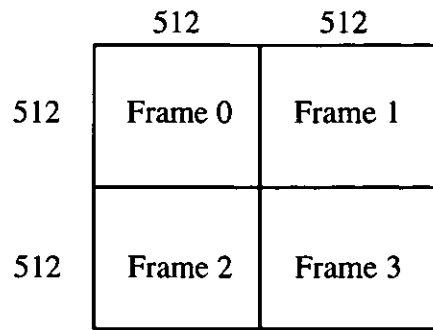


Fig. 2.4. Four 512×512 (8 bit) image frame buffer used by the vision system.

Each of these frame buffers can be used to store an image from the camera, it can also be used to act as an intermediate buffer during image processing operations to store temporary results. These frame buffers are labelled as frame 0, 1, 2, and 3, all which can be treated identically but also independently as frames ready for image storage. For example, to erode a binary image in frame 0, the frame will be assigned as the source while any of the four frames may be chosen as the destination. However, if the same frame is used as both source and destination, the original image will be overwritten by the new image. The MARZ program uses all four frames with frame 0 assigned for the original image of object (gray level image). The threshold image will be placed in frame 1, the processed image of the frame 1 will be put in frame 2, and finally frame 3 is kept for further possible processing such as eroding etc.

The PC-IMAGE software is a vision analysis package, possessing various capabilities such as filtering of unnecessary information, conversion of grey level images to binary level images, mathematical processing functions, etc. Its capability in this instance was utilised to determine golf ball dimple coordinate locations on the screen in pixel units. The golf ball image is viewed on the screen from which its centre and diameter were determined by reading the position of the cursor on the extreme edges of the golf ball image and the centre is determined from these readings. This visual process is subject to errors due to operator dependability although these errors are in the region of 1 to 2 pixels (1 pixel approximately equals to 0.2 millimetre when the ball is viewed from a height of 200 mm above its centre). The PC-IMAGE data is used for calibration to convert the pixel values to SI units. The data derived by the vision system needs to be referenced to a datum point and it was decided to locate the datum point at the centre of the ball because of the ease of location. A customised programme (MARZ) was developed to handle data generation from the vision system. This programme processes dimple visual information to give a series of X, Y, and Z coordinates for each dimple.

The data containing the coordinate positions of dimples with reference to the golf ball centre is output to a file for use on the CMM. In order to accurately measure the dimples on the CMM, a customised program named BALLINSP was developed. This software is used in collaboration with the CMM initialise software MM4/DCC-315, the two combined programs examine the coordinate location of each dimple, select a suitable tip orientation and then complete the inspection procedure.

2.6.2 Illumination and filtering system

Illumination of a scene is an important factor in image processing since a badly illuminated object often requires complex vision processing algorithms and techniques to provide high contrast and minimise reflections and shadows whereas a suitable illuminated object would require fewer processing algorithms to generate a similar result [54]. To use an illumination system for image processing several general principles need to be considered [1], the most important of them being; the output light level from the lamps, the spectral responses of the various optical components (e.g. lenses, filters, etc.), the reflectivity of the object being examined as a function of wavelength (i.e., its colour) and its smoothness, the spectral response of the image sensor, the performance of the camera, the spatial distribution of the light (i.e., uniformity), the polarisation of the light, the magnification of the optical system and the resolution of the digital images which are to be used. It should be noted that in image processing it is often cheaper to improve the lighting system than the image processing.

For high accuracy measurement the effect of the type of illumination on edge definition must be considered. The arrangement of the illumination system can cause the illumination to be partially coherent which can cause the measured edge position not to be detected.

The basic types of lighting devices may be grouped into the followings:

- i) Diffuse surface devices (typically fluorescent lamps and light tubes).
- ii) Condenser projectors (transforms an expanding light source into a condensing light source).
- iii) Flood or spot projectors (used to illuminate large surface areas).
- v) Collimators (used to provide a parallel beam of light on the subject).
- vi) Imagers (such as slide projectors and optical enlargers).

The lighting system which was required for this instance should have the capability to generate uniform contrast for the features on the golf ball surface and should illuminate the object in order to provide uniform, shadow free, and omni directional illumination. The difficulties experienced

were generated by the reflection and shadows from the ball surface and features since the object was not flat and had a shiny and reflective surface which made it impossible to use a standard lighting system. In some cases methods could be used to diffuse the object surface but the inspection accuracy may be affected. After considering many illumination sources a suitable lighting system was found to enhance the quality of the image in order to improve the derivation of the object dimensions. Details of these tests and arrangements are explained in chapter four.

The object of interest in this project is a golf ball with a reflecting surface finish, it was necessary to reduce reflection to a minimum in order to obtain a consistent results. A diffused illumination device in the form of a neon ring light proved to be suitable and in order to filter the direct light and generate a regular illumination from apex to equator a white paper filter was placed around the ball. Fig. 2.3 shows this filter arrangement.



Fig. 2.3. Filter arrangement.

CHAPTER 3

COORDINATE MEASURING MACHINE (CMM)

3.0 Introduction

CMMs are multi-axis devices with two to six axes of movement, each of which provides an output of position or displacement. These machines are available in both manual and automatic (computer controlled) models and are available in a wide range of sizes to provide for a variety of applications. They were designed to record the position of a probe as it moved along its coordinate axes, and also to probe points in 3-D space and give the position of the touched point or the centre of the probe point to micron accuracy. Softwares associated with CMMs enable them to alter the situation for different measurements rather than altering equipment mechanics or electronics. CMMs also have some means of providing output to the user (printer and etc.) and to other machines in a complete manufacturing system. The main objectives of CMMs are to measure and inspect complex 3-D components for both prismatic and sculptured surfaces.

A CMM can rapidly and accurately measure objects of widely varying size and geometric configuration, and can also measure the many different features of a part, such as holes, slots, studs without needing a range of tools. More importantly if any changes need to be made in a fixed measurement system for any reason this would increase the inspection cost and the time, however changes in the measurement or inspection routine of a CMM can be made simply by editing the computer programme that controls the machine. This flexibility and versatility is one of the principal advantages of CMMs. They have been manufactured with different structures and configurations which all work under the same principle. They are similar in concept to CNC machine tools which require a rigid construction with accurate positioning and sensors, direct current (DC) drives and an intelligent controller capable of performing data processing and communication tasks.

Although CMMs have shown they are good tools for performing fast accurate three dimensional measurements of mechanical components they may not always be suitable if the user cannot provide the correct operating environment, which is one of many primary factors which affect CMM performance.

To use the full potential of these machines linking them to CAD systems will enable more efficiency, flexibility and benefits, for example; inspection programs can be developed on the CAD

system and transferred to the CMM. Actual inspection data can be transferred from a CMM to a CAD system which could enable comparison of nominal data with actual part information [55]. The major aim of bringing CMMs to the point of production was to control the production process more fully. They play a vital role in the mechanisation of the inspection process and their traditional role as a 3-D measurement tool is expanding since they offer potentially viable solutions to a number of disputes facing manufacturers [36] such as;

- i) The need to integrate quality management more closely into the manufacturing process.
- ii) The realisation that the measurement process itself needs to be monitored and verified.
- iii) The elimination of fixtures and fixed gauges thus providing increased gauging flexibility.

3.1 CMM and it's elements

The CMM must be rigidly built to minimise errors introduced by unintended movements between the machine members and their movement along the axes of travel. Prior to considering the CMM elements it is important to stress that this type of inspection machine requires special foundations which may be several metres deep since they are generally delicatated pieces of equipment and their installation and usage need careful attention. The main components in a CMM are the base or bed, column, bearings, scales and encoders, probes, control consols/monitoring units, hardware and the software.

The base or bed is used for mounting or locating components, is generally made of granite for maximum stability and is usually provided with tapped holes for clamping purposes. The base stands on anti vibration mounts to absorb possible vibrations from within or from outside. In the past, it was essential that the bed of the measuring machine be perfectly flat, but with the advent of computer based error compensation, this characteristic has become far less vital.

The column will differ according to the type of CMM and generally comes as a square frame or gantry to support the complete machine head and attachments. It should have enough stability to withstand sudden shocks which could be generated from moving the head and the probe.

Bearings have a direct impact on the accuracy of all CMMs because of their effect on every motion of the machine along its axes. The current bearing assemblies in measuring machine can be the air or roller type, in a laboratory or a clean room where dust and dirt is minimum, air bearings are the best choice, since they move without friction and are therefore the most accurate.

The scales and encoders of CMMs show where the probe is located within the work envelope of the machine. There are mainly two types of scales, metal scales (stainless steel) and glass scales. The most accurate scales are glass since it easily polished, stable, and able to work with both trans-

mitted and reflected light. The ordinary glasses have expansion coefficients 15 to 30 per cent less than steel, and some special types have been developed which have the same expansion coefficient as steel. This material permits finer etching of measurement lines than steel or other commonly used materials.

Probes and sensors are the devices through which CMMs collect their measurement input. A wide variety of probes are currently available. Each of these probes has its own application and peculiarity. Apart from non contact probes such as laser probes and vision probes, there are contact probes such as hard probes, Touch Trigger Probes (TTPs), and CNC continuous contact probes [56].

The control system on CMMs is computer based and the machine motion can be operated from the computer keyboard or more usually from control consols. The control consols on CMMs are usually a hand held box (joy-sticks) with several function buttons. Some of the important functions of this unit are to allow the operator to take the probe to a start or a rest position, datum the probe and perform other manual tasks such as aligning the workpiece.

The computer technology has been given capabilities and versatility that are rapidly making CMMs essential to efficient manufacturing. Together the computer and the software programme manipulates the data gathered by the CMM into the forms required by the user. In addition, the computer also operates the CMM in DCC applications and functions automatically compensating for errors within the structure of the machine.

3.2 Types of probes and sensors used by CMMs

CMMs have evolved in one decade, from simple layout machines with manually operated systems, to highly accurate, automated inspection systems. A major factor in this evolution has been the development of 3-D probes and sensors for both contact and non contact applications together with motorised probe heads and automatic probe exchange system for unmanned, flexible inspection.

The probing system on a CMM consists of the probe, the stylus and the application software employed in using the probe [52,57,58]. In order to optimise the measuring performance of any probe system, it is important that potential sources of error associated with the techniques used are identified and the effects of probe application variants (stylus choice, trigger forces etc.) are quantified. The ANSI/ASME B891.1.12M [59] quotes " A major factor contributing to the total system measuring error (of a CMM) is the performance of the total probing system...". Obviously there are different types of probes with different technology, generally they are classified in two

main groups; contact probes and non contact probes.

3.2.1 Contact probes

Hard probes (mechanical solid probes) are one of the two main types of contact probes. These probes have been in used since the mid-1970s [56,57]. They were the original type used on CMMs and are available in a variety of configurations (ball, tapered plug, and edge) and continue to have broad application and utility, primarily on manual machines.

The second type of contact probes are the soft probes (kinematic/resistive electronic TTPs). The invention of this probe occurred during the manufacture of Rolls-Royce engines for the Anglo-French Concorde, when a unique solution was required for accurate pipe measurement. This 3-D sensor is capable of rapid, accurate inspection with low trigger forces. The probe is mounted on the CMM's quill, usually by means of a probe head. The section of TTPs which make contact with the surface of the object is usually made of a ruby sphere which have various sizes i.e., 0.2 to 8.0 mm and it is shown in fig. 3.1. Triggering is proceeded by limited pre travel as the stylus deflects. Pre travel is related to stylus length and gauging force and is automatically compensated during stylus tip calibration. In these probes the coordinates of the measured points on the surface can be found by combining the probe position at the instant of contact with the probe tip deflection which is required to trigger the probe [18,36]. Not only do the TTPs remove a major source of operator error, they greatly increase the flexibility of measurements and facilitate DCC CMMs. Because of their significant advantages, touch trigger probes are replacing hard probes in many applications. Fig. 3.1 shows the principle operation of a TTP.

The main differences of TTPs over hard probes can be stated as the TTPs give continues feed back in terms of probe location to the control system, they perform an automatic control of the forces applied by the probe on the measuring object, they are highly repeatable, and finally they have the capability of automatic transmission of position to the machine control system. Whereas hard probes have no mechanism for transferring the position data to the control system and it is not clear what forces are being applied on the workpiece. These concepts have been achieved by the kinematic electrical resistance mechanism within the design of the probe along with a spring mechanism which overcomes the forces involved in the measurement.

TTPs [60,61,62] have a kinematic re-seating mechanism which will restore the stylus ball or tip to its original position within a nanometer (1/1000 of micron). The principle operation engages a three point (kinematic) arrangement which is restricted in its degrees of freedom until the stylus is brought into contact with the workpiece. Following contact the mechanism begins to unseat against a restoring force provided by a spring until a highly repeatable trigger point is reached.

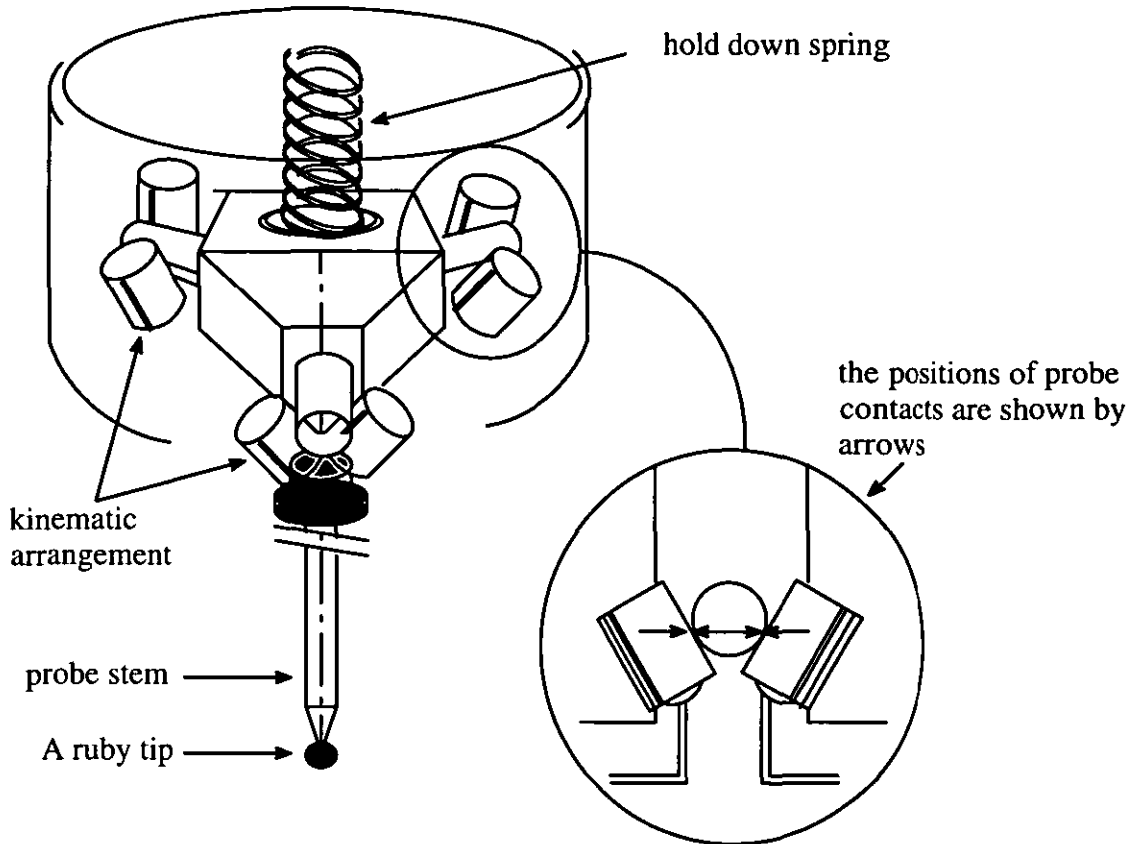


Fig. 3.1. Performance Characteristic of kinematic/resistive probes (Renishaw Publication).

The sensing system used in these probes uses electrical resistance, and the trigger incident (signal) is registered by the probe interface (CMM control unit) which monitors the probe contacts for a change in resistance. Once a preset trigger resistance threshold (trigger point) is reached the interface registers a trigger event and the signal is used by the CMM to latch its position counters to give a coordinate measurement at or near the instant of the surface impact. This trigger incident is highly repeatable and is not deteriorated by use. Fig. 3.2 shows the principle operation of this mechanism.

Triggering of this design of probe only occurs when the probe contacts actually break. The distance travelled by a probe between touching of a surface and the trigger incident is referred to as pre travel. It was stressed [60,61] that the probe pre travel was not a source of error from a probe of this design.

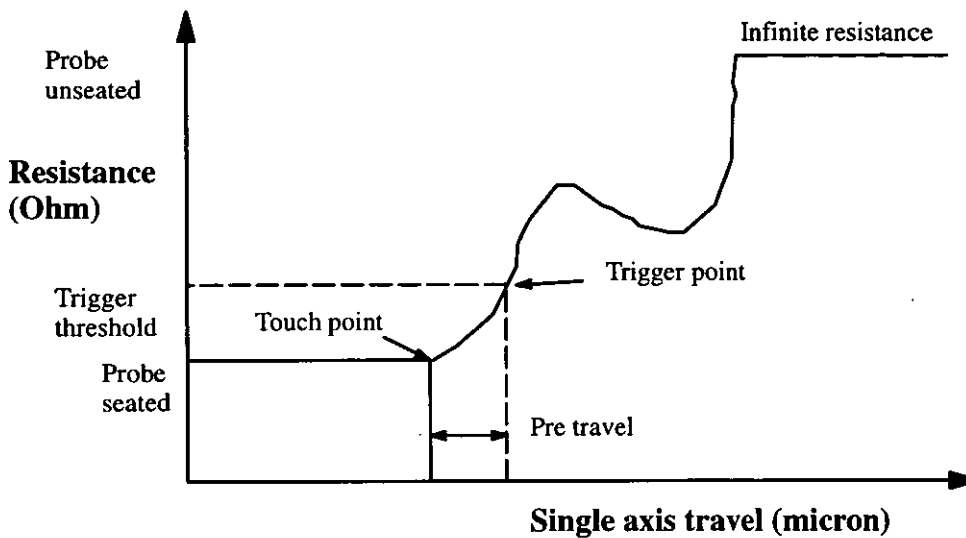


Fig. 3.2. Principle of operation of kinematic seating probes, electrical trigger characteristics (Renishaw Publication).

In addition, the repeatability of the measurement accuracy could be adversely influenced by the force variation encountered in different probing directions which could lead to measurement errors caused by variations in the stylus bending prior to triggering (a pre travel variation or "lobing"). Fig. 3.3 shows a plot of the trigger displacement error (pre travel) around a 360 probing plane with the characteristic lobing at three points approximately 120 degree apart, this becomes magnified when using longer or non-rigid stylus arrangements or increased trigger forces. It was mentioned [63] that a probe of this design could be only expected to function reliably up to a few million triggers.

Before using these probes they need to be datumed, also called calibration or qualifying which usually involves the probing of a precision reference sphere of precisely known diameter, and is a means of compensating for pre travel. The CMM software then calculates a best fit size for the sphere as measured by the probe (essentially averaging all the radii as measured) and compensates the stylus tip by giving it an effective diameter. Thus a physical 1 mm stylus tip is regarded by the controller as, for example 0.998 mm such that a more accurate idea of the true position is given during actual measurement cycle.

Finally, CNC continuous contact probes (touch scanner) are a specific group of probes which produce analog readings instead of the digital measurements. These probes are used for contouring measurements while the probe maintains contact with the workpiece as it moves along its surface. The probe is continuously moved against the workpiece and signals are transferred to the system computer control. The two primary types of this probe are force sensing and the displacement sensing probes. The force sensing probe uses strain gauge technology which measures force in-

Probe: Touch trigger (TP6)
Stylus: 50 mm

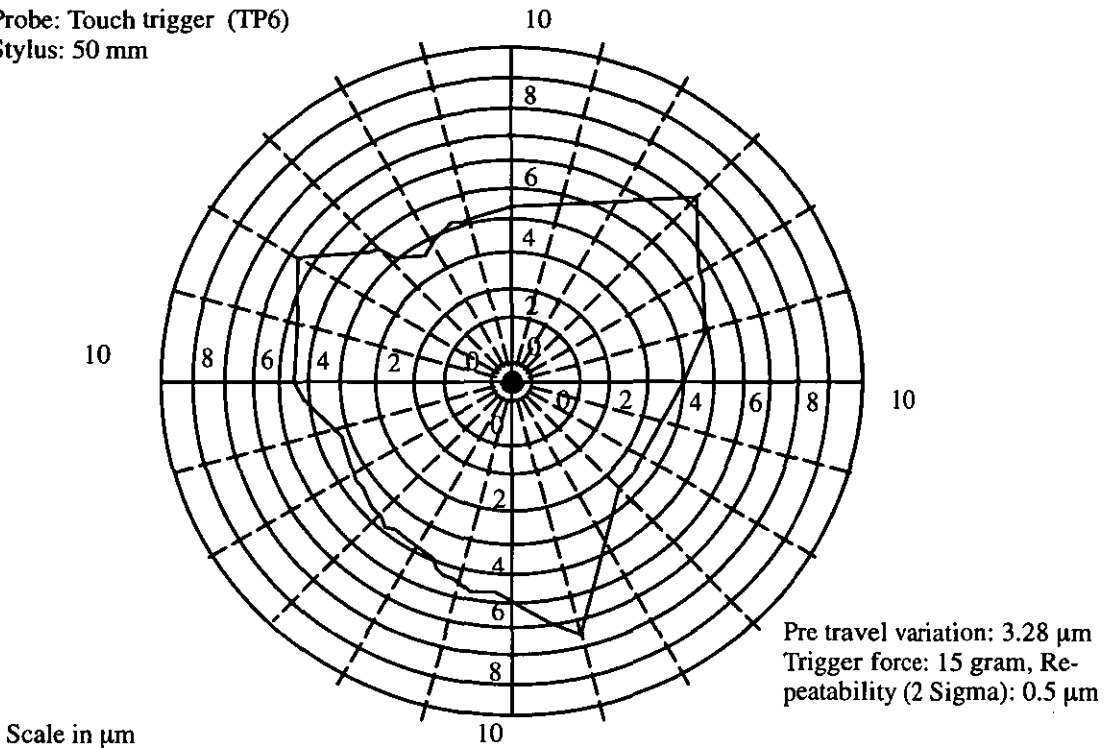


Fig. 3.3. Trigger displacement error (pre travel) around 360 probing plane (Renishaw Pub.).

stead of displacement. During the operation the system maintains constant force on the probe system and the signal is generated by calculating the change in the applied force. The displacement sensing probe uses a Linear Voltage Differential Transformer (LVDT) probe or digital scale technology, this probe measures displacement instead of force by maintaining the probe at a constant displacement from the workpiece [56].

The CNC continuous contact probes are more accurate in comparison with TTPs and are generally categorised as high costs probes.

3.2.2 Non contact probes

In general non contact probes have two advantages, they are capable of handling the undesirable effects of the touch probe, and have improved inspection speed. These probes can be sub divided into number of probe types such as non contact trigger probes, laser probes (sensors), Moiré fringes and the vision probes.

Non contact trigger probes in principle are similar to the contact touch trigger probes. With non contact probes, a beam of light is used to probe the workpiece from a set specific stand off distance. Lasers are generally used and can provide a non contacting measurement of both rigid and soft engineering materials. These probes utilize a number of techniques such as triangulation for the non contact 3-D scanning, gauging or inspection. Laser probes project a beam of laser light

onto the surface of the part. The position of which is then read by a triangulation arrangement through the lens in the probe receptor. These probes show considerable potential for automated measurement of complex surfaces.

The principle of laser triangulation can be explained as a laser beam is projected onto the surface of the object and the beam spot is viewed at the point of impact by a CCD camera. As the object moves relative to the beam, the point of impact moves further away from or nearer to the laser source, depending on the surface profile. As a result, the beam's position as seen by the camera moves along the line of photo cells in the CCD array. Fig. 3.4 shows the principle of a basic laser triangulation. The measuring resolution of this system depends on the size of CCD array and the distance between the nearest and furthest points to be measured on the object. For example, a CCD array with 1000 pixels (elements) measuring over a distance of 100 mm has a resolution of 0.1 mm. The overall accuracy of the system will also be 0.1 mm unless factors such as calibration or optical distortion introduce further errors. Fig. 3.5 illustrates the basic concept of the resolution of laser triangulation.

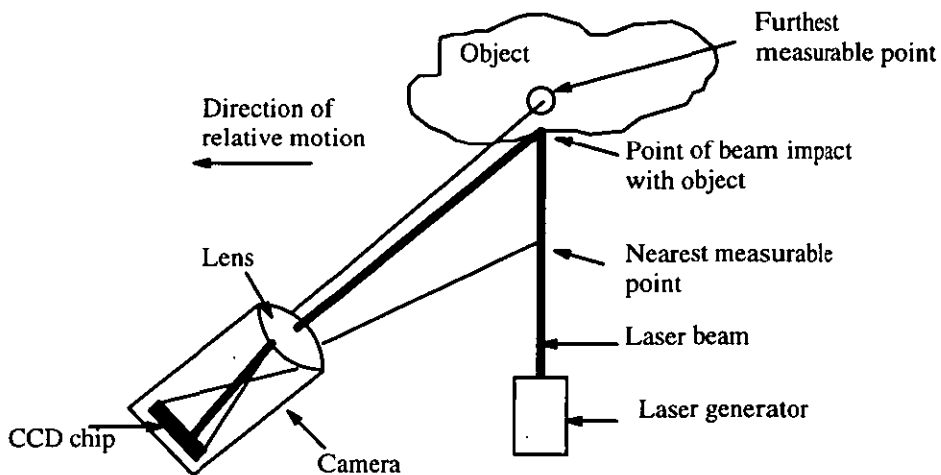


Fig. 3.4. The laser triangulation principle.

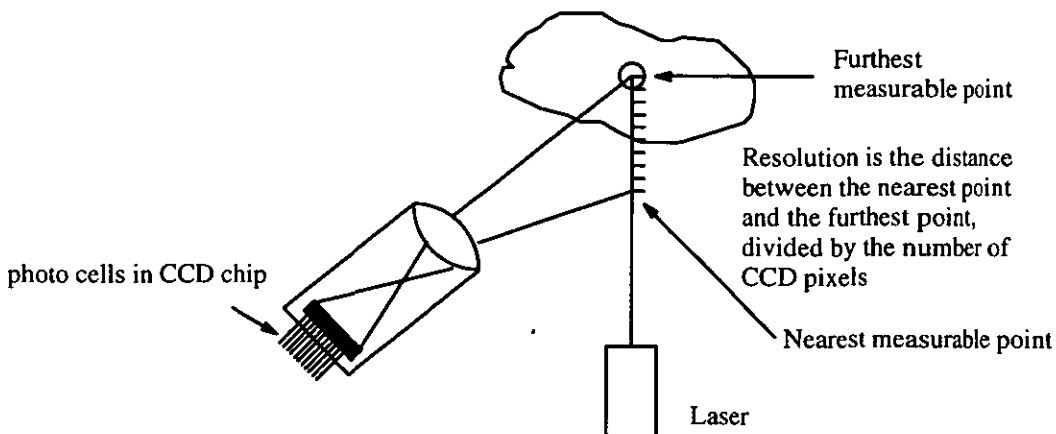


Fig. 3.5. Basic idea of resolution of laser triangulation.

In general, lasers are good at gauging depth and they provide their own light source, which is constant, bright, concentrated, and consistent, also they have the advantage of not working on the shadowing angle. In addition, a wide dynamic range, low optical crosstalk and high contrast can be counted as other advantages of laser probes.

3-D surface mapping Moiré sensors are not often used devices on CMMs. These sensors can be counted as a further extension of the triangulation devices which still use Moiré technology. They could provide a significant advancement [64,65] in 3-D non contact surface mapping techniques from laser line scanning and laser point triangulation methods. A miniaturised Moiré sensor can be mounted on a CMM probe pan/tilt head. This device can be used for the surface data mapping of complex parts. The sensor consists of three principle elements; 1) white light fringe projector, 2) solid state CCD video camera, and 3) microprocessor. The microprocessor is interfaced to a standard CCD camera resulting in the generation of 3-D surface points by reading the fringe patterns. In this technique a large number of lines or fringes are simultaneously projected by the white light fringe projector onto the part and viewed simultaneously in one video frame grab with the CCD camera. Analysing the distortions of these uniform fringe patterns would result in the generation of 3-D surface coordinate data. The sensor scans the part from a number of views in order to obtain a larger number of data coordinate patches. A developed software uses this raw data and orders it in arrays in order to be used for graphical representation of the object.

The last of these probes are the vision probes. This type of sensor are the most recent addition to the range of sensor systems currently in use. Genest [57] explained that this group of probes are especially useful when high speed 2-D inspection or measurement was required. However in some cases limited measurement capabilities in the third axis could be achieved using structured lighting techniques. In a vision probe system an electronic representation of the object is measured and evaluated and the various features of the workpiece (size, shape, location, and so on) are measured by analysing the edge of the component or the pixels intensities.

3.3 CMM measurement techniques

Prior to considering the CMM measurement techniques there are number of concepts related to part and machine set up that need considering. Normally for measurement of a part dimensions of the workpiece orientation must be determined in the direction specified on the engineering drawing. For this reason the workpiece reference plane should be set parallel with the machine reference plane and the workpiece reference axis should be aligned with the measuring direction (axis alignment). With advanced CMM control systems this is not necessary and these alignments

can be done by the CMM's computer system once the part coordinate system is established.

When a workpiece surface is measured using a probe, the coordinates of the probe centre are recorded and these coordinates must be compensated for by offsetting the probe radius to determine the actual workpiece dimensions. Currently CMMs are using data processing units and software which perform probe radius compensation either in response to specific commands, or using an automatic procedure which is based on the probe approach direction.

To measure a part it is necessary to establish a part coordinate system which is independent of the machine coordinate system. This is recognised as the part coordinate system, and it can be defined according to the drawing measurement datum surfaces and features on the workpiece. The part coordinate system is established by levelling and aligning the part (workpiece) to the measuring axis. It is important to set the part coordinate system that best suits the measurement tasks required with reference to the drawing, because the measurement data is represented in the coordinates in the part coordinate system.

3.3.1 Digitising, scanning and types of measurements by CMMs

CMMs can be arranged to scan or digitise the size and shape of an object or its contours by gathering raw data (in digital form) through sensors or probes. Digitising or scanning can be done from a feature or a surface by digitising a point, a plane, or a cluster of points on a specified area. These can either be measured as geometric shapes (flat surfaces as planes, holes as circles) or combined from separate features into new geometric shapes (i.e., two intersecting planes define a line, etc.).

Digitising a point in space or a point on a surface of component by a CMM is basically achieved by moving the sensing device (a probe) along the machine axes of travel until the probe contacts the object. The coordinates of the point (probe centre) will be recorded in Cartesian form for future use. To digitise a line or a plane it is important to take the points as widely spread as possible.

Digitising can be divided into five groups; point by point, contouring, zig-zag digitising, one way digitising and pencil mode (manual mode), fig 3.6 shows these tracing modes.

There are three general types of measurements for which CMMs are commonly used, geometric measurement, contour measurement and surface measurement.

Geometric measurement deals with elements such as points, lines, planes, circles, cylinders, cones, and spheres.

Contour or continuous path measurement has been defined as 2-D measurement of undefined curves (profiles) where the probe measures at certain intervals by taking points on the surface after each change of X and Y relative position in the machine axes. The measurement normally

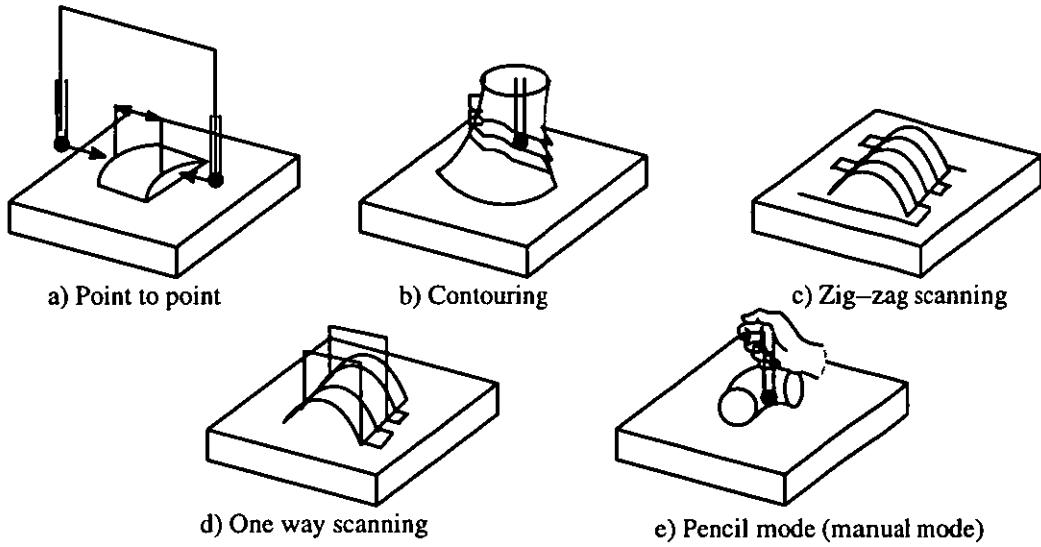


Fig. 3.6. Scanning and digitising modes.

scans a 2-D profile parallel to a reference plane which can be parallel to a machine axis, or at any angle to a machine axis. For example, measuring a circular contour requires a sine rate change in one axis and a cosine rate change in the other axis. Contour measurement deals with undefined, or irregular shapes, such as a turbine blade, surface of a shoe or a golf club. The contour measurement process in guided CMMs can deal with four types of curve scans; profile, curve, surface, and cylindric. Fig. 3.7 shows these methods.

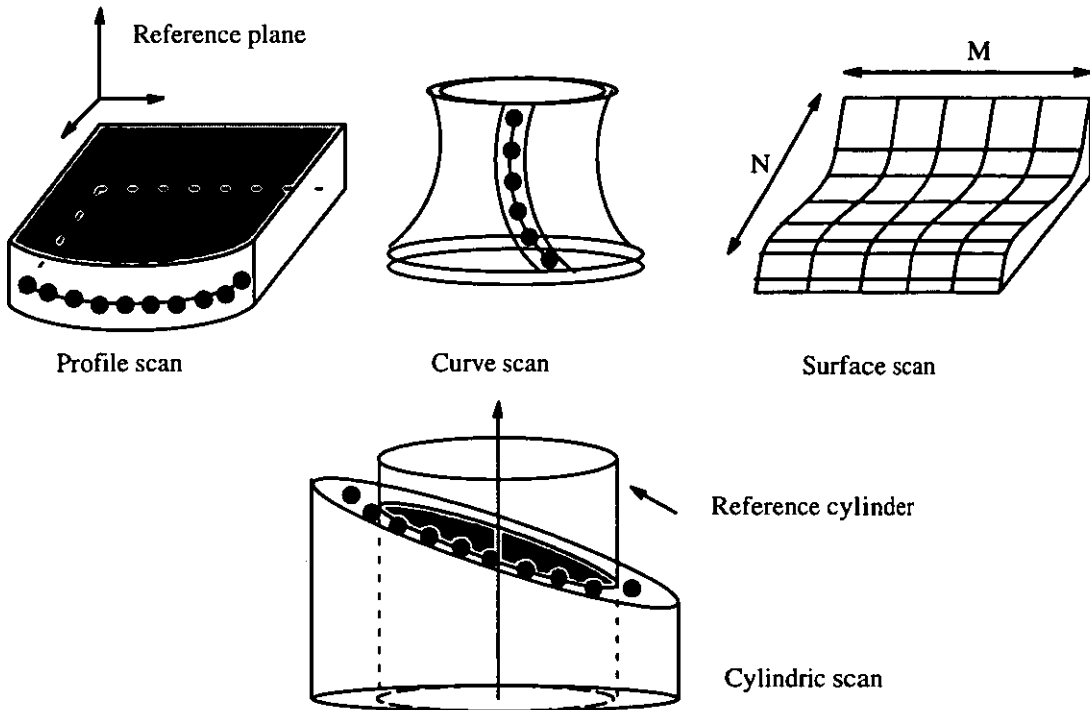


Fig. 3.7. Contouring four kind of curves (Brown and Sharpe).

In contour applications the required shape may not consist of lines or circular arcs but the curves might be either formed by a complex mathematical equation or a free form. It is common for the CMM's software to allow the normal shape to be entered directly or to be read in from other software packages, where the data points are then stored in order to be suitably displayed.

Surface measurement is a 3-D measurement of complex curves which would represent particular shapes, such as gear teeth or 3-D turbine blade.

3.4 Review on CMM applications, integration and related matters

The performance of CMMs and the necessity of them as an engineering tool have been dealt by many researchers [66,67,68,69,70]. They outlined the flexibility of these machines, roles and the justifications to invest in CMMs. The main other related areas to CMM can be named as probe technology [63], how to approach the objects by TTPs [20,21], assessing CMM software [71] and use of other type of probes (i.e., laser, 3-D scanners, analogue probes, Moiré fringes) [56,72,73,74] which worth considering.

Farmer and Smith [75] developed an integrated system using a low cost PC-based CAD system and a low cost CMM. They emphasised the integration of CAD and CMM with the principal objective of preparing inspection instructions and process measurements efficiently while conforming to relevant international standards. In their system model two types of information must be specified; a) instructions for the CMM operator such as how the part should be positioned or how the CMM should be set up; and b) instructions for the computer controlling the CMM such as the sequence of probe positions and the types of geometric features being measured. The measurement data for processing could be prepared in the form of a report, drawing or statistics for process control. The CAD system was used to prepare the product design specification (drawing) and a CMM inspection plan to the drawing. The inspection drawing was converted into Initial Graphics Exchange Specification (IGES) format and the information relevant to the CMM inspection procedure was separated from the IGES file and converted to a neutral format. At this stage the operator instructions and macros could be developed for controlling the CMM and the inspection procedure. The inspection report file from the CMM was edited and the data was standardised to suit the quality management system and additional reports (i.e., inspection reports, charts) could be prepared. It was not clear how the CMM inspection plan was developed. However, extraction of CMM inspection instructions from the files produced by the CAD system needed a high degree of expertise since grammar and syntax must be defined for the inspection instructions in order to be recognised by the IGES format. The system showed the feasibility of the integration of less expensive CAD and CMM's particularly for inspection and quality control

for manufacturers. However, their system did not consider automatic inspection of features and it required continuous user intervention.

Pahk et al. [76] developed a CMM and CAD inspection system for integrated mold manufacturing. The system was capable of measuring sculptured surfaces with some basic features such as; holes, slots and bosses. The features could be chosen in a CAD section in which inspection planning for each feature would be created. The output of the planning was the machine code for a specific CNC CMM. Error analyses arrangements in the CAD system allowed compensation to be made on received data from CMM and the evaluated errors would be graphically displayed. A least squares technique was used for error evaluation of basic features such as flatness, squareness and parallelism. Other error algorithm have been developed to calculate form and offset errors which were involved in tilting or translation of the sculptured surfaces on the mold plate. The system was based on the existence of the objects' CAD model which needed further research for both automatic inspection of the features on the designed model and to make the system applicable to complex products.

Oh et al. [77] researched on the use of CMM in reverse engineering, the process of making a part from an existing part rather than from a drawing.

They discussed five major steps of the reverse engineering cycle which were;

- 1). Measure and digitise the original part.
- 2). Transmit the CMM data to a CAD system.
- 3). Transforming the point data to a CAD model.
- 4). Generate NC tool path.
- 5). Produce a new part using the path programme.

Kwok and Eagle [78] discussed two major applications of reverse engineering by use of a CMM. The first application was creating CAD models of surfaces that are based on appearance rather than on engineering requirements examples such as shampoo bottles and automobile dashboards which are designed largely for their pleasing appearance, the CAD models of these crafted prototypes would be created by CMM digitising. The second application as mentioned earlier was to produce drawings of existing parts when the original design data were unavailable. The main similarity of these two studies [77,78,] to this work is in the process of creating the object on the CAD system by a CMM.

Sarkar and Menq [15] considered schemes for scanning compound surfaces by a touch probe CMM. Scanning compound surfaces required two important concepts; a) definition of the bound-

aries or character lines, and b) definition of regions bounded by the character lines. The boundary points could be digitised manually, by the use of vision techniques, or by enhanced CMM scanning procedures to define the character lines. The main concept was the division of the compound surface into a number of regions by the use of the character lines. The character lines signify the change in the surface shape which means each region will have no an apparent shape change. The position of the character lines could be visually detected and manually digitised or they could be determined by edge operators. However, none of these methods could be fully automated without manual intervention for a very general compound surface due to the degree of complexity. Also, for complicated 3-D objects with undercuts, scanning is difficult using a CMM without relocation or orientation.

The CMM probe technology and errors associated with them have been studied by many researchers, notably Reid [63] examined the fundamental requirements for the technology employed in a CMM probe sensor. He discussed that the principle of operation of Strain Guage Probes (SGPs) which eliminates the measurement uncertainty associated with lobbing by effectively triggering the probe at a constant force in all probing directions.

Smith [20] investigated the errors associated with variation in the angle of contact of a TTP. The error of a TTP reaches its minimum when the probe approaches the surface in the normal direction. Butler [21] researched into the nature of probe errors and factors that influence their performance with a proposed method of verifying the probe performance. Although the use of a SGP may improve probing for the majority of industrial applications, the developed probing strategy in this work supports the work of Smith and Butler [20,21] and minimised the errors associated with TTPs.

Cox [71] discussed methods for assessing and comparing CMM software quality. The methodologies for CMM software testing could be classified as:– i) correctness proving, the application of classical mathematical proving methods to metrology software, ii) self assessment using mathematical properties, in order to confirm that the computed solutions satisfies the original mathematical problem statement, and iii) black box testing through the use of reference data sets (soft gauges). The reference data sets are synthesized data sets that mimic actual measurement data. A good software should be consisted of: a) a rigid mathematical basis, b) good numerical analysis, c) careful algorithm design, and d) sound software implementation.

There is an increase in use of non contact probes with CMMs, Goh et al. [72] discussed the main advantages of non contact inspection and methods adaptable for the dimensional inspection of engineering components by the use of a compact solid state laser triangulation sensor on a CMM.

They were encouraged not to use a TTP due their limitations, such as possible local deformation, overshooting of the probe, critical surface finishes might be marred and slow speed of the measurement. Renishaw [79] developed a non contact probing system for the use with CMM to allow high speed scanning. The system used the triangulation principle within a laser light beam which was focused to a spot by the optics contained with the probe. The spot was typically focused between 20 and 100 mm from the probe. Since the majority of engineering materials are non-perfect reflectors, the surface would reflect the laser light in multiple directions. However, the system was able to operate with a portion of the scattered light which was focused onto a light sensitive detector.

Laser applications are rapidly increasing in the area of measurement, Bradley et al. [73] employed a 3-D laser scanning on a Mitutoya BHM 710 CMM to digitise object surfaces. The scanner operation was controlled on a terminal through a hierarchical menu. The scanner unit would move within the 3-D work envelop by the CMM and multiple passes could be made at any depth (providing the surface was within the scanners depth of field) across the prototype surface until satisfactory digitisation could be achieved. The servo motor position encoders of the CMM kept updating the scanner computer during data collection. The quoted accuracy of ± 0.05 mm could theoretically be increased by reducing the depth of field from the current 80.0 to 40.0 mm. The process would be used to reconstruct regions of the laser scanned object, which could be represented by a sub-set of the family of quadric surfaces, namely planes, cylinders, cones and spheres. Although the laser scanning accuracy was not as high as a CMM, it would be appropriate for many reverse engineering tasks and rapid prototyping of multi patch models.

Although there are some benefits with the use of non contact probes or scanners, there are some drawbacks with using them such as, high cost or complexity and less flexibility. However, they still attract specific applications in industry.

3.5 Factors affecting CMM performance

The CMM performance and its accuracy will be affected by many error sources which can be grouped into three categories: i) design errors, ii) environmental errors, and iii) operating errors. An evaluation of these errors will give the overall machine performance. Genest [57] believed that most errors in CMMs were of systematic kind, initiated from machine set-up and operating conditions rather than random. Therefore a series of initial considerations should be given when a CMM is to be used to give a high level of performance, the CMM should be placed in a suitable environment with adequate safeguards and protection for error free operation.

There are many sources of geometric inaccuracy in a three axis CMM which are; roll, pitch, yaw, scale error (linear positioning), straightness, and squareness. To ensure volumetric accuracy (explain later), every one of these factors must be tested. However, the majority of mechanical errors in the CMM may be refined using computer control and some of the others may automatically be compensated for by the use of powerful software algorithms during measurements [57].

Workpiece errors and probe workpiece interaction would be named as error sources which could be belong to the mechanical characteristics of the workpiece materials, examples of which could be hardness and roughness.

3.5.1 Geometric and kinematic errors on CMMs

In general it is impossible to manufacture a mechanically perfect machine, however it is important to be able to analyse the geometric errors associated with individual elements and to determine their effects on the machine's measurement accuracy. Geometric and kinematic error analysis tends to be of concern for the manufacturers of CMMs rather than the end user who is only interested in the accuracy to which he can measure using the machine. However, the geometric error of a CMM is one of the major sources contributing to the inaccuracy of a measured workpiece. The geometric error of a CMM is the error which is produced at the probe stylus due to dimensional and form errors of the elements of its kinematic linkage system, and the angular and positional misalignments between them. The accuracy of CMMs also depends on the accuracy of the position transducers and on the linear and rotary moving axes. Elshennawy [2] explained that geometric accuracy of the machine could be affected by the following factors,

- i) Errors in the form of different machine component shapes such as tables, guideways, etc.
- ii) Mechanical wear of linkages and joints which introduce undesirable effects such as lack of straightness and squareness, inadequate motion, etc.
- iii) Thermally induced errors due to variations in the operating environment which would cause structural changes.
- iv) Weight deformations caused by the weight of machine structure or the part being machined or measured.
- v) Errors in the control or measuring system which could be thermal, mechanical or electrical in nature.

3.5.2 Probe error sources within a kinematic/resistive probe

The electrically switching kinematic 3-D TTP was first available in 1972 and the principle of operation has not changed since then. Reid [60] explained that the potential probe error sources

within kinematic/resistive TTPs fall into two main types: random errors, and systematic errors which are generally application sensitive and could be either eliminated or minimised in practice.

The only random error source which could be associated with kinematic/resistive TTPs is the uni-directional repeatability which is present in all measurements taken. The repeatability of a probe is the competence of the probe to trigger at the same point each time and normally quoted statistically with a 95 per cent confidence level. The repeatability error of kinematic/resistive TTPs being typically less than $0.5 \mu\text{m}$. This is not likely to be the major source of measurement error on a CMM, however, its presence should be considered when appraising the measuring performance of any CMM or a probing system.

With kinematic/resistive TTPs systematic errors can be grouped into two main potential sources: pre travel variation and hysteresis. As mentioned before the degree of presence of these potential error sources are significantly influenced by the datuming and measuring techniques employed, the model of probe used, and the type of feature being measured.

Directional variation in probe pre travel may be as small as $\pm 1 \mu\text{m}$ if a good datuming technique is employed. The effective tip diameter of a probe (stylus tip) would be calculated by the CMM software and is applied to each point taken by the probe to give the true position of the inspection surface.

There are methods suggested by the standard bodies to establish the possible errors contributing to the total system measuring error by the probing system. A method is suggested by ANSI/ASME B89 standard for a probing system which lays out a performance test in order to establish the possible errors contributing to total system measuring error. The test involves taking 49 probe points over the surface of a test sphere using three different stylus configurations.

There are a number of considerations recommended [80,81,82] to optimise the use of the probe:—

- i) Keep the stylus configurations as short and rigid as possible.
- ii) Keep the probe trigger force (if applicable) as low as possible whilst ensuring reliable probe operation.
- iii) Datum the probe in the directions it will be used by taking at least five equispaced points spread over the surface of the datum sphere.
- iv) When measuring a feature with multiple points, take points sequentially around the feature, always trying to take more points than the minimum required.
- v) TTP accuracy varies as the stylus orientation varies. The best results can be obtained from a CMM by always approaching perpendicular to the part's surface and to use a large portion of the

feature.

vi) Follow the suggested measurement procedure by the CMMs and TTPs manufacturers.

vii) Ensure the probe holder is placed correctly to the machines' quill.

viii) Anytime the probe has been removed and reinserted into the CMM, the qualification must be re executed, because the probe can never be mounted identically and there are some inconsistencies on the probe stylus.

Probe hysteresis is often an overlooked systematic error which can be present in all types of probe design. It could occur as a direct consequence of the direction of the previous trigger and reseat and could be thought of as being backlash similar to other mechanical systems. Hysteresis error is generally of the same order of magnitude as probe repeatability and it is directly proportional to the stylus length and the trigger force in a TTP [60].

3.5.3 Errors due to environmental effects

Error due to environmental effects would generate a continuous error in the CMM and unless a recommended environment is prepared these factors are difficult to control. The environmental effects could be caused by;

Temperature. A stable temperature is necessary to avoid thermal distortion. This is particularly important if alloy or plastic components are to be measured. Specific operating temperature standards have not been established. One of the environmental requirements is the temperature at the location of the measuring equipment, for example the temperature in a laboratory doing interferometer calibration for 2 μm and for CMM to 10 μm accuracy should be held to $\pm 1/20$ °F. The nominal temperature should be 68 °F (20 ± 1 °C) to eliminate one of the correction factors when comparing results directly with National Bureau of Standards (NBS) [83].

Vibration. Many CMMs are mounted on anti vibration mounts; however, it is still important to minimise vibration in the vicinity of the machine. Some of the common sources of vibration are air compressors, punch presses, large mills and shapers (common machines in a workshops), etc.

Contamination. In order to keep maintenance to a minimum it is advisable to select a suitable site which is relatively free from contamination by oil, swarf, dust, humidity etc. The compressed air supply to the machine should be dry and oil free.

Electrical interference. The electronic desk should be supplied from a power line which is isolated from power cables supplying electrical equipment which may cause large voltage fluctuations or interference pulses.

Handling. Avoid touching the ground surfaces of columns or any other bearing ways with bare

hands. If it is necessary to move the machine manually, it is advisable to hold the Z column by the upper part of the probe mount [57].

3.5.4 Volumetric accuracy

As CMMs begin to be used to measure more complex parts, linear accuracy may not be sufficient to guaranty the level of measurement performance required. Therefore it is important to evaluate its volumetric accuracy, which is the performance of the CMM accuracy at any point within its three dimensional working envelope.

The maximum permitted error for volumetric accuracy is given by [84];

$$\text{Volumetric accuracy } U = A + \frac{BL}{C} \mu\text{m} \quad \dots 3.1$$

Where U is the maximum permitted error (volumetric accuracy) in measuring a known length of L millimetres in any position on the machine. A, B, and C are constants given in the specification of the particular CMM. BS6808 requires that the U shall be stated at a confidence level not less than 95 per cent. For example a CMM model with repeatability of 0.001 mm and the volumetric accuracy given as $2.8 + 3L/1000 \mu\text{m}$, the uncertainty on measuring a length is $2.8 \mu\text{m}$ plus an additional amount of $3 \mu\text{m}$ per metre of the measured length [84]. There are practical ways such as; laser measurement systems and Machine Checking Gauge (MCG) tests for determining volumetric accuracy of a CMM by the user. Dimensions and tolerance limits would be generally referred by implication to a theoretical temperature of 20°C .

3.6 The CMM systems used for this work

The two CMMs used for this project were of a moving bridge type which employ three movable components moving along mutually linear perpendicular guideways. The probe is attached via fittings to the vertical component. Fig. 3.8(a and b) show a Ferranti Merlin and a Micro Xcel Tesa CMM from the Brown and Sharpe Company.

The initial set of primary tests were undertaken on a Ferranti Merlin MKII series 750 CMM with a Hewlett Packard 9000 Series 300 computer control system [14]. The machine operates under full 3-axis computer numerical control (CNC) using the CMM initialise software named DCC-315. This software enables various standard measuring routines and calculations to be performed. The machine is of a gantry configuration which enables a $750 \times 750 \times 500$ (mm) envelope to be measured. The machine has an linear accuracy of 0.005 (mm) and a repeatability of 0.02 (mm).

The measuring head used for this work was a standard Renishaw PH9 motorised probe head. Through the CMM software the head allows for 20 probe orientation at 7.5 degree increments.

The touch probing was achieved using standard 0.3 mm, 1.0 mm, and 2.0 mm diameter spherical ruby tips.

During the course of the project a new CMM was purchased by the University which had the following advantages over the Ferranti Merlin. It allows the use of hundreds of probe orientations and generates direction vectors (IJK) of the measuring points. The machine is a bench type (425 Kg.), low cost and high performance measuring machine with an IBM compatible computer system which runs on SCO Xenix operating system. The machine enables users to toggle effortlessly between manual and DCC operation mode and operates under full 3-axis CNC with an initialise software named Micro-Measure-4 (MM4). The machine has a 457 x 508 x 406 (mm) measuring envelope with a linear accuracy of 0.005 (mm), a repeatability of 0.003 (mm), and a volumetric performance of $3 + 3L/1000$. The measuring head used for it was a standard Renishaw PH9 which allows for 700 probe orientations at 7.5 degree increments [82].

It was therefore decided to use the Tesa for the majority of the tests and the early developed system on the Ferranti was transferred to the Tesa CMM.

3.7 Future developments of CMMs

The future development of CMMs can be divided into: 1) software development and, 2) hardware development. The software development of a CMM needs to handle a variety of processes in real time with robust algorithms, a wide range of functions, a good interfacing system with CAD and CAM environments, and the possible need for handling vision data. A logical link to better sharing of information is needed to interface between the design data and the inspection data. The link between CAD and CMM allows information to be passed between the two systems, this interface is usually unidirectional from the CAD system to the CMM however, multidirectional links will be needed in the future. In addition, the CMM controllers of the future should have the capability of not only handling procedure commands (where the CMMs are asked to measure) but also the process geometry commands (where the CMMs will understand geometry commands and feature description commands) [85]. The connection of 3-D CMM to NC and CNC systems with off-unit programming opens possibilities for CIM with flexible measuring inspection to develop automatic probe changing systems without the requirement of subsequent recalibration [67].

An important part of the software development concerns interfacing which enables translating data between the systems. In order to advance and accelerate the production cycle of a part from design to manufacture it is important to allow part data to flow quickly and accurately between all those processes involved. There are a few such data interchange standards/methods currently available such as IGES, PDES, STEP, and DMIS [38,86]. DMIS has been specifically developed



Fig. 3.8(a). Ferranti Merlin CMM.



Fig. 3.8(b). Xcel Tesa CMM.

to provide a standard for bidirectional communication of inspection data between CAD/CAM systems, and DCC dimensional measuring equipment. In essence the specification is a dictionary of terms which establishes a neutral format for inspection programmes and inspection results. DMIS has evolved compatibility with IGES/PDES developments. Fig 3.9 shows a closed loop manufacturing environment where a fast design/manufacture/inspection environment can exist.

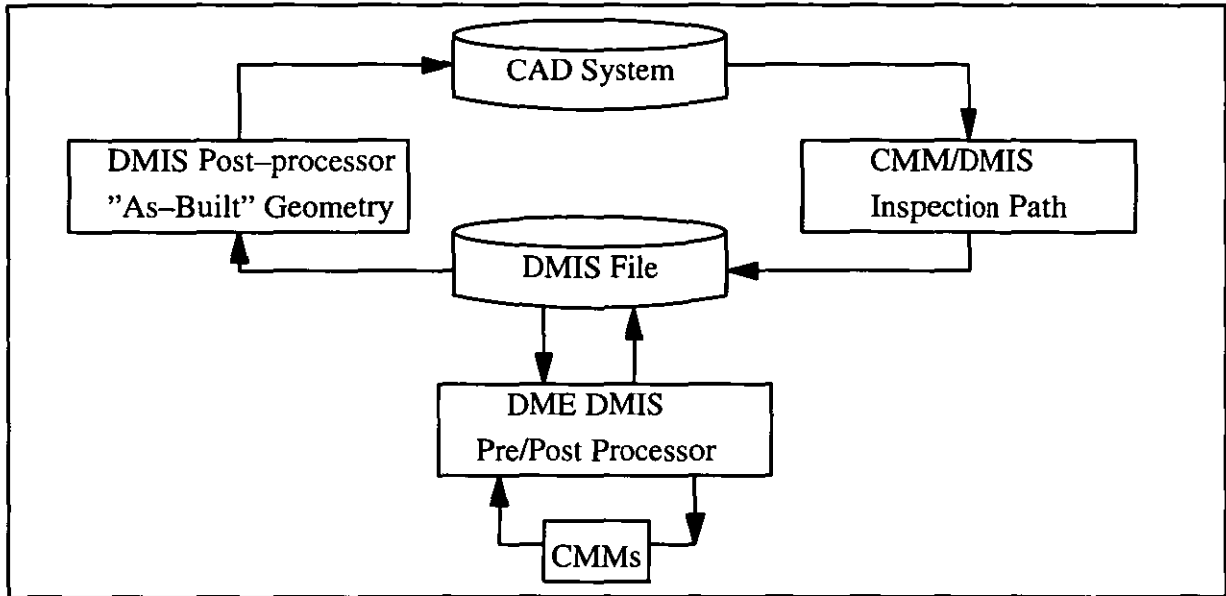


Fig. 3.9. A closed loop manufacturing environment.

By the use of DMIS as the data exchange standard, dedicated pre and post processors could be avoided. To date, the DMIS formatted inspection programme can be generated at several different CAD/CAM stations and transmitted through various standard network protocols to a variety of CMMs. Although there is less response from the engineering and quality assurance market place in Europe with regards to this specification, there is no significant difficulty in employing DMIS in industry. Development for translation using DMIS is currently under way in order to develop a general translator which can be used for any CMM, which undoubtedly would increase the demand for DMIS.

Further development of CMM hardware could be inspired by the need to minimise the part/machine set up time and the inspection time for part measurement. The CMMs physical structure has changed since they first came into being, however, their control system and measurement scales have not been given the same attention. One way to improve CMMs and enable them to measure faster with a high accuracy is to employ laser interferometer technology. Adding this form of non contact sensing device instead of the current optical system would also lower the inspection time at high accuracy [65]. Unfortunately at present these systems are also costly.

CHAPTER 4

FEATURE DETECTION USING MACHINE VISION AND A CMM

4.0 Introduction

Data collection of 3-D coordinate information from sculptured surfaces has been achieved by the use of contact and non contact techniques, however, the use of these methods is still causing some difficulties. When using a contact technique collection of data can be arranged by touching a point at a time which is a slow process. The specification of features for sculptured parts is still uncertain and generally lines or grids are marked onto the surface to identify features or patches. More sophisticated methods are required to enable this process be done faster. This feature detection and measurement strategy will include a systematic method for presenting the features in order for them to be easily identified, sorting of the detected features, development of an optimal procedure to measure features, and design of a strategy for the probe selection in order to minimise the probing error.

Prior to inspecting the surface features, their locations need to be identified and for special cases when the surfaces could have many features, a fast detection and reliable method is required. One possible method is to employ the use of a machine vision to identify the locations of the features. Because it is difficult to separate features on a sculptured part, they need to be enhanced by marking in order for them to be easily identified. The 2-D vision system used then determines the position of each feature which is treated as if it was on a similar horizontal plane, a set of algorithms and procedures were designed to analyse the problem.

For this research the selected objects were golf balls which are special cases of multi faceted feature parts albeit positioned around a regular object sphere and which also gives the opportunity for measuring multiple facets. For simple balls the dimple shape would be constant (one dimple shape repeated around the whole ball), whereas complex balls can have as many as eleven dimple sizes. It is apparent that there are no generic solutions for automated feature identification and detection and, one way of developing methods is by investigating special cases in order to learn rules and methods which can be applied elsewhere (e.g., shoe last inspection etc.). Jones and Mitchell [87,88] investigated and developed generic methods through studying feature based design of specific sculptured products, they concentrated in investigating solutions for one product from which methods and rules have been developed and applied elsewhere.

4.1 Golf balls

Although many books have been written about the history of golf, the true origin of the game has yet to be decided. The playing of a game resembling golf is evident in Dutch illustrations [89,90]

dating as far back as 1296. However historians agree that it was the Scots who taught the world to play golf. What is certain is that the game has existed for at least 500 years. This is known because an Act of Parliament dated 6 March, 1457 [90] clearly states that James II of Scotland had football and golf banned because their popularity strongly interfered with archery practice, important in those days for the defence of the realm against the English warriors.

A monopoly for ball manufacture was given in 1618 by James VI of Scotland to James Melvill and his associate for a period of 21 years [90] and referred to balls which were made from leather and stuffed with feathers. However feathery balls started to be superseded by the innovation of a new ball made from Gutta Percha in 1848. The Gutta Percha ball reigned supreme for almost 55 years, until it was superseded by the Haskell ball in 1902. The modern golf ball is a direct descendant of the Haskell rubber cored ball which brought improved performance and greater interest in the game. Today wound balls make up 20 per cent of the market with solid two piece and one piece balls the remainder. Manufacturers constantly strive to produce balls which go further etc. and, in order to maintain standards and control performance the twin governing bodies of the game, the Royal and Ancient (R&A) Golf Club and the United State of Golf Association (USGA), have placed a set of restrictions on ball design [91].

a. Weight

The weight of the ball shall not be greater than 1.620 ounces avoirdupois (45.93 gm).

b. Size

The diameter of the ball shall be not less than 1.680 inches (42.67 mm). This specification will be satisfied if, under its own weight, a ball falls through a 1.680 inches diameter ring gauge in fewer than 25 out of 100 randomly selected positions, in at a temperature of $23 \pm 1^\circ\text{C}$.

c. Spherical symmetry

The ball must not be designed, manufactured or intentionally modified to have flight properties which differ from those of spherically symmetrical ball.

The ball performance specifications outlined by the Rules of Golf [91] is that each ball type will be tested using 20 pairs of that type. One ball of each pair will be launched spinning about one specified axis; the other ball of each pair will be launched spinning about a different, but also specified axis. Differences in carry and time of flight between the two balls of each pair will be recorded. If the mean of the differences in carry is greater than 3.0 yards, and that value is significant at the 5 per cent level, or if the mean of the differences in time of flight is greater than 0.20 seconds, and that value is significant at the 5 per cent level, the ball type will not conform to the Rules of Golf.

d. Initial velocity

The velocity of the ball should not be greater than 250 feet (76.2 m) per second when measured on apparatus approved by the Royal and Ancient Golf Club of St. Andrews. A maximum tolerance of 2 per cent will be allowed. The temperature of the ball when tested shall be $23 \pm 1^\circ\text{C}$.

e. Overall distance standard

A golf ball under test should not cover an average distance in carry and roll exceeding 280 yards (256 meters) plus a tolerance of 6 per cent. The 6 per cent tolerance will be reduced to a minimum of 4 per cent as test techniques are improved.

The ball has to be designed to withstand impact speeds of up to 170 mph, which results in deformation on the club face to 70 per cent of the equator area, acceleration forces of 9000g, spin rates of 12,000 RPM [92] and is expected to fly with the accuracy of a bullet. Most manufacturers can produce acceptable balls but are limited from further advances by the Rules of Golf as explained previously.

One of the few design features which the ball designer has control over is the way in which the ball flies through the air and this is primarily affected by the dimple pattern. The major significance of dimples on balls is to create turbulence in the air flow around the ball, hence reducing the drag force. Although there are no rules concerning the dimple shape, most of them tend to be circular, with the "dish" shape generally spherical. The major reason for this arrangement is for ease of tool and die manufacture. A wide range of dimple shapes have been used in the past and presently multiple radii shaped dishes are becoming popular, but the surface shape still tends to be circular. Indirectly there are rules, concerning the dimple patterns which must be designed and manufactured to perform as if the ball were spherically symmetrical [91]. In order to achieve this end the position of the dimple on the ball is critical and dimples must be placed in symmetrical patterns, which cover the ball surface. These patterns are generally based on Archimedean Polyhedra and the five solids having regular faces or facets are known as Platonic Solids [93]. Fig. 4.1 shows the five Platonic Solids. The shapes are:

1. Tetrahedron: 3 equilateral triangles.
2. Cubic: 6 squares.
3. Octahedron: 8 equilateral triangles.
4. Dodecahedron: 12 regular pentagons.
5. Icosahedron: 20 equilateral triangles.

The tetrahedron has limited application in ball design, but the others are all used, often in combination, and with varying dimple diameters. It should be noted that occasionally small variations

in symmetry have to be accommodated, since the ball has to come out of a mould, split at the equator, and it is not practical for a dimple to cross the split line.

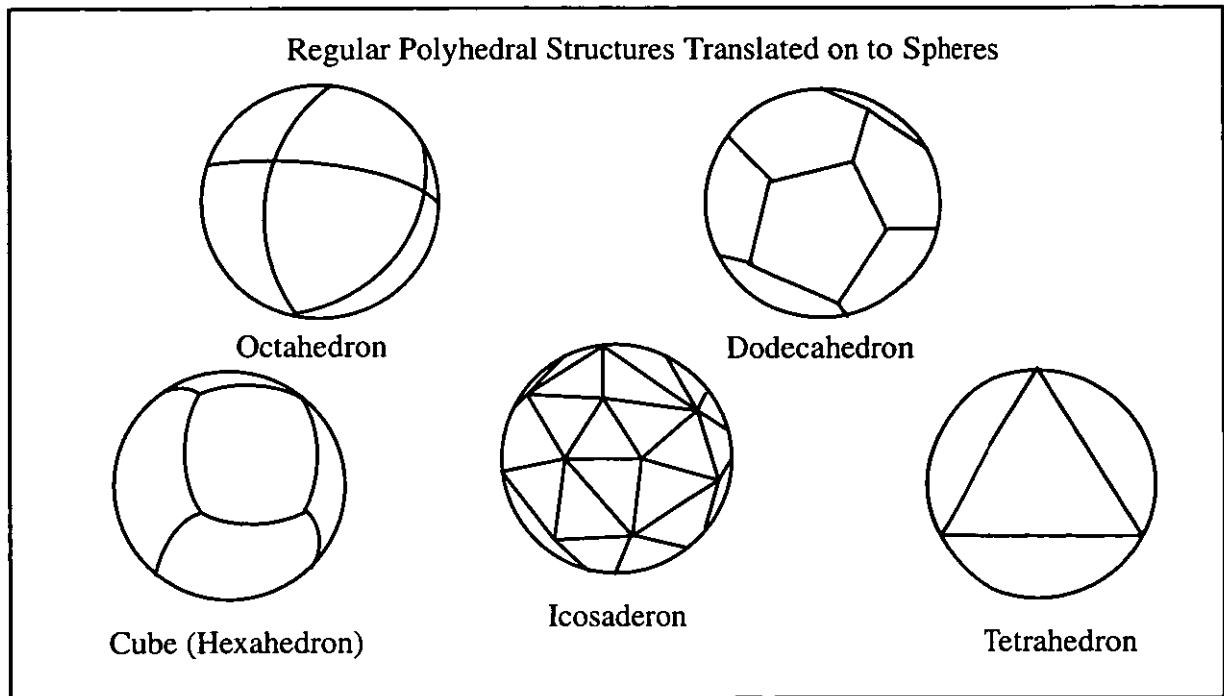


Fig. 4.1. Platonic solids.

The accuracy to which the dimples are manufactured and positioned is critical to the way in which the ball flies and the measurement of this three dimensional pattern provides the metrologist with a complex problem. At present balls contain between 250 and 500 dimples, with as many as 11 different dimple diameters. Variations in dimple depth as little as 0.0125 mm and variations in position of the order of 0.100 mm can cause significant differences in flight path. It is apparent that the measurement of the ball can be a complex and time consuming operation and for this reason it has been chosen as the example for this research work.

4.2 Review of vision system application methods for feature identification

The initial concept of the use of vision systems was for the identification and recognition of objects, however, these systems have now been employed in almost every branch of industry to carry out different tasks. The early work was primarily concerned with 2-D analysis but as optical systems and computing power developed 3-D solutions become available, but at a cost. Several of the more prominent developments have been reviewed to give an appreciation of the diversity of work in this field. Although these methods have merit in determining surface shape they have not been used for CMM applications.

Blake et al. [94,49] developed a method of active range sensing for the detection of features or objects, using the trinocular stereo method which employs two projectors each of which projects a pattern of stripes onto the object. Although this system could detect the general shape of the object, it could not equally process the image patterns on each side of the object which resulted in losing some of the data at the weaker side (the side opposite to the line of camera projection). This was caused by placing one camera at an angle to the projection axis of the light stripes. There was also a need for careful alignment of the patterns projector with the camera in order to avoid the computational expense of constraint propagation and the problem of ambiguity of the node positions (intersections of the light stripes). It was claimed that the system worked well in a laboratory environment over a working volume of a 50 mm cube with a depth of resolution of around 0.2 mm, however, there appears to be no significant industrial application of this method.

Celenk and Bachnak [95] designed a stereo vision method for 3-D information extraction and surface reconstruction of objects in a robot workspace. They used a number of camera pairs to view the objects. The camera pairs were defined with respect to a coordinate system datum and placed at the maximum allowable distance from the datum in order to use the minimum number of cameras that cover the workspace entirely. The system requirement was; a knowledge of the common area between the left and right images, relationship between image planes and scene domain, and the internal and external parameters of the system. The system was required to input an initial guess (prior knowledge) for the surface in order to be able to reconstruct the surface accurately. The degree of accuracy, speed of camera calibration or the matching procedure was not stated. Although this approach would have potential for a CMM it is believed to be expensive and complex.

Information about features can also be derived by image matching methods, Blisset et al. [96] developed a system for surface perception which was based on matching 2-D images in order to generate 3-D information. They developed a generic vision technique for locating surfaces in scenes from imagery using one or more moving T.V. cameras. In their scheme, information was extracted from a pair of video image sequences from different view points (originally taken from a single moving camera), and combined to form an explicit 3-D representation of the scene under observation. The approach was contrasted with model based vision in which predefined models of all expected or allowed objects were matched against what was observed on the image plane. The system was promising despite the fact that it involved complex procedures before 3-D information could be generated.

Shape measurement with the use of three view stereo analysis has been dealt by Ito and Ishii [97]. They used a stereo analysis method using three views, in which image correspondence could be

established from images taken from triangularly configured viewpoints. The method mainly worked by analysing the first and second images, with the third image used to avoid ambiguity. The method of stereo analysis selected edge points of elements as a matching unit between images. In order to use the system, the cameras needed to be calibrated which was done by observing several dozen circular marks (on a mark board) by a CCD camera which was placed at a known position. The system claimed to have advantages over the other stereoscopic methods, such as; the match points would be examined independently, and images threshold levels could be found faster. Unfortunately it appears that the system would experience some difficulty if it was applied to curved feature objects (due to the absence of an edge).

Fringe pattern interferometers have also been used for feature shape measurement of components. Burton and Lalor [98] researched on component shape measurement where they employed opto/computer techniques to determine the 3-D coordinates of feature points on a wide range of component surfaces. A fringe projection interferometer illuminated a surface to create interference patterns consisting of a series of equally spaced straight fringes. These fringes were projected onto a surface where a CCD camera was placed in a different direction to observe them. The analysis of the patterns by the use of Fourier transformation fringe analysis [99] revealed information about the shape of the surface. The system would have difficulty to be applied to small industrial products since a low resolution CCD camera was used.

4.2.1 Automated inspection by CMM

In order to inspect a feature automatically, it is essential to know its location which needs to be identified, manually, by the use of vision analyses, or during computer aided design. Once the feature location has been identified to a CMM, the machine needs to execute a programme or routine to assess the feature. The problems to be considered for sculptured features are, probe access, orientation, number of sample points, and efficient probing strategy.

Since 1980 a number of systems have been developed to enable automatic generation of CNC CMM codes for feature measurement and inspection directly from a CAD system [3,5,36,39,40,75,100,101]. The significant examples of these are presented, however, for sculptured parts with no definable features, these systems are difficult to apply and a new method needs to be developed to enable easier generation of measurement routines from the identified features.

Takeuchi et al. [4] worked on developing a method for automatic measurement of workpiece dimensions by placing it arbitrarily on the table of a CMM. The integrated system consisted of a CAD system, an image processing system and a CMM. The CAD/CAM system generated a measuring path through the solid modeling technique and measuring points for each primitive

shape on the workpiece. The image system was used to locate the position of the workpiece on the CMM table and algorithms developed to translate the CAD data to the coordinate system of the image. The system has been applied to workpieces having primitive shapes and further work is needed to develop strategies for more complicated objects.

The work of Pahk et al. [76] is considered here since they used a similar concept in order to develop a Computer Aided Inspection (CAI) system with a CMM for moulds having sculptured surfaces. Like Takeuchi et al. they used a CAD environment to select features to be inspected. The inspection planning and the distribution of measurement points has been controlled through the CAD planning system.

The configured system was based on three modules:— i) a CAD inspection feature selection module which dealt with the feature generation and selection, ii) a computer inspection system which dealt with inspection planning, path simulation and error evaluation, and finally iii) a CMM measurement operation module responsible for part alignment, measurement, and data saving or transferring to the CAD system. The part alignment was done by comparing the CMM measurement and the CAD data. The system has shown potential for sculptured part applications however a CAD model is required.

Medland et al. [102] developed a strategy to enable CMMs to inspect features by the selection of a set of sample points on a part (i.e., sample grid approach) and from these inferred information about geometric features. The objects were created as solid models by the use of a process plan and the tool motion over the solid block. A network of reference points was applied to the specified surfaces of the individual primitives used in the creation of the part. Through the procedure of the sample grid approach, the different features from an array of probing points would be deduced. The probing points are spread across the surface of the measured object and they would be eliminated if they were found laying inside or remote from the final solid. The creation of the sample grid was done during the feature construction within the CAD system. The work showed that an automatic inspection procedure could be created to integrate a CAD system with a CMM, however, the system only seemed to be suitable for prismatic parts.

Gupta and Sagar [5] worked on an automatic inspection process by integrating a CMM and CAD system. The system captured 3-D point data from a master component using the CMM in the teach mode and replayed the procedure for repetitive measurement of a batch of identical components in the replay mode. The measurement programme guided the operator through the measurement phases by requiring the operator to input the element types, the number of points and the direction of measurement. From the data points surfaces could be made and evaluation procedures were developed in the CAD system. However this tended to be a slow manual process.

4.2.2 Review of previous work at Loughborough University

There are number of methods, such as erosion, dilation, and coding/labelling which could be used within image processing systems to identify surface features. These methods have limitations and in previous work [103] dilation and erosion methods were used to identify surface dimples which resulted in a coarse determination of the approximate location of some dimple centre coordinates. Dimples in close proximity may appear to be joined and fig. 4.2 depicts the basic idea of using these methods for separating joined dimples. In fig. 4.2(a) two dimples are shown connected to one another. Figs. 4.2(b) to 4.2(d) show how the two dimples are deformed and separated.

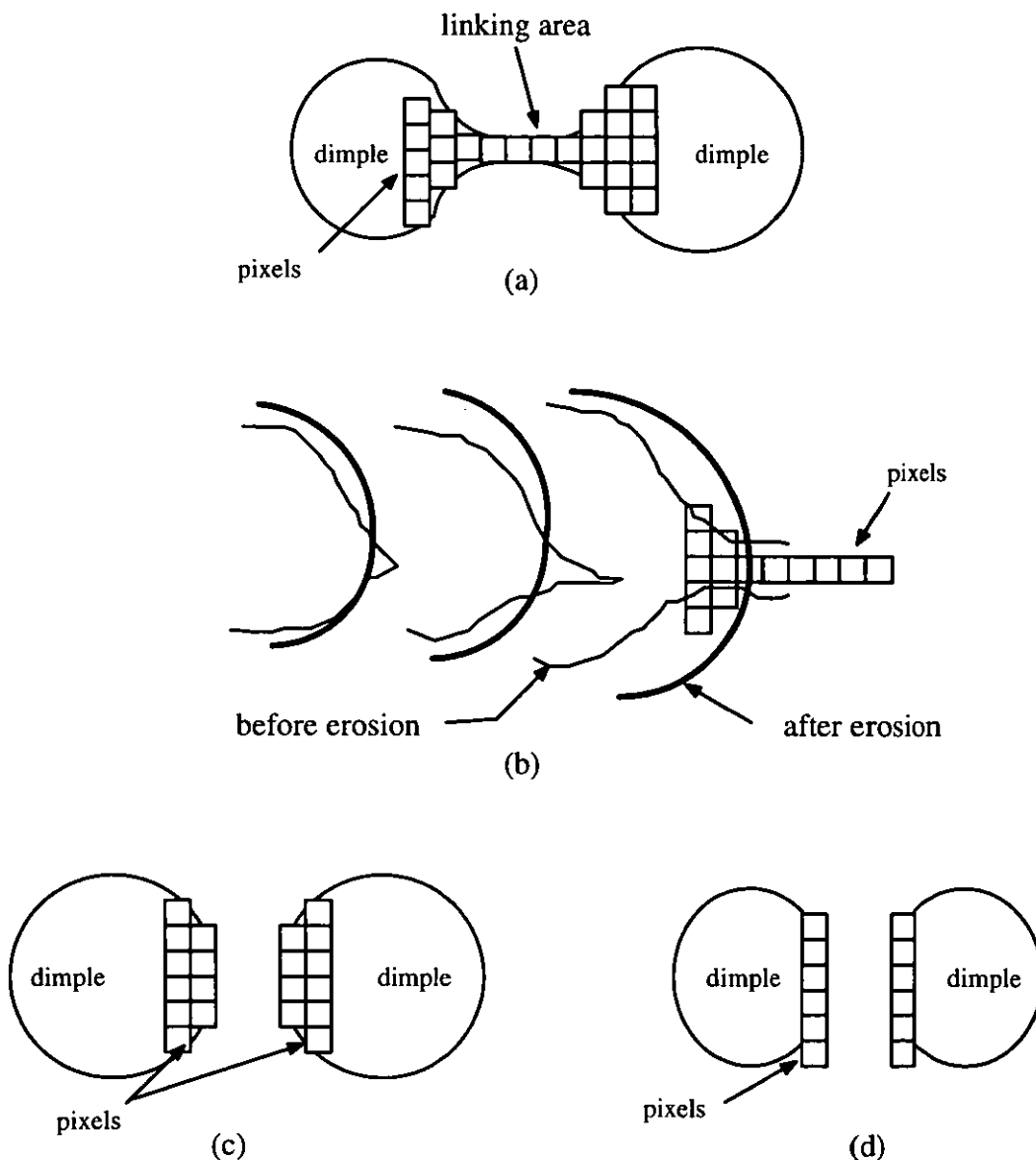


Fig. 4.2. Dilation and erosion effect on dimples.

The dilation and erosion methods for this work used the change of intensities of the pixels at the boundaries of the dimples. These methods have been applied to 2-D CAD drawings of golf balls.

The method used the difference in intensity level of the dimple boundaries to that of the background and by eroding and dilating the area within these boundaries, the centre of each dimple was reduced to a dot or small number of pixels.

One of the main problems with this method was not knowing the required number of iterations for each determination since the dimples were of different sizes and therefore some would reduce to one pixel sooner than others. The best result obtained was about 35 per cent of the dimples on a half of the cubic pattern ball. A major weakness of this approach was the inability to detect dimples around the golf ball equator where the majority of the dimples are concentrated. Dimples in this area needed fewer erosions to those at the centre of the ball image because the dimples in the centre are bigger and are more easily identified.

This result was achieved using a good quality 2-D CAD generated drawing, when using a real ball it is likely that the results would be worse.

4.3 Proposed integration method in this work

The use of 3-D CMMs for the measurement of objects is well established in manufacturing industries and the use of touch probe methods has enabled accurate measurements of prismatic parts. However, accurate measurement of sculptured surfaces still presents some problems and there is still no general automated inspection method or system available. Nevertheless, there are many CAD and CMM integration systems in which the CAD software helps to generate the inspection routines.

In many instances no CAD model of the objects exist and the "clay" model is in fact the design specification. In this situation the model needs to be measured in a suitable way such that the information can be input to a CAD system for further processing and development of manufacturing information. Programming of a CMM to suit such a system is a lengthy business and the ability to generate programmes automatically is not available. When a component has many features such as a golf ball the machine vision is an attractive solution to the problem of locating dimple centre coordinates which then can be transferred to a 3-D CMM for an accurate measurement of the dimples. Vision methods currently available do not have the required accuracy to measure the features accurately. However, a vision system could be used to provide an approximation of the component position which can be used to programme the CMM for probing.

This method is based on the concept of look and touch and consists of a Matrox machine vision system for the generation of the approximate location of the features and two CMMs, a Ferranti Merlin and a Brown and Sharpe Xcel Tesa. The CMMs were equipped with a Renishaw motorised probe head arrangement which inspects the features precisely to a high order of accuracy. The

system is integrated to a CAD system to represent the inspected model graphically and to model the errors within the product. This method should be applicable to many products about which there is a prior knowledge of the shape.

4.3.1 Method of feature detection

One of the main problems when looking at features using a vision system is determining the extent of features. In prismatic parts distinct edges are present which identify a feature and it is also possible to construct the feature shape by implication of the feature location, for example intersection of planes. However, the case of sculptured parts is more difficult due to not knowing the general shape of the features or the extent. Using a machine vision the information which could lead to recognition of the features could be interpreted from shadows, from surface discontinuities and suitable lighting, however, this is a subjective process. Preliminary tests using a vision system indicated that the features needed to be enhanced in order to identify them before digitisation. A number of different techniques were used to develop a simple technique for feature detection. In this study the feature marking method used is based on manually placing a small dot inside of each feature with a marker pen.

4.3.2 Identification of dimples

In order to develop a system to identify the dimple positions on a golf ball with the use of a 2-D vision system two stages were investigated; 1) use of 2-D models i.e., CAD plots and, 2) use of real golf balls.

In the first stage CAD 2-D drawings of golf balls were used with dimples shown as circles when they were close to the centre of the drawing, and deforming to ellipses towards the edge, fig. 4.3 is a 2-D CAD model of a golf ball which was produced to the design specification with circular dimples presented in a cubic pattern. The initial intention in the use of 2-D plots was to test and develop methods on clear images. Prior to identifying dimple centres the image needed to be prepared by removing unwanted portions from the image, e.g., surrounding marks etc.

To detect dimples on a white golf ball it was necessary to enhance the dimples from the background, since only a small number of dimples could be detected due to the lack of contrast between the features and the ball. There were a number of ways which dimples could be presented for image capturing such as; colouring dimples black or colouring the lands between the dimples, fig. 4.4 shows the colouring arrangements on golf balls. There were number of problems encountered when golf balls were used such as, they have shiny surfaces, no sharp edges which could be used to generate enough contrast for identification, and finally they are the same colour as the

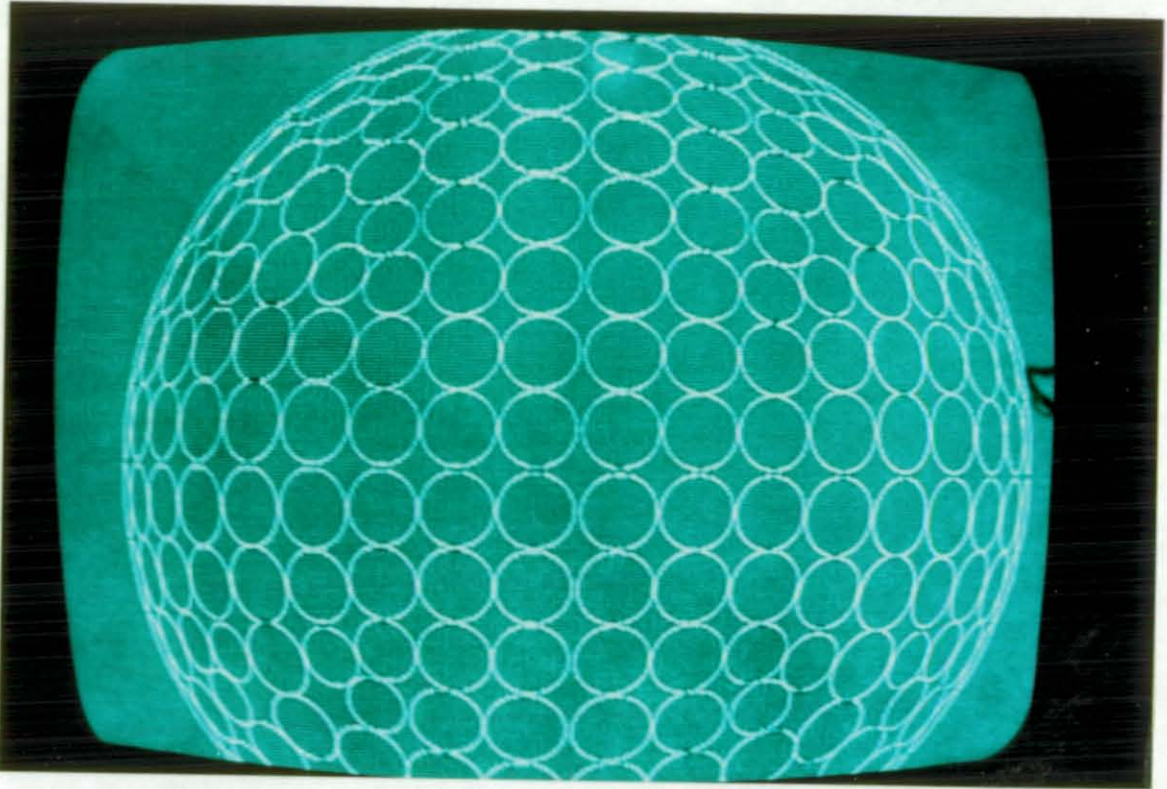


Fig. 4.3. 2-D golf ball CAD drawing (cubic pattern).

dimples. A number of experiments were done to matt the ball surface in order to reduce the reflectivity which had little success. A unique solution was needed in order to deal with above situations with a high degree of reliability. Eventually a simple dimple marking method proved to be the easiest, most reliable, fast and clean technique which was achieved by putting a black dot in the approximate centre of each dimple see fig. 4.5.

A reasonable black dot was assumed to have a diameter between of about 1.5 mm on the ball with relevant pixel representation of 13 to 17 pixels. A ball with 42.33 mm diameter was represented by the vision system for about 380 pixels in x-direction and 450 in y-direction.

When the dot colouring method was used nearly all the dimples were identified and only those which were found very close or connected to one another were identified as problems. A similar problem was detected when the dots were drawn too long or small. However, by adjusting the camera aperture and normal zooming it was possible to reduce the loss of dimples. All of the dimples in a pattern were detected when a reasonable sized dot was placed inside of each dimple, and up to 5 per cent error (about 10 dimples) was found when the whole image of the marked golf ball was examined. Using coloured lands took more time manually and an average of 20 per cent error was recorded.

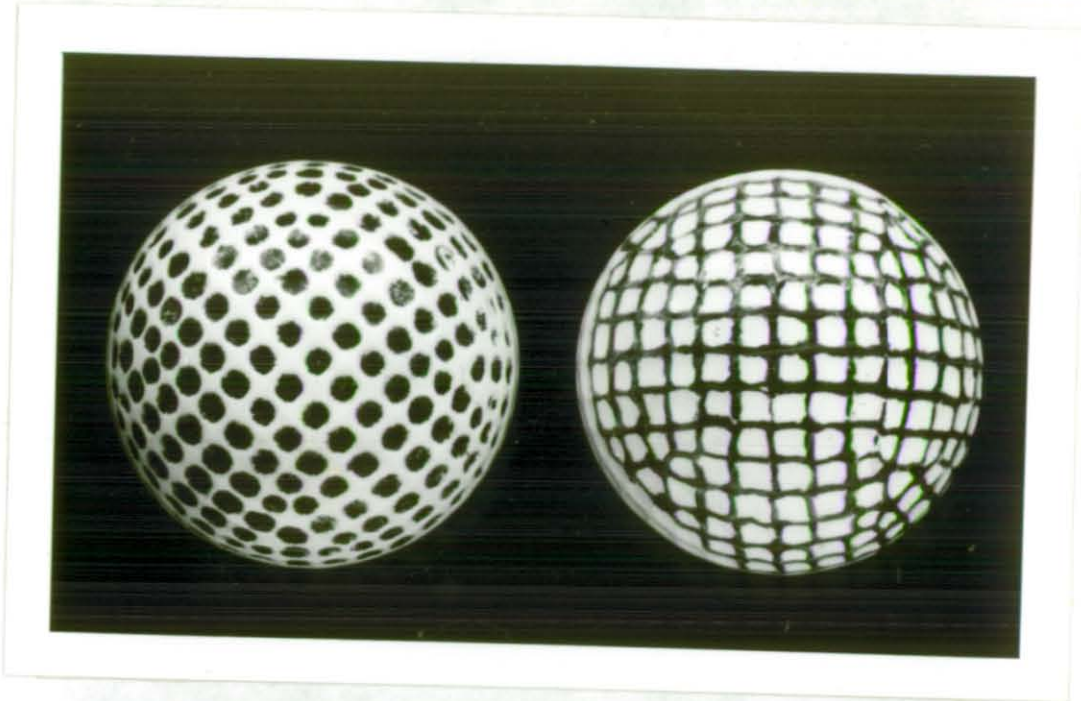


Fig. 4.4. Dimple Colouring Arrangements.

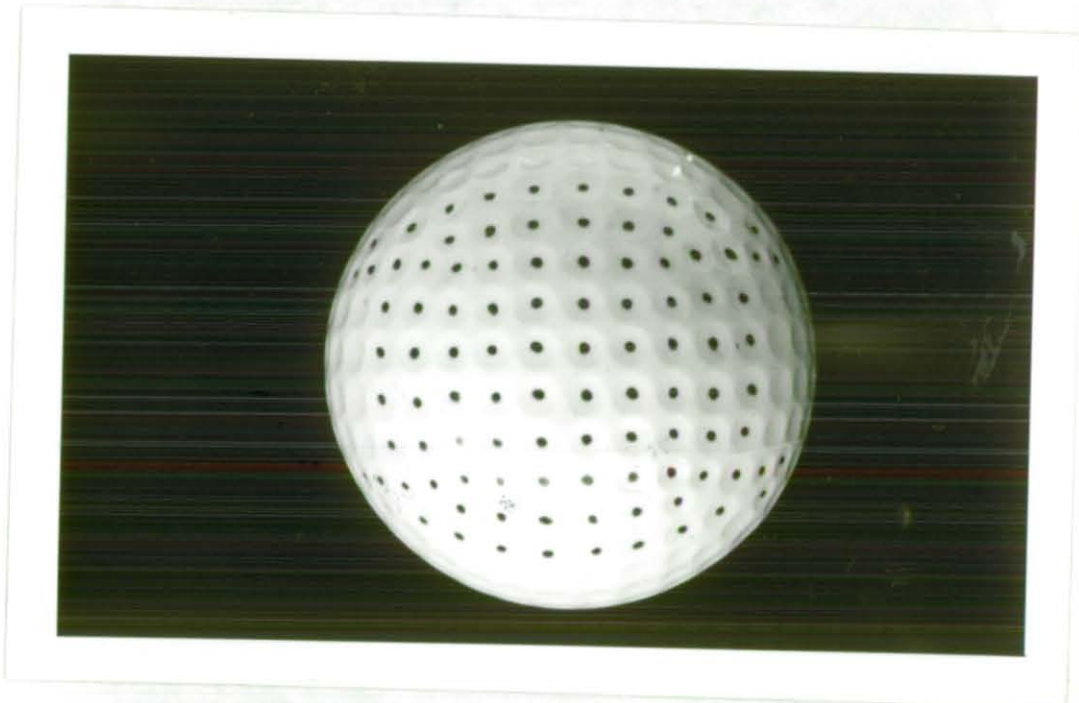


Fig. 4.5. Hand marked dimples on a golf ball.

4.3.3 Dimple centre detection from 2-D images

The method of dimple detection eventually used by the use of vision machine was named the "Route approach" which was designed to detect various size dimples (dimples between 2 to 5 mm of diameter). However, in real situations the diameter of dimples on golf balls rarely exceeds 3.5 mm. As mentioned earlier a dot (mark) was placed inside of each dimple and the system identifies

the centre of each dimple through assessing this dot by first detecting four edge points. The first two points will be detected through vertical pixel searching and the last two through horizontal searching. Fig. 4.6 depicts the procedure of finding a dimple dot centre. The method was arranged to analyse each pixel in the image in order to detect intensity differences. The pixel reader reads the intensity of the datum pixel (i.e. $X=0, Y=0$) which was placed at the top left side of the image. In a binary image, the dimples were given a zero intensity (black) and 255 to the background (white) in an image of 512 x 480 pixel resolution. The intensity level of each pixel in the image was then checked to determine if it is part of a dimple dot or not. In the binary image the dimple dots were given black intensity and when the pixel reader detected a black pixel along its route it changes its direction vertically downward and the point would be recorded as edge 1. The pixel reader continues reading pixels vertically downwards until a second change of intensity is found which should be a change of a black to white pixel. This point will be accepted as edge 2 and the mid point of these two calculated in order to guide to find edge 3 and 4 which uses a similar search procedure except in the horizontal direction. An imaginary horizontal line is drawn at the mid point between edges 3 and 4 to determine the dimple dot centre.

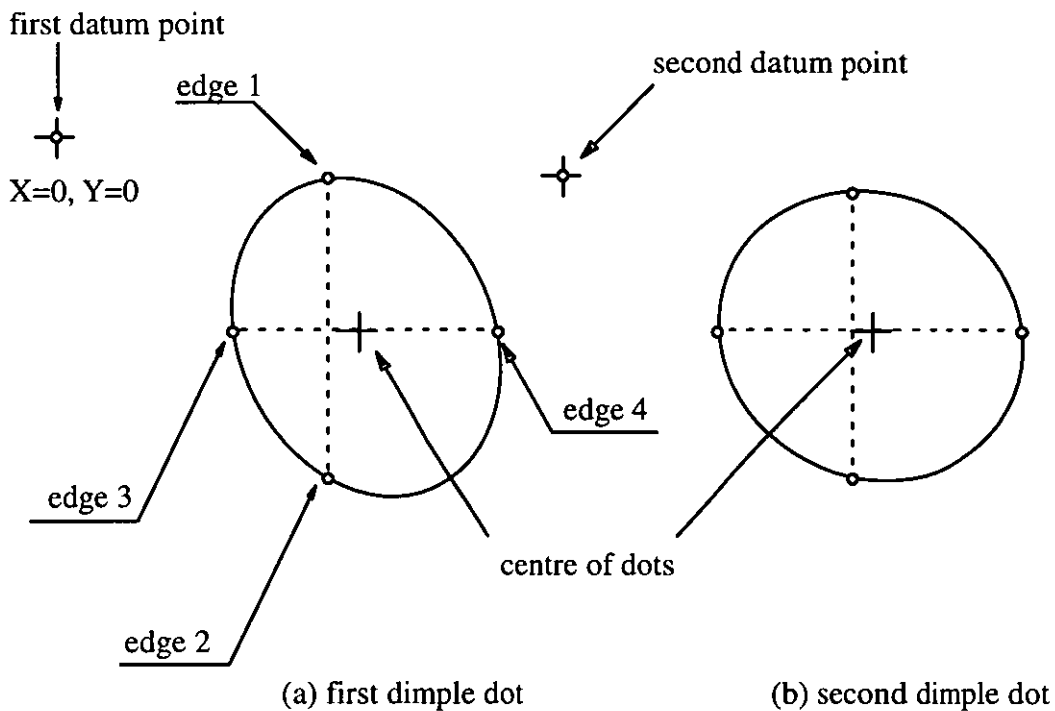


Fig. 4.6. The route approach method.

The above procedure was arranged to be repeated for the next dimple dot and so on until the entire image was examined. The recorded centres were arranged in X, Y format to be used for calculating the Z dimensions.

4.4 2-D lens correction factor for spherical products

When a 3-D data point is represented by a 2-D vision system, the system positions points from the object into a plane coordinate system. This is known as 3-D to 2-D translation which abandons the third dimension of the object. The dimple information is required in a horizontal plane as shown in fig. 4.7.

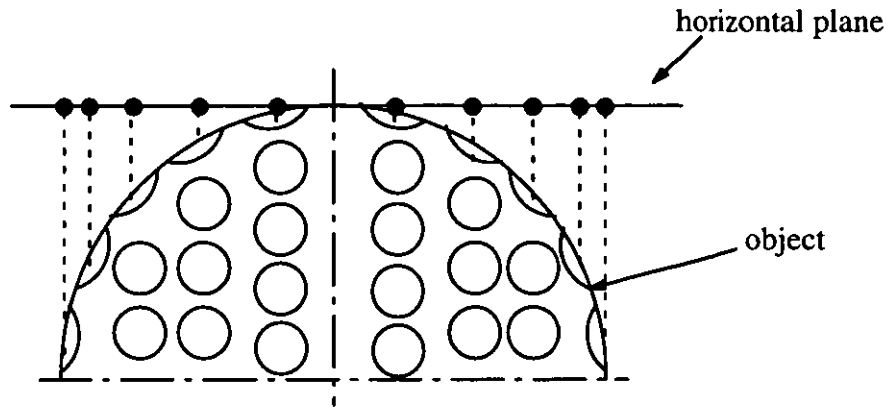


Fig. 4.7. Projection of dimples onto the horizontal plane.

Unfortunately most optical systems use lenses to focus light, which causes some discrepancy between the measured and the actual values. For golf balls the discrepancy values become significant especially for those dimples close to the equator and a Discrepancy Factor (DF) is required to compensate for them. The discrepancy acts radially from a point vertically above the object centre [32], and therefore the Discrepancy Radial (DR) error will be non linear. In this case the object is imaged on a plane CCD array at a distance f from the camera lens as shown in fig. 4.8. Point A on the object translates to point B on the map plane at a distance m from the origin. The required value is e . Fig. 4.8 shows the error as value g which translates to value DR on the CCD array. The calculation of this error is given in fig. 4.8.

An example is given for a ball with the following arrangement, r was selected between 8 to 0 mm, the ball radius R was 21.00 mm, a 25 mm focal length lens f with the camera placed at 200 mm above the object. The variation in DR error is plotted against radial distance r and is shown in fig. 4.9. It can be seen that a point remote from the centre of image will be significantly distorted.

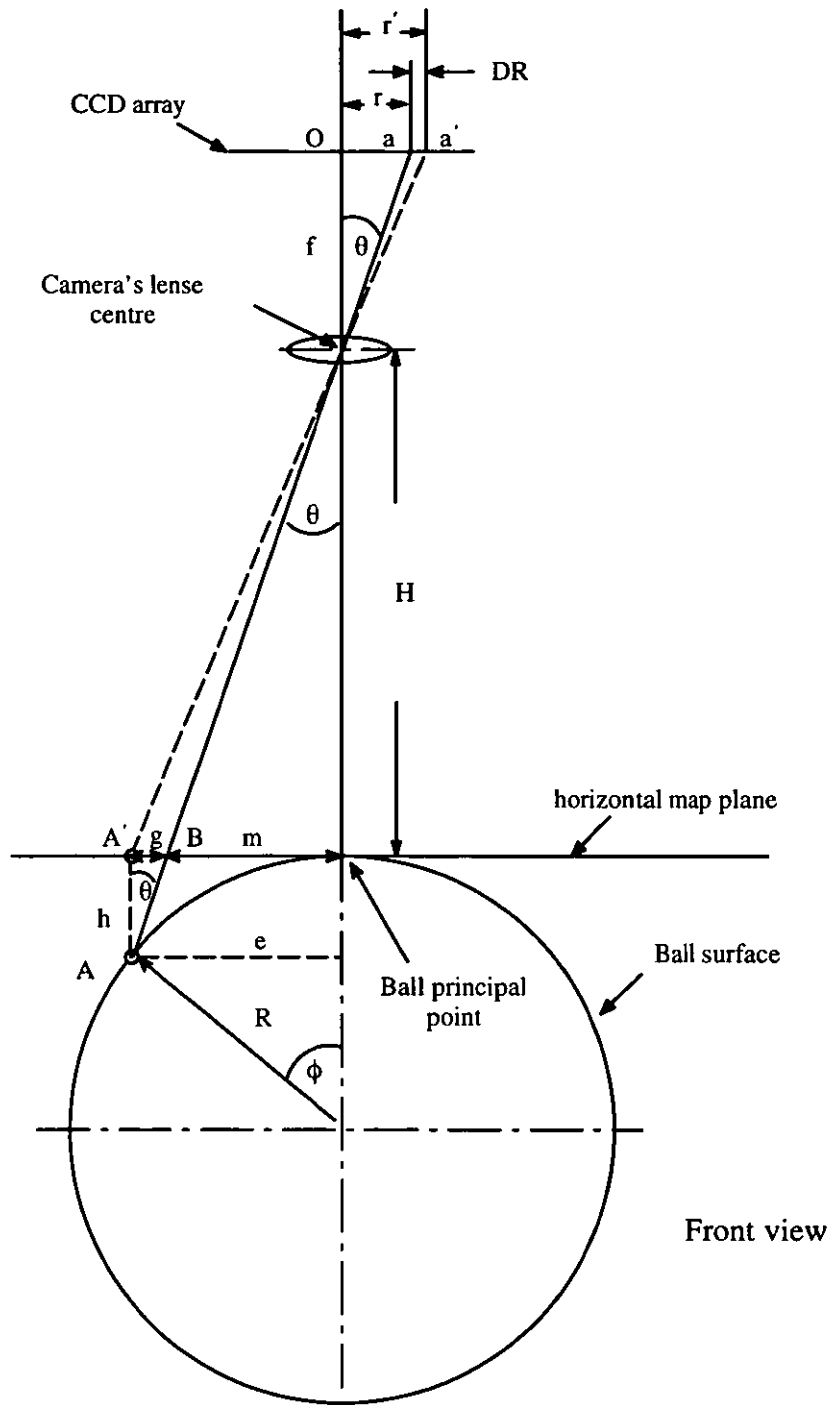


Fig. 4.8. Distortion in 2-D image processing for curved surfaces.

Where;

DR is distortion for ball curvature

a is actual image position

a' is theoretical image position

H is camera height above ball

r is radial distance from principal point to image point

R is the ball radius

f is the camera focal length

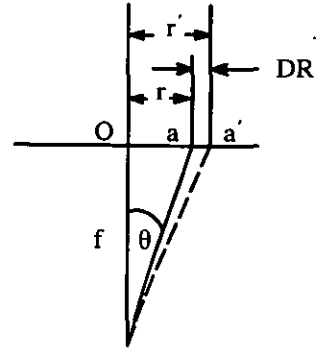
I, B, T, g, m, h, e, O, k and **P** are distances and locations.

From fig. 4.8 similar triangles:-

a) In the camera section,

$$r = f \tan \theta \quad \dots 4.1$$

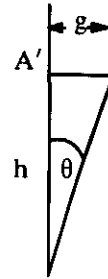
$$\tan \theta = \frac{r}{f} \quad \dots 4.2$$



b) On the ball surface;

$$g = h \tan \theta \quad \dots 4.3$$

$$\tan \theta = \frac{g}{h} \quad \dots 4.4$$



Equating expressions 2 and 4,

$$h = (g) \frac{f}{r} \quad \dots 4.5$$

From similar triangles POa and PTB,

$$\cos \theta = \frac{H}{k} = \frac{f}{I} \quad \dots 4.6$$

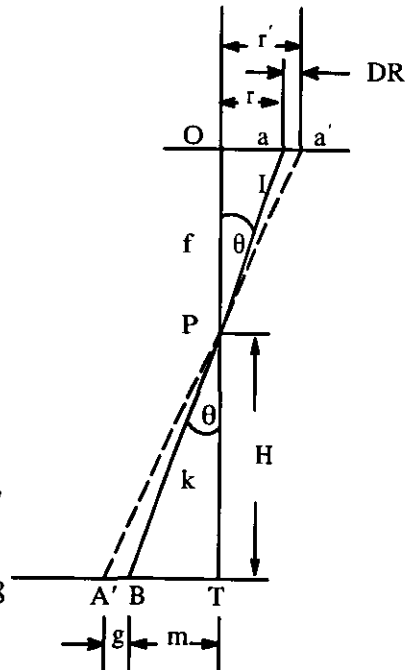
$$\therefore k = \frac{H}{\cos \theta} = H \sec \theta$$

$$I = \frac{f}{\cos \theta} = f \sec \theta$$

Also, from similar triangles PBA' and Paa',

$$\frac{DR}{g} = \frac{f \sec \theta}{H \sec \theta} \quad \dots 4.7$$

$$DR = \frac{gf}{H} \quad \dots 4.8$$



For the ball section;

$$e = m + g \quad \dots 4.9$$

$$e = R \sin \phi \quad \dots 4.10$$

$$m = H \tan \theta \quad \dots 4.11$$

Equating 9 and 10, and substituting 3 and 11 in 9 give,

$$R \sin \phi = H \tan \theta + h \tan \theta \quad \dots 4.12$$

$$R \sin \phi = (H + h) \tan \theta$$

also h can be expressed as;

$$h = R - R \cos \phi \quad \dots 4.13$$

$$R \cos \phi = (R - h)$$

To eliminate ϕ , (12)²+(13)²,

$$\begin{aligned} R^2 \sin^2 \phi + R^2 \cos^2 \phi &= (H + h)^2 \tan^2 \theta + (R - h)^2 \\ \cancel{R^2} &= (H + h)^2 \tan^2 \theta + \cancel{R^2} + h^2 - 2Rh \\ 0 &= (H + h)^2 \tan^2 \theta + h^2 - 2Rh \end{aligned} \quad \dots 4.14$$

Substitute 5 in 14 gives,

$$0 = (H + \frac{fg}{r})^2 \tan^2 \theta + (\frac{fg}{r})^2 - 2R(\frac{fg}{r}) \quad \dots 4.15$$

Also, substitute 2 and use from 8 in 15,

$$0 = \left[H + \frac{H(DR)}{r} \right]^2 \frac{r^2}{f^2} + \frac{(H)^2(DR)^2}{r^2} - 2R\frac{H}{r}(DR) \quad \dots 4.16$$

Rearranging 16 will give a quadratic equation in (DR);

$$\begin{aligned} 0 &= (H)^2 \frac{r^2}{f^2} \left[1 + 2\left(\frac{DR}{r}\right) + \left(\frac{DR}{r}\right)^2 \right] + \frac{(H)^2(DR)^2}{r^2} - 2R\frac{H}{r}(DR) \\ 0 &= (H)^2(DR)^2 \left[\frac{1}{f^2} + \frac{1}{r^2} \right] + 2H(DR) \left[\frac{Hr^2}{f^2r} - \frac{R}{r} \right] + (H)^2\frac{r^2}{f^2} \end{aligned} \quad \dots 4.17$$

(DR)² very small – ignore the term including (DR)²,

$$2H(DR) \left[\frac{Hr^2}{f^2r} - \frac{R}{r} \right] = - (H)^2\frac{r^2}{f^2} \quad \dots 4.18$$

$$2(DR) \left[\frac{Hr^2 - Rf^2}{rf^2} \right] = - \frac{Hr^2}{f^2}$$

$$DR = - \frac{Hr^2}{f^2} \times \frac{rf^2}{2[Hr^2 - Rf^2]}$$

$$DR = \frac{- Hr^3}{2[Hr^2 - Rf^2]}$$

$$DR = \frac{Hr^3}{2[Rf^2 - Hr^2]} \quad \dots 4.19$$

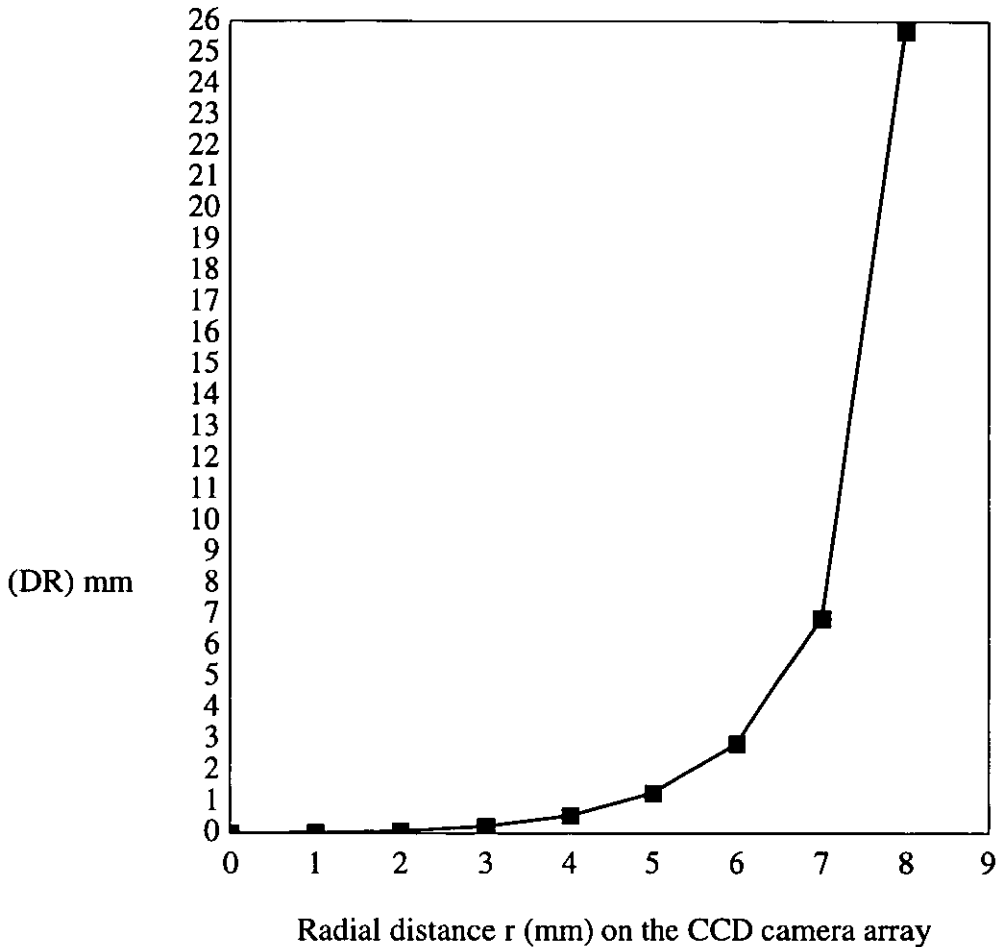


Fig. 4.9. Relationship of DR over a CCD camera array.

4.5 Calculation of feature height

One of the main problems with the use of a 2-D vision system for feature detection is determining the feature height in relation to a datum surface or reference point. A number of perceptive methods were considered by which the height of the surface features could be determined. The methods can be explained as Z-layer method, segmentation (zone approach), and 3-D calculation of dimple locations method which will be discussed in the following sections.

4.5.1 Z-layer approach

One method of obtaining height values is the Z-layer method if the shape of the product is known. The height of the feature was divided horizontally preferably in equal slices (n layers), see fig. 4.10 and the coordinate axis placed inside of the ball with Z-axis vertically upward. Once the object is identified by the vision system, the X and Y coordinates of each feature can be calculated by analysing the pixel location and the Z height selected according to these values. For example larger X and Y values indicate the lower Z layers. This approach was considered inadequate since the dimples are not positioned in a layer manner.

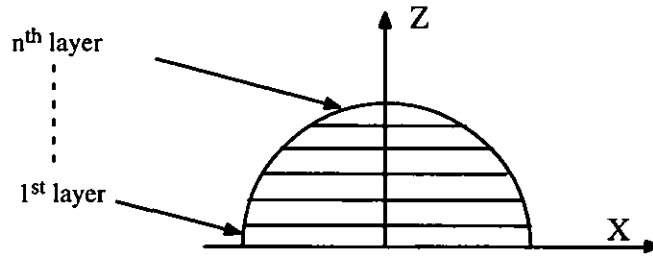


Fig. 4.10. Z-layer arrangement.

4.5.2 Segmentation approach

In this approach the object was sectioned into a number of segments and a probing strategy developed based on the probe access to each section. The position of a feature or dimple will then be matched with the segments in order to find the appropriate segment to which the Z height is previously determined with respect to the ball axis. Clearly there will be as many optimum probe orientations as there are dimples and in order to save time a limited number of zones was considered. After a number of experiments it was decided to divide the ball into 3 horizontal layers, see fig. 4.11(a). The ball was then divided into 8 segments, fig. 4.11.(b). The intersection of the horizontal and vertical sectioning produced 17 zones as shown in fig. 4.12. An intuitive approach has been used to create the probing zones and a more rigorous analysis may have produced a better result. The approach used was unable to organise the probe to be normal to the surface of each dimple and this had a direct effect on the accuracy of the dimple measurement.

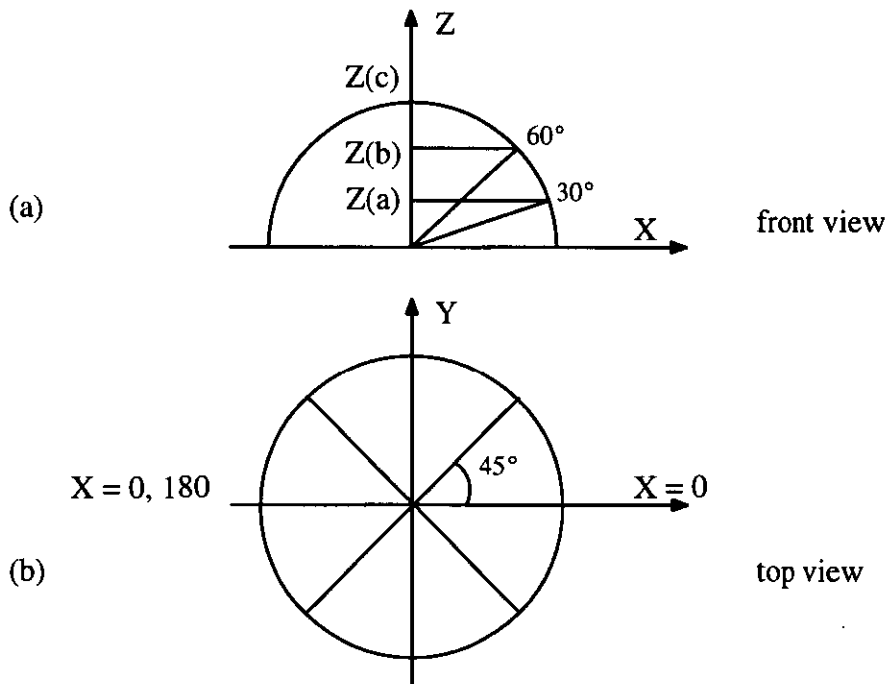


Fig. 4.11. Configuration of the positions for the Hob.

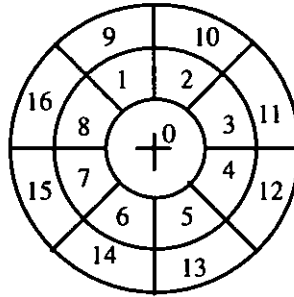
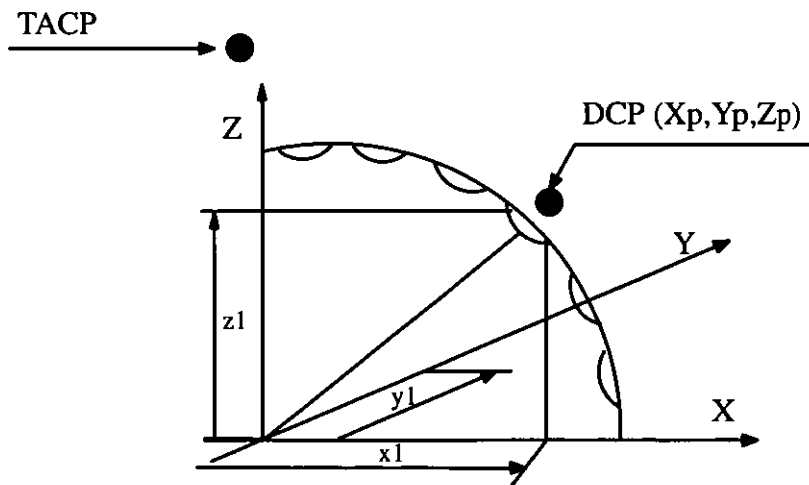


Fig. 4.12. The 17 tip position areas.

It is important to consider collision possibilities when moving the probe to its measuring position. The probe starts at the Tip Angle Changing Position (TACP) (100 mm above ball axis) and the required orientation selected. The probe is then moved to the Dimple Clearance Position (DCP) which is calculated from the dimple centre obtained from the vision system. The clearance coordinates are found by extending the dimple centre coordinates by 10 per cent, see fig. 4.13.



$$X_p = x_1 + (x_1/10)$$

$$Y_p = y_1 + (y_1/10)$$

$$Z_p = z_1 + (z_1/10)$$

Fig. 4.13. Tip angle changing position and dimple clearance position.

4.5.3 3-D calculation of dimple locations

As explained earlier, the use of a 2-D vision system will not give the depth or Z distance. In order to calculate the third dimension, an extensive set of tests were carried out on golf ball hobs which were made of high stainless steel with accurate dimple nominal positions. The dimples on the hob have been produced to a high order of accuracy (0.01 mm) by the process of Electro Discharge Machining (EDM). Fig. 4.14 shows two golf ball hobs and the balls on their holders. To reduce

the complexity of the 3-D calculation of dimple positions experience showed it better to move the vision system reference point from the top left corner of the image to the centre of the ball or hob.

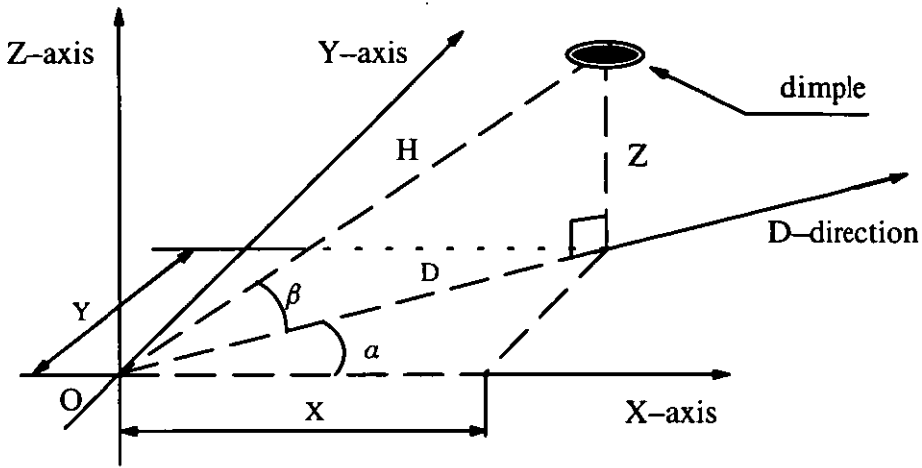


Fig. 4.14. Golf ball hobs and the ball holders.

The hob dimensions needed to be input into the system and the position of each dimple centre was calculated relative to the centre of the hob (datum point). The hob dimensions (the hob centre and the diameters in X and Y directions) were achieved quickly by the use of a piece of vision software named PC-Image marketed by Microsoft® company. The software was able to give the location of pixels on the image by screen digitising. The reference point was set at the centre of the hob and in order to calibrate the ball image for processing of the dimple positions, the diameter of the hob had to be measured by the CMM and converted into pixels.

Once the above procedures were completed the 2-D image would then be scanned to identify the dimples as discussed in section 4.3. The height of the dimple is dependant on its distance from the ball centre and its calculation is shown in fig. 4.15. It is assumed that the dimple centre lies on the ball sphere. Figs. 4.16 to 4.19 represent the process of dimple detection from an image which was captured by the vision system. After the detection of each dimple a black pixel was placed at the centre of the dimple and the final result was a set of X, Y and Z values in millimetres relative to the hob centre. Better images of processed dimple centre dots can be seen in fig. 5.16.

The dimple centre coordinates are then converted from pixel values into metric units for the CMM system.



$$D = \sqrt{x^2 + y^2}$$

$$\alpha = \arctan \frac{y}{x}$$

$$\beta = \arctan \frac{Z}{D}$$

$$H = \sqrt{D^2 + Z^2}$$

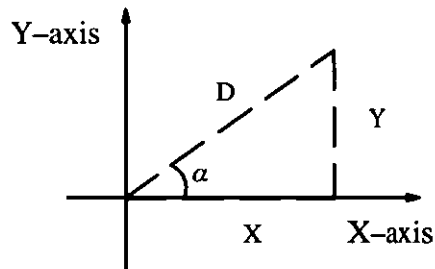
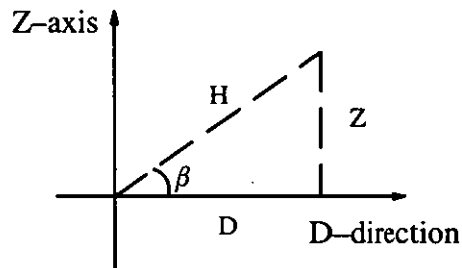
$$H = \sqrt{x^2 + y^2 + Z^2}$$

$$Z = H * \sin \beta$$

$$D = \frac{Z}{\tan \beta}$$

$$X = D (\text{abs}) * \cos \alpha$$

$$Y = D (\text{abs}) * \sin \beta$$



where ;

H is the distance from the ball surface,

O is the ball centre,

x,y are the vision dimple coordinates in mm,

X,Y,Z are the final dimple coordinates in mm,

alpha and beta are angles which make with the dimple.

Fig. 4.15. Calculation of a dimple coordinates.

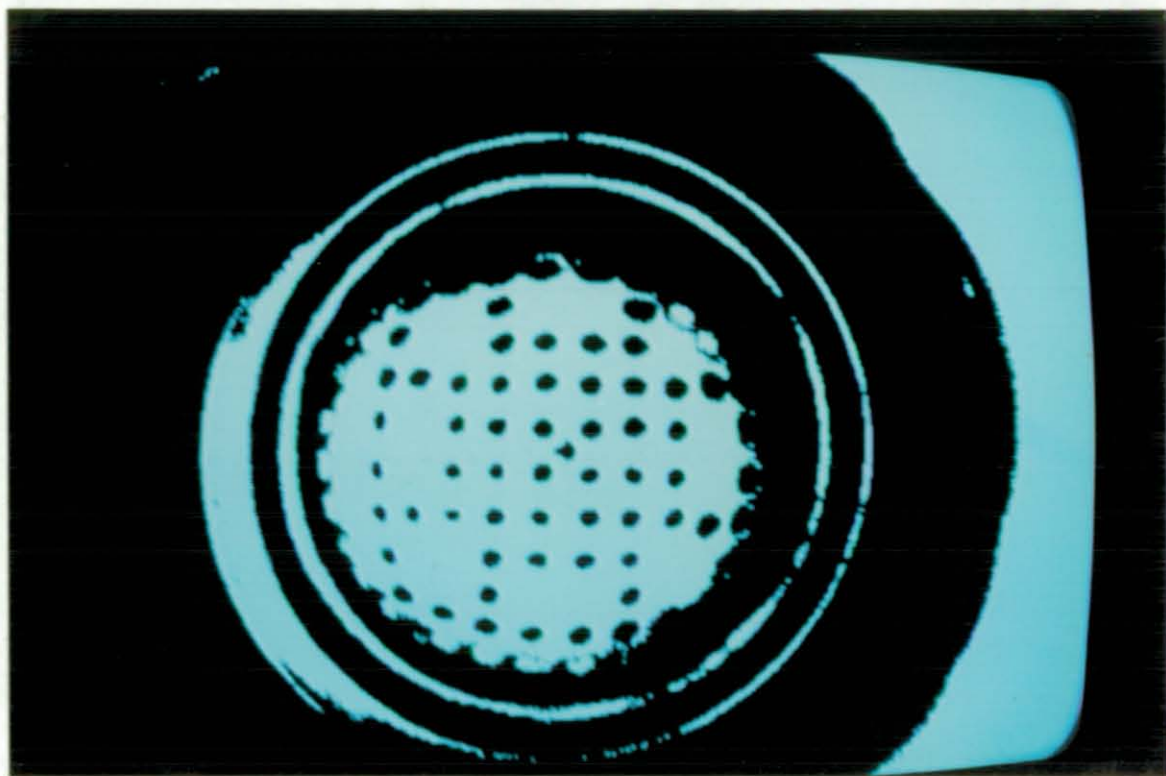


Fig. 4.16. Binary image of the golf ball hob.

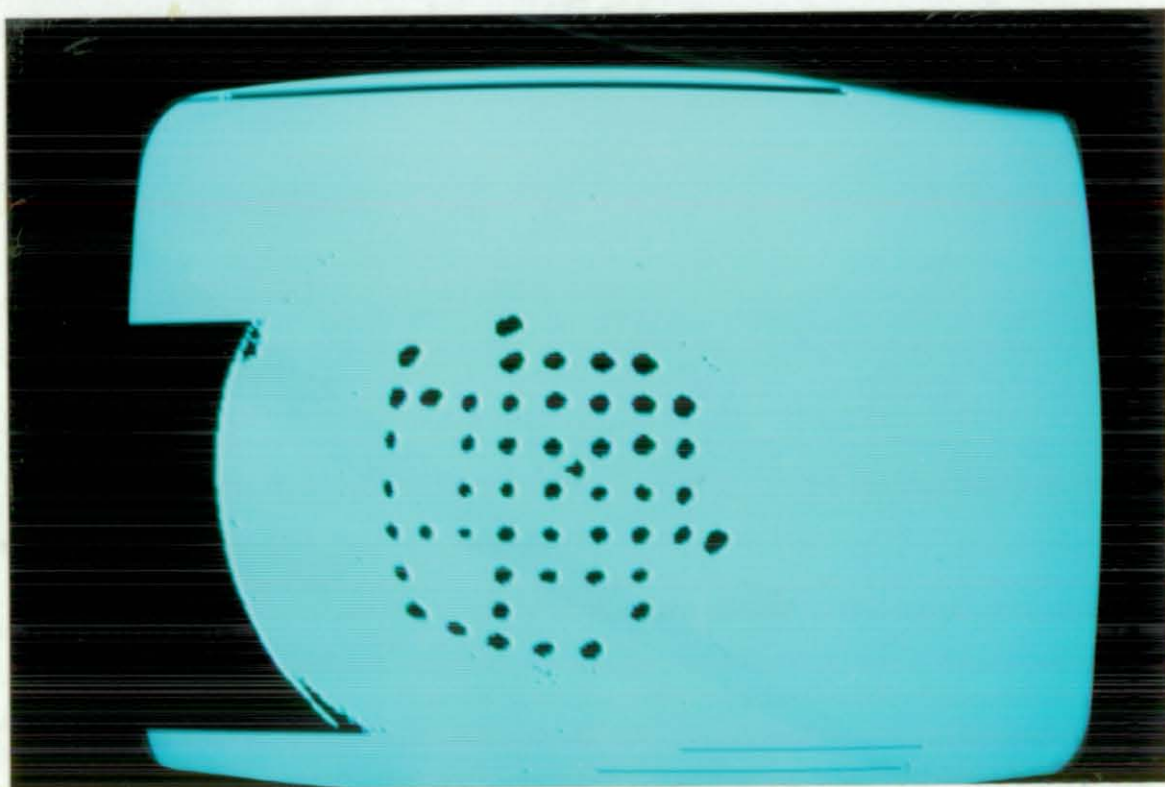
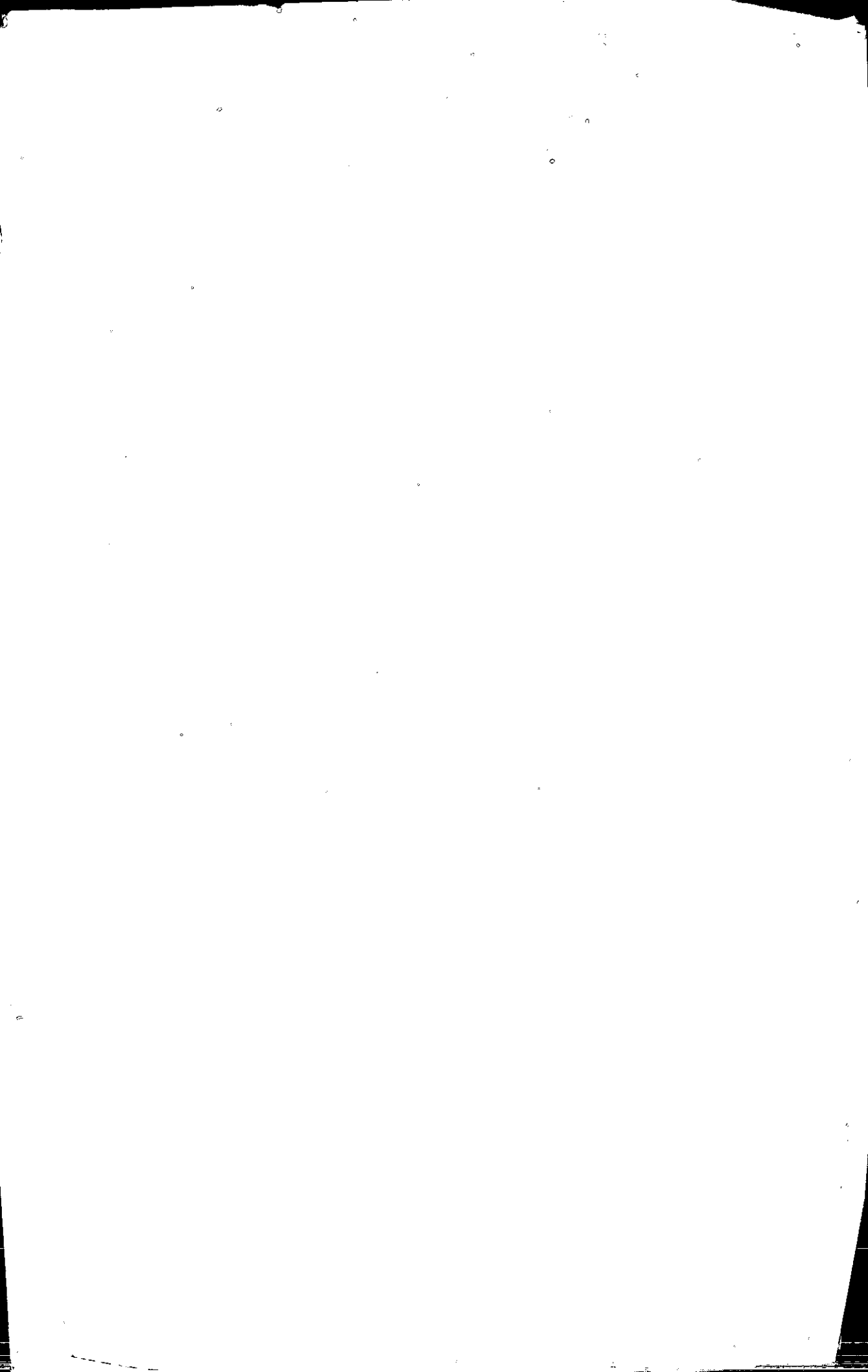


Fig. 4.17. Large unwanted black background is eroding.



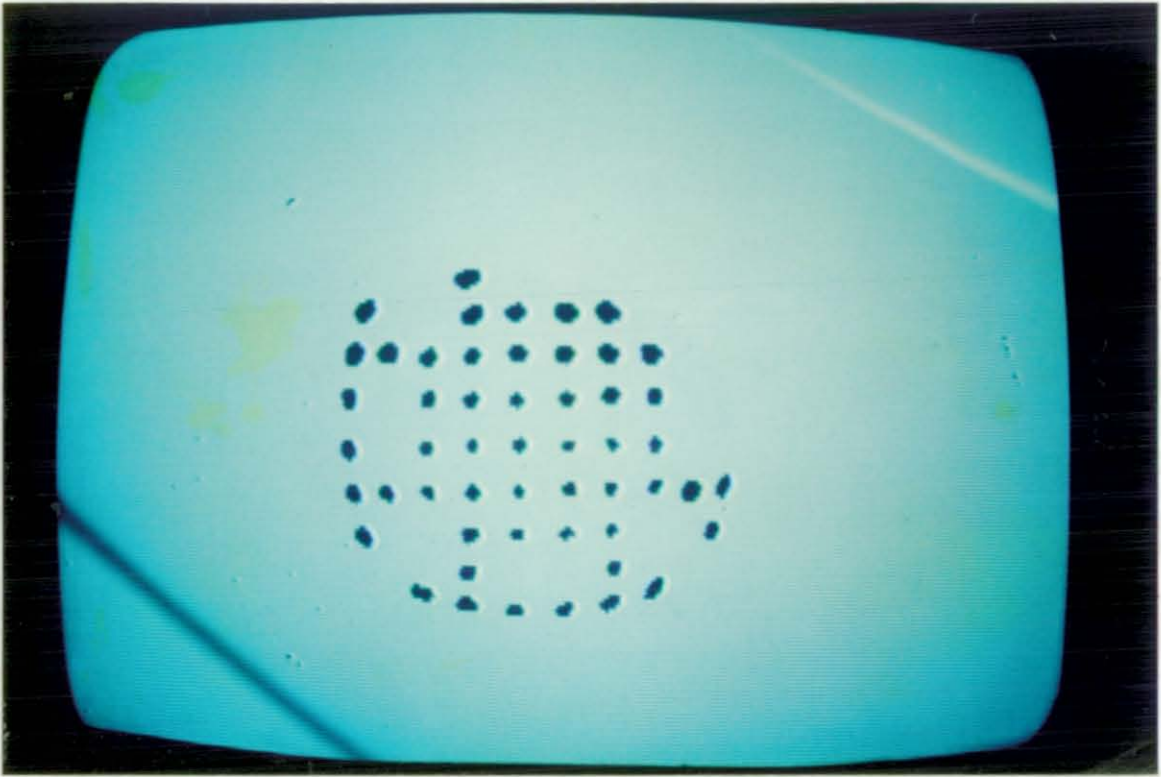


Fig. 4.18. Image with minimum unwanted interferences (final image for dimple analysis).

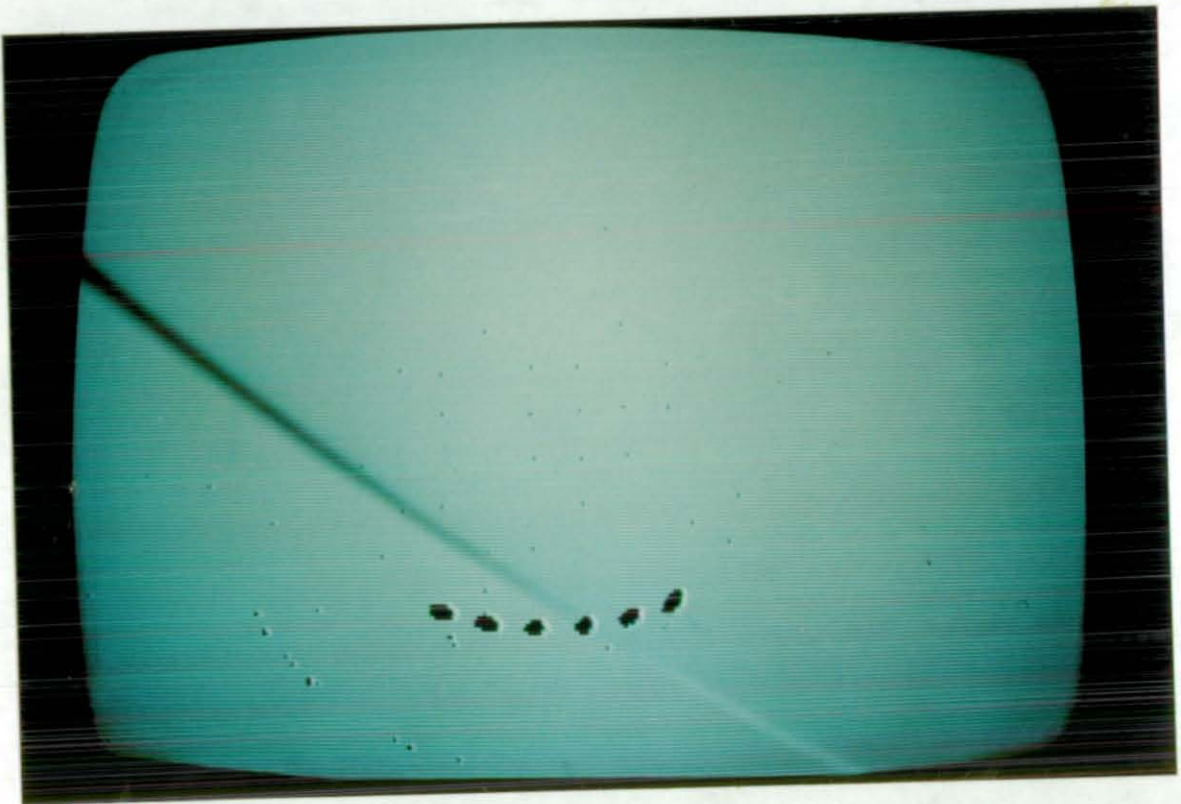


Fig. 4.19. Detecting each dimple and replacing it by a dot.

4.6 System of part and the ball holder

In order to measure a part feature in relation to its origin by a CMM, the part coordinate system and the origin were required to be established and aligned to the CMM axes. As mentioned earlier alignment is the procedure of relating the X, Y, and Z coordinates of a part to that of the machine. CMMs have the capability to do this once certain information about the part is given to them, such as a feature (a plane or a sphere) with a defined XYZ point. However, the feature that is selected to level the part defines the working plane in which the major and minor axes are defined with the third axis perpendicular to this plane.

For convenience of measurement the ball or hob is placed in a holder which generally has a square base, fig 4.20 shows a schematic diagram of the ball holder. This allows the object to be removed from the CMM and accurately replaced. However, the measuring procedure must be able to take the measured component information and align it to the CMM. The significant component dimensions for alignment are the centre of the ball, and a ball reference datum which is always a particular dimple.

The easiest alignment procedure for the hob and ball was using a plane (top plane) and two perpendicular lines (from two hob base edges) which best suited the purpose. In this alignment first the top plane was measured by taking four points then two points for each line were measured along front and side face of the hob (set as the major and minor axes). The intersection of the 2-D lines and the plane was the datum point. The next step was to translate this datum to the centre of the ball and in order to do that five points were needed to be taken from the ball surface to create a sphere. Although the part alignment process was done manually due to the use of various hobs and balls, it could easily be automated for each part.

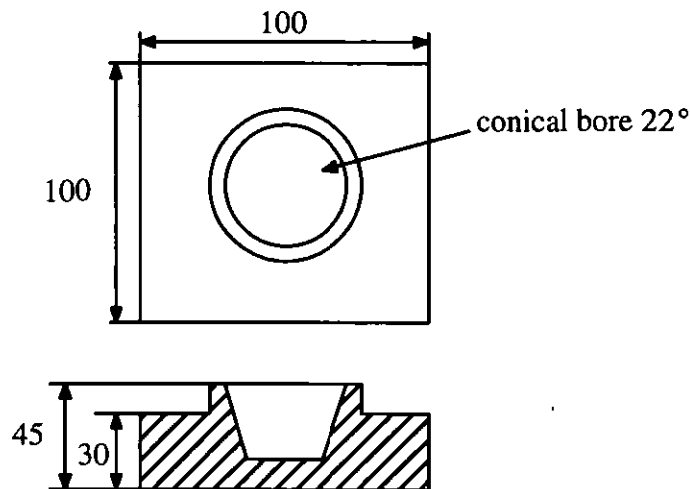


Fig. 4.20. A schematic diagram of the ball holder.

4.7 Probing strategy

Once the position of feature data points were known it was required to develop a strategy to guide the probe to inspect and assess the features. The probe needed to approach the feature normal to the work surface and avoid collision with the ball when moving from one side to the other. The most practical way was to guide the probe along a 3-D vector between the ball centre and each vision data point.

A dimple sphere was generated by taking five readings from each dimple enabling a second more accurate 3-D vector to be created between the dimple sphere centre and the ball. The feature was then measured once more using nineteen readings and a more accurate dimple sphere created. As mentioned before there are recommendations for the minimum number of points required to fit a geometric feature. Nineteen readings was found to be adequate, and readings beyond this did not increase the accuracy of the measurement significantly.

In order to achieve accurate measurements for each dimple, the CMM software required information about each tip and probe configuration (orientation, height, clearance etc.). As explained in chapter 3 each probe and probe orientation needs to be qualified or calibrated against a reference sphere. This process normally requires touching the reference sphere at 3 levels, 5 times in remote positions. In this case 25 readings were taken. This information was held in a qualification file. In order to keep the measurement accuracy as high as possible it is important that the qualification file should be executed every time the probe configuration is changed, and also executed periodically for system confirmation. The majority of CMMs have an automatic tip qualification software and there are usually two types of calculation for an effective probe diameter (the best possible tip diameter). The first is the computation of a single effective probe diameter for each probe being qualified and the other is based on the approach direction of the measurement point. In this case the latter method was used in which the CMM automatically computed the effective probe diameter from the touched points which improved the accuracy of the measurement.

4.7.1 Restrictions on different CMMs

Apart from the recommended procedures for use of a TTP there is a design restriction with the PH9 that the probe can only increment in steps of 7.5° in both horizontal and vertical planes. In addition to this some CMM software is only capable of saving a certain number of orientations, for example the Ferranti CMM could save up to 20 orientations in a calibration file while the Tesa CMM allows up to 700 orientations.

To measure each dimple it was required to use different probe orientations since dimples were spread all over the ball. In order to do this, two angles the yaw A and pitch B were needed to be

specified for the probe head. In the case of the Ferranti due to the system restrictions (7.5° increments and 20 probe orientations) it was necessary for each probe orientation to measure several dimples. It was practically found that intervals of 45° with a start angle of 22.5° for the probe head satisfied the restrictions. In order to limit the possible number of combinations for the Ferranti CMM to less than 20 it was decided to use three values of yaw angle i.e., 0.00° , 22.5° , and 67.5° the pitch angle B was also divided to give increments from -180° to 180° see fig. 4.21. In order to find the appropriate tip position for a dimple the dimple pitch and yaw values were matched to fig.4.21.

Tip No.	Angle A	Angle B	Tip No.	Angle A	Angle B
0.0	0.0	0.0	9.0	67.5	22.5
1.0	22.5	22.5	10.0	67.5	67.5
2.0	22.5	67.5	11.0	67.5	112.5
3.0	22.5	112.5	12.0	67.5	157.5
4.0	22.5	157.5	13.0	67.5	-157.5
5.0	22.5	-157.5	14.0	67.5	-112.5
6.0	22.5	-112.5	15.0	67.5	-67.5
7.0	22.5	-67.5	16.0	67.5	-22.5
8.0	22.5	-22.5			

Fig. 4.21 Selection of a tip angle for PH9.

The system of probe selection strategy on the Tesa was more comprehensive to that on the Ferranti since up to 700 orientations were possible, however a calibration file with 500 tip orientations was found to be adequate to allow a near normal approach probing to each dimple surface.

4.7.2 Dimple probing techniques

Because the dimple features are small a strategy (i.e., assessing) was needed to ensure that all of the readings would be taken from the inside of a dimple. In addition to this, a number of probing techniques were practiced from which the best solution was selected. In the assessing strategy the vision data was used as the starting point.

A small area around the vision data was assessed to identify a better possible centre for the dimple evaluation. Eight points were taken on a ring of 0.5 mm radius with 45° intervals. A 3-D vector created between each point and the ball centre. The point on the shortest vector on the ball surface was then selected and represented as the best centre for the dimple. This procedure repeated four times which gave a better dimple centre location. The original vision data was then replaced by this location (i.e., the improved dimple centre location) and used for the final dimple inspection. In the probing technique a small value (i.e., 0.5, 0.8, and 1.0 mm) was added to or from the im-

proved vision coordinate values to which the probe moved to take readings from the dimple. This procedure was repeated three times with five readings for the first time and nineteen for the second and third times to assure the accuracy of the measurement. Each set of readings was fitted into a sphere using a routine named Dimple Sphere (DS) and from the last set of readings the DS was constructed from which the dimple characteristics were calculated.

One of the main difficulties with the above methods was the way of incrementing probing points in order to take equally spaced readings from inside of each dimple. Since the CMM selects a 2-D working plane depending on the position of the dimple it was difficult to control the probe incrementation since the working plane constantly changed. It also should be remembered that it is not normal practice for a CMM to measure a very small portion of a feature and fit a feature into it since small errors can be significantly amplified.

The solution used was to develop a measuring approach by taking a vector from the ball centre through the detected dimple centre. Five points 1 mm apart were selected around the vector. These probed points gave a first approximation for the dimple sphere. However, this approximation gave a better indication of the dimple centre and chord diameter which allowed a more accurate approach vector to be calculated and the measuring points moved further apart. To enable accurate measurement to take place nineteen readings were taken for each dimple, one at the centre and six at three levels around the dimple centre point. To ensure the accuracy, repeatability and reliability of the measurement another set of nineteen readings were taken for each dimple in the same manner as before. The same measuring approach was taken for each dimple which took into account the required clearance position. The method was automated with a developed CMM programme named BALLINSP.

A set of equations were developed in order to calculate the required dimple characteristics e.g., dimple depth and chord diameter. Fig. 4.22 shows calculations to find the required information about each dimple. Fig. 4.23 is a flow diagram of the automated inspection procedure for dimples on golf balls.

parameters required are

- i. dimple sphere radius r ,
- ii. dimple depth w ,
- iii. dimple chord diameter x ,
- iv. dimple chord depth h .

where

R is the ball radius and constant.
 c is the distance between dimple and ball centres
 w and r are obtained from measurements.

from diagram

$$R^2 = (R - H)^2 + (x/2)^2$$

giving $x^2 = 4H * (2R - H)$ 1

also $x^2 = 4H * (2r - h)$ 2

equating 1 and 2 gives:

$$rh - RH = 1/2 \{(h - H) * (h + H)\}$$
3

$$w = H + h = (R + r) - c$$

subst. for $H = w - h$ in 3 gives:

$$rh - R * (w - h) = 1/2 \{((h - (w - h)) * w)\}$$

rearranging gives

$$h = \frac{w * (R - 1/2 w)}{R + r - w}$$
4

subst. for h in 2 gives x

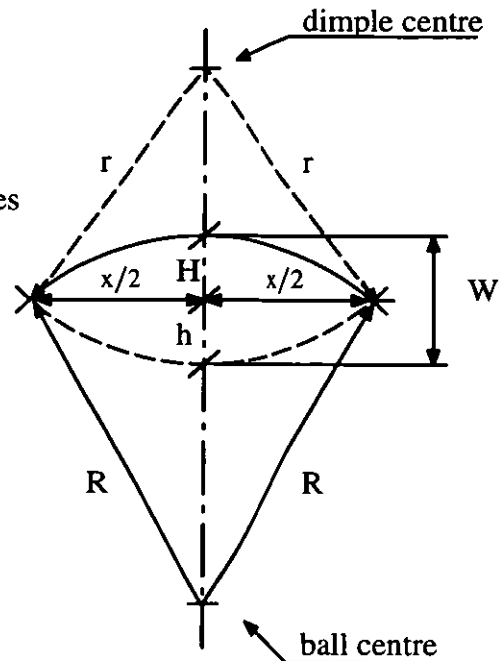


Fig. 4.22. A golf ball and a dimple intersection.

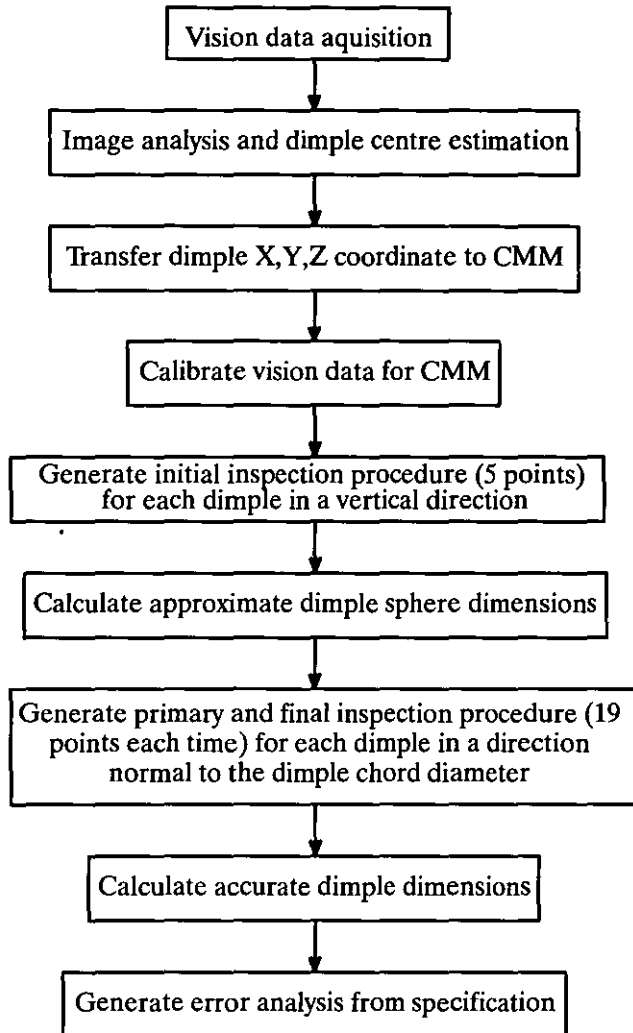


Fig. 4.23. Dimple inspection flow chart.

4.8 Discussion

In this chapter a fast feature identification and measurement procedure has been developed by employing an industrial vision system and a CMM for objects with spherical shapes and complex patterns.

Generally, feature identification can be the most difficult section of a detection system and one of the main reasons is that features are usually 3-D with no detectable edges or having primitive shapes. The common industrial vision systems are 2-D making depth determination difficult. One solution of feature determination is to enhance them in order for easy identification by a vision system. There are a number of ways to enhance the features, e.g., using surface markings

such as dots, grids, patterns and stripes, or use special light arrangement methods to generate a similar effect on the object surface. The developed method in this work was based on enhancing the features by marking and the most successful was simply to place a dot at the centre. The probing strategy for the CMM was developed based on knowing a point on each feature. With a prior knowledge of the feature shape it was then possible to detect and locate the dots by a set of developed algorithms and softwares which allowed the evaluation of the features to the machine highest accuracy. This method proved to be very simple and effective and may possibly be used elsewhere with some modifications to the system in order to be applicable to other forms of sculptured surfaces such as turbine blades, shoe lasts etc.

CHAPTER 5

MULTI-IMAGE SUPERIMPOSITION TECHNIQUE (MIST) FOR PATTERN FEATURES ON SPHERICAL SURFACES

5.0 Introduction

The feature identification process previously described can determine the approximate location of features on the object. Once these locations have been determined a measuring method can be employed to determine the actual position and characteristics of the features in relation to the main body. However, in the case of complex products with curved surfaces it is difficult to identify features close to and below the parting line or equator when they are viewed from one position above the object. One solution to this type of problem is to view the object a number of times from different directions and combine the information. The concept has been applied by other researchers [2,23,34,95] to measure approximate part shape, however, the integration of the method with a CMM for accurate identification and measurement of spherical or curved features has received little attention.

The generated technique for this work is named Multi-Image Superimposing Technique (MIST) which enables the inspection system to capture all features on the object of interest, and then calculate relevant feature data for an accurate inspection. The technique captures desired features within a detectable zone (an area of confidence for each captured image in order to prevent possible noise intrusion). Each feature location is defined by X,Y, and Z coordinates of its centre i.e., a feature datum coordinate. The coordinates describing the feature are related to the vision coordinate system and must be transformed to a common axis (i.e., world coordinate system) for consistency of the inspection results.

The objective of any feature identification system using machine vision is to obtain complete object and feature identification with the minimum number of viewing positions. Obviously the minimum possible viewing arrangements would be two (i.e., back and front) but this would not necessarily identify all aspects of the object. As more viewing positions are included then its obvious that parts of the object will be viewed a number of times. Early work [9] showed that for the golf ball situation in areas near the edge of the ball it was difficult to identify dimple features distinctly. It was decided to use 5 camera positions because of, ease of image manipulation, and to establish a method which was certain to lead to a satisfactory solution which could then be the basis for future improvement. However, this meant that there could be up to 3 overlapping areas,

shown as areas A in fig. 5.7. It was important to be certain that dimple information was not replicated as this would mean repeat probing of some dimples. A technique was required where it was possible to censor repeated features.

The area of certainty or confidence can be approximated to a circular ring and by knowing the size of the overlapped areas it was possible to determine the number of features covered by them. A number of mathematical methods and approaches were developed to model these areas. Features outside of the detecting ring would not be recorded but the ring dimensions need to be optimised in order to reduce the number of repeated features. The result of this modelling was the determination of complete coverage of the ball for the minimum processing time by trimming off the replicated data in order to achieve one set of data points.

5.1 Feature identification by multi-images

Although, researchers in the area of 3-D recognition use a vision system of some sort for their applications, they apply a variety of methods to recognise or identify parts. On prismatic parts where there are interfaces of surfaces or edges, these can be used to more easily locate the position of features, however, for curved surfaces without obvious edges, different solutions are needed.

In theory to detect features on a golf ball it should be possible to position a camera above the ball or hob and see all of the dimples on half of the object. Clearly those dimples at the centre of the ball will look circular, with the shape becoming more elliptical as the dimple moves towards the perimeter, fig. 4.3, visually it is still possible to identify centres but with increased difficulty. It was apparent that a more suitable technique was needed in order to capture all dimples.

Stereo vision has been used mainly to identify positions and shapes of 3-D objects. In this method two or more cameras are used to image a point on the surface of an object in different relative positions. By analysing the corresponding point in different images, the location of the required 3-D point can be calculated. The significant difficulty of a stereo system however, is to determine which point in one image corresponds to a given point in the other image. Furthermore, the two optical axes of the cameras should be aligned precisely to match the two images. Clenk and Bachank [95] used this method to extract 3-D information and to reconstruct the object surface in a robot workspace. The object of interest was viewed by n pairs of cameras. Cho et al [36] used a similar method by using one camera which was fixed to a CMM ram and arranged to capture two images along the X-axis of the machine. The object on the table of the CMM would have projected onto it a grid of spots in order to speed up the process of the point matching. The system would need further sophistication if the CMM was not used since small alignment errors would cause inaccurate results due to the incomplete stereo matching.

Other researchers [23,25,34,97] used multiple 2-D images to extract features for visual inspection and recognition. The main advantage of using this method over other 3-D surface analyses methods e.g. a stereo vision, is speed, ease of use and it is less complex to extract information from objects.

5.2 Proposed one camera multi-image superimposed method

In essence, an image superimposing technique is a method which maps (overlaps) images of the same scene on top of each other taken from different positions. If good analysis methods are available this allows more precise information of areas which are difficult to evaluate.

The MIST is arranged to determine and inspect three Dimensional Sculptured Surfaces (3-DSS), which have shapes, geometrical features or are of a free form nature. In image analysis it is necessary to determine a method to reference a feature, this reference value can be used to locate the feature from a global datum. For the objects in this case the reference point was the dimple centre and the datum was the ball or hob centre.

The proposed MIST employs the same vision arrangement as that used for the one camera method (chapter 4). In this technique feature information will be extracted from different images and referred to an individual reference point (i.e., datum) in each image. The datums selected were always the ball centre, errors in datum position of up to 1.0 mm have shown little effect on the dimple position values.

The MIST uses a number of different views from an object and the feature data for each view was arranged to be calculated in 3-D. The images are individually processed and the information related to each image stored in the same data file. The simplest case of using the technique was to utilise a minimum of two images from the object taken from different positions. This often would limit the application of the system since objects with hidden features would not be exposed by the camera regardless of the camera position. In order to establish the technique, the easiest case was chosen and that was to use five images from the object. The five images from the object were arranged to be taken with one image from the top of the object and four images from the sides of the object. The camera was positioned at 90 degree increments in both horizontal and vertical planes.

Views from the six sides of an object make up 100 per cent of the total object surface area, one side of the object would have 16.6 per cent of the object area. Therefore, in a system which uses five images, up to 83 per cent of the surface information could practically be detected. However, the precise amount would also depend on the object surface irregularities. With the use of this

method replication of some dimples was inevitable and a programme was developed to compare and select only one set of data for the features for probe measurement.

5.2.1 System configuration

The proposed system is shown in fig. 5.1(a and b). As shown in the figures, the camera was placed on the CMM table by means of a stand in two positions, above and at the side of the object. As explained earlier images were taken from five positions, one from the top and four from the object sides which were achieved by rotating the object (or hob) about the Z-axis while located on a rotary table (the accuracy of the table rotation was to seconds of a degree). The use of the rotary table enabled the system to achieve accurate steps of 90 degrees and to prevent backlash error, it was rotated continuously in one direction to each 90 degree position.

Although the objects to be measured for this research were spherical, a more general arrangement was also considered where the object was a cubic. This situation then needed five images to look at the five sides. Although fewer views might suffice, it provides an application for the more general case. However, for a reduced method (see section 5.6) it is possible to use three camera positions. The image capturing concept is shown in fig. 5.2, where the dotted lines show the cameras field of view.

It was best found to capture all five images by the vision system at the beginning of the test, and then to remove the vision system from the table for the rest of the process and the inspection. To calibrate the vision system with the object in order to match the camera positionings, an approximate location of the ball centre and the diameter of the ball in pixel values (X- and Y-directions) was required by the vision system. These values are referred to as the primary settings and are automatically used for calculating the scale factor (image ratio) for the image processing purposes. It was possible to find these locations manually by use of the Matrox vision software, however, fast determination was done by the use of PC-IMAGE software. In order to use metric units conversion of the pixel values was needed to be done to suit the CMM system and was achieved using equations 5.1 and 5.2.

$$\text{X-direction diameter (mm)} = \frac{(\text{Pixels in X - direction (unit)}) * \text{Ball dia. (mm)}}{\text{Ball dia. (in Y - dir.) in Pixels (unit)}} \quad \dots\dots 5.1$$

$$\text{Y-direction diameter (mm)} = \frac{(\text{Pixels in Y - direction (unit)}) * \text{Ball dia. (mm)}}{\text{Ball dia. (in X - dir.) in Pixels (unit)}} \quad \dots\dots 5.2$$

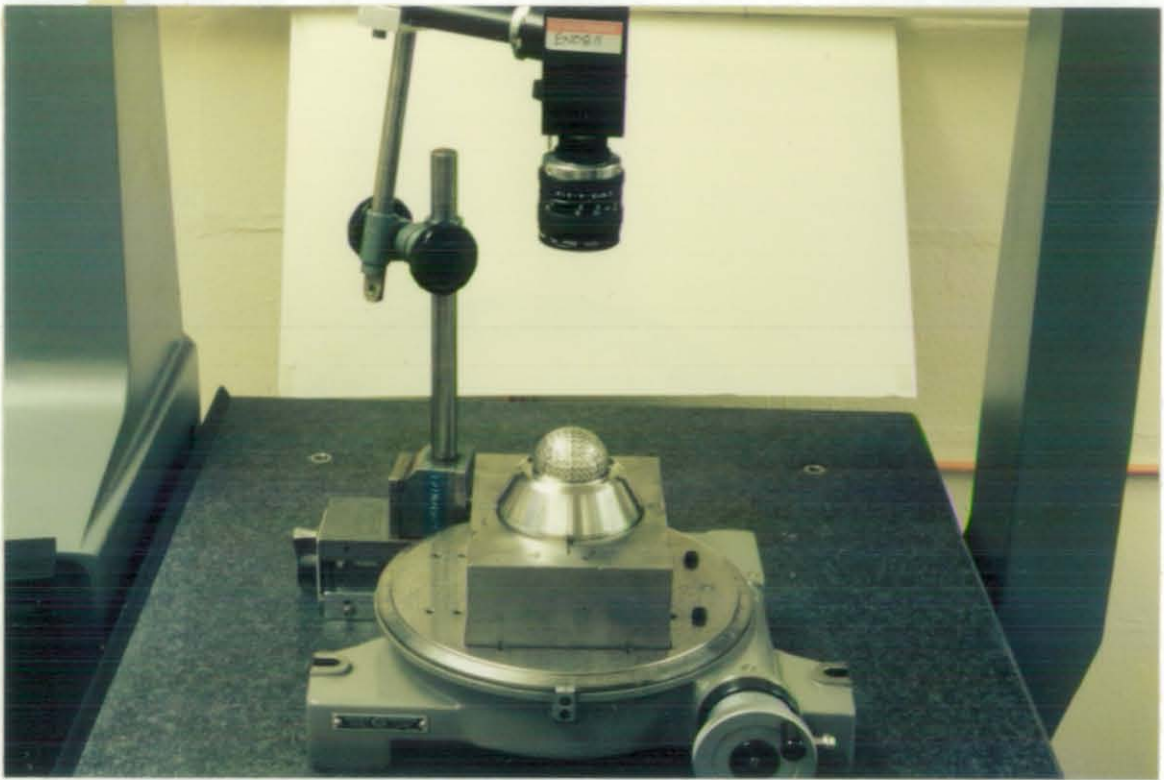


Fig. 5.1(a). The camera positioning on the CMM, for the top viewing.



Fig. 5.1(b). The camera positioning on the CMM, for the side viewing.

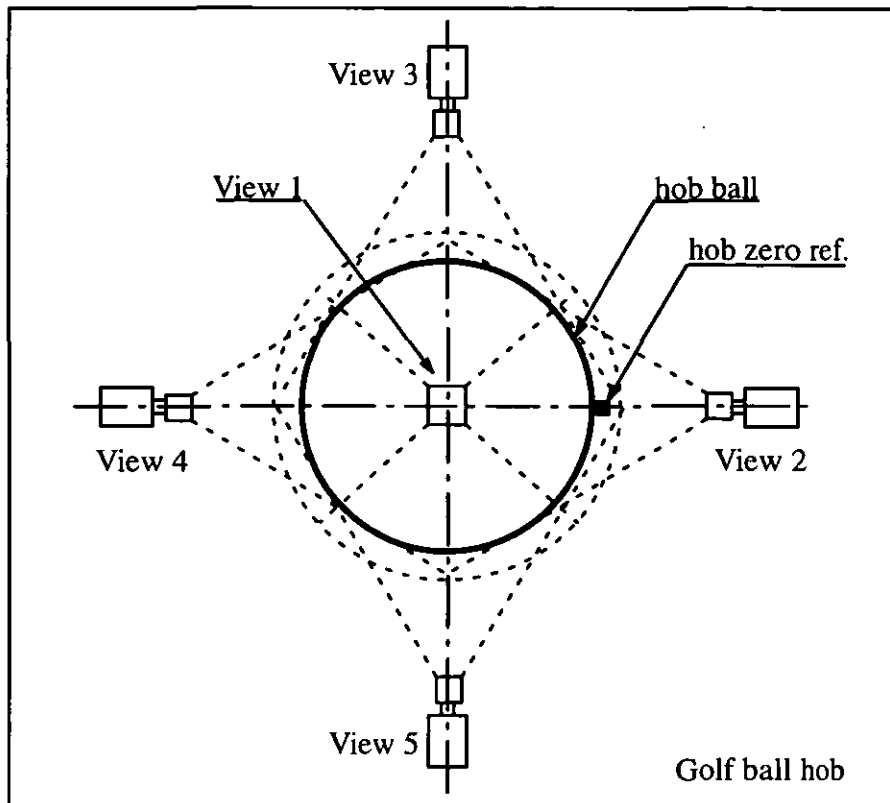


Fig. 5.2. Viewing segmentation of the hob by the vision system on the CMM.

5.2.2 Filter arrangement

A high quality image is achievable by using good illumination. Apart from the necessary characteristics i.e., intensity, size and shape of a suitable light source for each application, most of the time there is a practical need for a filter or an operation to regulate the illumination around the object. In this case surfaces of golf balls have a reflecting surface finish and there was a need to reduce reflection to minimum.

A diffuse illumination device in the form of a neon ring proved to be suitable light source and a paper filter was used to generate a regular illumination from apex to equator. The effect of the filter was the minimum of reflection with satisfactory illumination intensity. Fig. 5.3 shows the filtering situation with the camera placed at the side of the object.

5.2.3 Viewing arrangement and axes transformation

For each view the camera coordinate system was kept the same in order for the vision data to be referred to the same global axes. The position of repeated dimples would have a small difference in relationship to the coordinate system in each view, since the datum for each view would have a slightly different position. The ball views are shown in fig. 5.4, which gives the axes arrangement and sign conventions for the views and fig 5.5 shows the transformed coordinate axes for

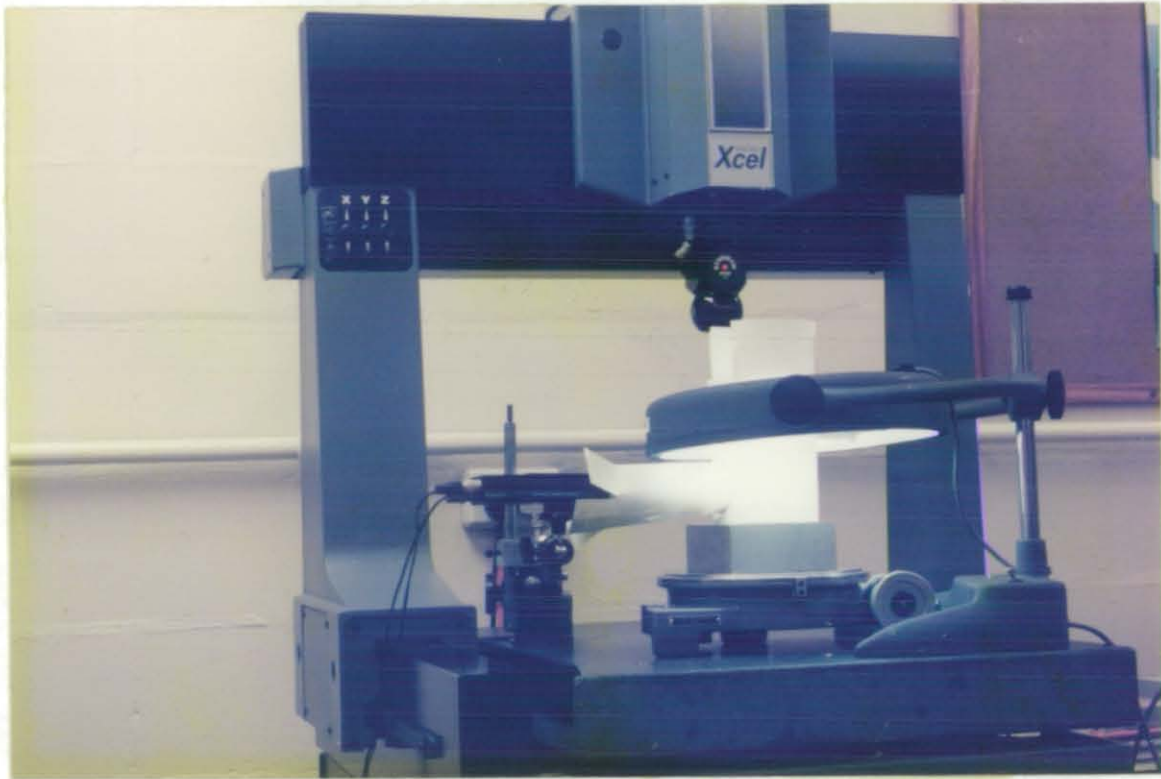


Fig.5.3 Filter arrangement for MIST.

each camera in order to suit the CMM. It is also can be seen from fig. 5.5 that each set of data belonging to an image needs to be addressed to the reference point.

5.3 Overlapped areas

During image capture there were areas in which dimples could be identified more than once, and these areas were created by overlapping up to three neighbouring images on the surface of the ball. In order to visualise the situation a hemispherical perspex model was generated with five image rings drawn on it to resemble the effect of viewing by the camera. Fig. 5.6 shows the physical model with image rings represented as the detectable image rings. From the model it was clear that when different diameter rings were used, a number of overlapping area segments or wedges would be generated and the number and size of these wedges would be dependant on the ring diameter. A wedge generally was formed by a minimum of two overlapping images and maximum of three. When an optimised image ring was used the number of repeated dimples were found to be a minimum. This situation is shown in fig. 5.6, where the shaded areas are detected twice. For image rings greater than the optimised values a number of additional overlapped areas (i.e., triple) were developed which are shown shaded in fig. 5.7 and marked as areas A. While for smaller detectable ring than the minimum there may be some overlap but there are areas which are not detected. This situation is shown in fig. 5.8, where the shaded areas are undetected regions.

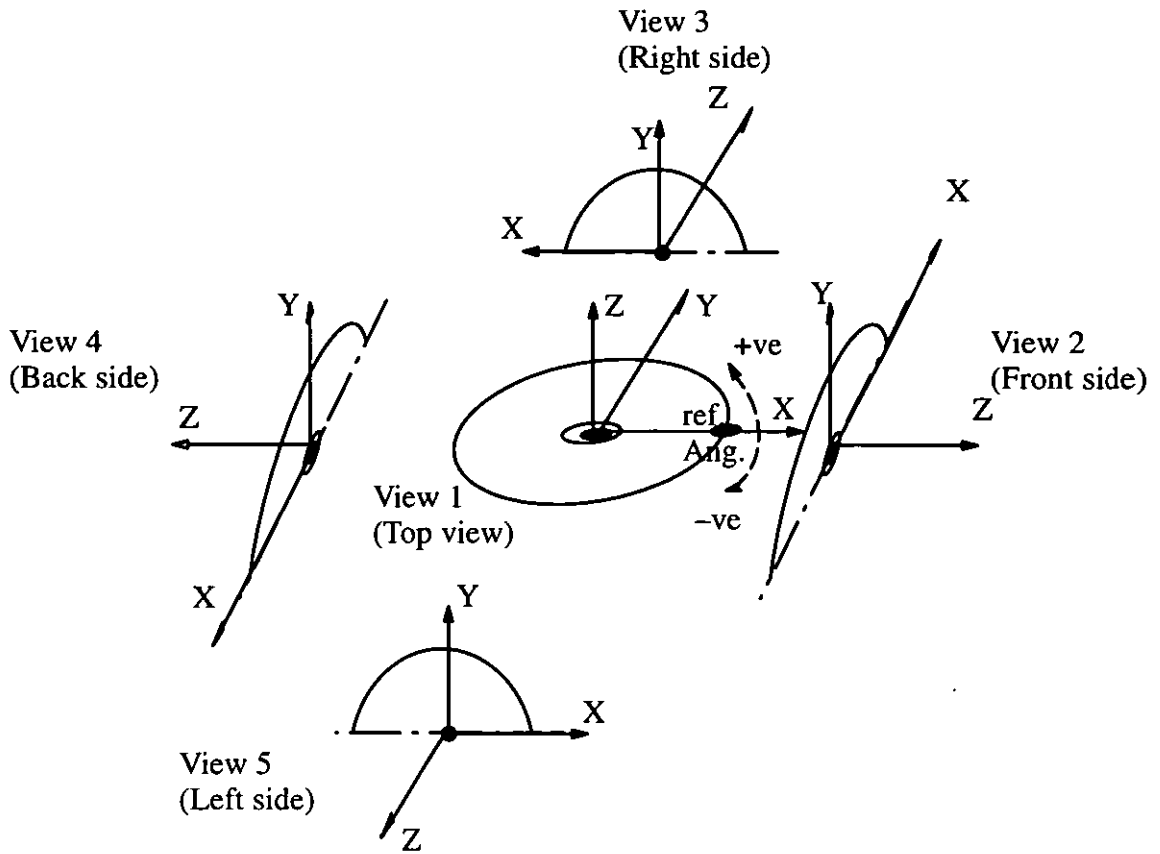


Fig. 5.4. Axes representation of the ball under the camera.

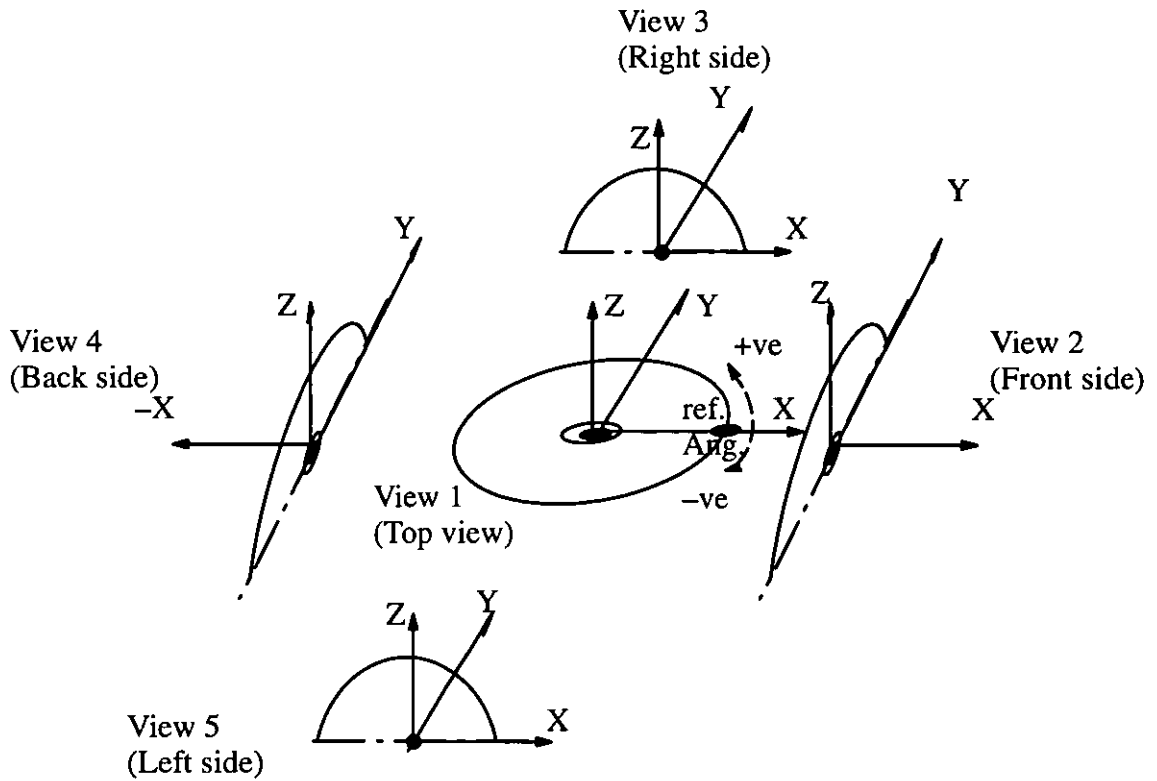


Fig. 5.5. Vision axes transformed to suit the CMM.

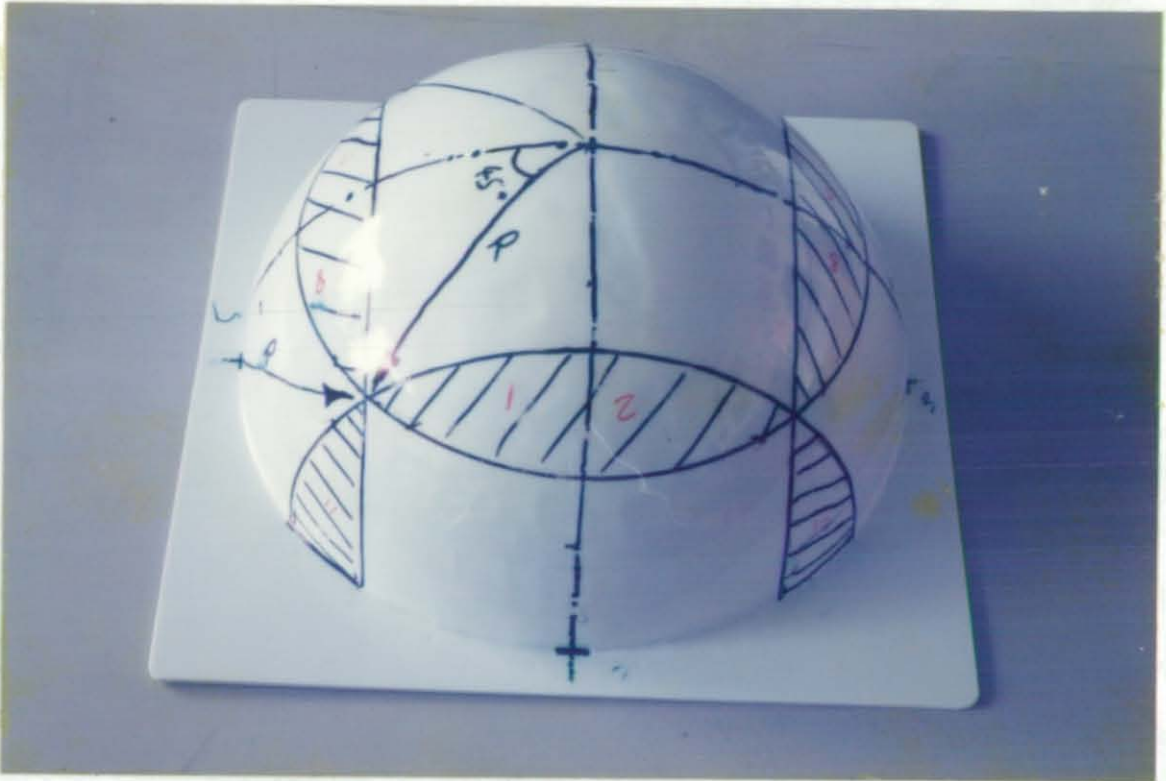


Fig. 5.6. Molded hemisphere for overlapping visualisation.

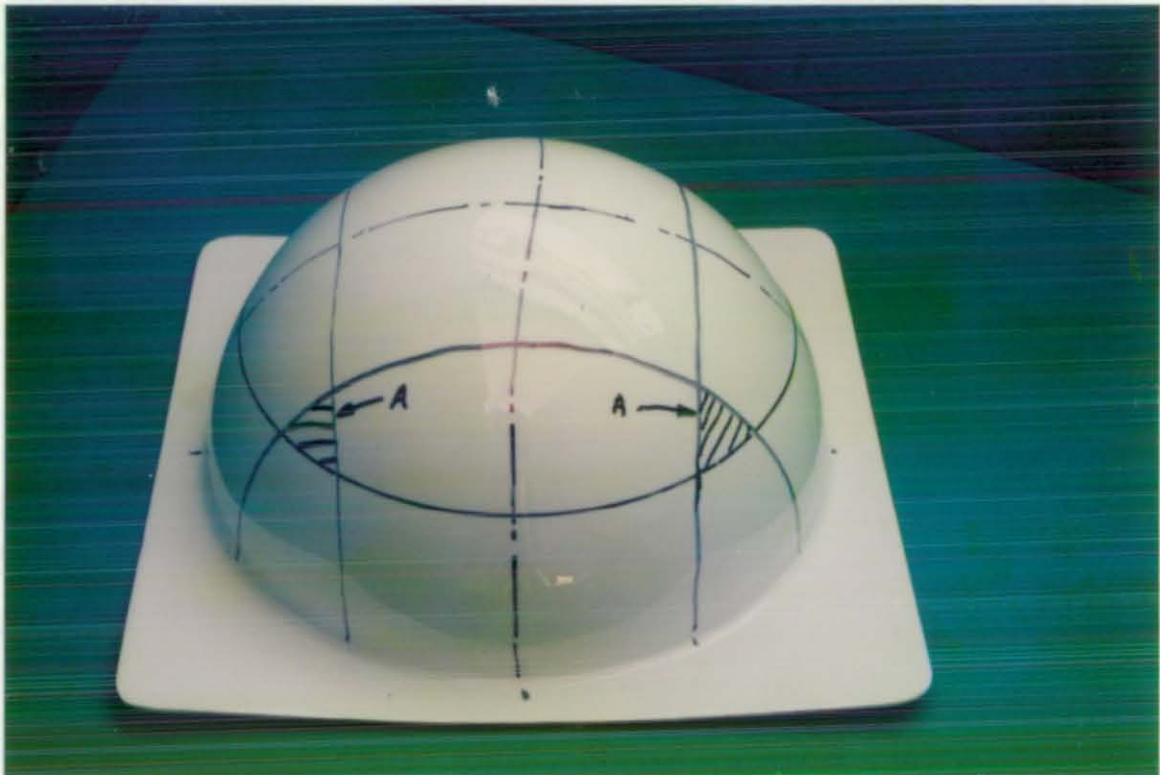


Fig. 5.7. Triple overlapped segments A.

It can be seen from the analyses that for an optimised case a ring with a radius of 17.51 mm was found for a standard ball with a radius of 21.45 mm. As mentioned earlier for a smaller detectable ring than the optimum value, some dimples would not be detected while some others may be detected more than once. This situation stays valid until the image ring gets smaller than 10.75 mm radius, where all rings touched one another, after which it is impossible to generate wedges see fig 5.8. The calculation of ring diameters and overlap areas are given in sections 5.4.1 and 5.4.2.

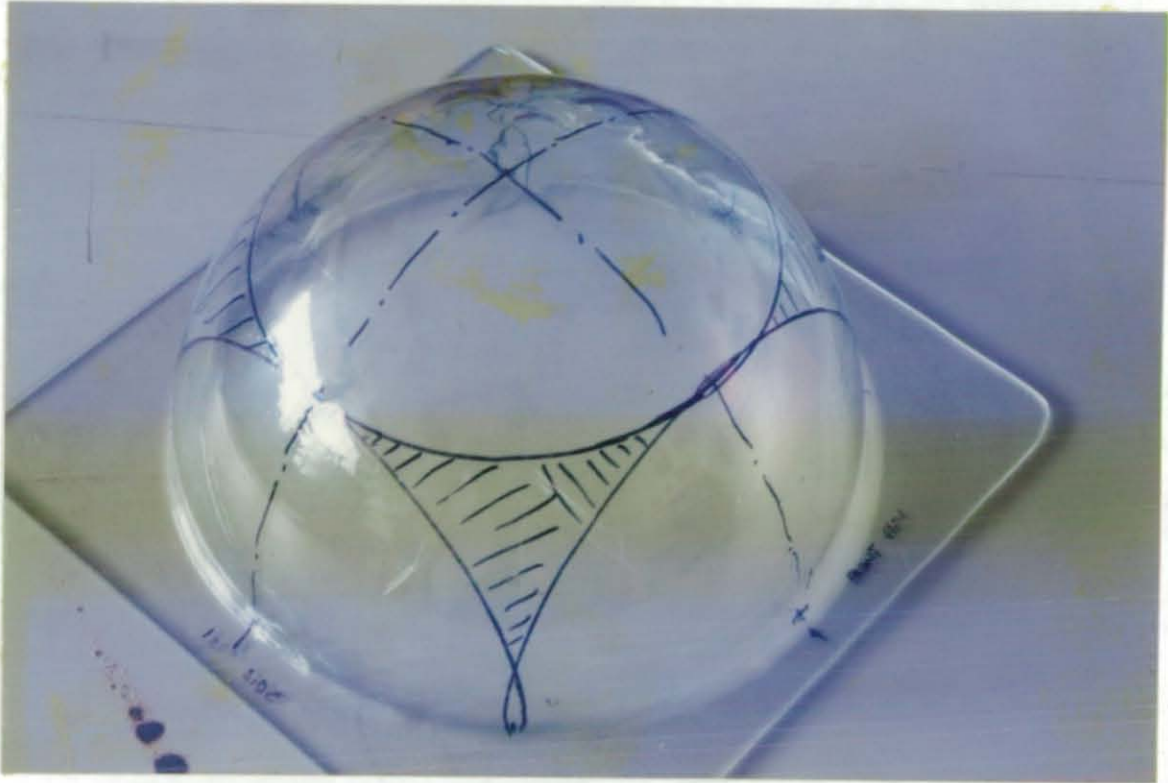


Fig. 5.8. No overlapping for rings smaller than the optimised diameter.

5.3.1 Data-set sorting

With the use of MIST the generation of repeated dimples was inevitable and in order to keep the inspection time to a minimum, a procedure was needed to measure each dimple once only. Three solutions were initially considered to overcome this problem, i) to set-up a method to be used at the time of detection, ii) to design a procedure to be used at the measuring stage on the CMM, and finally iii) to sort the data within the data file. It was found more efficient to sort a complete data file after all the dimples were detected by the various views which enabled repeated dimples to be censored.

The procedure of sorting was done by using a developed 'C' programme named "DimSort". Fig 5.9 shows the flow chart for data sorting.

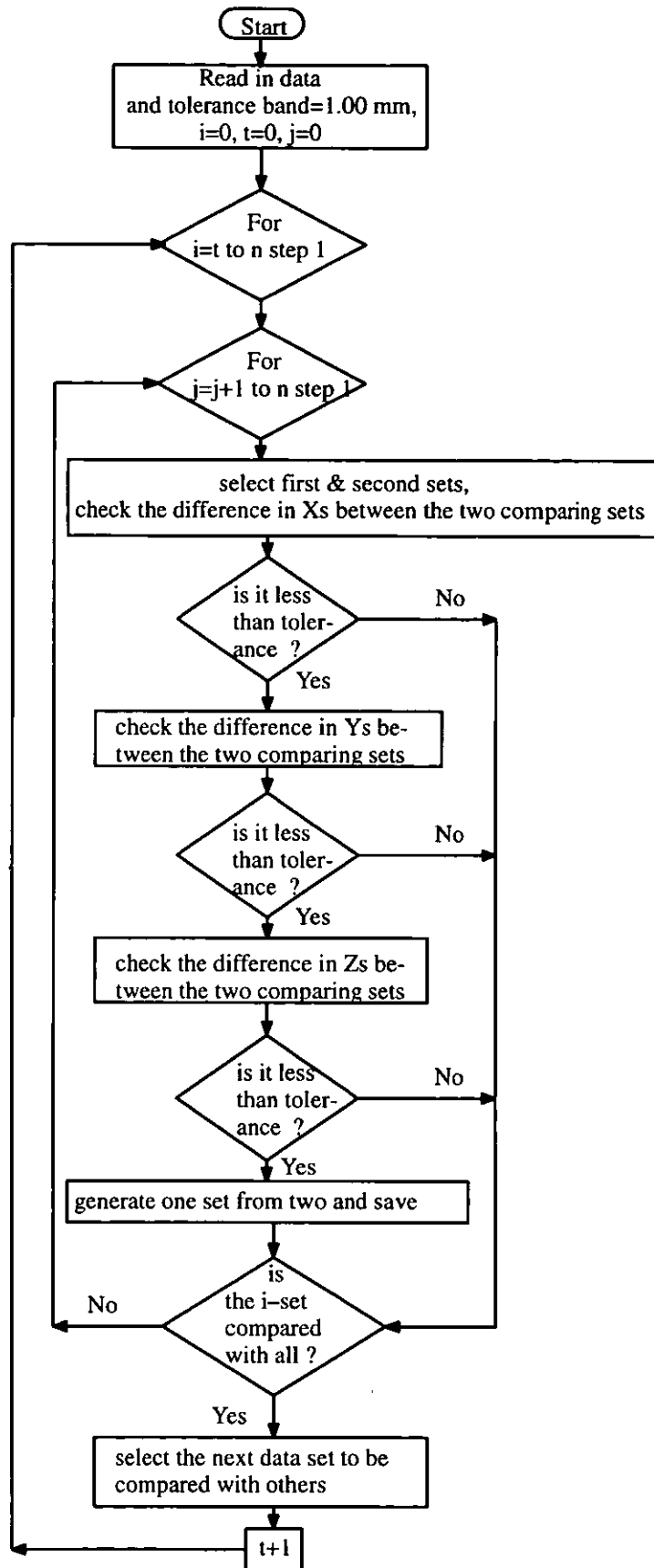


Fig. 5.9. The data set sorting flow chart.

The programme starts by reading in dimple data and placing it in a 3-D array. Each set of dimple coordinates is compared with others in order to find matched values within specified tolerance bands.

The tolerance band would vary with the golf ball type since they may have 11 different dimple chord diameters [9]. However, a 1.00 mm tolerance band was found to be acceptable for the majority of dimples. With a small amount of practice the most suitable band could be found for a particular ball. If the tolerance was too small there was a risk of losing some dimples. The comparison procedure continues in order to find other matching data since there could be more than one repeated set. It was found that averaging the repeated data sets was the best method to obtain the dimple centre to be used by the CMM. Once a complete set of data was obtained it was stored in a file for further consideration.

Various golf balls were tested using the above method with the machine under continuous supervision in order to check the amount of the repeated data for different tolerance bands. During the tests the original data from the MIST was continuously checked against the sorted file in order to assess the effect of the identification process for the repeated dimples, and also to evaluate the averaging method of the repeated data. Up to 90 per cent of the repeated data was detected and an average value substituted leaving the remaining 10 per cent to be measured more than once.

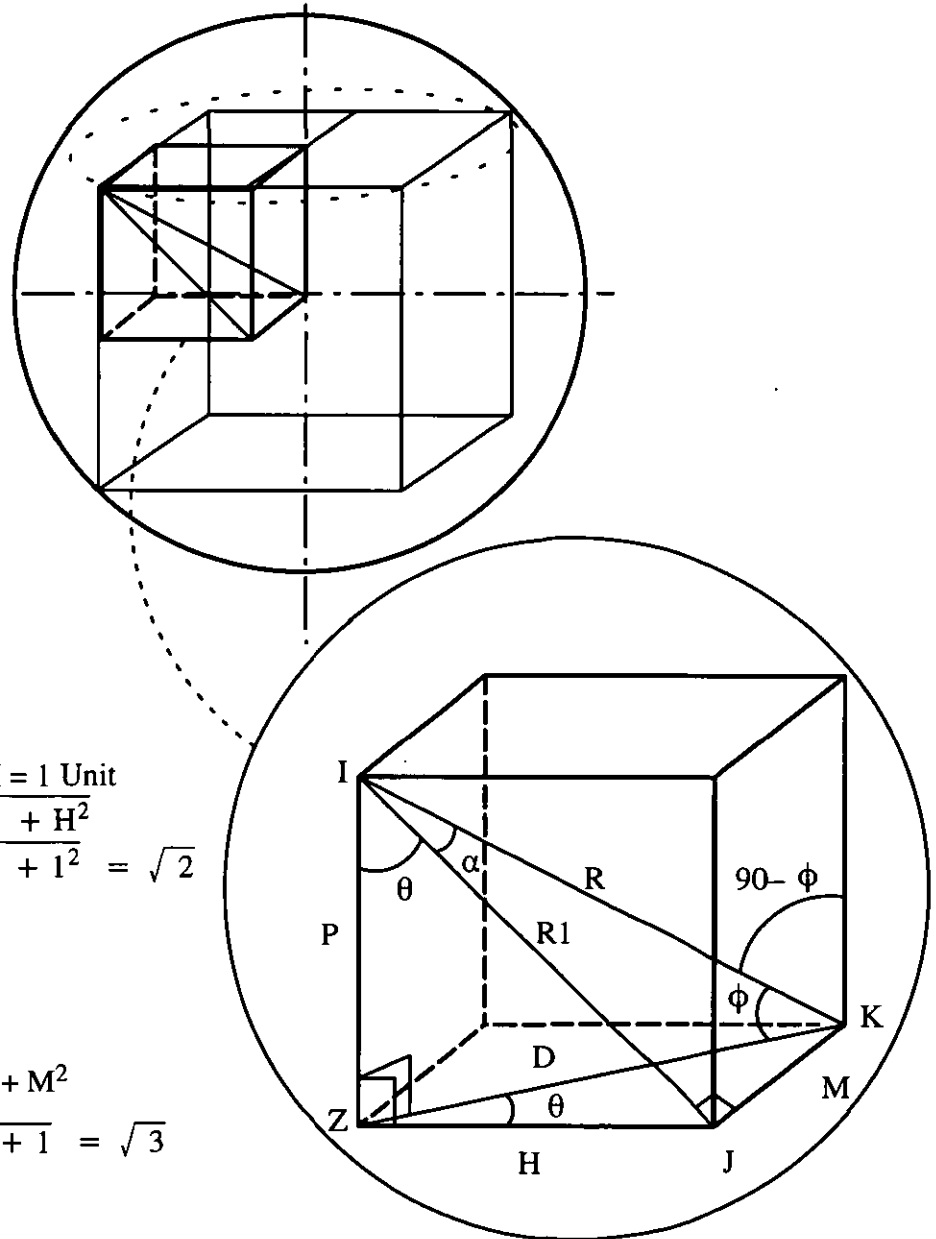
5.4 Mathematical evaluation of the overlapped areas

In order to minimise the number of repeated dimples from various views the size of the identification zone needs to be optimised. Experience has shown that they can be considered to be approximately circular in shape and therefore to develop a mathematical solution, circular identification zones or rings have been assumed. The procedure of calculating the detectable ring is shown in the next section and two methods were developed for calculating the identification zone. The first method uses an approximate evaluation and the second method follows a surface calculation [104,105,106]. The use of the approximation method also made it possible to speculate on an answer for the zone area. Once the detectable ring was identified the total area for five captured images was calculated and used to determine the overlapped area ratio to the ball surface from which the amount of repeated dimples can be identified.

5.4.1 Calculation of the detectable ring diameter for optimum overlap

In order to achieve optimum overlap when the MIST was applied to a sphere it was necessary to calculate the radius of the detectable ring (i.e., R_1) on a half hemisphere. This was done by

drawing circles on a sphere for zero overlap and then draw a box around them which resulted in a sphere with a square fitted inside. Fig. 5.10 shows this arrangement where the diagonal length of the box (i.e., R) is the radius of the sphere. The method of calculation is as follows:



Finding angle (α),

It is assumed that,

$$\begin{aligned}
 P &= H = M = 1 \text{ Unit} \\
 R1 &= \sqrt{P^2 + H^2} \\
 \therefore R1 &= \sqrt{1^2 + 1^2} = \sqrt{2}
 \end{aligned}$$

In Triangle IJK

$$\begin{aligned}
 R^2 &= R1^2 + M^2 \\
 R &= \sqrt{2 + 1} = \sqrt{3}
 \end{aligned}$$

Fig. 5.10. Sphere with a cube inside.

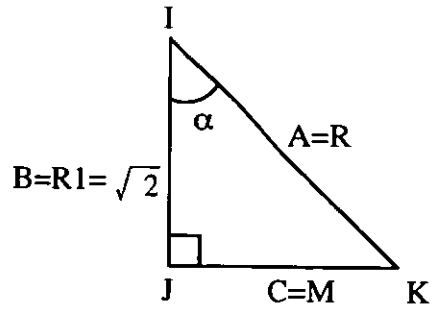
Using standard trigonometry Equ.

$$C^2 = B^2 + A^2 - 2AB \cos \alpha$$

$$\cos \alpha = \frac{B^2 + A^2 - C^2}{2AB}$$

$$\cos \alpha = \frac{2 + 3 - 1}{2\sqrt{6}}$$

$$\alpha = 35.26^\circ$$



$$R = 21.45 \text{ mm}$$

$$R1 = R \cos \alpha \dots\dots\dots 5.3$$

$$R1 = 21.45 \cos 35.26$$

$$R1 = 17.51 \text{ mm}$$

$$P = H = M \dots\dots\dots 5.4$$

$$R1 = \sqrt{2 H^2}$$

$$H = \frac{17.51}{\sqrt{2}}$$

$$H = 12.384 \text{ mm}$$

In triangle KZJ;

$$D^2 = H^2 + M^2 \dots\dots\dots 5.5$$

$$D = \sqrt{H^2 + M^2}$$

$$D = \sqrt{2 (H^2)}$$

$$D = 17.51 \text{ mm}$$

Total detected area for 5 images using the detectable ring

The total area for five images by the use of the detectable ring can be calculated by following method.

Top view

Detectable ring dia. = 17.51 mm

$$\begin{aligned} \text{Area} &= 2\pi R^2 \\ &= 2\pi(17.51)^2 \\ &= 1926.42 \text{ mm}^2 \end{aligned}$$

Side view

$$\begin{aligned} \text{Area} &= \frac{2\pi R^2}{2} \\ &= \frac{2\pi(17.51)^2}{2} \\ &= 963.21 \text{ mm}^2 \end{aligned}$$

Total areas for 5 images

$$\begin{aligned} \text{Total areas} &= \text{Top view} + 4 \times (\text{Side view}) \\ &= 1926.42 + 4(963.21) \\ &= 5779.27 \text{ mm}^2 \end{aligned}$$

5.4.2 The approx. overlapped evaluation method

To calculate the approximate overlapped area the radius of the optimised ring from previous section is used. To prevent the overlapped area a semi circle with radius of R is drawn and intersected with a plane at the calculated detectable ring. Fig. 5.11.a, 5.11.b, and 5.11.c show this arrangement. The total approximate overlapped area for the hemisphere is twelve times of the area A₃ which is shown in fig 5.11.c. This approximation treated the curved overlapped areas as flat surfaces.

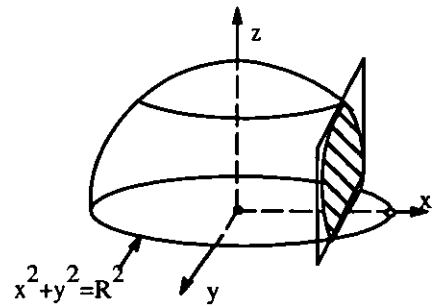


Fig. 5.11.a. Hemisphere sectioning.

$$\int \sqrt{A^2 - Z^2} dz = \frac{A^2}{2} \left[\sin^{-1}\left(\frac{Z}{A}\right) + \left(\frac{Z\sqrt{A^2 - Z^2}}{A^2}\right) \right]_0^{0.577R}$$

$$\int \sqrt{R^2 - X^2} dx = \frac{R^2}{2} \left[\sin^{-1}\left(\frac{X}{R}\right) + \left(\frac{X\sqrt{R^2 - X^2}}{R^2}\right) \right]_0^{0.577R}$$

$$A_1 = \frac{R^2}{2} \left[\sin^{-1}\left(\frac{X}{R}\right) + \left(\frac{X\sqrt{R^2 - X^2}}{R^2}\right) \right]_0^{0.577R}$$

$$A_1 = \frac{R^2}{2} \left[\left[\sin^{-1}\left(\frac{0.577R}{R}\right) + \left(\frac{.577R\sqrt{R^2 - (.577R)^2}}{R^2}\right) \right] - 0 \right]$$

$$A_1 = \frac{R^2}{2} \left[\sin^{-1}(0.577) + \left(\frac{.577R\sqrt{.666R^2}}{R^2}\right) \right]$$

$$A_1 = \frac{21.45^2}{2} (0.615 + 0.471)$$

$$A_1 = \frac{21.45^2}{2} (1.08)$$

$$A_1 = 249.84 \text{ mm}^2$$

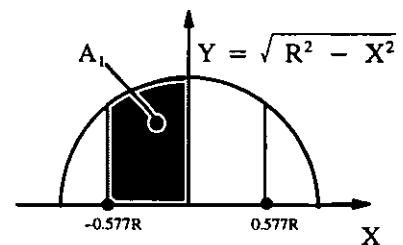


Fig. 5.11.b. Front view of the cut.

Area of A₂ for R = 21.45 mm

$$A_2 = .577R * .577R$$

$$= (.577R)^2$$

$$A_2 = 153.18 \text{ mm}^2$$

$$A_3 = A_1 - A_2$$

$$A_3 = 249.84 - 153.18$$

$$A_3 = 96.65 \text{ mm}^2$$

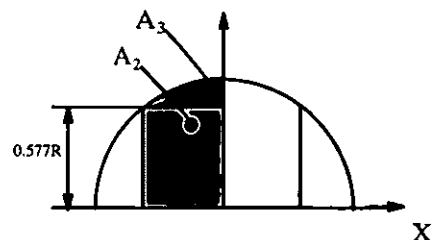


Fig. 5.11.c. Sectioning of the cut.

a) Total approximate area of the wedge sections around the ball

$$\begin{aligned} \text{Area} &= (A_3) * 12 \\ \text{Area} &= 96.65 * 12 \\ \text{Area} &= 1159.8 \text{ mm}^2 \end{aligned}$$

b) Total approximate percentage area of the wedge sections for five views

The value of the detectable ring of 17.51 mm was used for this calculation.

$$\text{Percentage (\%)} = \frac{\text{Total over lapped area for 5 views}}{\text{Total surface area of the ball for 5 views}} * (100)$$

$$\text{Percentage (\%)} = \frac{1159.8}{5779.27} * (100)$$

$$\text{Percentage (\%)} = 20$$

c) Total approximate percentage area of the wedge sections over the ball area

The value of the detectable ring of 17.51 mm was used for this calculation.

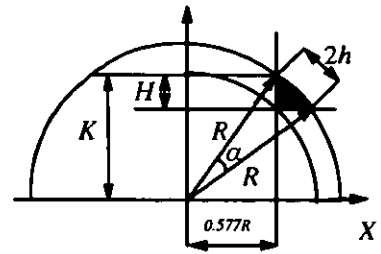
$$\text{Percentage (\%)} = \frac{\text{Total overlapped area for 5 views}}{\text{surface area of the ball}} * (100)$$

$$\text{Percentage (\%)} = \frac{1159.8}{1926.42} * (100)$$

$$\text{Percentage (\%)} = 60.21$$

5.4.3 The surface integration method

In order to calculate the surface of the wedge it was required to find the maximum angle (α) which generated this surfaces. Fig. 5.12.a, 5.12.b, and 5.12.c show the arrangement of the wedge outside the zone.



$$R^2 = K^2 + (0.577R)^2 \quad \dots\dots 1$$

$$\sin \left(\frac{\alpha}{2}\right) = \frac{h}{R} \quad \dots\dots 2$$

$$K = H + (0.577R) \quad \dots\dots 3$$

From 1,

$$K = \sqrt{R^2 - (0.577R)^2}$$

$$K = \sqrt{(1 - 0.332)R^2}$$

$$K = 0.8167R$$

Fig. 5.12.a. Schematic presentation of the wedge.

Subs. K in 3,

$$H = (0.8167R) - (0.577R)$$

$$H = 0.2397R$$

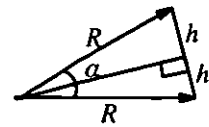


Fig. 5.12.b.

From triangle opposite,

$$2h = \sqrt{P^2 + P^2}$$

$$2h = \sqrt{(0.2397R)^2 + (0.2397R)^2}$$

$$2h = 0.339R$$

$$h = 0.1695R \approx 0.17R$$

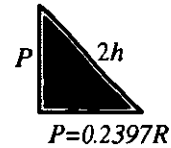


Fig. 5.12.c.

Subs. h back in 2,

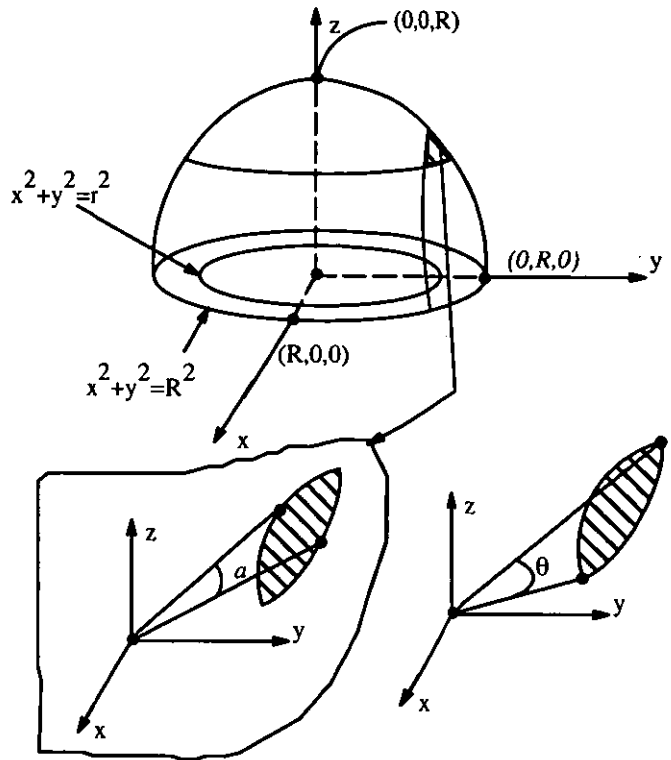
$$\sin \left(\frac{\alpha}{2}\right) = \frac{0.17R}{R}$$

$$\left(\frac{\alpha}{2}\right) = \sin^{-1}(0.17)$$

$$\left(\frac{\alpha}{2}\right) = 9.76'$$

$$\alpha = 19.52' \approx \frac{\pi}{9} \approx 20'$$

The evaluation of the surface integration for the wedge section at upper hemisphere is shown in fig. 5.13, the partial derivatives was used and the method as follows;



Where;

R = Radius of the ball

$R_1 = 21.45 \cos 35.26$,

$R_1 = 0.817R$

$Z = \sqrt{R^2 - X^2 - Y^2}$

Fig. 5.13. Schematic diagram of the overlapped wedge.

Solution: The partial derivatives

$$\frac{\partial Z}{\partial X} = \frac{-X}{\sqrt{R^2 - X^2 - Y^2}}$$

$$\frac{\partial Z}{\partial Y} = \frac{-Y}{\sqrt{R^2 - X^2 - Y^2}}$$

$$\iint dS = \lim_{r \rightarrow R} \iint \sqrt{\left(\frac{\partial Z}{\partial X}\right)^2 + \left(\frac{\partial Z}{\partial Y}\right)^2 + 1} \, dA$$

$$= \lim_{r \rightarrow R} \iint_{R_r} \sqrt{\frac{X^2}{R^2 - X^2 - Y^2} + \frac{Y^2}{R^2 - X^2 - Y^2} + 1} \, dA$$

Cartesian Form $= \lim_{r \rightarrow R} \iint \frac{R}{\sqrt{R^2 - X^2 - Y^2}} \, dA$ **Polar Form** $= \lim_{r \rightarrow R} \iint \frac{R}{\sqrt{R^2 - r^2}} \, r dr \, d\theta$

$$\begin{aligned} \text{area of one wedge section} &= \int_0^{\pi/9} \int_{R_1}^R \frac{R}{\sqrt{R^2 - r^2}} \, r dr \, d\theta \\ &= \int_0^{\pi/9} \left[-R \sqrt{R^2 - r^2} \right]_{0.817R}^R \, d\theta \\ &= \int_0^{\pi/9} \left(-R \sqrt{R^2 - R^2} \right) - \left(-R \sqrt{R^2 - (0.817R)^2} \right) \, d\theta \\ &= \int_0^{\pi/9} - \left(-R \sqrt{(1 - 0.6667)R^2} \right) \, d\theta \end{aligned}$$

$$\begin{aligned}
 &= \int_0^{\pi/9} (0.577)R^2 d\theta \\
 &= \left[(0.577)R^2\theta \right]_0^{\pi/9} \\
 &= \left[(0.577)R^2 \frac{\pi}{9} \right] \\
 &= 92.72 \text{ mm}^2
 \end{aligned}$$

a) Total area of all the wedge sections (12 sections)

Total area of all wedge sections which are generated by the overlapping is calculated below.

$$\begin{aligned}
 &= (92.72 * 12) \text{ mm}^2 \\
 &= (1112.70) \text{ mm}^2
 \end{aligned}$$

b) Total percentage area of the wedge sections around the ball over the total area of 5 images

$$\text{Percentage (\%)} = \frac{\text{Total over lapped area for 5 images}}{\text{Total surface area of the ball for 5 images (detectable ring)}} * (100)$$

$$\text{Percentage (\%)} = \frac{1112.70}{5779.27} * (100)$$

$$\text{Percentage (\%)} = 19.25$$

c) Total percentage area of the wedge sections around the ball over the total area of half of the ball

$$\text{Percentage (\%)} = \frac{\text{Total over lapped area for 5 images}}{\text{surface area of the ball}} * (100)$$

$$\text{Percentage (\%)} = \frac{1112.70}{1926.42} * (100)$$

$$\text{Percentage (\%)} = 57.76$$

5.4.4 Calculation of the Dead Zone Percentage (DZP)

As mentioned earlier when a smaller detectable ring than the optimum was used some dimples were not detected. In order to visualise the effect of using different rings it was necessary to calculate the DZP for the ball area and that for the total surface detected for each ring. This was carried out by calculating DZP for two selected different rings with 6.00 and 10.75 mm which both are less than the optimised ring diameter (17.51 mm). Prior to this calculation the thickness (t) should be calculated for each ring, fig. 5.14 shows this arrangement when t was calculated for the ring

radii of 6 and 10.75 mm for a ball radius of 21.45 mm.

By intersecting chord property [107]:

$$\begin{aligned} \text{for } a = 6 \text{ mm} \quad a^2 &= t(2R - t) \\ a^2 &= 42.90t - t^2 \\ t^2 - 42.90t + a^2 &= 0 \\ t^2 - 42.90t + 36 &= 0 \end{aligned}$$

$$\begin{aligned} \therefore t_1 \text{ and } t_2 &= \frac{42.90 \pm \sqrt{42.90^2 - 4(36)}}{2} \\ t_1 \text{ and } t_2 &= \frac{42.90 \pm 41.18}{2} \end{aligned}$$

$$t_1 = 0.86 \text{ mm}$$

$$t_2 = 42.04 \text{ mm (not applicable)}$$

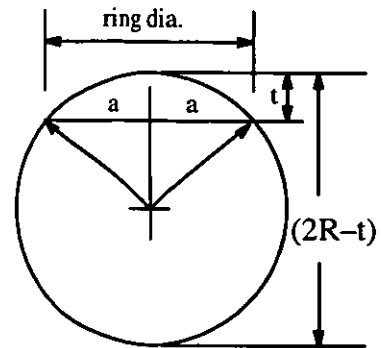


Fig. 5.14. Arrangement of finding height of a wedge.

for $a = 10.75 \text{ mm}$

$$t^2 - 42.90t + (10.75)^2 = 0$$

$$\begin{aligned} \therefore t_1 \text{ and } t_2 &= \frac{42.90 \pm \sqrt{42.90^2 - 4(10.75)^2}}{2} \\ t_1 \text{ and } t_2 &= \frac{42.90 \pm 37.12}{2} \end{aligned}$$

$$t_1 = 2.89 \text{ mm}$$

$$t_2 = 40.01 \text{ mm (not applicable)}$$

Total dead zone area for 6 mm ring:

Area of the half of the ball = 2890.90 mm^2

Total area of the multi images = Area of one complete circle + 4(half circle area)

$$\text{Total area} = 2\pi Rt + 4\left(\frac{2\pi Rt}{2}\right)$$

$$\text{Total area} = 2\pi(21.45)(0.86) + 4\left(\frac{2\pi(21.45)(0.86)}{2}\right)$$

$$\text{Total area} = 347.70 \text{ mm}^2$$

Dead zone area = area of hemisphere – areas viewed by the vision system

$$= 2890.90 - 347.70$$

$$= 2543.18 \text{ mm}^2$$

Dead zone area in percentage (%):

$$\text{Percentage (\%)} = \frac{2543.18}{2890.90} * (100)$$

$$\text{Percentage (\%)} = 87.97$$

The dead zone area for ring of 10.75 mm :

Total area of the multi image area's = Area of one complete circle + 4(half circle area)

$$\text{Total area's} = 2\pi Rt + 4\left(\frac{2\pi Rt}{2}\right)$$

$$\text{Total area's} = 2\pi(21.45)(2.89) + 4\left(\frac{2\pi(21.45)(2.89)}{2}\right)$$

$$\text{Total area's} = 1168.49 \text{ mm}^2$$

Dead zone area = area of hemishpere – areas viewed by the vision system

$$= 2890.90 - 1168.49$$

$$= 1722.40 \text{ mm}^2$$

Dead zone area in percentage (%):

$$\text{Percentage (\%)} = \frac{1722.40}{2890.90} * (100)$$

$$\text{Percentage (\%)} = 59.58$$

5.5 Experiments and results

Six different golf balls and two golf hobs were tested for feature detection and inspection by the proposed method see table 5.1. For each ball and hob the MIST was applied, and a number of different image rings were used and data files optimised by the use of the sorting method. The golf balls were selected from a range of ball types on the market, including two yellow coloured balls. From the table it can be seen that the Top Flite Magna SPALDING ball has an unusual design and it was selected since it was believed that some dimples intersected and this is not a common practice. The pattern on this ball is not designed from one of the Platonic shapes. However, it is a type of segmented design which does not necessarily behave as if it were spherically symmetrical. These balls all had spherical shaped dimples with various dimple chord diameters.

In order to analyse and compare the results between the balls a minimum area which would cover a dimple pattern on each ball was selected. However, patterns on the die separation line were not selected, since the dimples on this line may have been ground to remove excess plastic during

moulding.

Ball type	Colour	Diameter of ball mm	Dimple pattern	No. of dimples	No. of dimple types
Cubic hob	Steel	43.16	Cubic	440	4
Cubic ball	White	42.98	Cubic	440	4
Icos432 Hob	Steel	43.10	Icosdodecahedron	432	5
Icos432 Ball	White	42.67	Icosdodecahedron	432	5
Maxfli Tourltd MD	White	42.60	Dodecahedron	500	3
Slanzenger 2Piece	Yellow	42.78	Icosdodecahedron	420	4
Maxfli CD-90 Dura wound	Yellow	42.66	Icosdodecahedron	432	5
Maxfli CD-90 Dura wound	White	42.66	Icosdodecahedron	500	3
Top Flite Magna SPALDING	White	43.55	Segmented design	422	5

Table 5.1. List of the tested objects for this section.

All samples were tested by the same method and arrangement, the samples were placed individually on the CMM table where they were viewed and imaged by the vision system. After the camera was visually aligned in its position above and to the side of the object (see fig. 5.1), five images were taken from the object. Fig. 5.15 (a, and b) shows examples of the five images. Once the images were processed through the feature detection method in order to identify the dimple locations the data was then stored in a file for further processing. Fig. 5.16 (a, and b) shows examples of the processed images with each detected dimple highlighted.

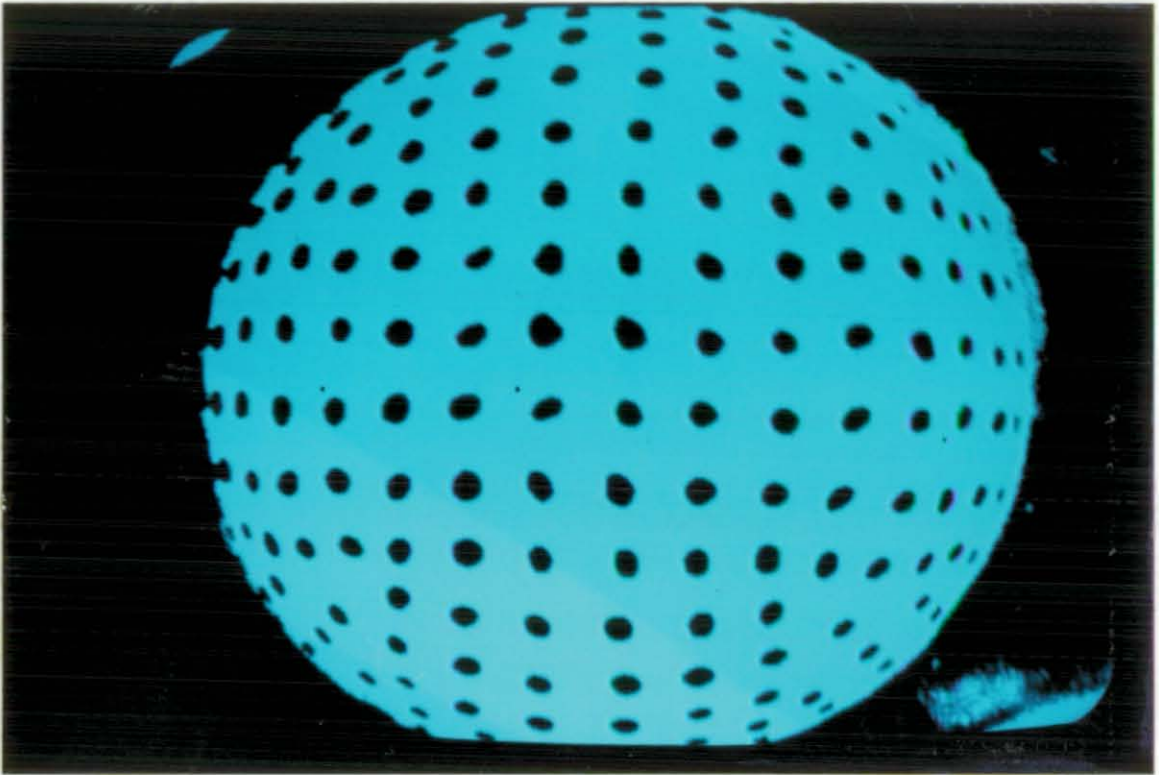


Fig. 5.15(a). Binary image of the golf ball (top view).

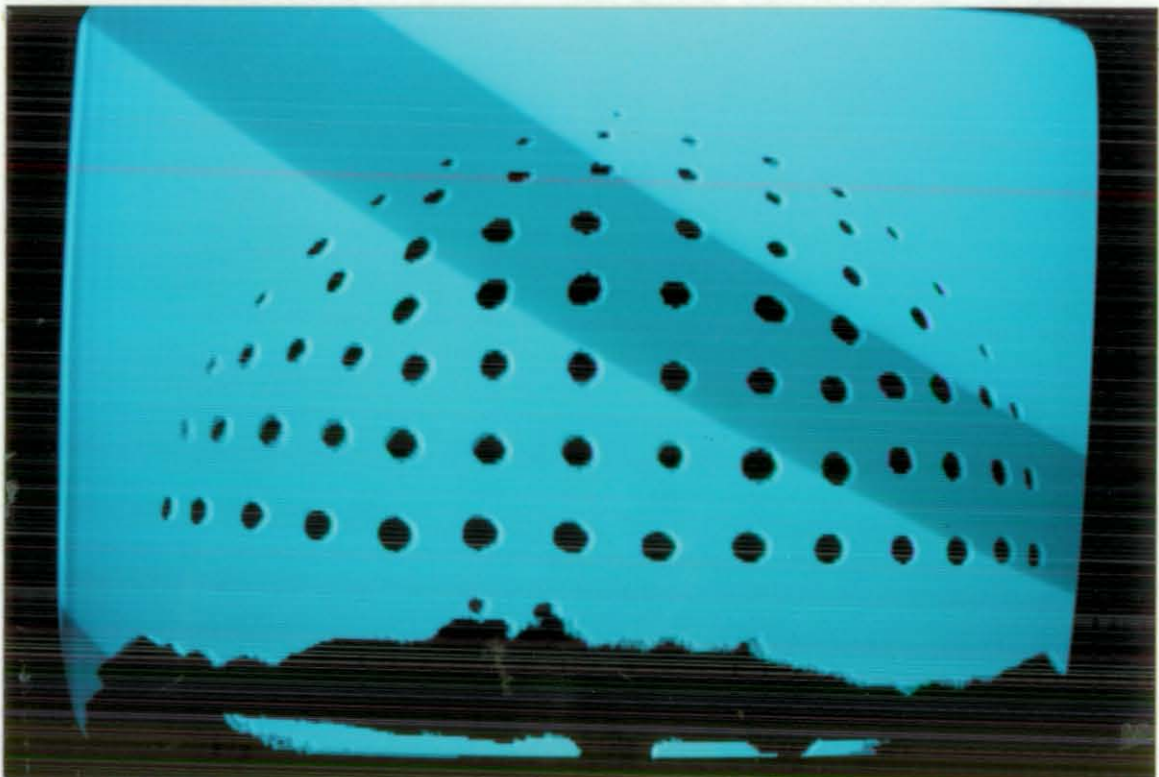


Fig. 5.15(b). Binary image of the golf ball (side view).

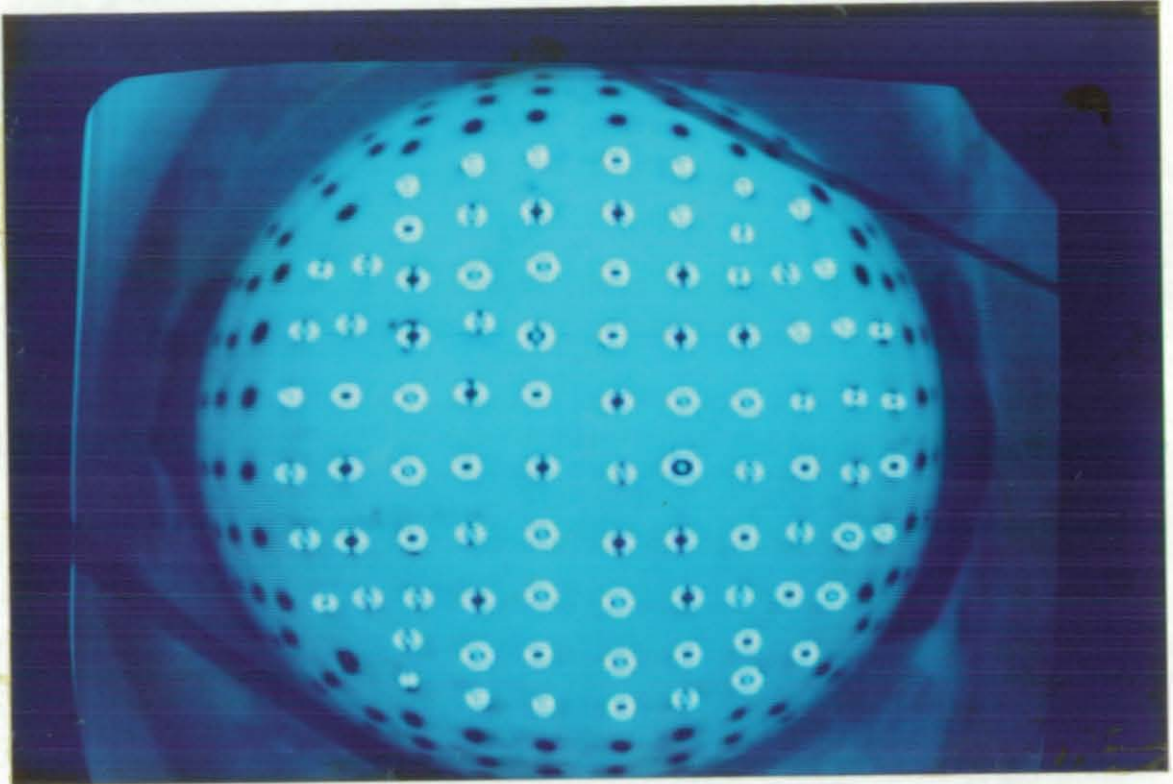


Fig. 5.16(a). Processed image by MIST (top view).

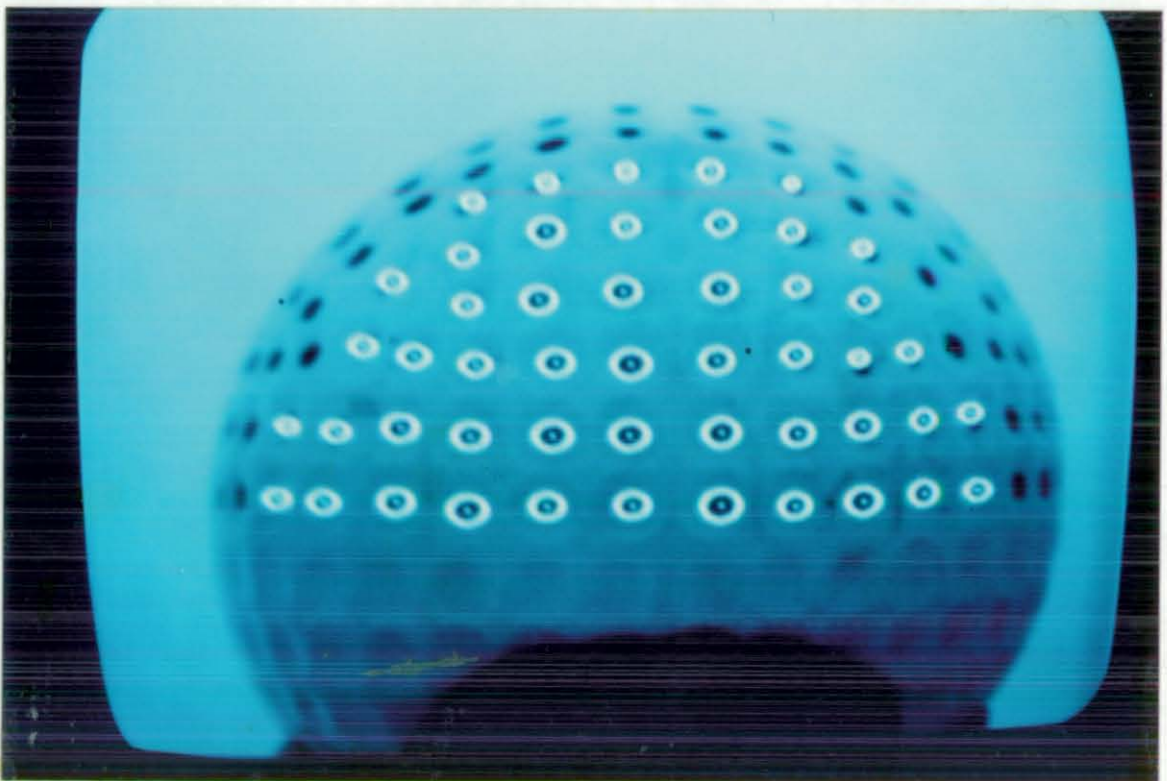


Fig. 5.16(b). Processed image by MIST (side view).

Each sorted data file was checked in order to determine the sorting process and a practical inspection was conducted for the relevant dimples. In order to check the validity of the CMM probing method three further methods were used on sample dimples to check shape and depth. One was the Taylor Hobson Talylin, the second was Universal Measuring Machine MU214B, and the third was laser scanner with the use of 3-D IsoSurf software.

The Talylin is an electronic instrument, capable of measuring surface finish and shape. The main parts of the machine are a measuring head which consists of a stylus and a shoe, an electric motor and a gearbox. The measuring head is drawn across the surface under test. The stylus and its arm are part of a circuit such that when displaced by the surface irregularities during traversing, the A.C. current flowing in the circuit modulates the amplitude. This is fed to an amplifier and causes a pen recorder to produce a permanent record of the displacement. The system accuracy was ± 0.2 microns with various magnifications.

The IsoSurf as a complete unit consists of three main parts, a distance measurement laser stylus (RM600), a motion controller (DMC-1000), and a 3-D software. The laser stylus is designed for non contact measurements between $0.01 \mu\text{m}$ and $600 \mu\text{m}$. The equipment contains a sensor and sensor interface and results are given to a four digit display and LED string. An infrared laser beam (780 nm) is focused on the surface [108] to a spot of 2 or $4 \mu\text{m}$ diameter, according to the type of sensor, which is reflected back to a focus detector. This device is capable of sampling rates of more than 500 per second. It can be interfaced to a variety of motors and drives. This controller provides several modes of motion for the laser stylus including gearing and user defined path following. The system accuracy was ± 5 microns.

The MU-214B machine [109] is an optical device frequently used for measuring workpieces produced in small batches. The measuring range (graduated length of the standard scale) is 75mm. Readings to 0.0005 mm , are made by means of the micrometer microscope fixed to the right hand side of the transverse carriage, while the sensitivity of the settings was $2 \mu\text{m}$. In this case the dimple chord diameter (distance between the two edges) was inspected through horizontal displacement of the machine table which carried the locating microscope and by accurate focusing of the latter on the edge of a dimple. The measurement of the dimple depth was subjective since there was no guaranteed way of locating the dimple centre under the optical head. The chord diameters of a few dimples were measured accordingly by the Talylin and the MU-214B. The laser scanner was used as an alternative to check on selected dimples in order to check profile and shape. However, the amount of time and effort required for using the laser device with its limitation on the range of measurement made it less attractive. The table 5.2. shows the results of these tests on

dimple chord diameter, where the bold figures show the maximum and minimum values found for each sample dimple measured by four measuring systems.

Sample No.	Ball type	Tesa CMM	Talylin	MU-214B	Laser Scanner	Max. variation
1	Icos432	4.108	4.064	3.978	4.030	0.130
2	Icos432	3.986	4.062	3.967	4.120	0.153
3	Icos432	4.049	4.166	3.966	4.002	0.200
4	Icos432	4.044	4.064	4.028	4.000	0.064
5	Icos432	3.973	4.160	4.033	4.010	0.187
6	Icos432	3.998	4.120	4.010	4.025	0.122

Table 5.2. Dimple chord measurement results on sampled dimples.

The maximum variation in chord diameter is 0.2 mm which compares favourably with the CMM measurements, since the positioning of the dimple under the instrument at its centre is subjective.

The MIST was practically applied to the selected balls and, the sum of detected dimples for example on half of a cubic ball was 220 which is 100 per cent. When different detectable rings were applied to the ball, an increase in the number of dimples was detected, consequently different ratios were attempted, table 5.3 shows results of these tests.

Detectable ring diameter (mm)	Number of dimple detected	Percentage (%) $\left(\frac{\text{Detected dimples}}{220}\right)$
15.00	167	76%
17.00	223	106%
17.50	240	109%
18.00	254	115.5%
18.50	273	124.1%

Table 5.3. Results for different detectable ring diameter on a cubic ball.

From the results it was possible to compare the ratio of detected dimples with the detectable ring diameter, for example a larger detectable ring will allow repeated detection of some dimples. Also from the table it can be seen it is not possible to determine an exact ring size in order to have 100 per cent detected dimples. The system will generally give more or less than the optimum value, the orientation of the ball, and the dimple markings i.e., size and the location in the dimple have a considerable influence.

The results from the tests are plotted and shown in fig. 5.17, 5.18, and 5.19, where fig. 5.17 shows the relationship between the detectable ring diameter and the detected overlapped area which is shown as the percentage of the overlapped area for the five images. The maximum overlapped area could reach as high as 200% for a ball hemisphere when the detectable ring radius reached the ball radius (i.e., 21.45 mm). A further point from Fig. 5.17 is the overlapped area has a faster growth after the detection ring passed 17.51 mm since triple overlapping is generated.

Fig. 5.18 and fig. 5.19 show how the detected area and dead zone area (the area where its dimples will not be detected) would have its maximum and minimum values. In fig. 5.18 the left hand side of the graph showed that when a zero detectable ring was used no dimple detection could occur, therefore the detected area became zero, and as the detectable ring reached the value of 17.51 mm the detected area reached its optimum value. As mentioned above when the ring passed 17.51 mm not only overlapped areas started to appear but also triple overlapped areas until they reached their maximum values when the ring reached the ball radius. Two things should be noticed from fig 5.18, first the graph is not linear, and second the maximum value of the total overlapped areas were more than 100 per cent. Fig. 5.19 shows the dead zone area as 100 per cent when the detectable ring is 0 mm and is 0 per cent when the ring is at the optimum value i.e., 17.51 mm. The sample calculation of the dead zone percentage given in section 5.4.4 has been used for generating fig. 5.19.

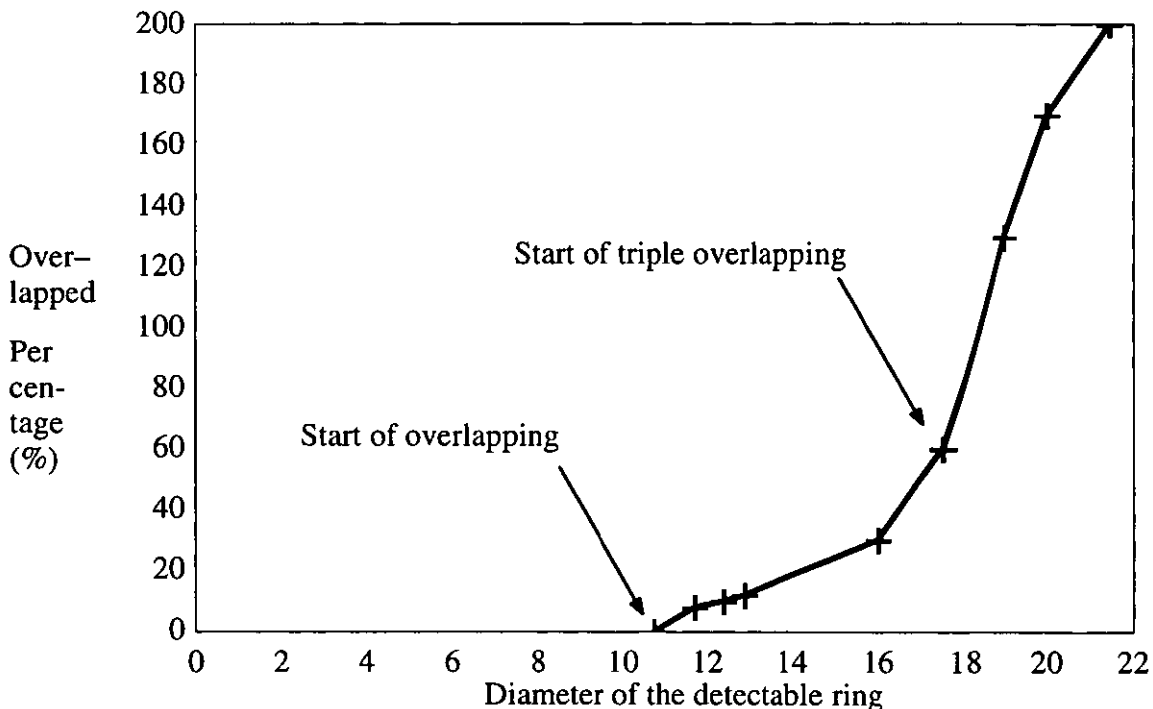


Fig. 5.17. Graph of overlapped area against detectable ring diameter for the ball.

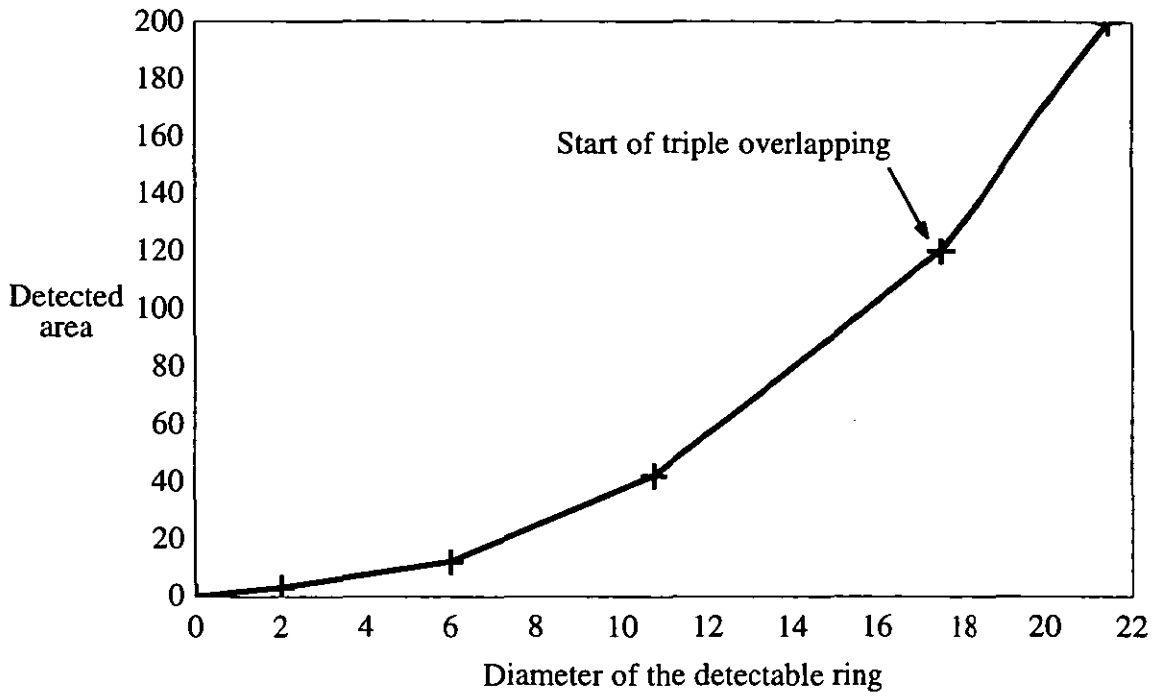


Fig. 5.18. Graph of the detected area against detectable ring diameter.

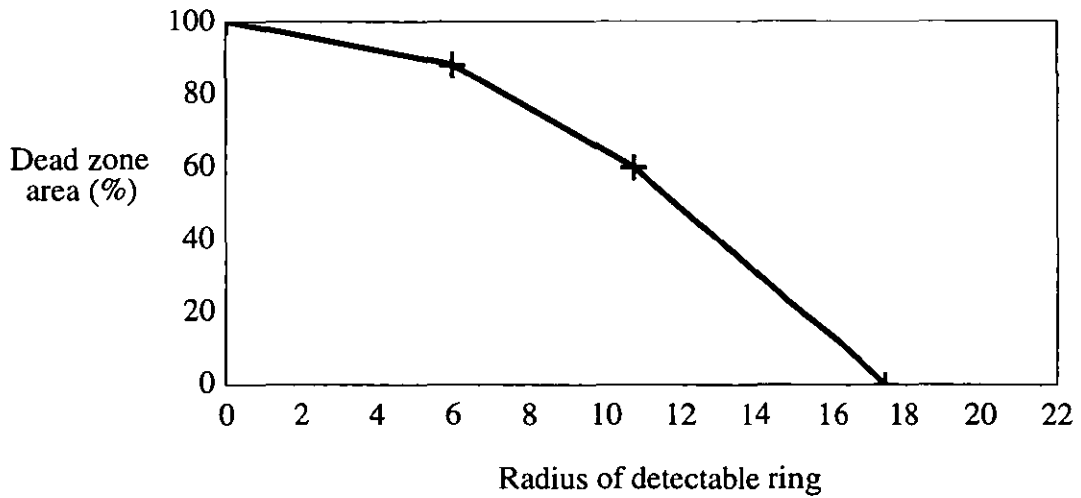


Fig. 5.19. Graph of dead zone percentage area against detectable ring diameter.

5.6 Reduced MIST

It should be possible to reduce the number of views from the five taken previously. One image is the minimum and earlier work [9] has shown this approach to have problems. It is anticipated that a 3 image system could be successful as shown in fig. 5.20.

The stages in this method would be same as that used previously with differences in calculating the axes transformations.

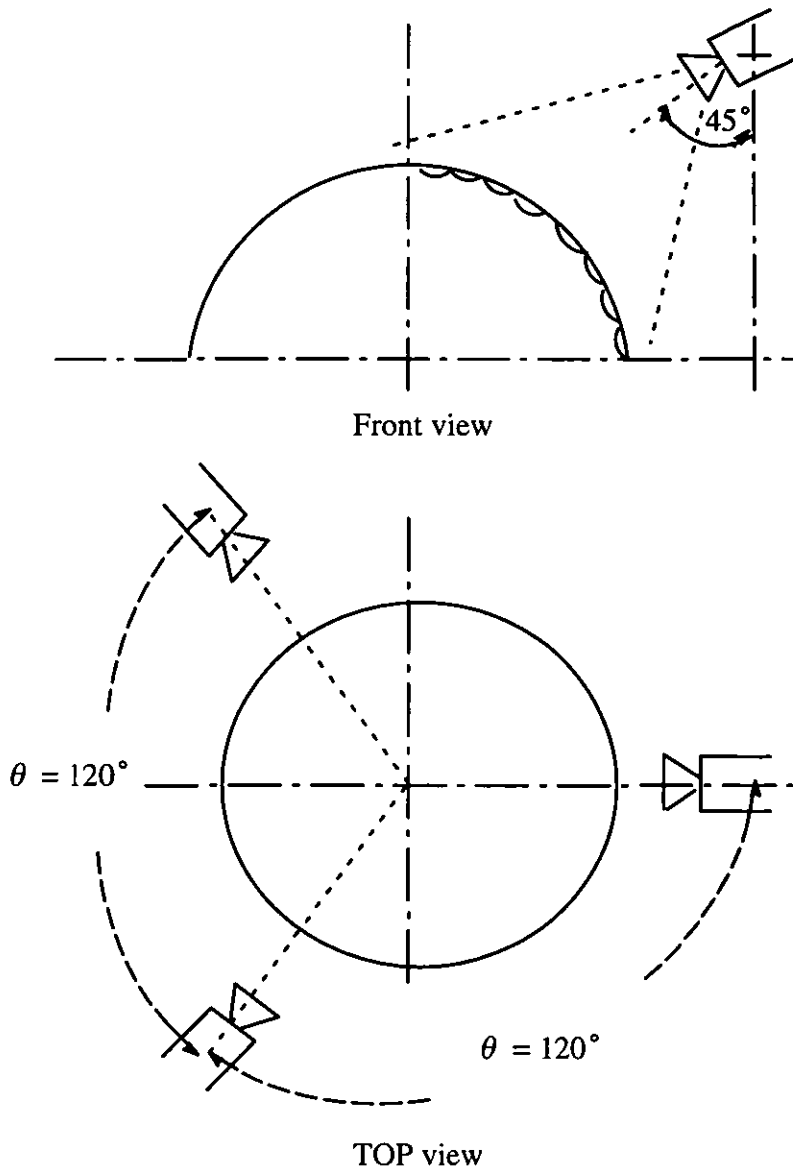


Fig. 5.20. Camera arrangement for reduced MIST.

5.7 Discussion

A one camera multi-image superimposed technique for surface feature identification has been discussed in this chapter. Although the technique was applied to spherical shapes, the concept can be studied, modified, and applied for non regular shapes.

The method used a one camera arrangement for the side views and also for the top view, while the object was placed on a rotary table, however, the technique could easily have used five cameras positioned around the workpiece at any location and the images fed into the vision computer system.

The common problem of illuminating an object which sometimes develops the most challenging section of a vision application has been solved by using a paper filter around the object of interest which resulted in a uniform illumination.

Applying the MIST to spherical shapes generated areas which double overlapped and in certain sections triple overlapped (sections A in fig. 5.7). The features in these areas will be detected two or three times. In order to minimise these areas, and consequently the amount of repeated data, a series of algorithms were developed. In addition to support the practical tests the overlapped areas were analysed mathematically.

CHAPTER 6

THE SYSTEM ERROR MODEL

6.0 Introduction

The importance of dimple location on golf balls originated from their effect on the flight of the ball. Size and shape inconsistency, positional inaccuracy and non symmetrical patterns are the main factors which would generate unexpected flight behaviour. In this research the mentioned manufacturing system errors were evaluated through the inspection of different (actual) hobs and golf balls. Once the actual dimple locations are determined it is necessary to determine the positional error. Each dimple will have an error with respect to its nominal position, however the error determined will be with respect to the set up position for measurement. Clearly if the datum plane is moved the error values will change. A method is required, which once the relative dimple positions are measured, will realign the datum plane to give the minimum error. At present the positional accuracy of dimples on tools and balls is assessed primarily through visual inspection and by practical testing of a number of balls from the pre production models in the field.

To obtain the minimised positional error for the dimples there are a number of methods from which a solution could be achieved. Some of these methods are capable of best fitting data to some geometrical features e.g., least squares best fit or interpolation method to handle data in the form of simultaneous algebraic equations in engineering using matrix notation. Mathematical solutions are also useful methods for minimising or maximising equations. They deal with functions of several variables for example to the 'm' power under a prescribed set of constraints from which the minimum or maximum points or coordinates can be calculated. The significant factor when using these methods is that the data must be represented by a function [110].

The error analysis method for dimple patterns needed to deal with n variables in 3-D space where there may not be an established function between the coordinates. In addition there is unlikely to be a pattern for errors at each coordinate, which makes it difficult since each error should be calculated individually, then compared with others and should satisfy a restricted pattern. It is unlikely that the solution for these problems could ever follow a deterministic equation due to uncertainties of the errors and their nature, however, a more iterative optimised approach could lead to a satisfactory solution.

6.1 Review on error evaluation methods

For any measurement to be of use there are two main criteria which must be satisfied, the measurement must use a system which is recognised and used by others in the field of application

(e.g, the International System of Units, ISO); and the degree of accuracy of the measurement must be known. It is inevitable to have errors, however, a system of evaluating differences (errors) should appreciate the type and source and should make appropriate compensation if necessary.

The British Standard BS5233 [111] (Glossary of terms used in metrology), section five considers the errors in two broad groups; errors in the results of measurements and errors of measuring instruments. Regardless of the sources of error there are many formal methods which can be used to evaluate and control error magnitude. They all aim to explain a sensible correlation between inconsistency or variations of data in tests with a model or specification.

Many researchers have developed methods and algorithms to model and analyse geometric error tolerance zones with the use of statistical analyses. They analysed and developed methods for engineering features such as holes, flat surfaces, surfaces of tooth gears etc. Although much work has been done there is little concentrated effort in any particular direction, some examples which have been tried are as follows:–

Lehtihet and Gunasena [112] discussed solutions for idealised statistical models for the relationship between the position tolerance specification of a single hole and production errors. They considered drilled holes in a flat plate, and used a series of statistical tests on the measured values which were taken by a CMM, to describe production errors and the position tolerance of a hole with regard of feature size and maximum material condition. Wang [113] developed a method to determine form feature tolerances of a machined part with sampled measurement points from a CMM and evaluated the minimum tolerance zone as a constrained optimisation problem with continuous functional relationships. He used a general purpose algorithm for constrained nonlinear optimisation, based on iterative formulation (explained in section 6.3.2). Elmaraghy et al. [114,115] used a similar concept to evaluate and determine actual geometric tolerances using CMM measured data. They developed a procedure for systematic comparison of geometric variations of measured features with their specified geometric tolerances by the use of algorithms and nonlinear numerical optimisation techniques to fit the data to the minimum tolerance zone on the surface of a cylindrical feature. They analysed measurement data by the use of point to point measurement rather than curve fitting. The optimisation algorithm determined the location of the centre point, or reference axis of the geometric element (i.e., cylinder) from which the calculation of the actual geometric tolerances was possible.

Litvin et al. [116] developed a method to minimise gear tooth surface deviations between the theoretical and real surfaces for the improvement of precision. They used a least square method to minimise the surface deviation in the direction of the normal to the theoretical surface.

There are other studies which analyse volumetric errors of machining a sculptured surface workpiece in order to generate a model for on line measurement of volumetric error of machine tools. Cho et al. [117] concentrated on the development of a generalised volumetric error model for multi axis machine tools based on a closed loop configuration with given error data. They used the volumetric definition of a 3-D error at the cutting point caused by the relative motion between the workpiece and cutting tool, which in turn was caused by the geometric error of each axis and alignment errors of the cutting tool. This enabled the volumetric error at the final cutting point to be obtained by calculating the difference between the required point on the workpiece and the tool position.

Regardless of the method of analyses there can be three different evaluation principles for establishing error: a) error within a plane or a surface can be compared with a known reference surface, b) points on the planes or surfaces may be compared to a reference plane, and c) the tendency error within a surface can be established.

6.2 Dimple pattern problems

A golf ball's dimple pattern has a significant role in determining the aerodynamic characteristics of the ball during the flight. In general the effectiveness of dimples is dependent on the number of dimples used and more importantly the dimple coverage (the amount of ball's surface area which is dimpled). Despite the fact that there is little acceptable proof, manufacturers continuously proclaim the performance of their products, for example some claim icosahedron (20 triangle) patterned balls with good uniform dimple coverage give more consistency in flight performance than octahedron patterned balls.

When considering dimple patterns, design and manufacturing problems have to be considered. The design of a pattern requires calculation of how many dimples to be used, dimple depth and diameters. The designers often use iteration methods to place dimples of particular characteristics within a specified area. The selection of these dimples may be from the experience obtained from other successful golf balls. This imperfect placement method will vary from pattern to pattern and will be dependent on the designers knowledge and intuition.

Dimple manufacturing problems are more related to machining and system errors. However, errors from these group may arise from a number of sources such as those related to positioning of the tool and the tooling errors. The precision which is required for dimple machining on a hob is to within $5\mu\text{m}$ in depth, $12.5\mu\text{m}$ in diameter and $25\mu\text{m}$ in position [118].

The simplest or most obvious error solution is to define a datum position on the ball or hob and simply state that all dimple positions could have errors from this specified position. This solution

has the obvious disadvantages that the datum position or the datum dimple might also have an error. A solution was therefore sought which would position a measured pattern with respect to the specified pattern such that the errors between the two would be minimised.

The order of difficulty could have been limited if dimples were only considered for their individual positional error, shape and size characteristics. However, each dimple is also required to be considered within a pattern which generates additional complexity. For example there is a restriction on dimple coordinates within a designed pattern when the length of each element of the pattern is not individually stretchable or extendible i.e., the dimple spatial relationships should stay constant. This indicates that if for example a triangular pattern with its three vertices is under consideration (dimples inside the triangle pattern are not considered), the coordinates of the three vertices are free to rotate or move along an axis in any direction as long as the whole triangle pattern moves and the angles between the sides do not change.

6.3 Possible solutions to dimple problems

In order to show error behaviour of dimples within a pattern and propose a method to reduce the errors to a minimum, many different methods of optimisation such as classical, iteration and data fitting methods were investigated. The classical solutions of optimisation are generally useful for finding the optimum of continuous and differentiable functions. These methods make use of the techniques of differential calculus in locating the optimum points. Since the practical dimple pattern problem involves objective functions which are neither continuous nor differentiable, the classical optimisation techniques are likely to have limited success. However, a study of the calculus methods of optimisation formed a basis for developing useful methods.

Interpolation methods [119] such as Lagrangian, allow curves or surfaces to pass through a set of points passing through a point for every coefficient in each equation. For instance, a first order equation will go through two points, while a quadratic will go through three. Each coefficient can be calculated by solving a set of simultaneous equations and substituting the coordinates of each point and other parameters into the curve or surface equations.

Data fitting methods such as least squares are popular for solving curve fitting and inverse problems [120] because they lead to easy computation. In these methods the gathered data from experiments is to be correlated into a convenient functional form. For example, the method could be used to calculate the best straight line approximation to a set of four data pairs, for minimum error the straight line should pass through all four data points. The main drawback of these methods is their lack of robustness, i.e., their strong sensitivity to a small number of large errors in a data set.

In the following sections a brief introduction and description of different optimisation methods and possible applications is discussed. Although only two of these methods were found feasible for further research it was considered worthwhile to have an appreciation about others available.

6.3.1 Introduction to optimisation

Optimisation is the act of finding or obtaining the best solution to a problem under a given set of circumstances. Optimisation can be defined as the process of finding the conditions that give the minimum or maximum value of a function and in practice this situation can be expressed as a function of certain decision variables. There is no single method available for solving all optimisation problems efficiently, hence a number of optimisation methods have been developed for solving different types of problems [121]. Mathematical models are often developed in order to analyse and understand complex phenomena and in this form the optimisation can be interpreted as finding the minimum or maximum of a function of n variables, $f(x_1, \dots, x_n)$, when n may be any integer greater than zero. The function may either be unconstrained (i.e., act freely) or subject to certain constraints on the variables of the function, for example function $g_i(x_1, \dots, x_n) = b_i$ for $i = 1, \dots, m$ [122].

Generally, logic models are structured to include four basic components:

- a) decision variables or unknowns which are to be found for the model,
- b) parameters which are inputs known either exactly or approximately and may or may not be adjustable by the analyst,
- c) constraints are conditions which limit the values that the decision variables can assume,
- d) objective functions are expressions which measure the effectiveness of the system as a function of the decision variables.

The decision variables are to be determined so that the objective function will be optimised. For problems which are not solvable by classical methods such as differential and variational calculus and involving experimentation, other methods of optimisation are required to be developed by gaining information about the function through direct measurement. These methods are optimum seeking procedures which search for the optimum of any function about which full knowledge is not available. The optimum searching methods are also known as mathematical programming techniques and are generally studied as a part of operations research. The operations research methods may be divided [121] into three groups: mathematical programming techniques (such as, linear, nonlinear, quadratic and geometric programming), stochastic process techniques (such as, statistical decision, queuing and renewal theory), and statistical methods such as, regression

analysis, cluster analysis and design of experiments, which are methods of analyses of experimental data.

6.3.2 Definition of optimisation problems

An optimisation problem involves minimising the objective function which would have a set of independent variables or parameters, and often includes conditions or restrictions that define acceptable values of the variables. The restrictions on the values of the variables are termed the constraint functions of the problem (e.g., the perimeter of a square, a triangle or a hexagon shape can be counted as a constraint for an individual problem). The solution of an optimisation problem is a set of allowed values of the variables for which the objective function assumes an "optimal" value. Generally, to optimise a process three basic components are required, a system model, an equation that represents the behaviour of the process, and finally the optimisation procedure which locates the values of the independent variables to produce the maximum or minimum objective.

In many practical problems the design variables cannot be chosen arbitrarily, since they have to satisfy certain specified requirements. The restrictions that must be satisfied in order to produce an acceptable design are collectively called design constraints. Other constraints, can be functional constraints and geometric or side constraints. The functional constraints represent limitations on the behavior or performance of the system while the side constraints represent physical limitations on the design variables such as availability, fabricability and transportability [121]. For example a real problem could be to design the nose cone of a vehicle, such that, when it travels at hypersonic speeds, the air drag is minimised. Hence, the objective function to be optimised is the drag and the parameters to be adjusted are the specifications of the structure of the nose cone. The optimisation required for this work was to determine a minimised value for dimple position errors arising between the given nominal values and the measured values of dimples on a golf ball.

6.3.3 Classification of optimisation problems

Optimisation problems can be classified in a number of ways which may be based on:–

- i) The existence and the nature of constraints, since any optimisation problem can be classified as constrained or unconstrained depending upon whether the constraints exist or not.
- ii) The nature of design variables. This class of sub groups may be divided into two broad categories. In the first category, the problem is to find values to a set of design parameters which make some prescribed function of these parameters a minimum. For example, the problem of minimum weight design of a prismatic beam subject to a limitation on the maximum deflection, such type of problems are called parametric or static optimisation problems. In the second cat-

egory the objective is to find a set of design parameters, which are all continuous functions of some other parameters that minimise an objective function.

iii) The physical structure of the problem. This class depends upon the physical structure of the problem. This leads to two types of problems, optimal and non optimal control.

iv) The nature of the equations involved. This class is based on expressions for the objective function and constraints. Linear, non linear, geometric and quadratic programming problems can be classified under this group.

v) The permissible values of the design variables. Problems in this group depend on the values permitted for the design variables and can be classified as integer and real value programming problems.

vi) The deterministic nature of the variables involved. Optimisation problems can be classified as deterministic and stochastic programming problems [121,123]. In deterministic problems if the process described by the model was repeated many times, the model will always yield the same set of output values for a given set of input values. In stochastic programming the parameters do not have fixed values, they are random variables which are defined on a common probability space, indexed by the elements of an ordered set which is called the parameter set.

In the following sections two main group of optimisations and least squares best fit are explained from which the most suitable methods will be discussed in detail.

6.3.4 Unconstrained optimisation

The unconstrained minimising or maximising of a function, say $f(x)$ is not subject to any constraints. The function may be a continuous variable or a discrete variable, or a mixture of the two. To solve unconstrained optimisation of functions differential calculus is used. To minimise a function of n variables $f(x_1, \dots, x_n)$ simply then n simultaneous equations should be satisfied:

$$\partial f / \partial x_j (x_1, \dots, x_n) = 0 \quad (j= 1, \dots, n) \quad \dots\dots\dots 6.1$$

However, differential calculus does not provide a method for solving such equations if they have no exploitable special structure. It is possible to solve the equations if the functions $Z_j(x)$ are all real valued.

$$Z_j(x) = 0 \quad (j= 1, \dots, n) \quad \dots\dots\dots 6.2$$

The equations can be solved by minimising the sum of squares of the residuals defined by

$$\sum_{j=1}^n (Z_j(x))^2 \quad \dots\dots\dots 6.3$$

The calculus approach is useful if the equations can be solved directly (i.e., if they are all linear) or to reduce the dimension of the problem [122].

If direct methods prove unsuitable then iterative methods can be used. Iterative methods are often useful for solving simultaneous equations once they have been transformed into a minimisation problem such as equation 6.3. Unfortunately, they are not so useful for solving the calculus equations [122], primarily because stationary points can be a minima or maxima i.e., a saddle point.

Several methods are available for solving an unconstrained minimisation problem. These methods can be classified into two broad categories of direct search methods and descent methods as shown in fig. 6.1.

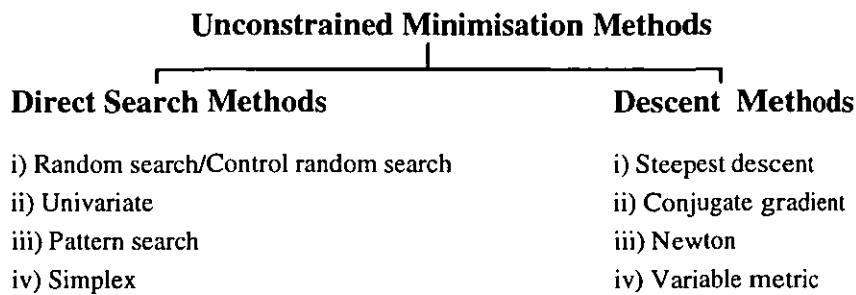


Fig. 6.1. Unconstrained minimisation methods.

The direct search methods require only objective function evaluations and do not use the partial derivatives of the function in finding the minimum and hence are often called the nongradient methods. The Random Search Method (RSM) places experiments randomly in the feasible region after it has been divided into a grid of discrete points. For the univariate method one variable at a time is changed in order to seek to produce a sequence of improved approximations to the optimum point. Since only one variable is changed the problem becomes a one dimensional minimisation problem. Pattern search methods are sometimes called function comparison methods, they are generally techniques [124,125] which begin with short excursions from the starting point to establish a pattern of improved values of the economic model. Based on these function comparisons the method continues acceleration in the direction established from the local explorations. When a failure is encountered, i.e., current value is less than the previous one, the technique will start over again with a new pattern by the use of a local explorations. Again, acceleration is performed in the new direction until a failure is encountered. The procedure continues in this fashion until an apparent optimum is reached. The simplex method is a numerical optimisation method which moves from one feasible solution to another in an iteration procedure [126,127].

The descent methods require, in addition to function evaluations, the evaluation of first and possibly higher order derivatives of the objective function. The descent techniques are also known as gradient methods, examples are the steepest ascent/descent method and conjugate gradient methods. In these methods the maximum would be sought by climbing rather than by elimination which results in locating the next block of experiments somewhere in the direction of the gradient, thus the maximum may be found through evaluation of the partial derivatives of the variables. Other geometric methods are called variable metric methods. These methods begin the search along a gradient line and use gradient information to build a quadratic fit to the model (profit function) [124].

In general, unconstrained minimisation methods are iterative in nature and hence they start from an initial trial solution and proceed towards the minimum point in a sequential manner. The general iterative scheme is shown in fig. 6.2.

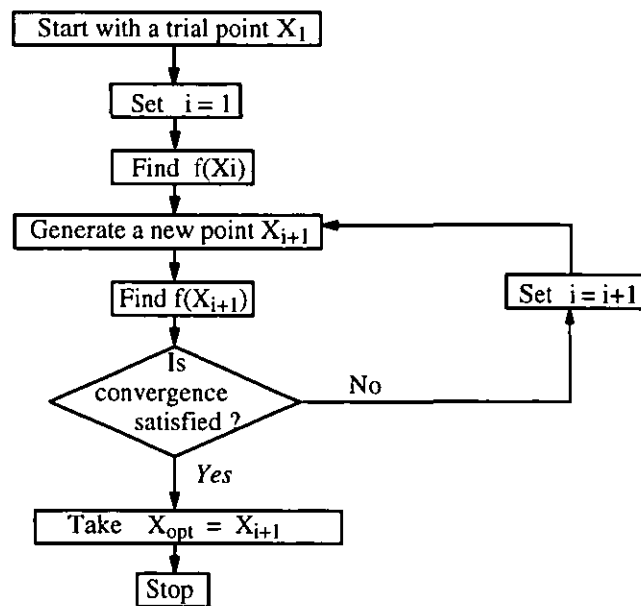


Fig. 6.2. General iterative scheme of optimisation.

6.3.5 Constrained optimisation

The two main groups of this optimisation are linear and nonlinear constrained programming optimisations. In optimisation of linear constrained programming, the objective functions and all the constraint functions appear as linear functions of the decision variables. However, the constraint equations in a linear programming problem may be in the form of equalities or inequalities. The special properties of linear programming allow methods to be developed by combining techniques from unconstrained optimisation and linear algebra.

In nonlinear constrained optimisation the constraints imposed upon the variables imply a certain nonlinear function. Methods for minimising this kind of functions can be divided broadly into two classes, those which set up an equivalent unconstrained minimisation problem by adding a penalty term to the objective function (i.e., barrier and penalty function methods), and those which seek to generate a sequence of feasible descent steps which would involve linear approximation to the constraints [124,128,129].

6.3.6 Least squares best fit

Least squares fitting algorithms are optimisation routines to approximate to linear (such as, line or plane) or non linear (such as, circles, spheres, cylinders and cones) functions by fitting features to a set of data points. For the 2-D case of curve fitting, a set of n points as $(x_1, y_1), \dots, (x_n, y_n)$ are given and it is required to determine a function $F(x)$ such that $F(x_i) \approx y_i$, for $i=1, \dots, n$. The method of least squares can be explained better by an example [120,130], if n pair of measurements, $(x_1, y_1), \dots, (x_n, y_n)$ are required to be fitted to a straight line of $y = a + bx$. The line should be fitted through the points so that the sum of the squares of the distances of the points from the straight line is to be minimum, the line is then in a unique position. The first task is to find estimated values of a and b such that the line gives a good fit to the data. At any point x_i the corresponding point on the line is given by $a + bx_i$, so the difference between the observed value of y and the predicted value can be given by

$$e_i = y_i - (a + bx_i) \quad \dots 6.4$$

The least squares estimates of a and b would be obtained by choosing the values which minimise the sum of squares of these deviations (i.e., residuals). Thus the sum of the squared deviations will be given by

$$S = \sum_{i=1}^n e_i^2 \quad \dots 6.5$$

$$S = \sum_{i=1}^n (y_i - (a + bx_i))^2 \quad \dots 6.6$$

The equality is a function of the unknown parameters a and b , which can be minimised by calculating partial derivatives $\partial S/\partial a$ and $\partial S/\partial b$, setting both these derivatives equal to zero, and solving the two simultaneous equations to obtain the least squares estimates, \hat{a} and \hat{b} , of a or b

$$\frac{\partial s}{\partial a} = \sum 2(y_i - a - bx_i)(-1) \quad \dots 6.7$$

$$\frac{\partial s}{\partial b} = \sum 2(y_i - a - bx_i)(-x_i) \quad \dots 6.8$$

When these are both zero:

$$\sum 2(y_i - \hat{a} - \hat{b}x_i)(-1) = 0$$

$$\sum 2(y_i - \hat{a} - \hat{b}x_i)(-x_i) = 0$$

Where sum over i from 1 to n gives,

$$n\hat{a} + \hat{b} \sum x_i = \sum y_i \quad \dots 6.9$$

$$\hat{a}\sum x_i + \hat{b} \sum (x_i)^2 = \sum x_i y_i \quad \dots 6.10$$

These two simultaneous equations in \hat{a} and \hat{b} are often called the normal equations.

6.4 Possible solutions worthy of evaluation

In order to design a method capable of optimising the errors within a measured coordinate system, a conventional approach to the problem by defining the objective function needed to be determined. In a conventional design procedure the aim is usually to find an acceptable or adequate method/design, which satisfies the functional and other requirements of the problem. However, there will always be more than one acceptable design and optimisation.

In simple measurement the objective function is the error between the design and actual values. In addition to determining the objective function, it was necessary to establish the system constraints, which were the simple's spatial position and its relationship within the platonic pattern. This kind of constraint which represents limitations on the behaviour of the system would be named a functional constraint.

In order to model the errors it was essential to identify if there was a pattern within them, since this could dictate the possible solution. However, it was found that the errors were not follow any pattern, therefore a practical optimisation method was needed which required the use of iteration methods. The majority of methods such as classical, stochastic, etc are found impractical for this problem due to the fact that there was no function which could explain the behaviour of the errors and they also needed a limit on the constraints.

One possible approach to this kind of problem was by optimising the data using CRS/RSM. One of the main advantages of using this method is that no limits are required on the degree of constraints within the system. The types of constraints were the size and the form or shape of the pattern which all should be kept unchanged. It was anticipated that the use of RSM would minimise positions for the actual data [121,125,131] and although, the solution to the problem was in three dimensions, a two dimensional solution was first developed for simplicity.

6.5 Proposed random search method for optimisation

As explained previously to classify an optimisation problem it is necessary to establish the nature of the problem, for a golf ball the dimples could not be grouped in a linear or nonlinear form. It was possible that the errors in a dimple pattern were generated through an imbiased machining system with other possible shortcomings being in the design specification i.e., selecting the wrong size dimple. The objective was to minimise positional errors. One of the most suitable methods was to use a numerical optimisation i.e., RSMs sub group of the direct search methods. These methods require only objective function evaluations and do not use the partial derivatives of the function in finding the minimum which makes them most suitable for simple problems involving a relatively small number of variables. The use of a RSM for this work was envisaged to be useful due to the nature of the problem i.e., not having prior knowledge of the behaviour of the errors, therefore, there appeared to be no solution using any direct methods.

6.5.1 RSM experiments on the golf ball patterns

The procedure of the RSM algorithm is shown as a flow diagram in fig 6.3. The method has been evaluated for a series of 2-D geometric pattern arrangements with arbitrary given points. For golf ball dimples there are two sets of data, nominal and actual. In order to visualise the effect of optimisation better, it was decided to assess graphically the pattern representation of dimples which were created from the actual and nominal data. Therefore, the graphical representation of the nominal pattern was assumed to be the target and that of the actual data was the objective to be minimised. In order to implement the technique for this problem it was required to develop a constraint function which was designed to be the sum of distances between these data points i.e., the target length was made of the nominal values and the objective was made of the actual values. In order to find optimisation positions for the target points each distance 'e' between the trial and the nominal point was stored for comparison to select the lowest value between them.

The dimple error minimisation will have a function of the sum of errors (i.e., objective function), with n variables (dimple centre coordinates).

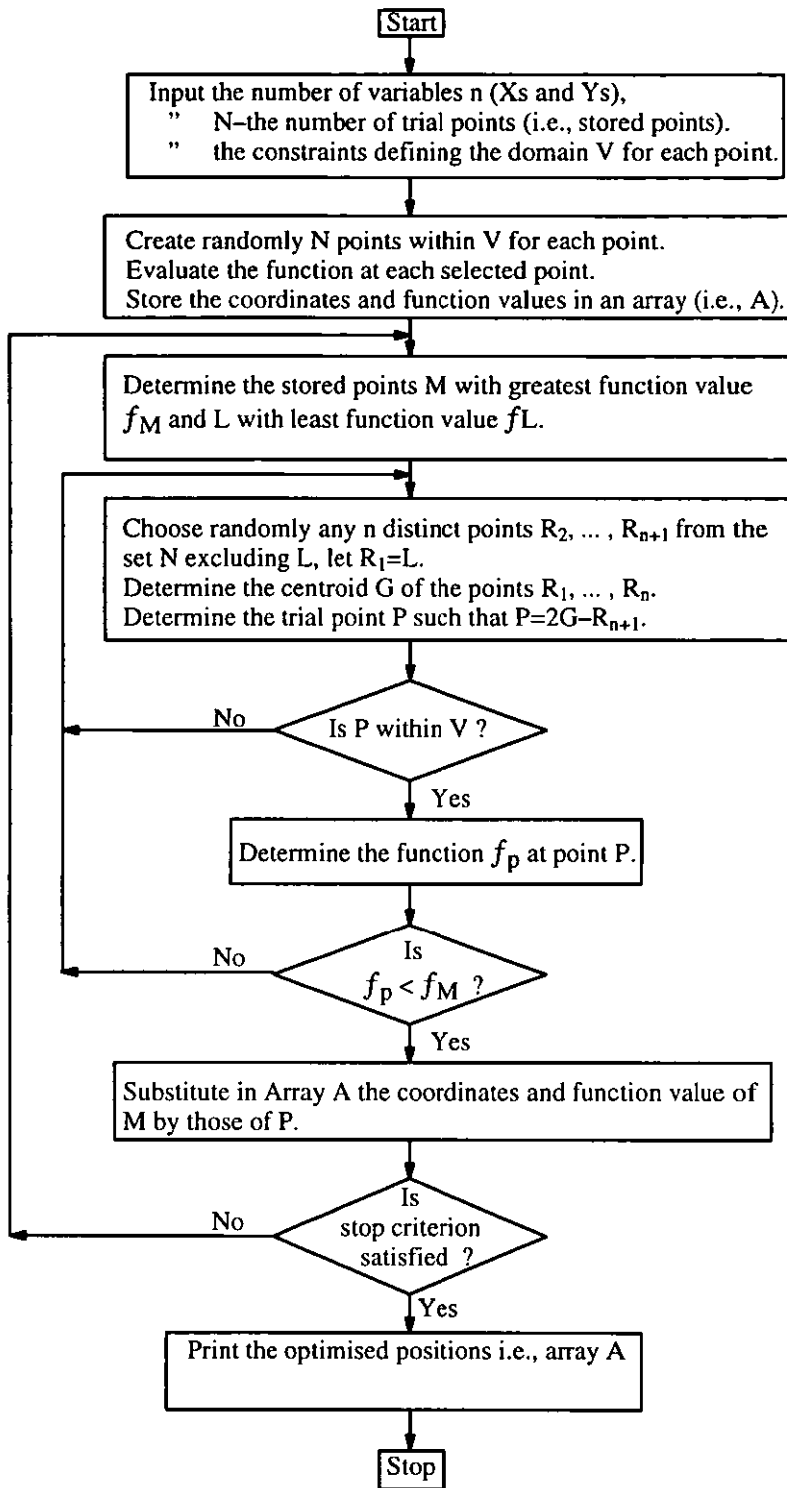


Fig 6.3. Flow chart of the random search.

$$f_P = \sum_{i=1}^n e_i \quad \dots 6.11$$

$$f_P = (e_1 + e_2 + e_3 + e_4 + \dots + e_n) \quad \dots 6.12$$

An initial search domain V was defined by specifying two limits (upper and lower) for each coordinate. A predetermined number of trial points N over the initial domain V were selected. The points were generated through a random generator. The concept of selecting the value for N is that the greater this value the more thorough the search and the higher the probability of discovering a global minimum would become. On the other hand the larger the value of N , the greater is the demand on computer storage and slower the convergence of the algorithm. The appropriate choice of N is a matter of experience, however the empirical rule recommended by Price [125] is $N = 10(n+1)$ where, N is the predetermined total selected points for search which dictates the trial, n is the number of variables e.g., for a 2-D triangle pattern with three corners which gives six variables (i.e., $n=6$), N would be 70, for a square pattern $N=90$ and $N=110$ for a pentagon pattern.

The error function evaluated at each trial and the position and function value corresponding to each coordinate were stored in array A . Then search and select the worst point (M) with the function value f_M and the best point (L) with its function value f_L which could be found in array A . 'n' distinct points R_2, \dots, R_{n+1} , were selected from the set N excluding L , since it was assigned $R_1=L$. These distinct points (R_2, \dots, R_{n+1}) are chosen at random from the N ($N \gg n$) in store and these constitute a simplex of points in n -space. The point R_{n+1} is taken (arbitrarily) as the pole (designated value) of the simplex and the next trial point, p is defined as the image point of the pole with respect to the centroid, G of the points. The centroid G of the points R_1, \dots, R_n would be determined and the next trial point computed through equation $P = 2G - R_{n+1}$ from a set of possible trial points for each corner. The position of P will be checked to be provided within the domain V . Fig. 6.4 shows the random number selection.

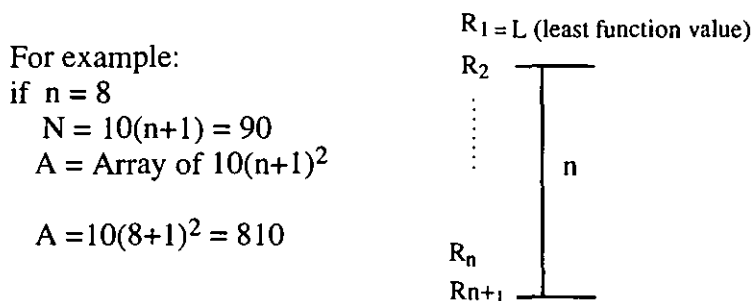


Fig. 6.4. Selection range of the random number points.

At each iteration the constraint function f_P was evaluated for each new trial point and was compared with the maximum available function value f_M (designed specification) within the gener-

ated set. If f_P was less than f_M , then M was replaced in array A by P, otherwise if either P failed to satisfy the constraints or $f_P > f_M$, then the trial was discarded and a fresh point was chosen from the trial set.

The search terminated when the stop criterion was satisfied; otherwise, the test would be repeated for other worst points. The application of the RSM is discussed below to show how the method can be applied for the problem of error minimisation on dimple positions for a square pattern. The method was also applied to a 2-D pentagon pattern in order to show the effect of optimisation better. To be able to carry out these tests, two sets of values were required. The first set of values were the nominal X and Y coordinates of dimples which were treated as the problem function values (objective function). The second set of the values was given in X' and Y' which were the measured values and were treated as the constraint values.

In this scenario the X and Y values were to have the specified values of the positions, and X' and Y' values were used to find the best minimised distance (error) between these two set of values. Fig. 6.5 shows a very simple case where four outside points ($X_1, Y_1, \dots, X_4, Y_4$) are the given coordinates and four inside points ($X'_1, Y'_1, \dots, X'_4, Y'_4$) are the measured values. The best result will be when the sum of e_1, \dots, e_4 are a minimum. The system was required to be given two sets of limits, one in the x-direction and one in the y-direction within which N random points will be chosen. It is important to be able to select realistic limits in order to reduce the convergence rate and have efficient searching. One possible way was to select an area zone below and above each of the coordinates points. For example, when X_1 and X'_1 are 10 and 15, the limits in x-direction can be selected from 8 to 17, and when Y_1 and Y'_1 values are 10 and 20 the limits in y-direction can be selected 8 to 22.

The system required a constraint function to be calculated, which in this instance was the total length of the measured points i.e., for the square pattern, the length of 4 sides which can be simply calculated by the equation 6.13.

$$\begin{aligned} \text{Constraint function} &= \text{Length of } (P_1 + P_2 + P_3 + P_4) && \dots 6.13 \\ &= \sqrt{(x'_2 - x'_1)^2 + (y'_2 - y'_1)^2} + \sqrt{(x'_3 - x'_2)^2 + (y'_3 - y'_2)^2} + \sqrt{(x'_4 - x'_3)^2 + (y'_4 - y'_3)^2} + \\ &\quad \sqrt{(x'_1 - x'_4)^2 + (y'_1 - y'_4)^2} \end{aligned}$$

and the centroid of points can be found by,

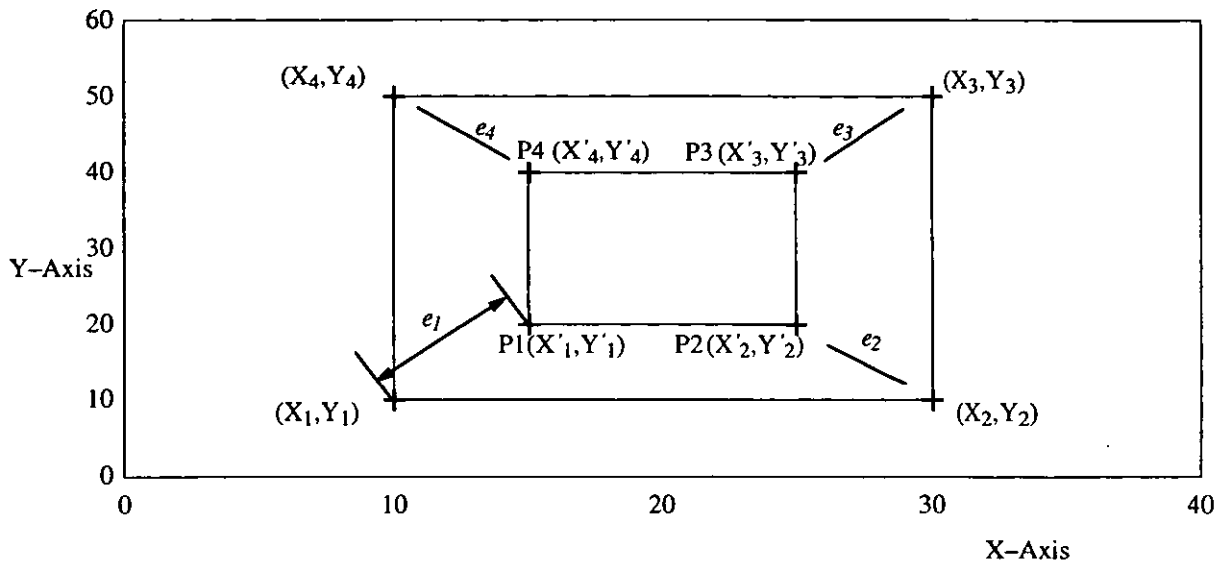


Fig. 6.5. Four points square optimisation.

$$\bar{X} = \frac{1}{m} \sum_{i=1}^m X_i$$

$$\bar{Y} = \frac{1}{m} \sum_{i=1}^m Y_i$$

The output is the optimised coordinates of the best possible position for the points which gave the minimum distances between the nominal and the measured values. A series of 2-D patterns were examined for validation, such as a 2-D line, triangle, and square where in each, a set of actual and nominal points was selected with some exaggerated differences in order to see the optimised results comfortably. In the following section a detailed example of this method is applied to a pentagon pattern.

Pentagon pattern

In this example the X and Y coordinates of the nominal pentagon had a total of 10 variables which were represented by X_1, Y_1 to X_5, Y_5 and the actual pentagon coordinates represented by X'_1, Y'_1 to X'_5, Y'_5 . The problem required to minimise the actual vertex positions. In order to minimise the objective function f which is the sum of errors e_1 to e_5 (2-D distances between the actual and nominal coordinates) the equation 6.12 was used, for example an error distance for one vertex can be calculated as $e_1 = \sqrt{(X_1 - X'_1)^2 + (Y_1 - Y'_1)^2}$ subject to the total length (L) of the polynomial (constraint function) where $L = l_1 + l_2 + l_3 + l_4 + l_5$.

A programme was developed and written in Fortran named RSM based on the Price controlled random search optimisation method [131]. The programme required the length of the designed pattern, the domain for each corner (upper and lower), the number of trails N and the values of the variables. The procedure is as follows:-

The given variables were, (i.e., nominals)

$$(X_1, Y_1) = (03, 05)$$

$$(X_2, Y_2) = (13, 05)$$

$$(X_3, Y_3) = (15, 12)$$

$$(X_4, Y_4) = (08, 19)$$

$$(X_5, Y_5) = (01, 12)$$

The measured values, (i.e., actuals)

$$(X'_1, Y'_1) = (02, 4.5)$$

$$(X'_2, Y'_2) = (13, 5.5)$$

$$(X'_3, Y'_3) = (16, 13)$$

$$(X'_4, Y'_4) = (10, 20)$$

$$(X'_5, Y'_5) = (02, 12)$$

Domain V in X-direction selected as,
(lower-upper limit)

$$01 - 04$$

$$12 - 14$$

$$14 - 17$$

$$07 - 11$$

$$00 - 03$$

Domain V in Y-direction selected as,
(lower-upper limit)

$$04 - 06$$

$$04 - 06$$

$$11 - 14$$

$$18 - 21$$

$$11 - 13$$

$$\begin{aligned} \text{Constraint length} &= \sqrt{(x'_2 - x'_1)^2 + (y'_2 - y'_1)^2} + \sqrt{(x'_3 - x'_2)^2 + (y'_3 - y'_2)^2} + \sqrt{(x'_4 - x'_3)^2 + (y'_4 - y'_3)^2} + \\ &\quad \sqrt{(x'_5 - x'_4)^2 + (y'_5 - y'_4)^2} + \sqrt{(x'_1 - x'_5)^2 + (y'_1 - y'_5)^2} \\ \text{"} &= \sqrt{(13 - 2)^2 + (5.5 - 4.5)^2} + \sqrt{(16 - 13)^2 + (13 - 5.5)^2} + \sqrt{(10 - 16)^2 + (20 - 13)^2} + \\ &\quad \sqrt{(2 - 10)^2 + (12 - 20)^2} + \sqrt{(2 - 2)^2 + (4.5 - 12)^2} \end{aligned}$$

$$\text{Constraint length} = 47.154 \text{ mm.}$$

The optimised values (i.e., X_{opt} , Y_{opt}) were calculated to be,

$$(X_{\text{opt}}, Y_{\text{opt}}) = (2.99, 4.99)$$

$$(X_{\text{opt}}, Y_{\text{opt}}) = (13.00, 4.99)$$

$$(X_{\text{opt}}, Y_{\text{opt}}) = (15.00, 12.00)$$

$$(X_{\text{opt}}, Y_{\text{opt}}) = (7.96, 20.79)$$

$$(X_{\text{opt}}, Y_{\text{opt}}) = (0.99, 12.00).$$

Fig. 6.6 shows the graphical representation of the above example. Although it can be seen that the optimised positions of the actual points are satisfactory, the pattern is distorted which is not acceptable. This was caused by having only one constraint function i.e., the length of pattern. Also from further experiments on different dimple patterns it was revealed that optimising the positional errors on the length of the other polynomials produced the same result. An extra constraint was introduced in the programme on these patterns in order to keep the angles between the shapes constant which was not successful, due to the excess amount of restriction created. The programme was unable to process this condition.

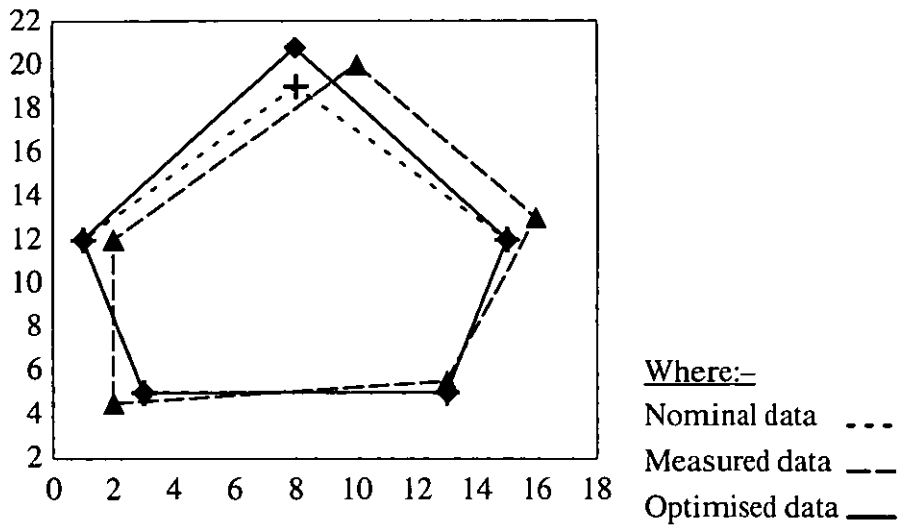


Fig. 6.6. 2-D Pentagon pattern optimisation by RSM.

Further analysis indicated that the optimisation process would be time consuming and it would be impractical to implement the RSM on the golf ball patterns, since determining the domains i.e., Vs for each point (i.e., 250 points) and constraint functions for the lengths as well as the angle or shape of the pattern would be a laborious task. However, if the problem could be arranged to optimise only dimples on the pattern line of the golf balls and the pattern distortion was not a problem, this approach could possibly be of the simplest and most practical method for this case.

6.6 Proposed Least Squares Best Fit Optimisation Method (LSBFM)

In order to minimise dimple positional errors a virtual centre for each dimple was required to be calculated. This point was named the Surface Virtual Point (SVP) and was defined as the centre of the dimple at the nominal ball radius and could be generated from the intersection of the ball and the dimple fig. 6.7 shows a schematic generation of this point.

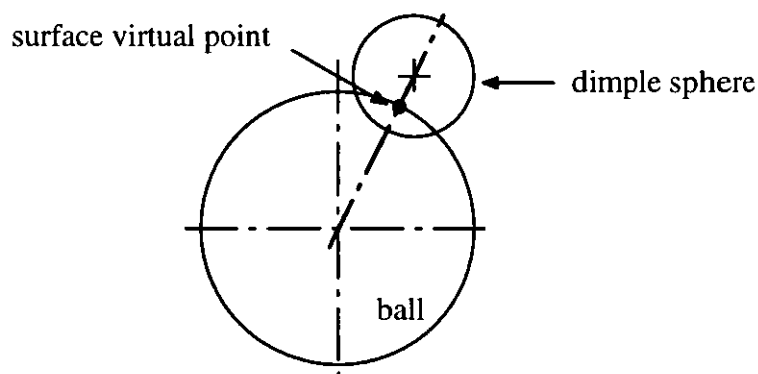


Fig. 6.7 Dimple virtual point.

The importance of these points was appreciated when the nominal and actual data needed to be compared in order to establish possible production variances which may then improve the production of the part by finding the source of variation.

The error at each virtual centre should be calculated individually and then compared to that of other centres in order to satisfy a restricted pattern. A survey of literature has revealed no analytical method for assessing this type of 3-D error optimisation.

In essence, the proposed optimisation method finds the best point positions for the errors by use of a number of trials on the objective function in order to give critical values or a set of minimum values subject to certain constraints on the control variables. 3-D optimisation was used for each trial, with the calculation of the objective function for all the points in three axes.

A comparison was made between the nominal designed values to those of the actual data which were obtained through measurement on the CMM. The required limits on the data were selected no wider than the distance between two dimple thus, the relationships between the dimples was ensured.

The software employed for this section of the project was developed and written in C and its flow diagram can be found in fig. 6.8. The programme requires a tolerance zone which depends on the size type of dimples used on the ball and permits the points to be assessed in three axes for both negative and positive directions. One of the outputs of the programme was the optimised positions of the actual points and some others were the length of the objective function, and the value of residuals. Sequentially a small value in different directions was added or subtracted to the coordinates and the objective function evaluated. The objective function was then recorded and compared in order to select the objective function with the minimum value which would refer to the best position of the data. The method of optimisation was arranged in cartesian form, however, the polar approach would have a similar concept and is explained later.

6.6.1 Cartesian approach

The first step is to create an objective function, an example of which can be the location of the dimples on the surface of a ball. The dimples are machined in relation to the ball center as well as to a pattern. The machining of the dimples requires positioning in 5 axes, which results in some error between the specified and actual positions. These positional errors generally do not occur in a controlled manner. Once the positional errors are established a method is required to minimise the errors in a controlled process.

The objective function for this problem was based on the distance between the nominal positions and the actual positions. The objective function needed to be minimised which required the cal-

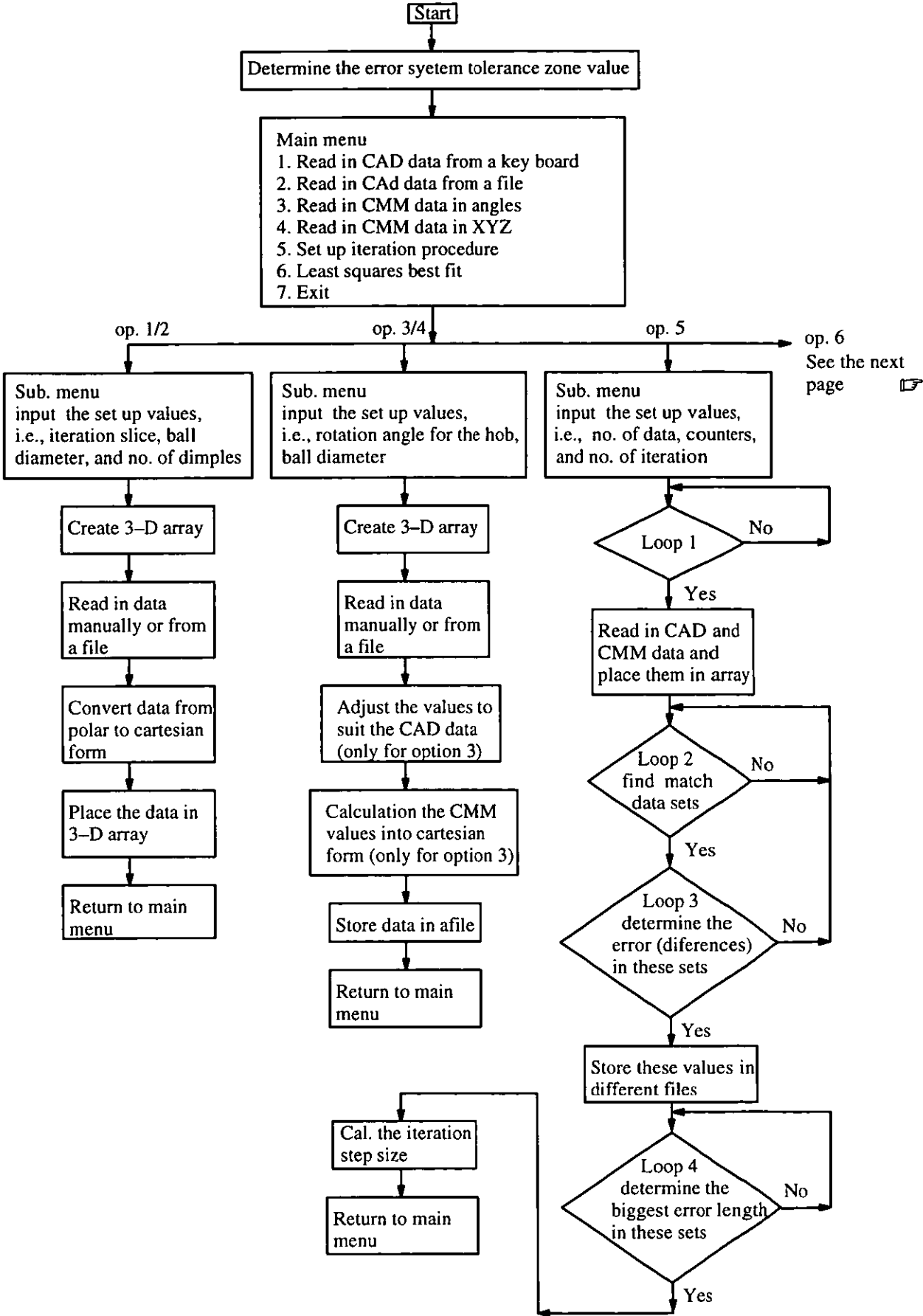


Fig. 6.8. Flow diagram of the programme of least square best fit.

op. 6

From previous page

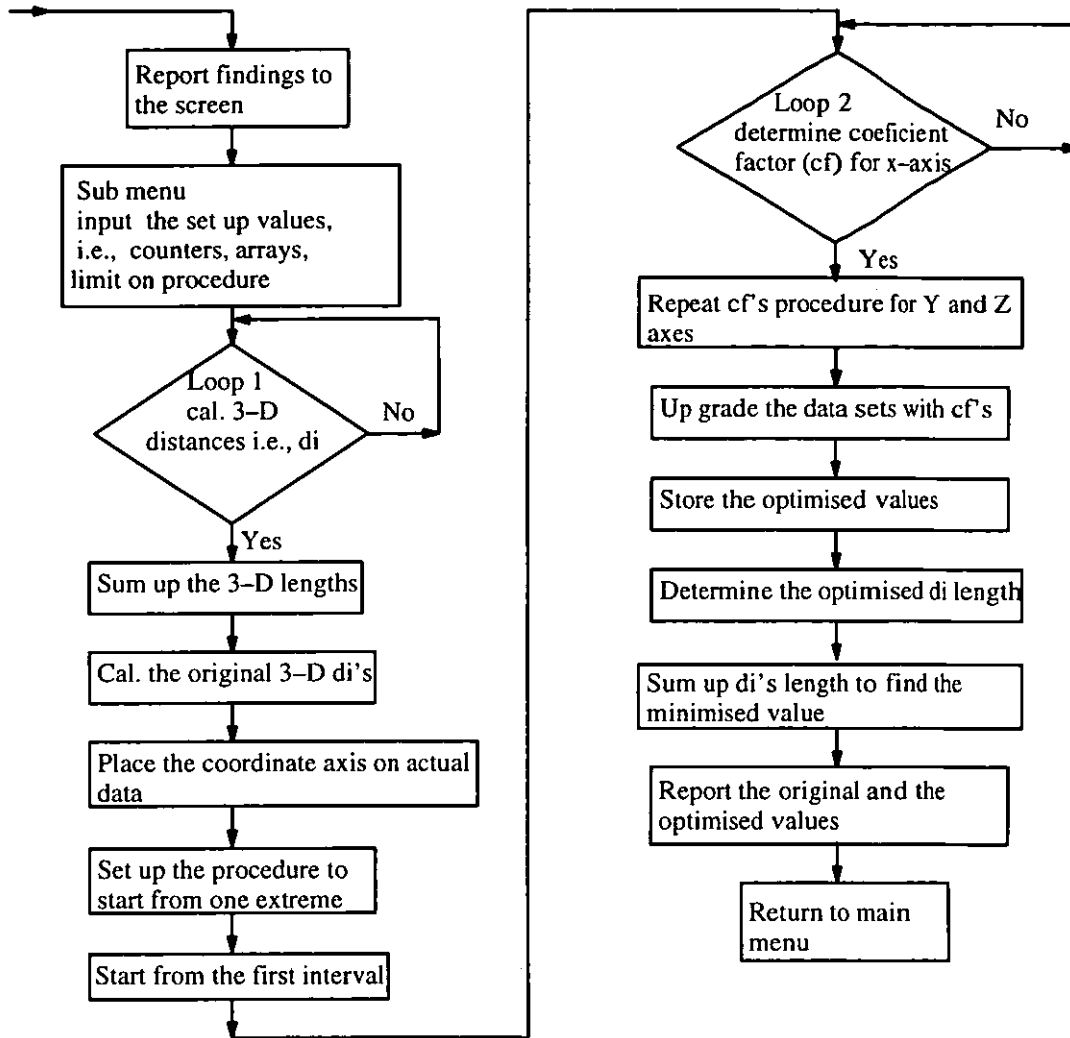


Fig. 6.8. Flow diagram of the programme of least square best fit.

culuation of the distance between each pair of related data points (i.e., a nominal and actual point). The total summation of these distances was represented by the objective function. A method was then required to move the pattern of points toward the position, where the sum of the error lengths would present the least value of this function. The optimisation was performed by an iteration procedure.

The new position for the pattern of points was the best minimised arrangement that could be found for the existing errors. The iteration needed to be controlled to arrive at a minima and one way of handling it was by using the points in cartesian coordinates. As mentioned before, there could be as many as 250 dimples on half of a ball, consequently 250 errors would be accounted for in each trial. The related distance between each of the designed values and that of the actual

value was named d_i with i designating the number of dimple. The use of this method would not restrict the amount of data, and the objective equation can be written as:-

$$E = \sum_{i=1}^{i=n=250} (d_i)^2 \quad \dots 6.14$$

$$E = \sum_{i=1}^{i=n=250} [X_{n_i} - X_{a_i} \pm (\Delta X)]^2 + [Y_{n_i} - Y_{a_i} \pm (\Delta Y)]^2 + [Z_{n_i} - Z_{a_i} \pm (\Delta Z)]^2 \quad \dots 6.15$$

Where E is the objective function, ΔX , ΔY , and ΔZ are the iteration step sizes, and d_i is the error between each data pair set.

One of the important factors in this method was how the iteration could be controlled. The best position for each piece of data was when its positional error was zero and ideally that was achievable when all the nominal points and the actual points could be coincidentally located. To initiate the iteration a starting point was required, logically in such an iteration a starting point could be a point with the worst global characteristic (i.e., a pair of data points which gave the maximum separation length). The worst case of the error length was the maximum calculated error length which could be found between the axes of a data set (i.e., $|X_{max}|$, $|Y_{max}|$ or $|Z_{max}|$), however, a simple solution would be to take the largest absolute length value which could be found within the set, i.e., $|(X_n - X_a) + (Y_n - Y_a) + (Z_n - Z_a)|$.

6.6.2 Calculation of the domains

The values of $\pm X_{max}$, $\pm Y_{max}$ and $\pm Z_{max}$ are the extremes which will be selected for the iteration domains. The 3-D error lengths can be determined in relation to the ball centre, by calculating the distance between the actual and nominal data. In order for the optimisation to proceed the largest possible error between the data sets i.e., the largest 3-D error between the data sets was selected and the domains for three axes were set, based on this value. This would cover any error between the data sets in any plane.

Once the domains are determined an imaginary box was created and placed on the actual data. A local coordinate axis was placed at the centre of the box with the domains at negative and positive sides of the axes, where each axis represented error in that direction with indexed intervals, e.g., X_{int} . Fig. 6.9 schematically shows this arrangement.

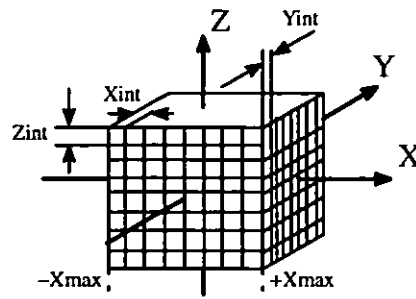


Fig. 6.9. Visualization of error limits for three axes.

The process starts from the actual data with the limiting values divided equally into reasonable size intervals i.e., 0.01 mm to produce an accurate optimisation. The iteration procedure always started from one extreme and worked through the intervals to the other extreme. This process is repeated for the three axes in turn by increasing the iteration step for each run. The minimum and maximum values of error lengths for all the dimples were stored separately. The minimum for each objective function for each axis would represent the optimised case for that axis. From each optimised function, the iteration coefficient in each direction was then selected and would be added to all actual data coordinates in order to generate the optimised dimple centres.

The procedure of calculation of the minimum dimple error is summarised as follows:–

1. Determine the maximum and minimum lengths of 3-D error distances for the nominal and actual values, a schematic sample is shown in fig.6.10 where the Virtual Length (VL) and Centre Length (CL) are shown for a dimple. The largest length will be kept as the reference. The virtual lengths were used for the 3-D error distances.

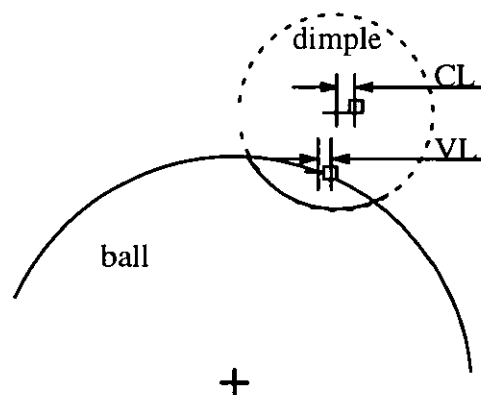


Fig. 6.10. Error distances for a dimple.

2. Select an iteration step size based on the maximum value found.

3. Divide the limits into equal intervals for both positive and negative directions similar to that in fig. 6.9.
4. Run the process for each axis.
5. Calculate the squared length of errors for each pair set.
6. Repeat step 5 for all the dimple pairs.
7. Repeat step 5 for all combinations of the intervals.
8. Sum the squared error lengths for each iteration.
9. Compare the calculated error lengths for each iteration to find the minimum for three axes.
10. Determine the correction factor for each axis from step 9.
11. Find the 3-D optimum location in X, Y, and Z values from the minimum cases .
12. Place the original error axes found from step 11 in the new error axes arrangement for one more investigation.
13. Repeat step 3 to step 9 to possibly arrive at a better accuracy around the optimum point.
14. Determine the new locations (optimised) by adding/subtracting the correction factor to the actual data locations.
15. Evaluate the optimised positions by graphical representation of the actual and optimised data to that of the specified values.

A series of tests were carried out on cubic and icosddh 432 hobs to support this theory. The dimples on the hobs were measured three times to ensure consistency of the results. Each of the measured data was processed by the proposed optimisation method and new values were calculated. In order to represent the results graphically on the Unigraphics CAD system it was necessary to distinguish this data by using different colours for data sets, e.g. the nominal data was represented with colour red. A sampled set of the optimised results for the cubic and icosddh 432 hobs are listed in appendix A.

In order to study the results an example from the icosddh 432 sets (appendix A) is selected and explained in detail in fig 6.11:–

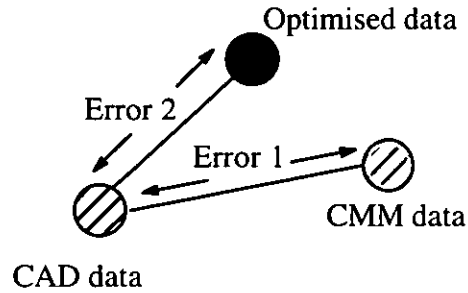


Fig. 6.11. Error optimisation for a set of dimple.

Distance	Minimum	Maximum
Error 1	0.0028	0.0158
Error 2	0.0013	0.0141

Table. 6.1. Variations for a sampled dimple data.

In fig.11 the distance between the CAD and CMM data is designated as Error 1 i.e., the system spatial error, and that between the CAD and optimised as Error 2. The table 6.1 consists of selected dimple sets which produced the minimum and maximum distances within the optimised data. The Error 2 values are those to be minimised. Fig. 6.12 and 6.13 show the graphical error representation of the actual (red), nominal (yellow) and the optimised (green) position for a few dimples, individually and in a pattern.

6.6.3 Polar approach

Many curves such as circles and cardioids are more easily described in polar coordinates which implies that it is also easier to use polar coordinates in order to compute the length of such curves [110]. In this section the procedure of finding the arc length between the nominal and actual data is presented. The method calculates the 3-D arc length between the data and minimises the arcs in a similar manner to that in the cartesian approach. The polar approach was investigated and showed very small variations in order of 0.002 mm to that of the cartesian method. Therefore, it was satisfactory to treat the arcs as straight lines. Details of the polar concept is in appendix B.

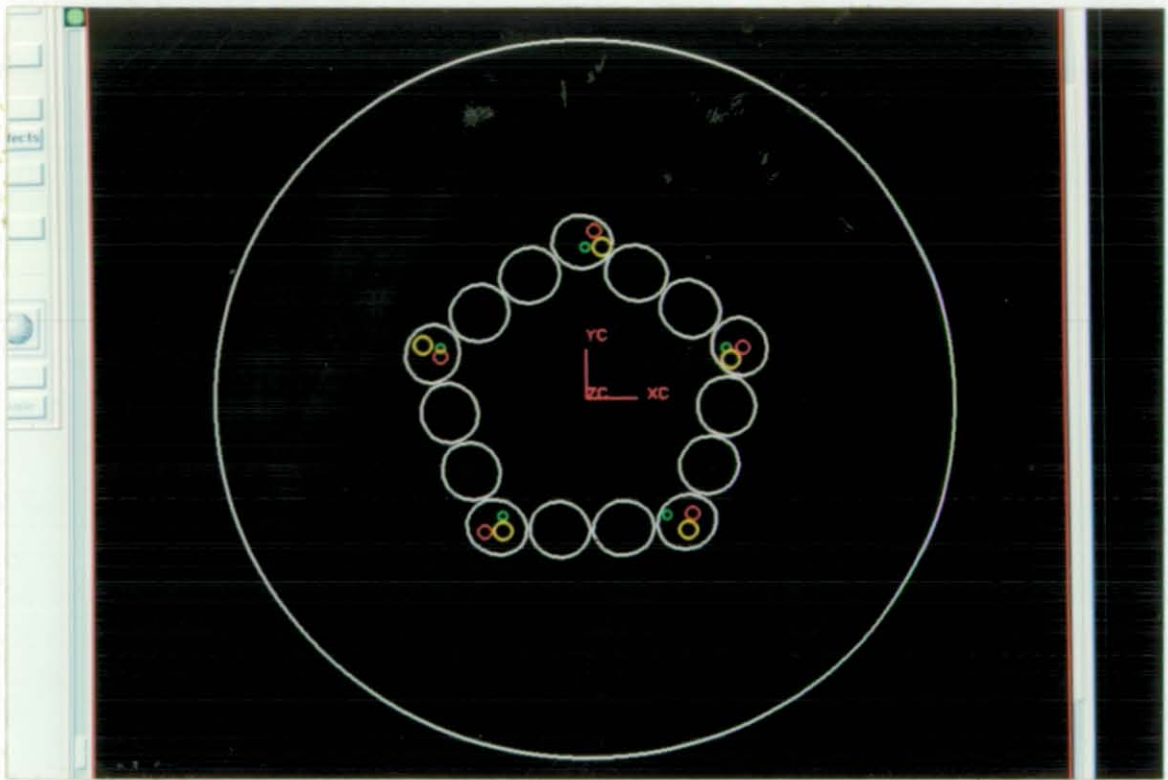


Fig. 6.12. Individual error representation for a pattern.

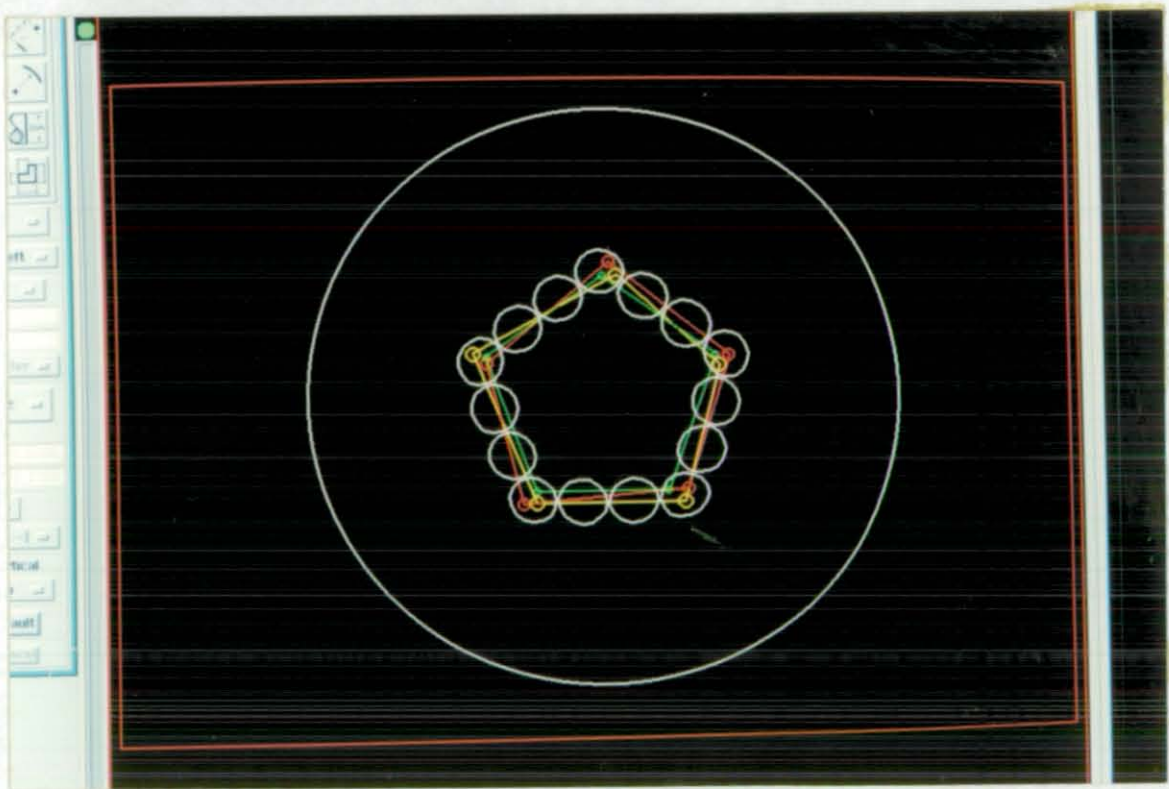


Fig. 6.13. Pattern error representation for a selected set of dimples.

6.7 Discussion and Results

In this chapter a system error model has been presented for dimple patterns.

The most obvious error solution is to define a datum position on the ball or hob and simply state that all dimple positions could have errors from this specified position. This solution has the obvious disadvantages that the datum position or the datum dimple might also have an error. A solution was therefore sought which would position a measured pattern with respect to the specified pattern such that the errors between the two would be minimised. A criterion is that the dimple spatial relationships (specified and actual) should stay constant.

Many different methods of optimisation and data fitting were investigated from which the CRS or RSM and least squares method were found to be feasible. The RSM method of optimisation was found simple and efficient with a very high percentage of success, despite the fact that the optimised positions were selected through a random procedure. The major disadvantage of this method is the distortion of the dimple pattern, consequently altering the spatial dimple relationships. A series of simple different patterns were experimented with to study the optimisation behaviour. Fig 6.6 shows clearly the effect of distortion on the pattern by the procedure. This system has the potential to be applied by deploying more constraints in order to prevent the patterns from distorting. The main disadvantage of this would be the time required for the system to process data.

The LSBFM was found to be successful due to its fast processing time. The proposed method finds the best point positions for the errors by the use of a number of trials on the objective function which was developed in order to give a set of minimum values to certain constraints on the control variables. In order to show that the method is applicable to any type pattern and also to have a less complex visual representation of the procedure a series of test were carried out on square patterns. Fig. 6.14 shows an implementation of LSBFM on square patterns with different error variation. Although the patterns are shown in 2-D the actual practice was done in 3-D. In Fig 6.14(a,b, and c), intentionally one corner of the original patterns was chosen to be varied in order to see the effect of optimisation better. In each figure a different amount of variation was used for the corner point. From the figures it can be seen that regardless of the variation sizes the optimised patterns have not been distorted, and, have been moved to the optimised locations.

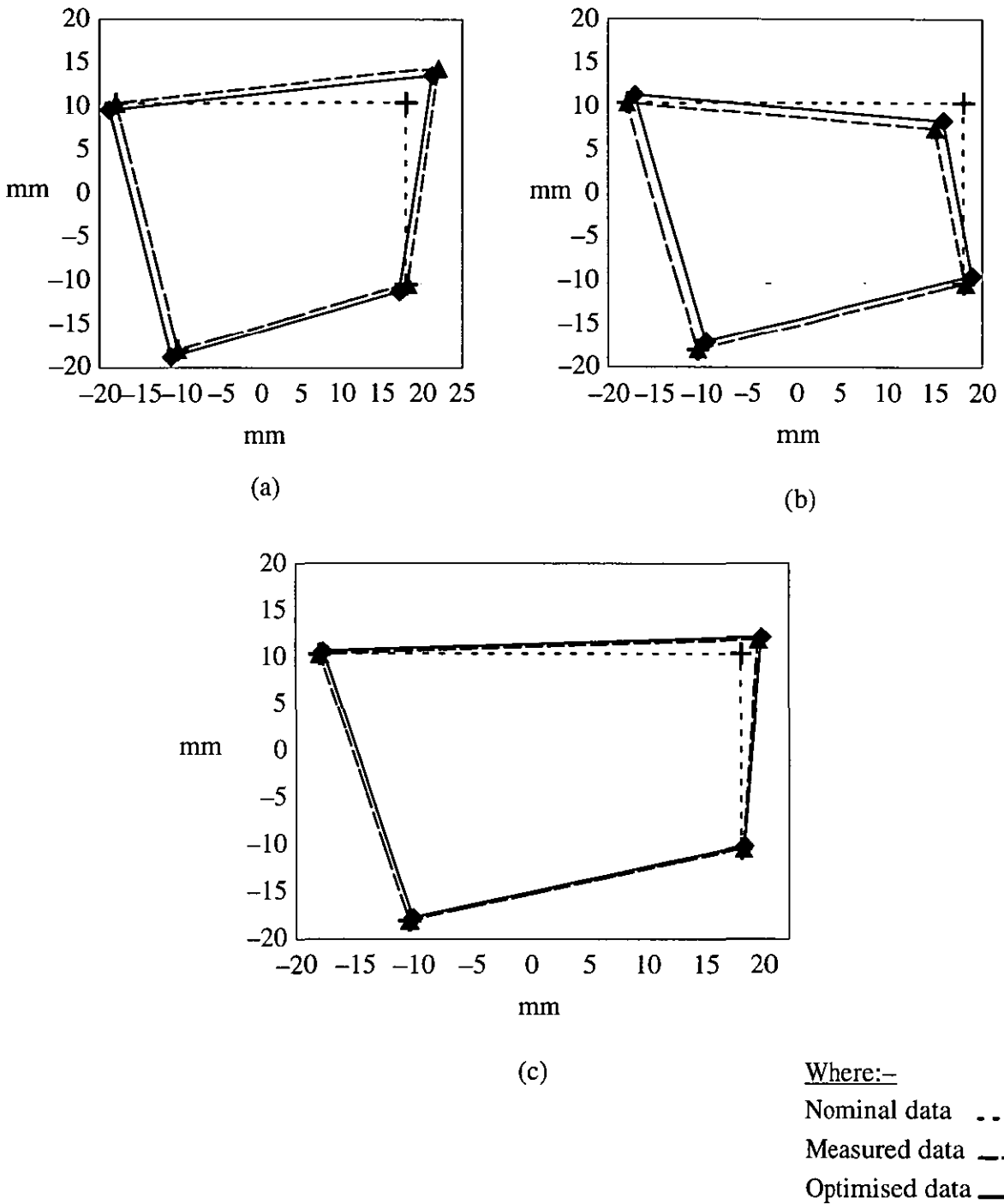


Fig. 6.14. LSBFM on square patterns.

The method of optimisation for golf ball objects was arranged in the cartesian form due to the small nature of the errors, however, the polar approach would have a similar concept. The reasons why the polar approach was not used, were the negligible different values in arc length and that of a straight line, excessive computation time, and the overall the difficulty of using it overruled

applying it, a simple calculation of the error with the use of polar and cartesian method is in appendix B in order to appreciate the amount of variation for an arc and straight line.

One of the main difficulties regarding the positional error for dimples was specifying the possible error which could be generated by the CMM. The designed (dimple locations) was presented by θ and ϕ angles from a reference (datum) dimple. In order to address the dimples it was necessary to align the reference dimple to the CMM axes. In the case of the icosddh 432 hob specification the reference dimple was given by a type A dimple, dimple number 16 positioned at $\theta=0.000^\circ$ and $\phi=22.762^\circ$ (degrees), however when this dimple was measured on the actual hob by the CMM, θ was found to be 16.728° and $\phi=0.241^\circ$. The measured data was adjusted to these values for the error modelling. One of the problem or inaccuracy of the system is the datum dimple might be in error which in this case referring all other dimples to the datum dimple could generate a situation where the correct dimples will be assumed wrong.

CHAPTER 7

INTERFACING CAD AND CMM

7.0 Introduction

CAD and CMMs have been available for some time, but until recently they have been largely used individually. In recent years the practicalities of integrating a CAD system with a CMM have changed dramatically because of the savings which can be made by using them concurrently in manufacturing and inspection industries. In order to allow such integration to happen component geometry information needs to be transferred from the CAD system to a CMM or vice versa by data files developed through a standard protocol. There is a need for an inspection planner to take the designed model consisting of specification of the part geometry, dimensioning and tolerancing information to produce an automatic inspection plan and programmes with detailed instructions. One of the practical applications of CAD and CMM integration is seen in mould design, where the CAD system is linked to one or more CNC machining centres [55,132].

With the rapid development of CMMs and associated softwares data can be more quickly and accurately collected by using various probing systems to sense a surface or feature, and used to create CAD drawings for documentation, or a part programme for an appropriate machine tool. One prime use of CMM data collection is to evaluate the part dimensions against the specified values in order to establish errors with the further enhancement of showing the graphical representation of their existence. There are many industrial environments where the CAD and CMM link [39,40,55,75,85,101,132,133,134] to give benefits. Reverse engineering where the CAD model is created by using data collected by a CMM is also a significant application area particularly for sculptured parts which may have been hand crafted.

In the following section the term CAD is used for a system which is accompanied with an inspection post processor module as one unit.

In order to achieve an effective and useful integration between an inspection module of a CAD and CMM the following needs to be considered [40]:

- i) Generation of inspection programs.
- ii) Creation of a data format for transfer of inspection information to CMM.
- iii) Compatible CMM software which can interpret CAD generated files.
- iv) Use of a data format for transfer of inspection results back to CAD.

Conceptually, for a CAD directed CMM there are three main areas to be considered. The first area concerns with the creation of an inspection file in the CAD inspection module which uses the

design data. The second area deals with the definition of all features to be used in the process, including all datums and attributes. The final area takes responsibility of determining the inspection paths for each feature which can usually be previewed graphically on a CAD system.

In this work the integration is between a Tesa CMM and the Unigraphics (UG) 3-D CAD modeller. Ideally automatic transfer of a set of data which represents dimples on a golf ball would be through a local network. The data was arranged in the form of X, Y, Z centre coordinates of the dimples accompanied by the dimple diameter. Due to unavailability of the software at the time in order to perform an automatic transfer of data between the two systems, the work was manually carried out by inputting data into the CAD system. The work planned to use the UG spreadsheet application named UG/Xess with a user function to process the model (see recommendation for future work). The UG/Xess allows creation and update of a UG family of parts and these tables can also be imported from other PC spreadsheet applications. UG expressions are converted to formulas in UG/Xess, so users quickly see changes to the model when different values are used. In order to support and appreciate the inspection procedure and also to visualise the order of precision a graphical comparison was generated between the actual and nominal data (section 7.4).

7.1 Review of CAD and CMM integration

The issue of CAD and CMM interfacing has been the subject of research for a number of years in order to improve the speed of inspection and overcome the difficulty of measuring complex parts. This has been influenced mainly by the increasing roles of CMM's as a fast, flexible, and accurate measuring tool in a high demand automated production area, however the majority of work has been for prismatic parts. Cowling and Mullineux [39], McCarthy and Genest [55], Farmer and Smith [75], Powaser [133] and others have studied the importance of inspection process requirements. They agree that for an efficient integration between the two systems a standard file format is crucial.

The role of CAD and CMM integration has been one of the main objectives of the National Research Council of Canada (NRCC) [3] in order to develop an automated machining cell. In their system a closed loop inspection system inspects production from the cell and communicates the results to the cell controller. Through this integration the measured data from the CMM is transferred to the CAD computer for analysis.

As mentioned previously Takeuchi et al. [4] used a vision based system to develop an automated inspection environment. They also used a solid modelling CAD/CAM system named P-CAPS to generate the CMM measuring path for the manufactured parts. From the CAD data a set of measuring points on the workpiece were selected and each feature measured automatically in turn

as they were constructed by the CAD system. The system is useful only for mechanical parts which are composed of a combination of primitives.

In a Computer Aided Inspection (CAI) system Pakh et al. [76] developed an interactive and integrated inspection system for moulds having sculptured surfaces with some basic features such as holes and slots.. The CAD system contained the model from which features were selected manually for inspection and inspection planning was arranged for each feature. Osbaldiston et al. [135] attempted to combine CAD and CAI in an interactive programming environment with the target criteria to produce a system capable of extracting geometric information for prismatic parts from any CAD system supporting IGES in order to generate inspection part programmes. In their system the data was used to form the basis of an interactive programming environment capable of generating inspection part programmes conforming to the DMIS. The methodology of their work was to extract 2-D geometric data from an IGES file and recreate the drawing as accurately as possible by the Graphical Kernel System (GKS) on the chosen output device. The DMIS part programme for this file was then generated by instructing the system with the type of commands required at any particular points in the part programme i.e., an accompanying piece of code to specify the feature for example cir. for a circle.

Lu et al. [100] researched into establishing an AI inspection path planning system to avoid repeated routes and to provide the best movement path between the components. Their attention was based on optimal path planning for the whole measurement task which included finding the shortest inspection path for multiple components. The AI path planning system required input of component information which could be read into the data processing unit through CAD files, from a vision system data file or input manually.

It is apparent that automated inspection planning is an extremely complex subject, and further research is needed to develop this area. Unfortunately, all the interfaces which have been developed between the CMM and CAD to date have been for particular CAD systems. Since there is no universal translator for this link, it was seen necessary to arrange a link between the UG CAD and the Tesa CMM for this work.

7.2 Generation of CAD data/Reverse engineering of parts

The use of computers to create product designs is primarily a geometry based activity which is organised to manipulate coordinate data points into lines, planes, and other geometric shapes. Free formed and complex surfaces require considerable data to represent them, and generation of this data is not an easy task. If the component has been designed during a crafting process so that it is the design specification, the collection of data of part requires intelligent analysis, es-

timization of features and the density of points to be sampled to give good surface representation. It is useful wherever possible to build a feature with a known set of properties and then transfer it to the CAD system. In order to identify and provide a suitable set of data for the CAD system in this work it was necessary to appreciate the systems requirements and the information required for the integration and modelling.

CMMs have a variety of methods for generating the information necessary to create an inspection procedure, two such methods are manually inputting information, or using the system routines to measure a feature. A stream of data points which is generated on the CMM can be grouped and transferred to the CAD database and can be used to generate a graphical representation of the object. In order to manipulate prismatic part data into geometry shapes a feature identification code is needed to accompany each group of data e.g., if the data is taken from a cylinder a code which identifies the cylinder should accompany the data. In a reverse situation i.e., linking CAD to a CMM, an additional element such as a probe path for inspection of the designed feature is necessary to be added to the transferring data file. In the case of free form geometric shapes other arrangements need considering, e.g., selection of one or more reference points to which the group of data can be referred. When a CMM inspection is to be conducted by a CAD system it is advantageous to create the inspection procedure for a part where the part data base resides.

Exchanging data between CAD and CMMs is now conducted by writing the data into a standard format such as DMIS which allows the user to create an off line inspection programme in a common format suitable for a broad range of CMMs. The DMIS format language is conceived as a universal standard for all inspection files to be generated on the CAD systems on which that part was designed. However, there could be a number of potential problems for interfacing:-

- i) Difference in speed of execution of inspection files on the CMM due to verifying errors.
- ii) Clashing of the probe with the workpiece due to misplaced trust of DMIS interface files.
- iii) A high degree of expertise is required to understand interfacing and CMM operation.
- iv) Potential dangers of accessing CAD files by non CAD operators.

As mentioned earlier, for each data file to be transferred between two systems an identification code is required to accompany each operation or element. In order to decode elements a similar code reader is required at the user end. An example of the use of DMIS for coding a feature is given below where a boss is represented [38]:-

F(BOSS)=FEAT/CYLNDR,OUTER,CART,75,50,25,0.00,0.00,1.00,25.00

At the CMM end, a decoder is required to understand this format. For complex surfaces it might be easier to use data points with extra information such as a vector representation or methods en-

abling them to be grouped into a cluster of data which would then be easier to understand and manipulate. Each data set should be organised to have enough information to relate the data to a reference location. An easy situation is when the data sets belong to a product with a reasonably established global datum e.g., if there is a hole or an edge, but when a sculptured part is used a more complex solution may be necessary. When considering manipulating CMM data sets (e.g., dimple coordinates) on a CAD system it is necessary to have them in a file in the form of X,Y,Z coordinates preferably with IJK vector representation. The data sets can be organised into a format readable on the CAD system and in the case of knowing the feature shape, the model easily generated. However, it will become more tedious where the tolerance dimensions are needed to be added to the process.

In order to represent a suitable set of data for the CAD system a series of practical tests were carried out on several golf balls by the Tesa CMM.

The centre coordinates were determined using the vision system, transferred to the Tesa CMM database and the machine was then driven to each position to measure the feature and generated dimple information. The measured data was arranged to give:–

- i) The X,Y,Z coordinate location of dimple centres.
- ii) The shape of dimples.
- iii) 3–D virtual centres i.e., X_v, Y_v, Z_v (see fig. 6.7).
- iv) The length of dimple chords (x in fig. 4.21).
- v) The depth of dimples in relation to the dimple edge (h in fig. 4.21).
- vi) The intersection distance between the dimple sphere and the ball (W in fig. 4.21).
- vii) The dimple sphere diameter (r in fig. 4.21).

The whole process including data sorting on the vision system (explained earlier) for measuring 220–250 dimples took less than 5 hours. This gave an improvement of more than 10 times that of the manual method. This data was then transferred to the UG modeller in order to build the golf ball CAD model.

7.3 CAD generated models

CAD has been employed in engineering not merely to generate models but also to produce drawings, document designs, generate shaded images and animated displays, perform engineering analysis on geometric models e.g., finite element analysis, and also to perform process planning and generate NC part programs. The choice of the modeller mainly depends upon the application which indicates there is no single solution for all problems. For example the surface form used

to model a bottle body may not be adequate to model a car body. Early CAD systems focused on improving the productivity of draftsmen while more recent systems are focused on modelling engineering objects. For reverse engineering usually a number of points are taken from a feature or a surface from the object and then used to model the object on the CAD system.

One possible way of presenting results is by identifying points on the products and listing them against the specified point values. From this data the product errors can be assessed and if required additional measuring point values can be arranged. The main drawback of using this technique is establishing a datum. The situation will be simple when the datums for the products are reasonably well established, for example if there is a hole or an edge. But when a sculptured part is used establishing a datum position is more difficult since the part is made of continuous curves. In this instance the object is spherical and the ball centre can be used as a datum, but the dimple pattern can start at any point and establishing a datum position for the dimple pattern is difficult. The method of fitting patterns for error analysis has been discussed in chapter 6. It can be seen that the errors are small and it is difficult to represent these graphically unless some method of enhancement is used.

There are generally three types of geometric modelling, wireframe, surface, and solid modelling. Wireframe modellers tend to be used for simple representation and in the past the main differences between a solid modeller and a surface modeller has been in their ability to model complex surfaces and generate mechanical properties. These differences are not now so apparent and in this work a solid modelling system has been used to model the dimpled surface at the ball and assess the errors.

7.4 Interfacing and 3-D graphical presentation of results

A valid solid modeller would have representation schemes such as domain; the class of objects that the scheme can represent (i.e., the geometric coverage), validation; the range and the set of valid models it can produce, and completeness; an ability to provide models with sufficient data for any geometric calculation in order to produce a valid model. A representation scheme is defined as a relationship that maps a valid point set into a valid model [136].

The solid modeller which was used for this part of the work to model the measured product was the 3-D Unigraphics (UG) from Electronic Data Systems (EDS) Corporation. UG is an interactive CAD/CAM system, designed as a flexible and cost effective method of automating design, drafting, and manufacturing functions. The CAM functions provide NC programming for modern machine tools using the UG design model to describe the finished part. UG is a fully 3-D system that allows accurate description of almost any geometric shape. There are number of UG

software applications such as, drafting, modelling, assembly modelling, analysis, manufacturing operations, sheet metal forming, programming languages, quality control, digital mock-up, and interfaces to convert files into documents i.e., Interleaf® (technical publishing software). These tools enable the modeller to be used for a wide range of applications.

The majority of CAD systems usually require the development of a piece of software in order to allow two systems to integrate and work with the same data. Due to unavailability of the UG/Xess module automatic interfacing between the CMM and CAD was not fully developed and in this instance manual interfacing was achieved as the result of this concept. As explained in section 7.0 interfacing the two systems was planned to allow data from the CMM to be transferred into the CAD system to manipulate them to generate golf ball models.

The 3-D measured data in cartesian form was transferred from the CMM to the UG 3-D modeller system in order to generate the model. This was carried out by manually inputting the dimple centre coordinate values (X,Y,Z) accompanied with the dimple diameter. A sphere was required to be generated on to which the features (dimples) could be embedded. Figure 7.1 shows the interaction of the dimple spheres with the ball and the resulting trimmed dimple shapes. Figure 7.2 shows the wireframe representation for a complete dimple pattern and figures 7.3 and 7.4 the trimmed representation. It is possible to identify gross errors e.g., if two dimples overlap, however it would be difficult to show which dimple was in error and if the errors are small then it may not be possible to detect them usually at all. It is obviously difficult to determine which dimple features and there may be several, are in error unless a method for error enhancement can be developed.

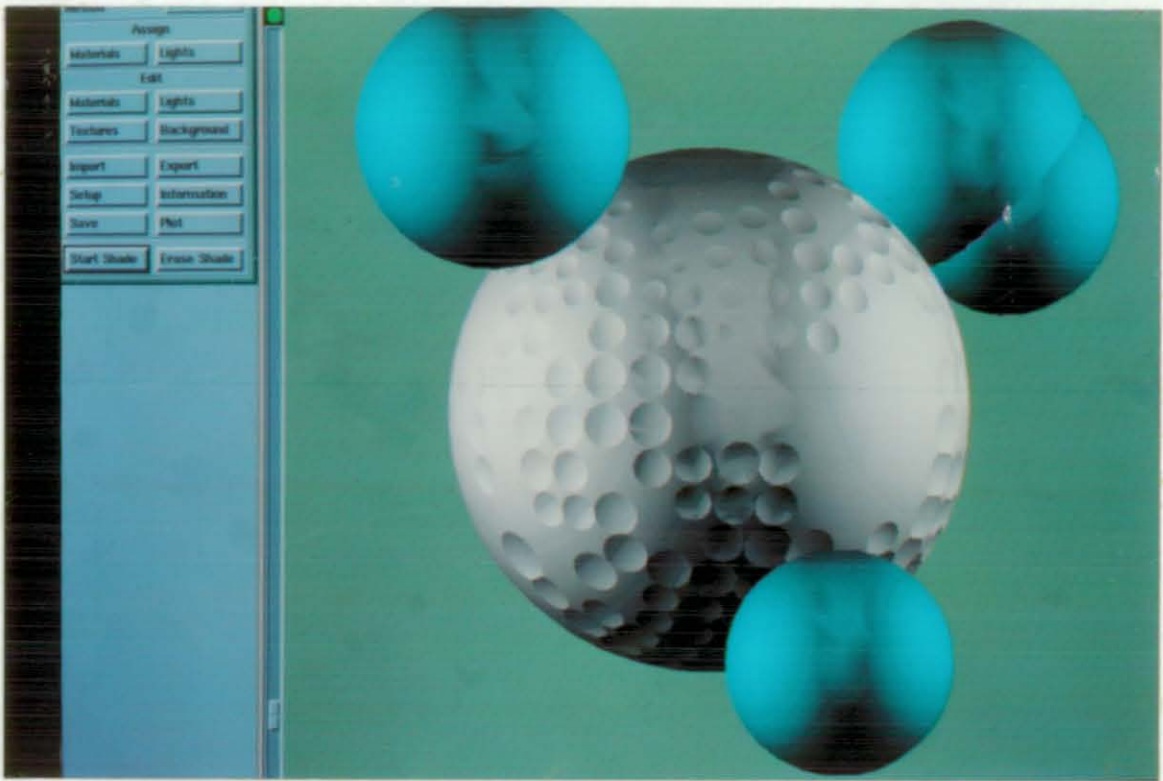


Fig. 7.1. Creation of a golf ball on UG.

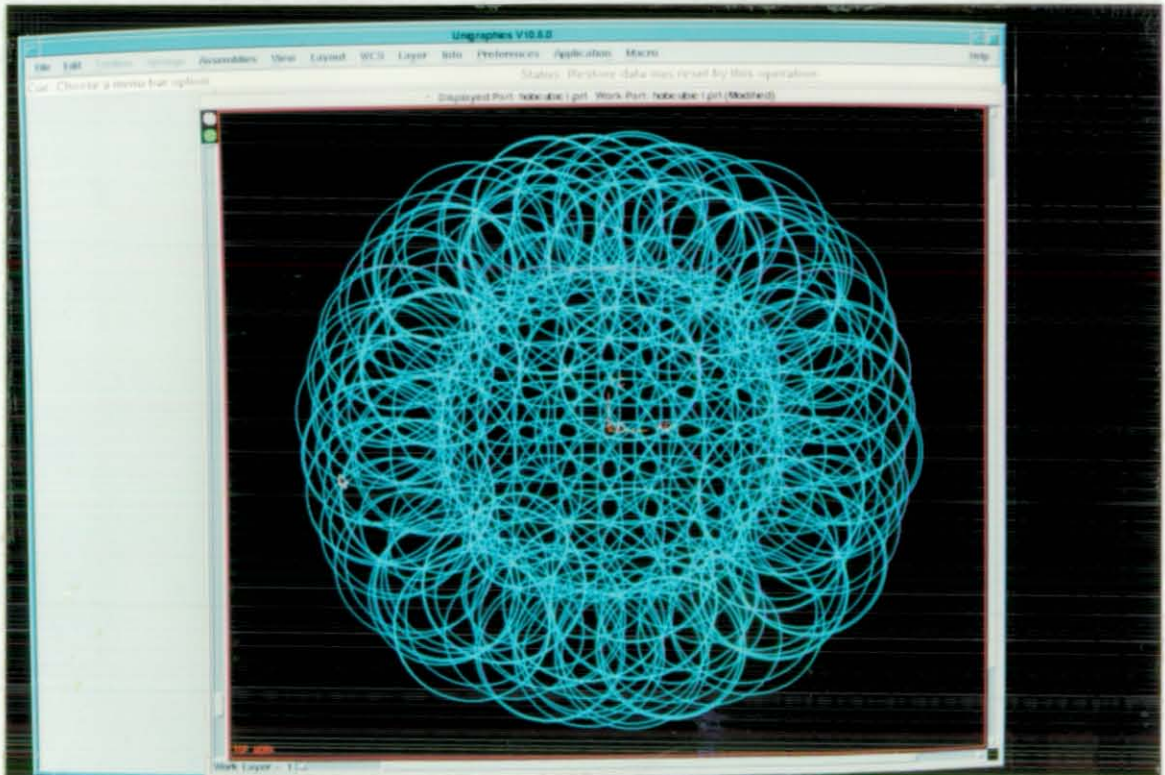


Fig. 7.2. Wireframe model of the complete golf ball model.

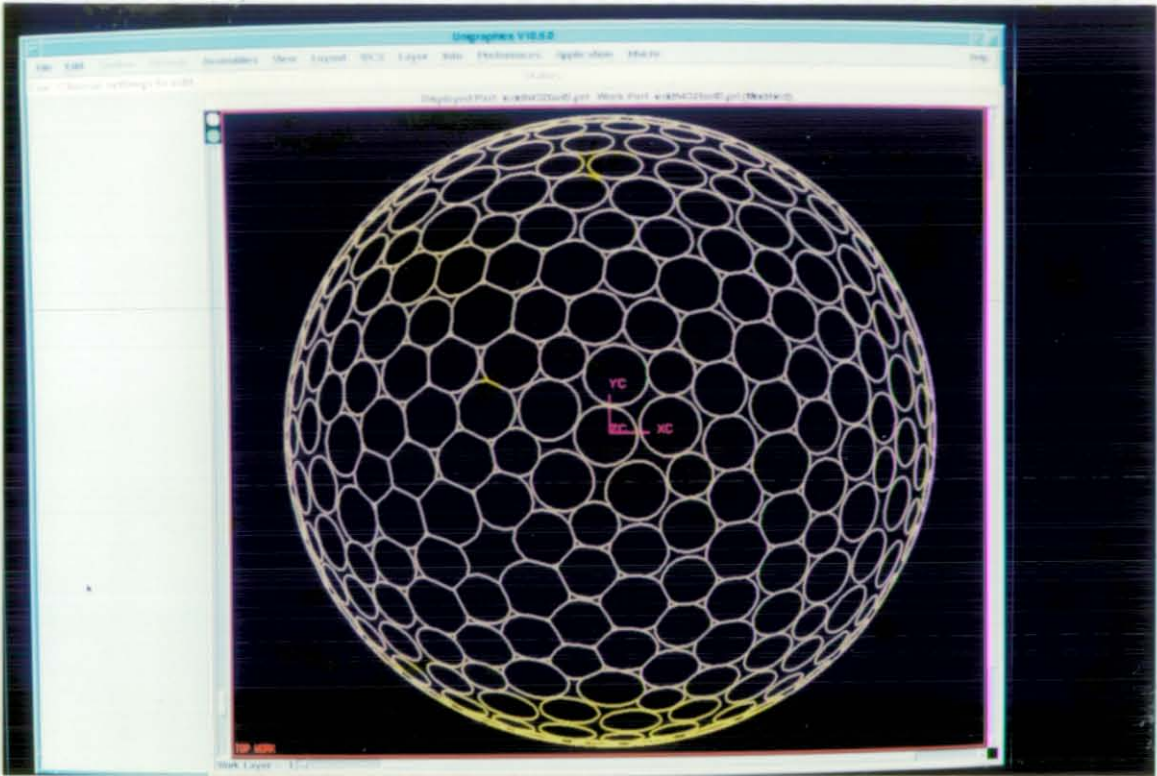


Fig. 7.3. A completed model with all features on.

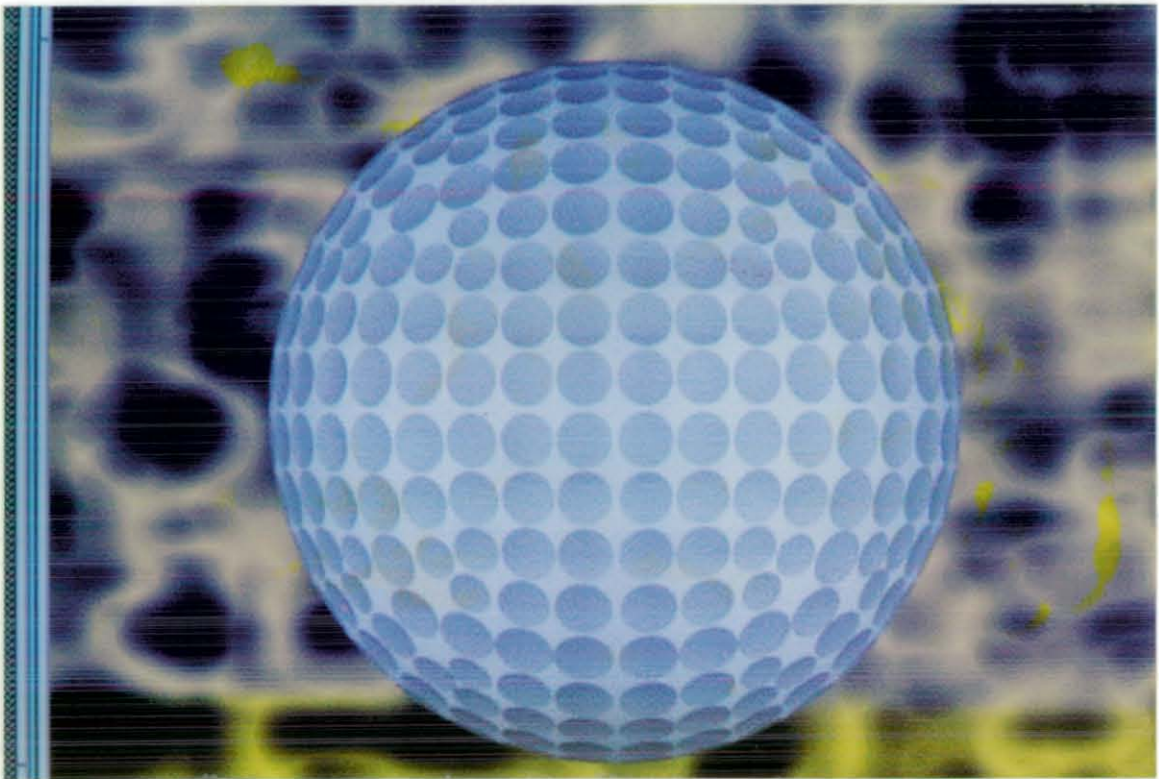


Fig. 7.4. The shaded model of the generated golf ball.

Fig. 7.5 shows a situation where dimple A is overlapped with dimples B,C,D, and E and in order to produce information automatically relating to dimple positions or to show the amount of error for each dimple a concept named Automatic Error Representation Scheme (AERS) was designed to use colouring of the dimples which are in error.

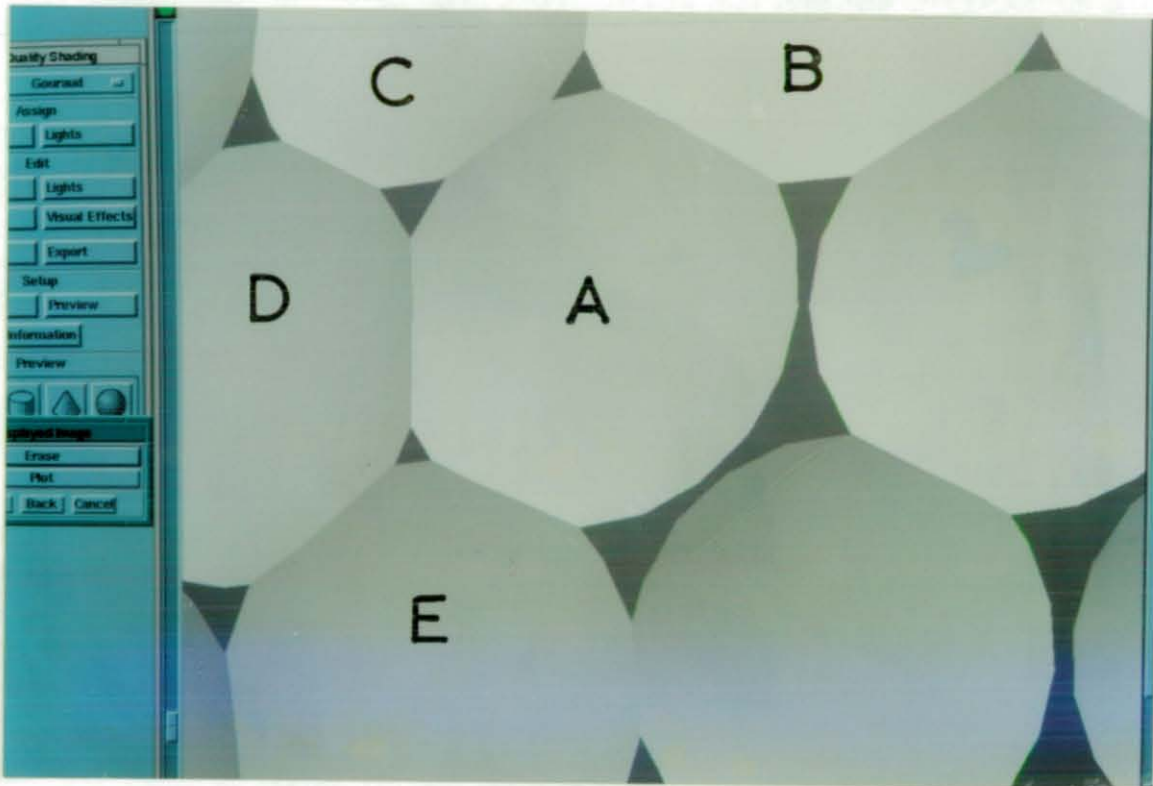


Fig. 7.5. Overlapping of more than two dimples.

The errors regarding dimples on the ball can be listed into three groups:-

- a) Errors relating the spacial positions of the dimples.
- b) Errors in connection with the shape of dimples.
- c) Errors relating overlapped dimples.

Although the AERS was not fully developed due to insufficient knowledge of the data structure of the UG, a manual process was carried out. Each model was checked for the three types of error in turn and the result of each analysis recorded and shown separately. A model will be checked first for the error of type a, by comparing the designed and actual values, the result of this comparison will be shown as a model with dimples coloured in different shades, depending on the amount of error e.g., four colours can be used to grade the error. Fig. 7.6 shows a sample of this concept together for each type error with different colour codes. For example a yellow colour can be used for errors between 0.001 to 0.01 mm, blue for 0.01 to 0.1 mm, green for 0.1 to 0.5 mm

and red for 0.5 mm and above which would represent the worst situation. The model will be then checked for the b type error by assessing the circular shape of dimples with each dimple checked for variation in diameter. Finally, the overlapped dimples will be checked which need more attention since they can have a combination of errors such as being oversized, undersized or misplaced from their nominal positions. The colour shading arrangements were planned to be used for each error type in order to ease understanding. There could be a situation where combined errors exist, in such a case dimple shading could result in ambiguity, therefore a supplement or extra method such as coding could be employed. For example codes or error values can be arranged to appear by or on the relevant dimples in each image.

The result of each colour shaded evaluation will be arranged to be shown in different images by calling each one up on request on the CAD screen, a schematic sample of such error evaluation is shown in fig. 7.6, where (a) shows the dimples deviated from their nominal positions, (b) shows shape error of dimples and (c) resembles overlapping of two dimples. From the figure it can be seen that the same colour codes with respect to the error size were used for three error types.

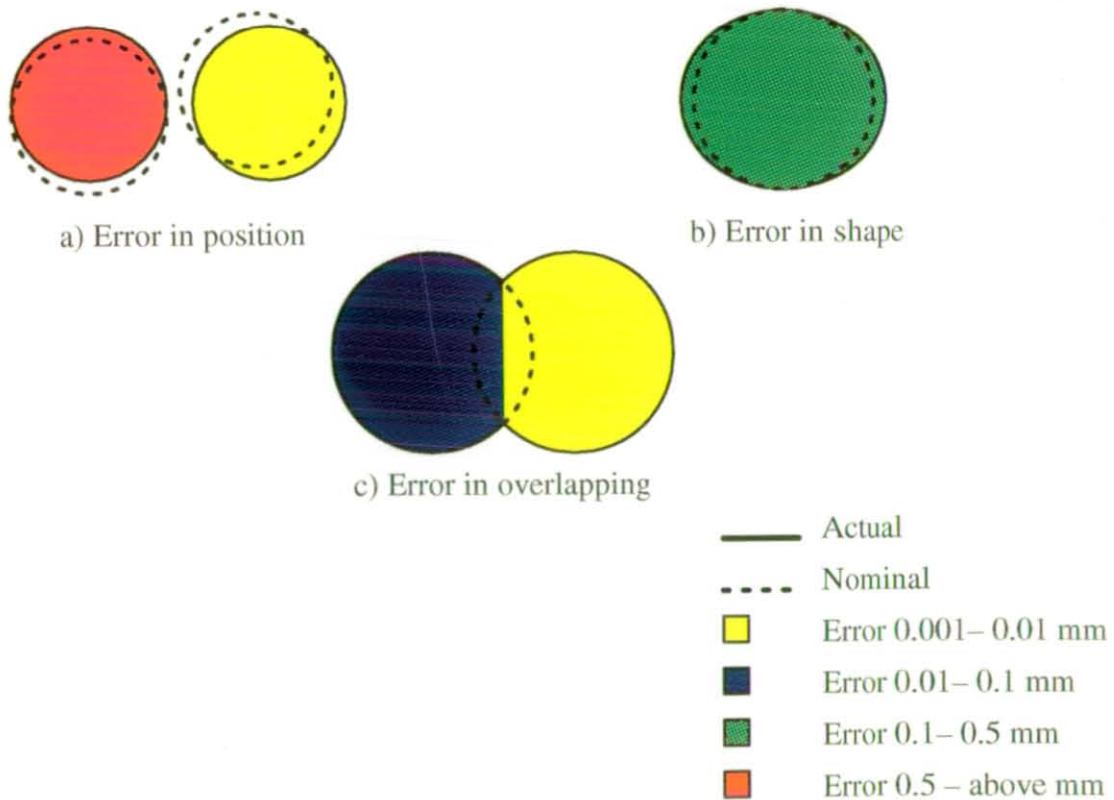


Fig. 7.6. Error colour coding for dimples on a golf ball.

7.5 Machine code generation for an optimised measurement

The generation of machine code for CNC CMMs can be a laborious process and when it is done correctly can have a direct effect on time saving for machining operations. In CNC measurement the probe samples specific regions of the part and does not cover all areas as in machining. Therefore code generation for an optimised measurement requires suitable path planning and probing strategy.

The area of path planning for CMM automatic inspection has been studied in recent years, especially for parts having complex geometry such as dies and moulds. Automated planning of a collision free inspection path using CAD model information requires a hierarchical planning system and automatic selection of probe angle for particular features. The principle of generating inspection paths for a CMM requires analysing the geometry of the existing part model in order to determine the measurement points. The inspection path can then be obtained by directly connecting these measurement points with their clearance points. However, due to the complexity of most CAD measurement system structures the generated inspection path is more easily created for relatively simple parts or features [10].

In order to achieve an inspection system the following steps are required to be considered. First an inspection plan needs to be determined which consists of selection of a probe, orientation of a probe based on accessibility, and measurement locations including clearance point(s) for each feature. Secondly the inspection procedure needs to determine the number of measurement points required to ensure the feature quality. Once the above steps are completed the collision detection for each individual path segment needs implementing

As mentioned in earlier chapters CAD and CMM links have been set up in recent years through a DMIS format which gives a bidirectional data exchange standard [37] between the two systems by creating a neutral file format for inspection programmes to be down loaded to the CMM and for data following inspection to be sent back to the CAD system for analysis. An example of this is Brown and Sharp's Microquindos and Mitutoyo's CMMCAD software. The packages are able to import CAD data from a variety of CAD systems and present it in wireframe form to the user. The user must identify and select all the features to be inspected, the software will then find each feature in its database and calculate the necessary inspection points. The probe path is planned for each feature, but collision detection is still left to the user to check during graphical simulation of the programme.

Although advanced computer programming techniques for current CMMs are equipped with various routines which enable them to be programmed for almost any measurement tasks, as yet

they are not as advanced as machining programming systems. They all require the part to be set up and aligned on the machine table prior to the measurement.

Some of the important advantages of CAD driven CMM are the time savings which can be achieved in comparison to that of a CMM on line programming technique. For example, in on line programming the CMM needs to be stepped through its measurement routine in order to complete the programme and the CMM can not be used during development of the programme while, within a CAD and CMM system the CMM can be continuously measuring with the old programme until the new program becomes available. Also through the CAD and CMM interface a much easier analysis of the measured results can be performed, for example the user may learn where to better sample the surface and how to interpret the results.

To drive a CMM from a CAD system the first step is to set up the part database which contains both actual and measured data. The next step is to use the commands to build up the part programme. Path planning can be divided into two section [37], sequence of probing and clash avoidance. In the former the datum features should be inspected first to establish the location of the part in the work envelope. The probing points on a feature can then be selected with the aim of achieving the minimum inspection time. Evaluation of measured data then requires fitting the points to the corresponding features on the CAD model.

In essence an optimised measurement can be referred to as an automatic inspection procedure which should support 3-D inspection, detect and prevent collisions of the trajectories of the probe with the part and the selection of the measurement routes for the minimum inspection time.

7.6 Discussion

In this chapter a study of interfacing CAD and CMM has been presented along with the methods for analysing the data generated by the inspection machine.

The current CMMs have been equipped with powerful softwares which allow them to produce automated measurements, analysis, and also 2-D graphical representation. However, when the part is complex or has a free form surface modelling of the part on the CMM becomes tedious and often unsuccessful. The use of a robust modelling system such as a 3-D CAD modeller in combination with a CMM may then be necessary for part or error representation.

Connecting these two systems together will allow the benefits of a CAD system for the CMM measurement such as tolerancing and specifying the measuring approach direction together with the possibility of intelligent inspection planning giving a Computer Integrated Manufacture (CIM) environment.

A key factor to the future growth of CAD and CAI is the development of universal (versatile) interfaces for design, inspection, and manufacturing applications. Although progress has been made, CAD and CMM interfacing still needs further development to achieve higher flexibility, intelligent inspection and enhanced automation. The future of CAD and CMM is bright, with the price of hardware continually decreasing while the CAD's speed and CMM performance are increasing.

As discussed earlier the most effective interfacing solution for CAD and CMM systems is to have and use an universal translator between the different type of CMMs. Apart from the obvious versatility benefits, such as the increase in the measurement quality by eliminating manually intensive data entry techniques and increases in machine availability, this solution has the advantage that all measuring systems will have similar specifications. This process has already started with the development of DMIS which is evolving to maintain upward compatibility with IGES/PDES/STEP standards developments [38], where an inspection file can be produced from scratch and exported into any CAD/CAM system.

Through the CMM/CAD/CAI interface, programming efforts can be placed in the quality assurance office enabling a response to engineering product releases and change orders with new and updated inspection data required to meet manufacturing needs [38]. From the CAD and CMM link not only can an inspection strategy be implemented, but also a more strict regime can be introduced to diagnose the cause of problems after errors have been detected.

The accurate and automatic inspection of curved surfaces has not received significant attention and due to changes of surface curvature in three axes accurate measurement can be difficult. The number of such surfaces found in the aerospace industry alone means that the inspection of complex and curved surfaces is a critical part of the manufacturing process, and traditional methods of inspection are time consuming and limited in application [133]. At present there are always some elements remaining to be defined by the user such as, which part and feature should be inspected, to what degree of precision, and a strategy for doing so [39].

Unless there is a gross error in dimples so that one dimple cuts another one, it is very difficult to detect that through a CAD visual representation. The majority of the errors relating to dimples on a ball are small therefore a colour shading arrangement (explained earlier) which depends upon the error size may be an ideal method. This method can easily show the errors relating the spatial positions, the shape and the overlapped dimples. Once the model is evaluated the result of the analyses can be shown graphically on the CAD monitor.

CHAPTER 8

DISCUSSION

Automated inspection and measurement of complex, free form or sculptured products to high orders of accuracy is a laborious and time consuming process, since for exact specification an almost infinite number of points would be required. One of the most effective way of measuring these products is by the use of a CMM but in order to measure or sense a feature or a surface it's location needs to be identified. One possible way of identifying these locations is by employing a perception system, such as a vision machine.

Vision systems are being used increasingly to automate the measuring processes and their use can help to identify product shape and features but unfortunately for high accuracy their cost is prohibitive. If an integrated inspection system could be developed which could identify the surface features quickly, then measure them to high accuracy with speed and suitable analysis the above mentioned problems could be avoided. Such a system was developed in this work which consists of an inexpensive 2-D machine vision with a CNC CMM incorporating probing.

Several experiments were performed to demonstrate the effectiveness of the proposed methods, and the results show that the automated inspection for sculptured surfaces can be achieved successfully with reduced cost. The following discussions are based on the experiments carried out during this work which have led to a set of guide lines for operation.

- **Feature specification.** One of the main problems when looking at features using a vision system is determining the extent of features. In prismatic parts distinct edges are present which identify a feature and it is also possible to construct the feature shape by implication from the feature locations, for example intersection of planes. The specification of features for sculptured parts is uncertain due to not knowing the general shape of the features or the extent, generally lines or grids are marked onto the surface to identify features or patches.

It is apparent that there are no generic solutions for automated feature identification and detection, and one way of developing methods is by investigating special cases in order to learn rules and methods which can be applied elsewhere (e.g., shoe last inspection etc.). The selected objects in this work were golf balls which are special cases of multi faceted feature parts albeit positioned around a regular object sphere. For simple balls the dimple shape would be constant (one dimple shape repeated around the whole ball), whereas complex balls can have as many as eleven dimple sizes.

A number of techniques were used to develop a simple method for feature detection by the use of a 2-D vision system and it was found that feature marking was the most suitable for the pur-

pose. This method was based on human or industry perception of the feature and then manually placing a small mark (dot) inside of each feature with a marker pen.

- **Feature detection and enhancement by 2–D machine vision.** As mentioned earlier, feature identification can be the most difficult section of a detection system and one of the main reasons is that features for sculptured parts are usually 3–D with no detectable edges or having primitive shapes. In order to identify the location of the surface features for sculptured surfaces and in special cases when the surface could have many features, a fast detection and reliable method is required. Using a machine vision the information which could lead to the recognition of the features could be interpreted from shadows, surface discontinuities and suitable lighting. However, this is a subjective process.

3–D feature identification methods are available [25,28] but expensive and complex and the common industrial vision systems are 2–D making depth determination difficult. One solution for feature determination is to enhance them for easy identification by a vision system. A marking method can determine the approximate position of the features regardless of their shapes or orientations. As remarked earlier, with a prior knowledge of the feature shape it was possible to detect and locate the marks by a set of developed algorithms and softwares which then allowed the evaluation of the features to the highest CMM accuracy. This method proved to be very simple and effective and may possibly be used elsewhere with some modifications to the system in order to be applicable to other forms of sculptured surfaces such as turbine blades, shoe lasts, golf clubs etc. A limitation with the technique is the ability to place the identification mark in the approximate centre of the feature.

- **Feature identification in 3–D.** One of the main problems with the use of a 2–D vision system for feature detection is determining the feature height in relation to a datum surface or reference point. Three methods were initially considered, Z–layer, segmentation and 3–D calculation. The main problem with the Z–layer approach is selecting layers such that they contain complete features i.e., dimples. Dimple patterns do not follow such rigid rules and any layer selected will inevitably cut through some dimples. To a reduced extent this problem is also apparent with the segmentation method since the segments contain layers.

To reduce the complexity of the 3–D calculation of dimple positions and by knowing that these features are always on a spherical object it was found more appropriate to move the vision system reference point from the top left corner of the image to the centre of the ball or hob. The height of the dimple is generally dependent on its' distance from the ball centre and it was assumed that the dimple centre lies on the ball sphere with a known radius. It was then possible to calculate the approximate Z–heights of the identification dots using trigonometry.

When an optical 2-D vision system is used to represent a 3-D data point some discrepancy between the measured and the optical values will be generated. This optical discrepancy acts radially from a point vertically above the object centre. In this work a 2-D correction factor was developed to compensate for this optical effect. Although this was developed and tested for golf balls it was not used since the calculated centres were adequate for the measurement process for larger objects a correction would have to be used.

- **Multi-image feature detection.** It is obvious for efficient feature detection to use only one camera position. However, when one camera position was considered, it was found that the features in areas where the surface curvature changed rapidly tended to merge together and on the outer extreme of the ball could not be detected. Therefore, multi-images were used in order to identify features in these areas. The generated technique (MIST) viewed the object of interest a number of times from different directions and combined the information, for curved objects it is likely that there will be areas which could be identified more than once. In the case of the golf ball these areas were created by overlapping up to three neighbouring images of the surface.

In order to minimise the number of views it is necessary to have some confidence in the information available in any one image. In the case of the golf ball confidence in feature identification diminishes away from the ball centre. The dimples that can be identified with confidence can be contained within an approximate circular area or ring of about 18.5 mm radius. In this work 5 views were used to develop the methods. The situation for 100 per cent ball cover is shown in fig 5.6 which gives a radius of 17.51 mm. Fortunately all dimples in these areas can be confidently identified which might not be the case for more complex products. Ideally the overlapped areas shown in fig. 5.6 should be kept as small as possible. Despite the fact that the data sorting algorithms were developed to censor the detected repeated data sets, this could not guarantee 100 per cent sorting. The method applied to the cubic golf balls by using 17.51 mm radius image ring to detect 220 dimples on a half ball which resulted in about 50 per cent of the dimples being identified more than once.

- **Data sorting and censorship.** With the use of MIST the generation of repeated dimples was inevitable and in order to keep the inspection time to a minimum, a procedure was needed to measure each dimple once only. It was found more efficient to sort a complete data file after all dimples were detected, which enabled repeated dimples to be censored. Various golf balls were tested with the data sorting method (the DimSort programme explained in chapter 5) with the machine under continuous supervision in order to control the method efficiently. Up to 90 per cent of the repeated data was detected and an average value substituted leaving the remaining 10

per cent to be measured more than once. In a more complex component this amount of repeated measuring could increase and represent a significant system inefficiency.

● **Probing strategy.** Once the position of features was known it was required to develop a strategy to guide the probe to inspect and assess the features (chapter 4). As discussed in chapter 3, it is extremely important that the probe approach direction to the object surface be normal and the probe accurately calibrated (probe datuming). A non normal approach gave inaccurate results with measurement variations up to 25 μm when ten dimples at different locations were measured. When the probe was calibrated following the procedure suggested by ANSI/ASME B89 1.1.12M and BS7172 with the probe approaching the surface as normal as possible, a difference of up to 10 μm was recorded. The following techniques will ensure more accurate results.

- i) Measure the features at least 3 times to obtain three sets of results with the first set being used to obtain an estimate of feature shape for more extensive measurement by the second and third sets.
- ii) Measure the feature with equispaced measuring points, a larger number of points resulted in the generation of a better feature.
- iii) Measure most of the feature with the approach normal to the direction of the feature.
- iv) Use a reasonably slow speed for measurement.
- v) Calibrate the stylus regularly in the direction it will be used.
- vi) A clean probe and the measuring surface should always be prepared prior to measurement.
- vii) Use as short a probe as possible.
- viii) Take readings from as large an area of the feature as possible.

Fig. 8.1 shows the possibility of generating inaccurate dimples when only a part of a feature is measured, since small errors can result in significant variation if extrapolated to a larger surface.

Touch trigger probes all have a pre travel effect before the exact location is recorded (chapter 3). If a surface on a body is to be measured precisely (see fig. 8.2), the approach direction needs careful consideration to account for this problem. Sculptured surfaces represent a particular problem since the surface curvature can change significantly. For high accuracy work this could mean that the probe approach would need to continually vary during the measurement of a feature. Clearly this may not be a practical solution and the metrologist should be aware of the likely inaccuracy that can result for a common probe approach for a feature. This limitation is usually not a significant source of error and can be minimised when procedures are followed for the probe datuming.

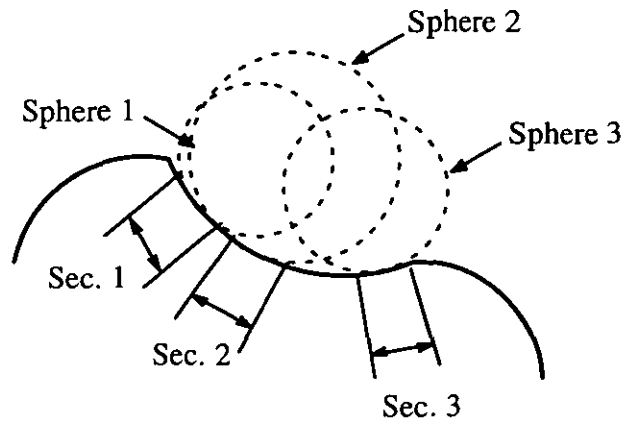


Fig 8.1. Different feature generation.

It was found through a series of practical tests on different golf balls and hobs that if the recommended probe calibration method was followed, the errors related to probing are reduced. The effect of bad and good calibration for measurements of dimples on a same ball (icosdhh 432) can be seen in figs. 8.3 and 8.4.

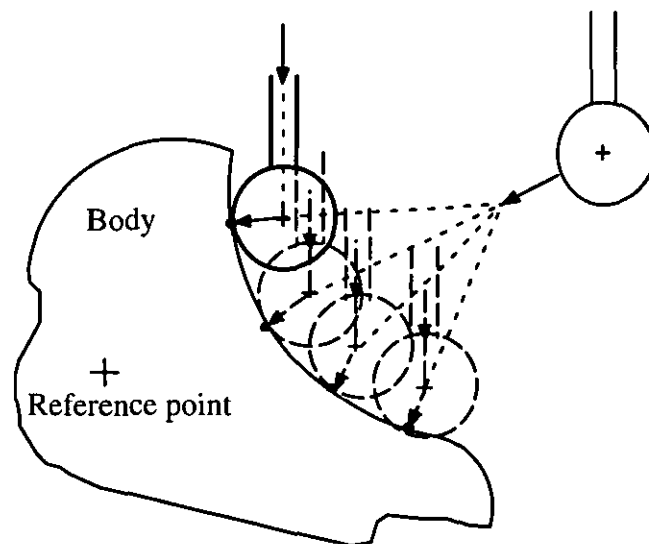


Fig. 8.2. Direction of free formed surface probing.

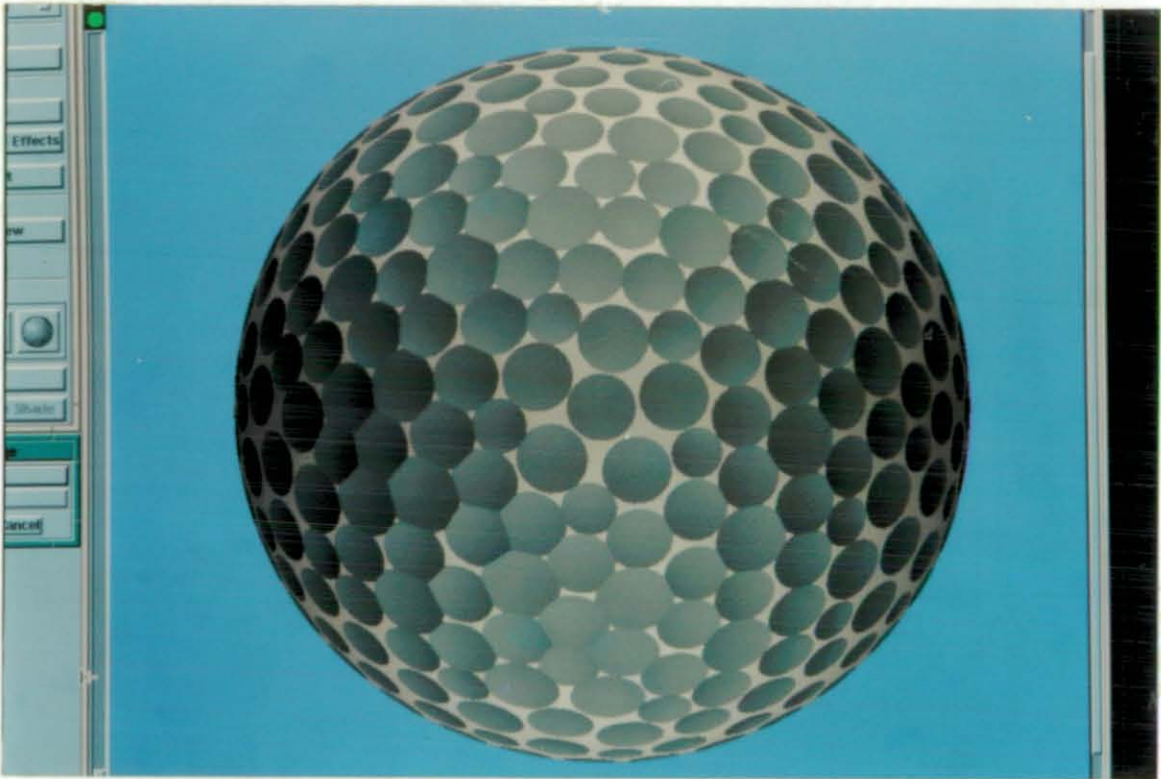


Fig. 8.3. CAD model of the measured ball with inaccurate probe calibration procedure.

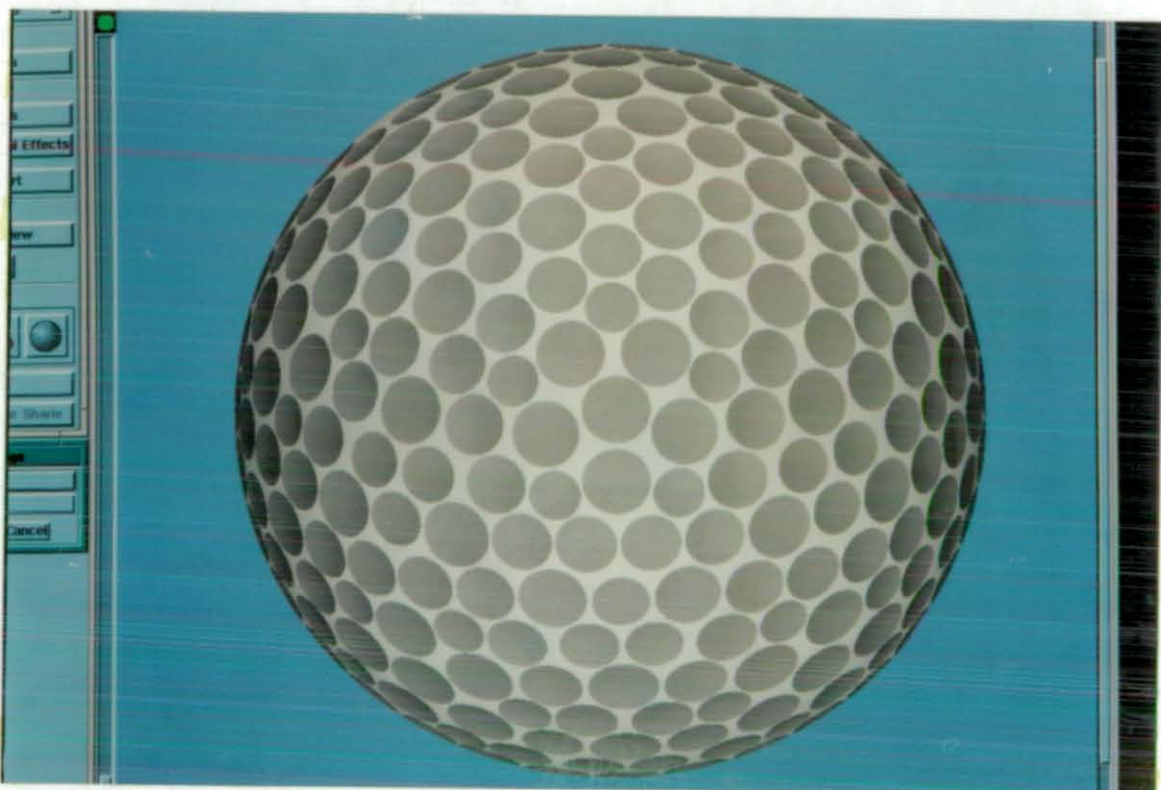


Fig. 8.4. CAD model of the measured ball with accurate probe calibration.

It was originally assumed that when features were measured with the minimum possible number of points (e.g., four points for a sphere) the result would be of reasonable accuracy. However, the practical tests [137] showed that significantly more points (up to five times the suggested number was used for this case) are required to determine a feature of reasonable accuracy. One possible reason for this increased number of readings is that the area of dimple probing was small i.e., 3.5 mm diameter, and a small error in measurement would be magnified irregularly. The algorithms within the CMM were used for feature measurement to generate shapes and experiments were developed to check them for the accuracy which was confirmed.

The approach to the probing strategy used for measuring the dimples was to generate a vector from the ball centre to the detected dimple centre along which the probe took readings from the feature surface.

- **CNC code generation for CMM.** Once the position of feature data points was known a strategy was required for the CMM to inspect and assess the features. The CNC code generation in this research was incorporated with an auto probe selection strategy. This method was designed to automatically measure the identified features. The method uses the feature position, orientation and X,Y,Z vision system data, to automatically select a suitable tip orientation (chapter 4) for an optimal evaluation of the relevant features by executing a developed CMM programme. The programme consists of a series of routines and algorithms to perform an automatic measurement of golf balls and hobs.

In this instance the features are of similar shape, but for more complex parts if prior feature knowledge is available a library of feature measurement algorithms could be accessed and used where required.

- **Error optimisation model.** The importance of dimple location on golf balls originated from their effect on the flight of the ball. Positional inaccuracy of dimples and patterns are some of the main factors which would generate unexpected flight behaviour. Presently the positional accuracy of dimples on tools and balls is assessed primarily through visual inspection and by practical testing of a number of balls from the preproduction models in the field. In order to evaluate this error and minimise it the least squares best fit method (LSBFM) was designed and applied to 3-D scattered data points. The model used the nominal data as the reference and optimised the actual data generated through the CMM measurement. The model worked on finding the maximum possible error within the measured dimples and progressed through an iteration on the objective function, to certain constraints in order to arrive at a situation where the errors were minimised. This method considerably reduced pattern errors and could be applied to problems of this nature where errors between the nominal and the actual data need to be minimised.

The LSBFM was found to be simple and successful due to its fast processing time and ease of appreciation. The main shortcomings of this method can be broadly listed as; a) not showing the direction of errors from which possible relationships could be found, and b) it is not integrated into the UG CAD system in order to perform an automatic graphical representation. However, error model tests for two hobs were successfully carried out and the results were studied manually (two sets of results can be seen in appendix A). A total of 220 and 213 dimples were measured on the two hobs used. The nominal and measured values were fed into the error modelling system in order to produce an optimise model. The results of these tests were the optimised locations for the measured dimples with an average error reduction of about 40 per cent. From the results (appendix A) the maximum and minimum error variations between the error lengths of CAD–CMM and CAD–optimised values for the cubic hob were recorded as 7.7 μm , 1.0 μm and those for the icosdhh432 hob were 4.6 μm , and 1.1 μm .

• **Virtues of this work.** The research advances the 3–D automatic inspection of features on sculptured surface products through the application to a specific product. Although the system was applied to golf balls which are complex products to inspect, it could be applied to other products which can be featurised and which have not been measured automatically to date e.g., golf clubs, bottles, and shoe lasts.

The proposed integrated inspection system has the following virtues,

- i) A 100 per cent surface feature detection,
- ii) Measurement time saving up to 10 times in comparison to the conventional method with minimum operator interference,
- iii) An accurate measurement consistency to a few microns for all the features,
- iv) Simplicity of the surface feature detection and measurement procedures,
- v) An inexpensive and effective system in comparison to other rival systems.

CHAPTER 9

CONCLUSIONS

This research presents a developed method of automated inspection for sculptured surface products by integrating a CMM and 2-D vision system. The research outlined in this work may be applied to free formed surfaces but some modifications such as specifying reference points for the surfaces needs to be developed. The system was developed on golf balls which are considered to be a special instance of a product with surface features. The conclusions can be summarised as follows:–

- Automated identification of surface features is difficult for sculptured surface products.
- Careful illumination of products can help enhance features particularly with the use of a fluorescent light source and filtered light. A suitable illumination system was achieved by the use of a fluorescent ring light and filtering using white paper filters.
- If prior knowledge of feature shapes is available, then a feature and its position can easily be identified by the use of a small mark or dot in the approximate centre of the feature to an accuracy of 0.2 mm.
- If prior knowledge of the part or feature is available using a single 2-D image of the part enables a 3-D shape to be probed.
- It is possible to generate a library of probe measuring routines for feature types and apply them to identify features automatically for accurate measurements, < 0.01 mm.
- The use of multiple images achieves a more comprehensive view of a product in particular for areas of rapidly changing surface curvature and this allows 100 per cent surface/feature cover. However it is necessary to censure formation in overlapped image areas to reduce repeated inspection.
- The savings in measurement time for this "look and touch approach" compared to traditional inspection methods can be considerable. In the cases investigated of dimples on golf balls saving in the order of 10 times have been achieved.
- In order to assess component accuracy datums are required which are difficult to establish for sculptured products. The method of fitting measured feature patterns to the design specification

using a three dimensional least squares technique proved successful, the examples used reduced the errors by 40 per cent.

- The use of a CAD modelling system to enhance component error by colour coding error types has many advantages for unambiguous interpretation by operators.

CHAPTER 10

RECOMMENDATIONS FOR FUTURE WORK

In this research several topics were handled to implement an automated inspection of sculptured surfaces with the use of a machine vision. Recommendations for future research in order to improve the proposed system are listed below:

- **Optimisation of probe orientations.** An optimisation method for probe orientations can be employed in order to inspect features which could use the same probe orientation. This will reduce the inspection time. Presently there is no control on the size of the marks placed inside of the features which resulted in an unpredictable feature detection order, meaning they will be measured in the order they were detected. A significant effect of this is the generation of too many unnecessary probe movements. If a controlled feature detection or a feature sorting method could be arranged in a way that grouping the features which could be probed with the same probe orientation, the inspection time could be minimised.
- **Feature identification/Marking other sculptured parts.** The feature identification method is of interest and for multiplicity of features on a part a more comprehensive method should be investigated. The dot marking method proved successful for circular features, however a more difficult case is when the features on the surface have more than one shape, for example dimple shapes based on triangle, squares, pentagons, or a mixture of all. For such cases an advanced marking method is required to be developed in order to help the vision system to identify these features. One way of arranging the advanced marking method could be using combined marks such as, dots, arrows, triangles, crosses and other possible practical symbols. Routines and algorithms are required for the vision and CMM to identify and process these marks.
- **Optimum (reduced) view positions.** Further practices should be developed for applying the MIST to objects using an optimised view positions, in order to reduce the automated inspection time further. This will be possible by using some trigonometric relationships between the camera locations and the part coordinate system.
- **Application of the MIST to other featured sculptured parts.** The proposed MIST should be applied to other featured sculptured parts (non-regular objects) such as a golf club or shoe last which have not been measured automatically to date. A starting point for this is to use the advanced marking method. The approximated locations of these marks can then be determined by referring them to one or different datums. The direction of these marks can also be identified by using some developed algorithms within the detection method. This could be an answer to the

inspection or identification of complex free formed sculpture surfaces where specifying the direction and the correct location of the patches and surfaces is one of the most difficult parts of the process.

- **Application of the MIST to prismatic parts.** The MIST with the marking method can also be applied to objects which consists of prismatic features such as blocks, pockets, spheres, bosses etc., Although a number of researches [102] have been devoted to this area, the simplicity and effectiveness of this method could justify it.
- **Automated CAD model and error generation.** The CAD generated models of the measured balls and hobs should be researched further in order to use the UG/Xess (explained in chapter 7) for automatic CAD modelling. This could also allow an automatic 3-D CAD representation of errors using colour coding explained earlier on the optimised model on the UG CAD system.
- **Illuminating the object.** Although a solution was achieved for this case (explained in chapter 4), there is still further work to be carried on lighting methods and systems. One possible way is to use diffuse lights around the workplace in order to create regular illumination. Another successful approach could be to use indirect lights by utilising umbrella reflection arrangements. The above methods can be arranged to illuminate the object from a distance up to a few meters.
- **Efficiency and probe motion.** The CNC CMM code generation for feature measurement was mainly considered with respect to taking successful measurements rather than optimising the speed of measurement. Work is required therefore on this aspect in order to speed up the process. As explained earlier each dimple was probed three times (5, 19, and 19) which gave 43 readings and for a ball with 250 dimples a total of 10750 probings has to be carried out.
- **The LSBFM errors analysis for other complex features.** An additional area of research can be developed by investigating the application of the LSBFM of error optimisation to surfaces of other sculptured parts. In such a case a relationship for each patch or surface to a datum point and consequently to a global (master) datum point needs establishing. By comparing the actual and nominal data of each surface the possible error between them and also for the neighbouring patches could be identified. Once the amount of errors are determined an optimisation method could be applied.
- **Future integration between CAD and CMM.** A series of practical work needs carrying on in the area of CAD and CMM integration in order to utilise the full ability of communication between the UG CAD and Tesa CMM.

REFERENCES

- [1]. Batchelor B.G., Hill D.A., Hodgson D.C., *Automated Visual Inspection*, pub. by IFS (Publication) Ltd, U.K., 1985.
- [2]. Elshennawy Ahamad K., *The role of inspection in automated manufacturing*, Computers ind. Engineering 17(1–4), 1989.
- [3]. Berg B.VanDen, *Closed loop inspection of sculptured surfaces in a computer integrated environment*, Proc. 8th Int. Conf. Automated inspection and product control 1, 1987.
- [4]. Takeuchi Yoshimi, Shimizu Hiroyuki, Mukai Ikuo, *Automated Measurement of 3-Dimensional Coordinate measuring Machine by means of CAD and Image Data*, Annals of the Int. Institution for Prod. Eng. Research (CIRP) 39/1/90, 1990.
- [5]. Gupta V.K., Sagar R., *APC-based system integrating CMM and CAD for automated inspection and Reverse engineering*, Int. J. Advan. Manuf. Tech. (IJAMT), 1993.
- [6]. Al-Kindi G.A., Baul R.M., Gill K.F., *An example of automated two-dimensional component inspection using computer vision*, IMechE 205, 1991.
- [7]. Merat Francis L., Radack Gerald M., *Automatic Inspection Planning Within a Feature-Based CAD System*, Int. J. of Robotics & Comp.-Integ. Manuf. (IJRCIM) 9 No.1, 1992.
- [8]. Mahon James, *Automatic 3-D inspection of solder paste on surface mount printed circuit boards*, Int. J. Materials Processing Technology (JMPT) 26, 1991.
- [9]. Zarifi A., Jones R., *Automated Measurement of Golf Balls Using Machine Vision Assistance*, J. of Quality of world Today Supplement (QWTS), March, 1994.
- [10]. Yau Hong-Tzong, Menq Chia-Hsiang, *Path Planning for Automated Dimensional Inspection Using Coordinate Measuring Machines*, Int. Conf. on Robotics and Automation (IEEE), 1991.
- [11]. Corrigan M.J., Bell R., *Probe and Component Set-up Planning for Coordinate Measuring Machines*, Int. J. of Comp. Integ. Manuf. (IJCIM) 4 No.1, 1991.
- [12]. Cho H.D., Jun T.T., Yang M.Y., *Five-axis CNC milling for effective machining of sculptured surfaces*, Int. J. of Production and Research (IJPR), 1993.
- [13]. Brown and Sharp Company, *TESA CMM Publication*, 1993.
- [14]. Ferranti International Ltd. Scotland U.K. *The Merlin CMM manual*, 1988.
- [15]. Sarkar Biplab, Menq Chia-Hsiang, *Scanning compound surfaces with no existing*

- CAD model using touch probe of a Coordinate Measuring Machine**, Intelligent Design and Manufacturing for prototyping (IDMP) 50 (PED) Winter ASME, 1991.
- [16]. 3D Scanner Ltd., **FACIA: Medical Surface Scanner**, 3D Scanners Ltd South Bank Technopark 90 London Rd SE1 6LN, 1991.
- [17]. Champ Peter, **Reverse Engineering in Industrial Applications using Laser stripe Triangulation**, Colloquium digest No. 1994/054, IEE, March, 1994.
- [18]. Duffie N., Bollinger J., Riper R., Kroneberg M., **CAD directed inspection and error analysis using surface patch databases**, CIRP 33–No.1, 1984.
- [19]. Duffie N., **CAD directed inspection and error patch databases**, CIRP 33–No.1, 1987.
- [20]. Smith D., **Touch Probe Attack Angle Problems**, Quality Today, Sept. 1987.
- [21]. Butler Clive, **An investigation into the performance of probes on coordinate measuring machines**. Industrial Metrology 2–part4, 1991.
- [22]. Zuech Nello, **Applying Machine Vision**, John Wiley and Sons, Inc. ed. John Wiley and Sons, U.S.A., 1988.
- [23]. McMichael D., **Fusing Multiple Images and Extracting Features for Visual Inspection**, IEE Factory 2000, 1992.
- [24]. Schneider Carl., Sinnreich Kurt, **Concept of an optical coordinate measurement machine**, SPIE 1395, 1990.
- [25]. Clarke T.A., Ellis T.J., Robson S., **High accuracy 3–D measurement using multiple camera views**, Colloquium digest No. 1994/054,, IEE, March, 1994.
- [26]. Urquhart C.W., McDonald J.P., Fryer R. J., **Active Animate Stereo Vision**, British Machine Vision Conference (BMVC) 1, 1993.
- [27]. Seibert Michael, Waxman Allen M., **Adaptive 3–D object Recognition from Multiple Views**, IEEE Trans. Patt. Anal. Machine Intelligent., Vol. 14, No. 2, 1992.
- [28]. McDonald J.P., Lambert R., Fryer R.J., **3D Measurement Using Stereo Scene Coding**, IEE. Colloquium digest No. 1994/054, March, 1994.
- [29]. Griffiths B.J., Wang Y., Wilkie B., **AI Vision for Inspection**, ACME WISEACME.002, 1993.
- [30]. Scalkoff Robert J, **Digital Image Processing and Computer Vision**, John Wiley & Sons, Inc. New York, 1994.
- [31]. Gonzalez Rafael C., Woods Richrd E., **Digital Image Processing**, Addison–Wesley

Publishing Company, Inc., Reading., 1992.

- [32]. Wolf Paul R., *Elements of Photogrammetry*, 2nd. Ed. Vol. 1. McGraw-Hill, Inc. 1983.
- [33]. Martin W.N., Aggarwal J.K., *Volumetric descriptions of objects from multiple views*, IEEE Trans. Patt. Anal. Machine Intelligent., Vol. 5, No.2, 1983.
- [34]. Liu Cheng Hsiung, Tasi Wen Hsiang, *3D Curved Object Recognition from Multiple 2D Camera Views*, Computer Vision Graphics and Image Processing 50, 1990.
- [35]. Edwards J., Clements P., Murgatroyd S., *Machine vision integration and information support: methods, models and tools*, Int. J. of CIM, Vol. 6, No. 5, 1993.
- [36]. Cho M.W., Kim M.K., Kim K., *Flexible Inspection System Based on Vision Guided Coordinate Measuring Machine*, Int.J.Prod.Res. (IJPR), Vol. 33, No. 5, 1995.
- [37]. Harris J.R., Rockliffe S.C., Smith G., Hill T.M., *A review of on-line and off-line programming facilities for coordinate measuring machines*, Factory 2000, 1994.
- [38]. Daniels Glynne E., *DMIS: a quality Standard*, J. of Quality Today, January 1992.
- [39]. Cowling G.J., Mullineux G., *Toward an Intelligent CAD-CMM Interface*, Engineering with Computers 5, 1989.
- [40]. Schartz Mark H., Karadayi Recep, *Making the CAD to CMM Interface More Effective*, Society of Manufacturing Engineers (SME), MS89-530, 1989.
- [41]. Fu K.S., Gonzalez R.C., Lee C.S.G., *Robotic control, Sensing and intelligence*, McGraw-Hill International Editions, New York, 1988.
- [42]. Frost and Sullivan, *Machine Vision*, Engineer Technical File No. 223, August 1993.
- [43]. Sension Advanced Computing, *Advance Computing News*, Kane International Limited, 7 Craftwood Square, Martland Mill Industrial Estate, Wigan, WN5 0LG, 1994.
- [44]. Data Cell Co., *Image Matters 2*, Newsletter, 1994, West End Rd, Mortimer Common, Reading, Berks RG7 3TF, U.K.
- [45]. Taylor Barry, *Placement: Vision and Integration*, Electronics Manufacture and Test July/August 1991.
- [46]. Purnell G., Khodabandehloo K., *Vision for Robot Guidance in Automated Butchery*, J. of Robotic Systems, Advanced Techniques and Applications 10, 1992.
- [47]. Azar I., Weston R.H., *A vision reference model for systems integration*, Int. J. of CIM, 1 No. 4, 1992.

- [48]. Svetkoff D.J., Smith D.N., Doss B.L., *Automatic Inspection of Component Boards Using 3-D and Greyscale Vision*, Microelectronics 13, 1987.
- [49]. Blacke Andrew, *Double Grid Maps 3D Shapes Precisely*, Eureka on Campus Autum, 53, 1991.
- [50]. Brown Joe, *Vision Systems Get Better at Doing What Eyes Can't*, Power Transmisson Design 5, 1991.
- [51]. Pastorius W.J., *Robots in Aerospace Manufacturing*, SME MS89-162, 1989.
- [52]. Harding Kevin G., *Sensors for '90s*, Mechanical Engineering 106, part 4, 1991.
- [53]. *MVP-AT user's manual*. Matrox Electronic Systems Limited, 1988.
- [54]. Grover M.P., Weiss M., Nagel R.N., and Odrey N.G. *Industrial Robotics*, McGraw-Hill International Editions, 1988.
- [55]. McCarthy Brian, Genest David H, *Getting your CMMs and CAD system to talk*, Machine and Tool Blue book 85 part 6, 1990.
- [56]. Graund Bill, Maggiano Larry, *Smart Contact Scanning*, Conf. Applying Imaging and Sensoring technology to CMM Applications, Pub. SME, 1993.
- [57]]. Genest David H., *Coordinate Measuring Machines*, Inspection Equipement and Techniques, Brawn & Sharps Publication, U.S.A., 1993.
- [58]. Renishaw CMM product Group 4, *General Product*, Bulletin, 1992.
- [59]. ANSI/ASME B89 1.1.12M, *The American National Standard For Coordinate Measuring Machine*, 1989.
- [60]. Reid Colin *performance Characteristics of Touch Trigger Probes*. Renishaw Metrology Publication U.K. 1993.
- [61]. Traylor Alan, Jarman Tom, *Performance Characteristics of Touch Trigger Probes*, SME MS90-266, U.K., 1990.
- [62]. Modjarrad Amir and Dukiewicz Peter, *Development of a small novel 3-Dimensional high accuracy probe for CMMs*, Quality Europe 36, Part 1, U.K., 1991.
- [63]. Reid Colin, *Probe Technology Beyond Accuracy*, Conf. Applying Imaging and Sensoring technology to CMM Applications, SME Pub., 1993.
- [64]. Fitts John M., *Miniature 3D surface mapping moire sensors for the CMM*, Applying imaging and sensoring technology to CMM applications 1, U.S.A., 1993.

- [65]. Owen Jean V., *Are Laser Measuring Up?* Manufacturing Engineering 104 part 1, January 1990.
- [66]. Kunzmann H., Waldele F., *Performance of CMMs*, CIRP 37–No.2, 1988.
- [67]. Danzer H.H., Kunzmann H., *Application of 3–Dimensional Coordinate Measuring Machines for problem Investigation and upstream quality assurance*, CIRP 36–1, 1987.
- [68]. Paolino Richard F., Genest David H., *Justifying the CMM*, Carbide and Tool Journal, 21 part 4, 1989.
- [69]. Daschbach James M., Sairamchandar R., S., *Coordinate Measuring Tool*, SME MS89–528, 1989.
- [70]. Oetjens Thomas J., *New Developments in Coordinate Measuring Machines for Sheet Metal*, Autofact 19, 1989.
- [71]. Cox M.G., *Assessing CMM software quality*, J. of Quality Today, January 1992.
- [72]. Goh K.H., Bell R., *The applicability of a Laser triangulation probe to non–contacting inspection*. Int. J. Prod. Res. (IJPR), Vol. 24 No.6, 1986.
- [73]. Bradley C., Vickers G.W., Milroy M., *Reverse Engineering of Quadric Surfaces Employing three–dimensional Laser scanning*, Institute of Mechanical Engineering 208, 1994.
- [74]. Dalglish G.F., James R.D., Randeree K.H., Aitchison D.R., *Laser–Based inspection of cutting tools for advanced manufacturing systems*, Factory 2000 October, 1994.
- [75]. Farmer L. E., Smith G., *Integrating CAD and CMM Inspection*, International Mechanical Engineering Congress 91 part 8, 1991.
- [76]. Pahk H.J., Kim Y.H., Hong Y.S., Kim S.G., *Development of Computer Aided Inspection System with CMM for Integrated Mold Manufacturing*, CIRP 42–1, 1993.
- [77]. Oh kaytack, Daschbach James M., Abella Robert J., *CMM Application in Reverse Engineering–Integrating CMM With CAD/CAM for Existing Parts Without Drawings*, SME MS89–529, MS89–529–1 MS89–529–9 1989.
- [78]. Kwok Wai–Lun., Eagle Paul J., *Reverse Engineering: Extracting CAD Data From Existing Parts*, Mechanical Engineering 113 part 3, 1991.
- [79]. Renishaw Ltd. *High Speed Scanning of 3–D Surfaces*. Quality Today Januaray, 1992.
- [80]. Spokes Ben, *CMM – Style Machine Tool Inspection Probing*, Final year undergraduate project Manufacturing Eng. Dept., Loughborough University, U.K., 1993.
- [81]. Morton Danny, *Systematic and spatial errors, their measurement and compensation*

- method applied to CMMs*, School of Eng., Huddesfield University, U.K. 1994.
- [82]. Brown & Sharpe, *Measuring equipment Catalogue*, Brown & Sharpe Pub., Tesa Metrology Ltd., Telford, Shropshire, U.K. 1994.
- [83]. Dallas D.B., *Tool and Manufacturing Engineering Hand Book*, 3rd Edition, Pub. by SME, 1976.
- [84]. W.A. Metrology pub. U.K., 1993.
- [85]. Zink Joseph H., *The Role of Coordinate Measuring Machines in Assuring Quality*, Computer Integrated Manufacture REVIEW Summer, 1988.
- [86]. Palframan Diane, *At Last Industry Can*, J. of Manuf. Sys., April 1993.
- [87]. Jones R., Mitchell S.R., Newman S.T., *Feature-Based Systems for the Design and Manufacture of Sculptured Products*, Int. J. Prod. Res., Vol.31, No.6, 1993.
- [88]. Mitchell S.R., Jones R., Newman S.T., *A Structured Approach to the Design of Shoe Lasts*, Journal of Engineering Design, Vol.6, No.2, 1995.
- [89]. Olman John M., Olman Morton W., *The Encyclopedia of Golf Collectibles*, Books Americana Inc., 1985.
- [90]. Pinner John, *The History of Golf*, The Apple Press Ltd., 1988.
- [91]. The Royal and Ancient Golf Club of St. Andrews, *Rules of Golf*, 1991.
- [92]. Daish B.C., *The Physics of Ball Games*, English University Press, 1972.
- [93]. Wenninger Magnus J., *Dual Models*, 1st Ed., Cambridge University Press, 1983.
- [94]. Blake A., McCowen D., Lo H.R., Lindsey P.J., *Trinocular Active Range-Sensing*. University of Oxford Dept. of Engineering Science, 1991.
- [95]. Celenk Mehmet, Bachnak Rafic A., *Multiple Stereo Vision System For 3-D Object Reconstruction*, Jour. of Applied Systems Analysis, 1990.
- [96]. Blisset R.J., Stephens M.J., Sparks E.P., *Surface Perception and Localisation Using Passive Vision*, 9th Int. Conf. Automation Inspection & Product Control, 1989.
- [97]. Ito Minoru, and Ishii Akira, *Range and Shape Measurement Using Three-View Stereo Analysis*, IEEE, 1986.
- [98]. Burton David R., Lalor Michael J., *Non-contact Precision Measurement of Shape in a Manufacturing Process*, Application of Computers to Manufacturing Engineering Directorate September Conf. Sheffield University. ACME.000, 1993.

- [99]. Takeda M., Mutoh K., *Fourier Transform Profilometry for Automatic Measurement of 3-D Object Shapes*, Appl. Optics, Vol 22, 1983.
- [100]. Lu C.G., Myler P., Wu M.H., *An Artificial Intelligence Path Planning System for Multiple Tasks Inspection on Co-ordinate Measuring Machine*, Matador Conf. 31th, 1995.
- [101]. Atkins N.W., Derby S., *An Interactive Graphics Application for Computer Aided Development of Inspection Programs for Coordinate Machines*, Advances in Design Automation (ASME) Design Technical Conf. Part 1, 1989.
- [102]. Medland A.J., Mullineux G., Rentoul A.H., *Measurement of Features by a Sample-Grid Approach*, Tenth National Conf. on Manufacturing Research, VIII, 1994.
- [103]. Shield S.J., *Automated measurement of Golf Balls*, BEng. Final Year Project, Man. Eng. Dept. Loughborough University, U.K., 1990.
- [104]. Anton Howard, *Calculus with Analytic Geometry*. 4th ed. Anton Textbook Inc., 1992.
- [105]. Bajpai A.C., Mustoe L.R., Walker D., *Advanced Engineering Mathematics*, John Wiley and Sons, Ltd. 1977.
- [106]. Mustoe L.R., *Worked Examples in Advanced Engineering Mathematics*, John Wiley and Sons Ltd., 1988.
- [107]. Dobinson John, *Mathematics for technology*, Hazell Watson and Viney Ltd., 1972.
- [108] Rodenstock, *RM600 laser stylus*, 1991.
- [109] *Universal measuring machine MU-214B*, Societe Gtevoise Ltd, Switzeland.
- [110]. Ellis Robert, Gulick Denny, *Calculus With Analytic Geometry*, 4th ed. Harcourt Brace Jovanovich Inc., U.S.A. 1990.
- [111]. The British Standard BS5233, *Glossary of terms used in metrology*.
- [112] Lehtihet E.A., Gunasena U.N., *Statistical Models for the Relationship Between Production Errors and the Position Tolerance of a Hole*, CIRP 39 part 1, 1990.
- [113] Wang Yu, *Minimum Zone Evaluation of Form Tolerances*, Advances in Design Automation (ASME) 2, Symposium on Flexible Automation, 1992.
- [114] Elmaraghy W.H., Wu Z., Elmaragh A., *Evaluation of Actual Geometric Tolerances using Coordinate Measuring Machine Data*, Advances in Design Automation 19-1, 1989.
- [115] Elmaraghy W.H., Elmaraghy H.A., Wu Z., *Detemination of Actual Geometric Deviations Using Coordinate Measuring Machine Data*, ASME Manuf. Review 3-1, 1990.

- [116] Litvin F.L., Zhang Y., Kuan C., Handschuh R.F., *Computerized Inspection of Real Surfaces and Minimization of Their Deviations*, Int. J. Mach Tools Manufac. 32, No. 1/2, 1992.
- [117] Cho J.H., Cho M.W., Kim K., *Volumetric error analysis of a Multi-Axis Machine Tool Machining a Sculptured Surface Workpiece*, Int. J. Prod. Res. (IJPR), Vol.32–No. 2, 1994.
- [118]. Jones & Shipman Plc., *Rotary Table is Just the Tee*, J & S Technology Autumn No. 10, 1993.
- [119]. Bowyer Adrian, Woodwark John, *Introduction to Computing with Geometry*, 1st ed. Information Geometers Ltd, GB., 1993.
- [120]. Hensel Edward, *Inverse Theory and Applications for Engineers*, 1st ed. Prentice Hall Advanced Reference Series, 1991.
- [121]. Rao S.S., *Optimization Theory and Applications*, Wiley Eastern Limited, New Delhi, 1979.
- [122]. Beale E.M., *Introduction to Optimization*, John Wiley & Sons 1988.
- [123]. Taylor Howard M., Karlin Samuel, *An Introduction to Stochastic Modeling*, Revised Edition ed. Academic Press, Inc., USA, 1994.
- [124]. Pike Ralph W, *Optimization for Engineering Systems*, 1st ed. Van Nostrand Reinhold Company, New York, 1986.
- [125]. Price W.L., *Global Optimization Algorithms For a CAD Workstation*, J. of Optimization Theory and Applications 55–1, Oct. 1987.
- [126]. Abdy P.R., Dempster M.A.H., *Introduction to Optimization Methods*, 1st ed. Chapman and Hall Ltd, London 1974.
- [127]. Gill Philip E, Murray Walter and Wright Margaret H., *Practical Optimization*, Academic Press, Inc. 1988.
- [128]. Gill P.E., Murray W., *Numerical Methods for Constrained Optimization*, 1st ed. Academic Press Inc. Ltd., London, 1974.
- [129]. Scales L.E., *Introduction to Non-Linear Optimization*, 1st ed. Macmillan Publishers Ltd., London, 1985.
- [130]. Kreyszig Erwin, *Advanced Engineering Mathematics*, 4th ed. John Wiley & Sons, New York, 1979.
- [131]. Price W.L., *A Controlled Random Search Procedure for Global Optimization*, proc.

Towards Global Optimization II North-Holand Pub. Co., 1978.

[132]. Capes Philip, Harding Maria, *Computers Grasp Moulding Data*, Metalworking Production, January 1992.

[133]. Powaser Dave, *Linking CAD and CMM*, Automation (Magazine for manu. management and Eng.) April 1991.

[134]. Sivayoganathan K., Balendran V., Czerwinski A., Keats J., *CAD/CAM Data Exchange Application*, Nineth National Conference on Manufacturing Research, VII, 1993.

[135]. Osbaldiston S.L., Sivayoganathan K., Al-Dabass D., *An Intelligent, Interactive Programming Environment for Co-ordinate Measurement Systems*, 5th Conf. on Production Research 1, 1989.

[136]. Zeid Ibrahim, *CAD/CAM Theory and Practice*, 1991

[137]. Zarifi A., Jones R., *Errors in Measurement of Sculptured Surfaces Using a 2-D Vision System and Coordinate Measuring Machine*, Production and manufacturing Engineering Conference, Oct. 1993.

APPENDIX A**LSBFM RESULTS FOR CUBIC AND ICOSDHH (432) PATTERNS**

The LSBFM was applied to the cubic and icosdhh 432 hobs and the followings are results of these tests in mm, where Error1 is the 3-D distance between CAD and CMM values, Error2 is the CAD and optimised values and variation is the difference between the Error1 and Error2.

Cubic Pattern

Dimple No.	Error1 (CAD-CMM)	Error2 (CAD-Optimised)	Variation (Error1-Error2)
0	0.0118	0.0078	0.0040
1	0.0113	0.0083	0.0030
2	0.0101	0.0078	0.0023
3	0.0099	0.0089	<u>0.0010 (Min. Var.)</u>
4	0.0090	0.0083	0.0007
5	0.0114	0.0094	0.0020
6	0.0087	0.0080	0.0007
7	0.0109	0.0099	<u>0.0010</u>
8	0.0125	0.0112	0.0013
9	0.0130	0.0113	0.0017
10	0.0137	0.0112	0.0025
11	0.0112	0.0091	0.0021
12	0.0132	0.0118	0.0024
13	0.0123	0.0112	0.0011
14	0.0115	0.0102	0.0013
15	0.0113	0.0090	0.0023
16	0.0105	0.0089	0.0016
17	0.0132	0.0118	0.0014
18	0.0125	0.0102	0.0023
19	0.0142	0.0111	0.0031
20	0.0108	0.0072	0.0036
21	0.0093	0.0071	0.0022
22	0.0078	0.0062	0.0016
23	0.0103	0.0087	0.0016
24	0.0095	0.0081	0.0014
25	0.0099	0.0079	0.0020
26	0.0111	0.0080	0.0030
27	0.0106	0.0074	0.0032
28	0.0109	0.0091	0.0018
29	0.0127	0.0102	0.0025
30	0.0129	0.0098	0.0031
31	0.0089	0.0067	0.0022
32	0.0104	0.0074	0.0030
33	0.0128	0.0084	0.0044
34	0.0103	0.0091	0.0012
35	0.0069	0.0046	0.0023
36	0.0089	0.0073	0.0016
37	0.0122	0.0101	0.0021
38	0.0106	0.0077	0.0029
39	0.0106	0.0083	0.0023

Appendix A. LSBFM results for cubic and icosdhh (432) patterns

40	0.0103	0.0066	0.0037
41	0.0139	0.0101	0.0038
42	0.0149	0.0111	0.0038
43	0.0111	0.0071	0.0040
44	0.0084	0.0059	0.0025
45	0.0096	0.0063	0.0033
46	0.0102	0.0076	0.0026
47	0.0115	0.0072	0.0043
48	0.0113	0.0085	0.0028
49	0.0117	0.0099	0.0018
50	0.0098	0.0075	0.0023
51	0.0048	0.0023	0.0025
52	0.0129	0.0088	0.0041
53	0.0116	0.0105	0.0011
54	0.0070	0.0057	0.0013
55	0.0106	0.0087	0.0019
56	0.0072	0.0047	0.0025
57	0.0128	0.0091	0.0037
58	0.0104	0.0084	0.0020
59	0.0059	0.0027	0.0032
60	0.0081	0.0049	0.0032
61	0.0086	0.0046	0.0040
62	0.0089	0.0051	0.0038
63	0.0107	0.0087	0.0020
64	0.0099	0.0072	0.0027
65	0.0106	0.0074	0.0032
66	0.0119	0.0090	0.0029
67	0.0098	0.0064	0.0034
68	0.0131	0.0110	0.0021
69	0.0107	0.0091	0.0016
70	0.0110	0.0083	0.0027
71	0.0098	0.0069	0.0029
72	0.0116	0.0069	0.0047
73	0.0069	0.0037	0.0032
74	0.0073	0.0041	0.0032
75	0.0112	0.0091	0.0021
76	0.0109	0.0098	0.0011
77	0.0108	0.0081	0.0027
78	0.0105	0.0082	0.0023
79	0.0118	0.0083	0.0035
80	0.0132	0.0101	0.0031
81	0.0147	0.0106	0.0041
82	0.0077	0.0042	0.0035
83	0.0114	0.0092	0.0022
84	0.0098	0.0068	0.0030
85	0.0113	0.0091	0.0022
86	0.0109	0.0084	0.0025
87	0.0106	0.0086	0.0020
88	0.0109	0.0072	0.0037
89	0.0107	0.0087	0.0020
90	0.0103	0.0079	0.0024
91	0.0108	0.0083	0.0025
92	0.0092	0.0071	0.0021
93	0.0096	0.0072	0.0024
94	0.0127	0.0097	0.0030
95	0.0103	0.0092	0.0011
96	0.0112	0.0080	0.0032
97	0.0124	0.0110	0.0014

Appendix A. LSBFM results for cubic and icosdhh (432) patterns

98	0.0113	0.0095	0.0018
99	0.0114	0.0100	0.0014
100	0.0109	0.0096	0.0013
101	0.0125	0.0101	0.0024
102	0.0142	0.0101	0.0041
103	0.0109	0.0091	0.0018
104	0.0126	0.0114	0.0012
105	0.0149	0.0103	0.0046
106	0.0117	0.0092	0.0025
107	0.0139	0.0114	0.0025
108	0.0108	0.0081	0.0027
109	0.0102	0.0064	0.0035
110	0.0079	0.0052	0.0027
111	0.0109	0.0080	0.0029
112	0.0088	0.0061	0.0027
113	0.0109	0.0091	0.0018
114	0.0116	0.0096	0.0020
115	0.0119	0.0096	0.0023
116	0.0105	0.0085	0.0020
117	0.0078	0.0059	0.0019
118	0.0103	0.0083	0.0020
119	0.0092	0.0072	0.0020
120	0.0098	0.0083	0.0015
121	0.0099	0.0069	0.0030
122	0.0098	0.0077	0.0021
123	0.0118	0.0101	0.0017
124	0.0129	0.0089	0.0040
125	0.0137	0.0077	0.0060
126	0.0122	0.0112	<u>0.0010</u>
127	0.0128	0.0108	0.0020
128	0.0100	0.0070	0.0030
129	0.0131	0.0083	0.0048
130	0.0101	0.0091	0.0010
131	0.0099	0.0069	0.0030
132	0.0109	0.0084	0.0025
133	0.0119	0.0090	0.0029
134	0.0111	0.0091	0.0020
135	0.0108	0.0088	0.0020
136	0.0113	0.0063	0.0050
137	0.0089	0.0068	0.0021
138	0.0079	0.0058	0.0021
139	0.0069	0.0054	0.0015
140	0.0075	0.0053	0.0022
141	0.0107	0.0087	0.0020
142	0.0108	0.0076	0.0032
143	0.0108	0.0068	0.0040
144	0.0137	0.0060	<u>0.0077 (Max. Var.)</u>
145	0.0136	0.0103	0.0033
146	0.0099	0.0061	0.0038
147	<u>0.0037 (Min. Err.)</u>	<u>0.0013 (Min. Err.)</u>	0.0024
148	0.0069	0.0036	0.0033
149	0.0045	0.0011	0.0034
150	0.0067	0.0026	0.0041
151	0.0049	0.0024	0.0025
152	0.0046	0.0024	0.0022
153	0.0049	0.0027	0.0022
154	0.0131	0.0087	0.0044
155	0.0138	0.0097	0.0041

Appendix A. LSBFM results for cubic and icosdhh (432) patterns

156	0.0089	0.0068	0.0021
157	0.0094	0.0074	0.0020
158	0.0109	0.0084	0.0025
159	0.0108	0.0078	0.0030
160	0.0139	0.0079	0.0060
161	0.0127	0.0076	0.0051
162	0.0122	0.0102	0.0020
163	0.0148	0.0088	0.0060
164	0.0124	0.0084	0.0040
165	0.0159	0.0115	0.0044
166	0.0131	0.0119	0.0012
167	0.0137	0.0093	0.0044
168	0.0106	0.0069	0.0037
169	0.0109	0.0079	0.0030
170	0.0107	0.0070	0.0037
171	0.0109	0.0092	0.0017
172	0.0110	0.0090	0.0020
173	0.0111	0.0091	0.0020
174	0.0114	0.0084	0.0030
175	0.0129	0.0106	0.0023
176	0.0105	0.0079	0.0026
177	0.0108	0.0088	0.0020
178	0.0103	0.0088	0.0015
179	0.0142	0.0095	0.0047
180	0.0119	0.0091	0.0028
181	0.0129	0.0089	0.0040
182	0.0142	0.0110	0.0032
183	0.0108	0.0088	0.0020
184	0.0118	0.0088	0.0030
185	<u>0.0154 (Max. Err.)</u>	<u>0.0121 (Max. Err.)</u>	0.0033
186	0.0129	0.0099	0.0030
187	0.0131	0.0119	0.0012
188	0.0137	0.0099	0.0038
189	0.0109	0.0083	0.0026
190	0.0109	0.0079	0.0030
191	0.0107	0.0070	0.0037
192	0.0119	0.0092	0.0027
193	0.0098	0.0060	0.0038
194	0.0111	0.0091	0.0020
195	0.0114	0.0084	0.0030
196	0.0109	0.0086	0.0023
197	0.0105	0.0079	0.0026
198	0.0108	0.0088	0.0020
199	0.0123	0.0101	0.0022
200	0.0142	0.0115	0.0027
201	0.0119	0.0101	0.0018
202	0.0129	0.0109	0.0020
203	0.0124	0.0102	0.0022
204	0.0108	0.0087	0.0021
205	0.0118	0.0089	0.0029
206	0.0118	0.0078	0.0040
207	0.0142	<u>0.0121</u>	0.0021
208	0.0122	0.0109	0.0013
209	0.0119	0.0089	0.0030
210	0.0123	0.0110	0.0013
211	0.0108	0.0077	0.0031
212	0.0098	0.0065	0.0033
213	0.0108	0.0082	0.0026

214	0.0102	0.0085	0.0017
215	0.0129	0.0109	0.0020
216	0.0117	0.0089	0.0028
217	0.0119	0.0091	0.0028
218	0.0108	0.0064	0.0044
219	0.0109	0.0087	0.0022
220	0.0101	0.0089	0.0012

Icosdhh 432 Pattern

Dimple No.	Error1 (CAD-CMM)	Error2 (CAD-Optimised)	Variation (Error1-Error2)
0	0.0110	0.0068	0.0042
1	0.0103	0.0066	0.0037
2	0.0085	0.0049	0.0036
3	0.0112	0.0072	0.0041
4	0.0098	0.0061	0.0038
5	0.0119	0.0076	0.0043
6	0.0116	0.0073	0.0043
7	0.0115	0.0074	0.0041
8	0.0103	0.0065	0.0038
9	0.0079	0.0046	0.0033
10	0.0088	0.0053	0.0035
11	0.0135	0.0091	0.0044
12	0.0104	0.0065	0.0039
13	0.0096	0.0059	0.0037
14	0.0085	0.0052	0.0033
15	0.0077	0.0042	0.0034
16	0.0094	0.0056	0.0038
17	0.0126	0.0082	0.0045
18	0.0085	0.0050	0.0035
19	0.0082	0.0049	0.0033
20	0.0127	0.0083	0.0044
21	0.0087	0.0053	0.0035
22	0.0108	0.0070	0.0038
23	0.0115	0.0076	0.0039
24	0.0117	0.0078	0.0039
25	0.0089	0.0055	0.0034
26	0.0073	0.0042	0.0031
27	0.0063	0.0036	0.0027
28	0.0078	0.0046	0.0032
29	0.0085	0.0052	0.0033
30	0.0092	0.0058	0.0034
31	0.0078	0.0045	0.0032
32	0.0077	0.0046	0.0031
33	0.0103	0.0068	0.0036
34	0.0079	0.0050	0.0029
35	0.0068	0.0040	0.0028
36	0.0084	0.0053	0.0032
37	0.0070	0.0047	0.0024
38	0.0118	0.0088	0.0030
39	0.0101	0.0073	0.0028
40	0.0098	0.0071	0.0027
41	0.0067	0.0045	0.0022
42	0.0082	0.0057	0.0026
43	0.0071	0.0047	0.0024
44	0.0048	0.0028	0.0020

Appendix A. LSBFM results for cubic and icosdhh (432) patterns

45	0.0048	0.0027	0.0020
46	0.0086	0.0060	0.0026
47	0.0090	0.0077	0.0013
48	<u>0.0158 (Max. Err.)</u>	<u>0.0141 (Max. Err.)</u>	0.0017
49	0.0102	0.0087	0.0014
50	0.0073	0.0060	0.0013
51	0.0089	0.0083	0.0006
52	0.0063	0.0033	0.0030
53	0.0097	0.0058	0.0038
54	0.0100	0.0060	0.0039
55	0.0088	0.0052	0.0036
56	0.0071	0.0041	0.0030
57	0.0086	0.0052	0.0035
58	0.0086	0.0052	0.0034
59	0.0085	0.0053	0.0031
60	0.0076	0.0045	0.0031
61	0.0076	0.0044	0.0032
62	0.0081	0.0049	0.0032
63	0.0083	0.0050	0.0032
64	0.0089	0.0057	0.0032
65	0.0101	0.0063	0.0038
66	0.0081	0.0046	0.0035
67	0.0042	0.0019	0.0023
68	0.0040	0.0018	0.0022
69	0.0038	0.0018	0.0021
70	0.0032	<u>0.0013 (Min. Err.)</u>	0.0018
71	0.0036	0.0017	0.0019
72	0.0052	0.0030	0.0022
73	0.0038	0.0021	0.0017
74	0.0027	0.0014	0.0013
75	0.0027	0.0016	<u>0.0011 (Min. Var.)</u>
76	0.0032	0.0015	0.0017
77	0.0053	0.0030	0.0023
78	<u>0.0028 (Min. Err.)</u>	0.0015	0.0013
79	0.0033	0.0017	0.0016
80	0.0058	0.0035	0.0023
81	0.0070	0.0044	0.0026
82	0.0071	0.0045	0.0026
83	0.0035	0.0021	0.0014
84	0.0037	0.0020	0.0017
85	0.0039	0.0019	0.0020
86	0.0049	0.0024	0.0025
87	0.0033	0.0016	0.0017
88	0.0110	0.0068	0.0042
89	0.0102	0.0063	0.0039
90	0.0085	0.0051	0.0034
91	0.0085	0.0051	0.0034
92	0.0070	0.0038	0.0032
93	0.0072	0.0041	0.0032
94	0.0096	0.0060	0.0036
95	0.0073	0.0041	0.0032
96	0.0099	0.0059	0.0039
97	0.0109	0.0068	0.0041
98	0.0120	0.0077	0.0043
99	0.0100	0.0061	0.0039
100	0.0136	0.0090	<u>0.0046 (Max. Var.)</u>
101	0.0093	0.0058	0.0035
102	0.0099	0.0064	0.0035

Appendix A. LSBFM results for cubic and icosdhh (432) patterns

103	0.0084	0.0050	0.0034
104	0.0070	0.0040	0.0031
105	0.0084	0.0050	0.0034
106	0.0103	0.0063	0.0040
107	0.0102	0.0063	0.0038
108	0.0116	0.0075	0.0041
109	0.0105	0.0066	0.0038
110	0.0107	0.0070	0.0037
111	0.0089	0.0057	0.0032
112	0.0085	0.0054	0.0032
113	0.0078	0.0048	0.0031
114	0.0044	0.0020	0.0024
115	0.0062	0.0035	0.0028
116	0.0078	0.0045	0.0033
117	0.0098	0.0063	0.0036
118	0.0107	0.0070	0.0037
119	0.0112	0.0074	0.0037
120	0.0092	0.0058	0.0034
121	0.0084	0.0052	0.0032
122	0.0061	0.0034	0.0027
123	0.0074	0.0044	0.0030
124	0.0072	0.0043	0.0028
125	0.0080	0.0048	0.0032
126	0.0066	0.0038	0.0028
127	0.0072	0.0041	0.0030
128	0.0093	0.0061	0.0032
129	0.0091	0.0060	0.0032
130	0.0088	0.0057	0.0031
131	0.0074	0.0046	0.0028
132	0.0071	0.0045	0.0027
133	0.0083	0.0054	0.0029
134	0.0070	0.0042	0.0028
135	0.0072	0.0045	0.0027
136	0.0060	0.0034	0.0026
137	0.0065	0.0038	0.0027
138	0.0084	0.0056	0.0028
139	0.0071	0.0046	0.0025
140	0.0060	0.0037	0.0023
141	0.0054	0.0031	0.0022
142	0.0056	0.0033	0.0023
143	0.0105	0.0080	0.0025
144	0.0104	0.0080	0.0024
145	0.0077	0.0056	0.0022
146	0.0070	0.0050	0.0021
147	0.0084	0.0062	0.0022
148	0.0096	0.0075	0.0021
149	0.0119	0.0096	0.0023
150	0.0117	0.0093	0.0023
151	0.0086	0.0066	0.0020
152	0.0075	0.0056	0.0019
153	0.0065	0.0046	0.0018
154	0.0073	0.0054	0.0019
155	0.0070	0.0051	0.0019
156	0.0055	0.0038	0.0017
157	0.0060	0.0042	0.0017
158	0.0093	0.0055	0.0038
159	0.0084	0.0051	0.0034
160	0.0098	0.0062	0.0036

Appendix A. LSBFM results for cubic and icosdhh (432) patterns

161	0.0091	0.0056	0.0035
162	0.0077	0.0046	0.0031
163	0.0080	0.0047	0.0033
164	0.0091	0.0055	0.0036
165	0.0106	0.0065	0.0041
166	0.0080	0.0052	0.0029
167	0.0078	0.0049	0.0028
168	0.0081	0.0052	0.0029
169	0.0093	0.0062	0.0030
170	0.0071	0.0044	0.0027
171	0.0053	0.0030	0.0023
172	0.0078	0.0052	0.0026
173	0.0086	0.0056	0.0029
174	0.0070	0.0044	0.0027
175	0.0071	0.0044	0.0027
176	0.0070	0.0043	0.0027
177	0.0061	0.0036	0.0025
178	0.0080	0.0055	0.0025
179	0.0064	0.0042	0.0022
180	0.0102	0.0074	0.0027
181	0.0079	0.0057	0.0022
182	0.0076	0.0053	0.0023
183	0.0057	0.0036	0.0021
184	0.0127	0.0082	0.0045
185	0.0105	0.0066	0.0039
186	0.0135	0.0092	0.0043
187	0.0094	0.0059	0.0034
188	0.0076	0.0048	0.0028
189	0.0096	0.0063	0.0032
190	0.0094	0.0059	0.0035
191	0.0072	0.0044	0.0028
192	0.0091	0.0053	0.0037
193	0.0123	0.0080	0.0042
194	0.0113	0.0072	0.0041
195	0.0101	0.0064	0.0037
196	0.0107	0.0069	0.0038
197	0.0092	0.0057	0.0035
198	0.0122	0.0084	0.0039
199	0.0081	0.0053	0.0028
200	0.0094	0.0060	0.0035
201	0.0093	0.0060	0.0033
202	0.0059	0.0030	0.0029
203	0.0112	0.0076	0.0036
204	0.0132	0.0095	0.0037
205	0.0091	0.0062	0.0029
206	0.0063	0.0038	0.0025
207	0.0081	0.0051	0.0031
208	0.0145	0.0125	0.0021
209	0.0118	0.0099	0.0019
210	0.0061	0.0046	0.0015
211	0.0064	0.0049	0.0015
212	0.0073	0.0057	0.0016
213	0.0063	0.0048	0.0015

APPENDIX B

POLAR APPROACH

A point in a plane has polar coordinates (r, θ) and cartesian coordinates (x, y) relative to a coordinate datum. To convert from the cartesian coordinates system to a polar coordinate system the equations below can be used for all values of r and θ , fig. app.1 depicts this situation.

$$x = r \cos \theta \quad \text{and} \quad y = r \sin \theta \quad \dots 1$$

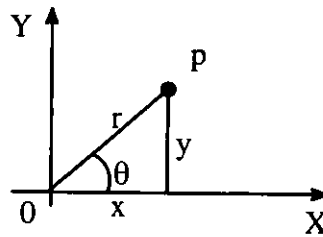


Fig. app.1. Polar coordinate of a point.

It is possible to compute a length in polar coordinates of a non negative function f defined on α , and β with $0 \leq \beta - \alpha \leq 2\pi$ (fig. app.2). The polar graph of f is the set of points (x, y) with polar coordinates (r, θ) satisfying $r = f(\theta)$ and $\alpha \leq \theta \leq \beta$. The representation of a polar graph has

$$x = f(\theta) \cos \theta \quad \text{and} \quad y = f(\theta) \sin \theta \quad \text{for} \quad \alpha \leq \theta \leq \beta \quad \dots 2$$

Fig. app.2 shows the length of a curve in 2-D space. In general, to find a curve length, the behaviour of the function have to be found within the limits α and β .

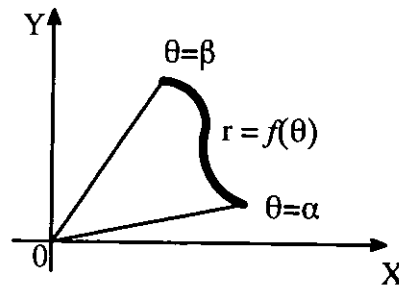


Fig. app.2. Polar graph of f .

$$\begin{aligned}
 \text{length of a curve in polar coordinates} &= \int_{\alpha}^{\beta} \sqrt{\left(\frac{dx}{d\theta}\right)^2 + \left(\frac{dy}{d\theta}\right)^2} d\theta && \dots 3 \\
 &= \int_{\alpha}^{\beta} \sqrt{[f'(\theta) \cos \theta - f(\theta) \sin \theta]^2 + [f'(\theta) \sin \theta + f(\theta) \cos \theta]^2} d\theta \\
 &= \int_{\alpha}^{\beta} \sqrt{(f'(\theta))^2(\cos^2 \theta + \sin^2 \theta) + (f(\theta))^2(\sin^2 \theta + \cos^2 \theta)} d\theta \\
 &= \int_{\alpha}^{\beta} \sqrt{(f'(\theta))^2 + (f(\theta))^2} d\theta && \dots 4
 \end{aligned}$$

Where r is radius of curve
 $f(\theta)$ is function of θ
 $f'(\theta)$ is derivative of f respect to θ

Length of arc in 3-D space

If a segment is cut out of a sphere with radius r and points O,1,2,3, and 4 as shown in fig. app.3, the arcs between points 1and2, 1and4, 1and3, etc. are examples of arcs in 3-D space. The orientation of the arc lengths is random, however they are easier calculated if they are considered with respect to one plane for example the arcs 1and2, or 3and4 have some variation in angle θ but the constant angle ϕ while arcs 1and3 or 2and4 have variations in both angles θ and ϕ . In order to appreciate this concept the length of the arc between points 1and4, or 2and3 with angle $\phi_2 - \phi_1$ in circle with radius r can be found by

$$\text{arc } \widehat{1-4} = r (\phi_2 - \phi_1) \quad \dots 5$$

The length of arc between points 1and2 which consists of angle $(\theta_2 - \theta_1)$ in a circle radius $r_1 = r \sin(\phi_2)$, so that

$$\text{length of arc } \widehat{1-2} \approx r (\theta_2 - \theta_1) = (r \sin \phi_2)(\theta_2 - \theta_1) \quad \dots 6$$

and consequently, the approximation length of an arc $\widehat{1-3}$ can be found by,

$$\text{length of arc } \widehat{1-3} \approx \sqrt{[r(\phi_2 - \phi_1)]^2 + [r(\theta_2 - \theta_1)]^2} \quad \dots 7$$

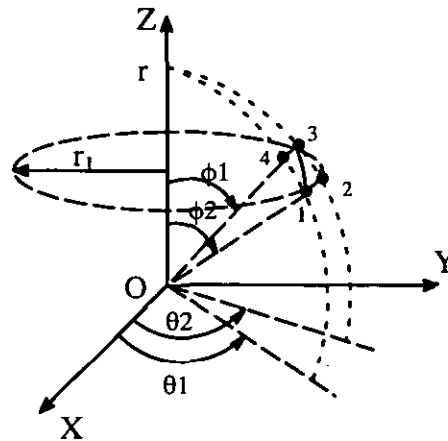


Fig. app.3. Spherical wedge in 3-D.

Since, in practice the arc lengths such as arc $\widehat{1-2}$ or $\widehat{1-3}$ are very small in comparison with the ball diameter and the errors are much smaller, therefore, it is acceptable for the lengths to be treated as 3-D straight lines.

For the case considered here the actual position of dimples are acceptable until the point where the dimples overlap (i.e., the land width between dimples is effectively zero). If the maximum amount of land between dimples can be as much as 2.00 mm. This amount is selected as the worst case since values bigger than this would be detected through the visual inspection of the process and it is reasonable to treat the arc length as a straight line.

Although the optimisation process has been applied to the actual data in cartesian form, the same process can be applied for polar arrangement. The steps for minimising the errors between the nominal and virtual centres are as follows:–

1. Determine the maximum and minimum arc lengths of 3-D distance for the nominal and actual virtual centre points.
2. Determine the polar angles of θ and ϕ for the points which create the maximum arc length.
3. Determine the maximum calculated angle for the points.
4. Set up a grid (the horizontal and the vertical step size of the grid will have equal intervals), noting that the smaller the step size the longer it takes to process data and the better the result may be.
5. Calculate equivalent of the angle step size in mm (i.e., $\Delta\theta = \Delta X$ mm).
6. Calculate arc length for each pair of virtual surface points. Fig. app.4 shows the mathematical equations which could be used for calculating arc lengths in 3-D.
7. Run the process for each axis.

8. Apply the error equation to find the minimum arrangement for $\Delta\theta$ in mm.

$$E = \sum_{i=1}^{i=n=250} [X_{n_i} - X_{a_i} \pm (\Delta X)]^2 + [Y_{n_i} - Y_{a_i} \pm (\Delta Y)]^2 + [Z_{n_i} - Z_{a_i} \pm (\Delta Z)]^2$$

9. Repeat step 8 for all dimple pairs.

10. Repeat step 8 for all combinations of the intervals.

11. Sum the squared lengths for each iteration.

12. Use the least squares length for the total points.

13. Select the minimum least squares length.

14. Determine the correction factor for each axis.

15. Determine the new optimised positions.

16. Evaluate the optimised positions graphically with those of actual and nominal positions.

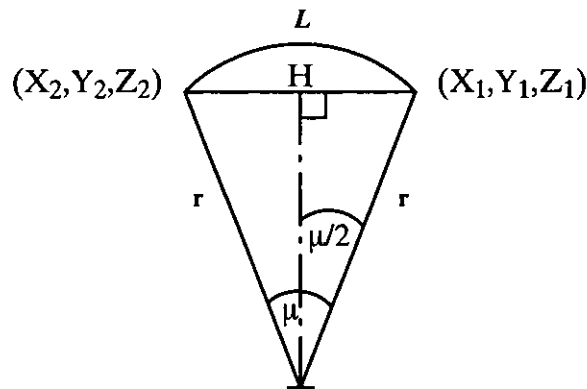


Fig. app.4. Arc length representaion.

$$H = \sqrt{(X_2 - X_1)^2 + (Y_2 - Y_1)^2 + (Z_2 - Z_1)^2} \quad \dots\dots\dots 8$$

$$\sin \frac{\mu}{2} = \frac{H}{2r}$$

$$\frac{\mu}{2} = \sin^{-1} \left(\frac{H}{2r} \right)$$

$$\mu = 2 \left(\sin^{-1} \left(\frac{H}{2r} \right) \right) \quad \dots\dots\dots 9$$

The arc length (L) in that plane can be calculated

$$\text{arc length (L)} = r\mu \quad \dots\dots\dots 10$$

Example

It is assumed that the arc error between the two neighbouring dimples would not be as much as 2.00 mm and also the maximum positional error. Applying the method to a sample dimple with only one angle (μ) which is considered in one plane on a ball with radius of 21.45 mm, the CAD and CMM data are fabricated values only for calculation purpose.

CAD data			CMM data		
X ₁	Y ₁	Z ₁	X ₂	Y ₂	Z ₂
16.83	12.23	5.61	16.61	12.52	5.61

using equation 8

$$\begin{aligned}
 H &= \sqrt{(X_2 - X_1)^2 + (Y_2 - Y_1)^2 + (Z_2 - Z_1)^2} \\
 &= \sqrt{(16.61 - 16.83)^2 + (12.23 - 12.52)^2 + (5.61 - 5.61)^2} \\
 &= 0.364 \text{ mm}
 \end{aligned}$$

from equation 9

angle between the two dimples

$$\begin{aligned}
 \mu &= 2 \left(\sin^{-1} \left(\frac{H}{2r} \right) \right) \\
 &= 2 \left(\sin^{-1} \left(\frac{0.364}{42.90} \right) \right) \\
 &= 0.0169^\circ
 \end{aligned}$$

from equation 10 the arc length is

$$\begin{aligned}
 L &= r\mu \\
 &= 21.45 * 0.0169 \\
 &= 0.362 \text{ mm}
 \end{aligned}$$

Therefore a difference between the values using the straight line and the arc length equations is

$$0.364 - 0.362 = 0.002 \text{ mm}$$

From the above calculation it is acceptable to treat the arc lengths as straight lines. The land between two dimples can vary and generally is not more than 2.00 mm, but the minimum would be a zero land since overlapping of two dimples is not allowed. But for the design and production aspects the dimples should be positioned and manufactured to the highest accuracy.

